Investigation of the Leaching and Oxidation of a Secondary Lead Refiner's Slag

Craig Beautement BSc (Eng)

Supervisor: A. Lewis

Submitted to the University of Cape Town in fulfilment of the requirements for the degree of Master of Science in Engineering

Environmental Process Engineering Research Group
Department of Chemical Engineering
University of Cape Town
Rondebosch, South Africa

June 2000

Acknowledgements

I would like to thank:

- *My supervisor, Alison Lewis for a learning experience*
- *Tiah Carleton thank you for your understanding, support, help and compassion. Your presence when things got rough pulled me through.*
- *My family for the amazing support they have provided me*
- *Harro von Blottnitz and Joachim Petersen for the guidance they provided*
- *Sue Buerger and the rest of the members of the 'Greenhouse' for all your help and friendship*
- *UCT Chemical engineering staff members*
- *Helen Divey and Shireen Mjacu for the analytical help*
- *Willie van der Merwe and Roley Tolmay at the local refiner*
- *Kai, Mark and Graeme for keeping life interesting*

Abstract

Secondary lead refiners produce a slag as a furnace waste product. Its disposal to a landfill represents an economic loss and an environmental hazard. The environment hazard arises from toxic heavy metals (notably lead) and soluble sulphides. Of the processes reviewed to reduce this hazard, the BROSS process was most suitable. This process was demonstrated at pilot plant scale to convert the sulphides present in the slag to sulphate and recover 90 % of the lead present in the slag for recycle back to the secondary lead process furnaces.

This study set out to experimentally investigate the leaching and oxidation processes of the first step of the BROSS process (termed leach – oxidation) as applied to the slag of a local refiner. The process goals that may be achieved by leach – oxidation are the removal of the soluble sulphide component from the slag and conversion of the sulphur present in the slag to aqueous oxidised species, thiosulphate and sulphate. The summarised objectives of this study were to:

- characterise the local slag with respect to the components relevant to leach – oxidation,
- determine the effect of varying the process conditions on the thiosulphate conversion,
- investigate each of the subprocesses occurring during leach – oxidation with respect to the: sequence of occurrence; effect of varied process conditions, identification of the conditions under which each of the subprocesses becomes rate determining and the applicability of theoretical rate equations where relevant.

Sulphide components were identified in heterogeneously distributed matte phases in the form of soluble $Na_2S.FeS$ and insoluble FeS. Sodium components were identified in the slag phase in the form of Na_2O and bound up in silicate matrices.

Under the base conditions selected for this investigation, 55 % - 60 % of the slag sulphur was converted to thiosulphate and less than 0.5 % to sulphate in 48 h. Under these conditions, approximately 12 % of the extraction of sulphur from the slag was due to dissolution of the soluble sulphide and the rest was found to occur via oxidative leaching of the insoluble sulphide. Aqueous sulphide was typically removed from the reactor solution within 18h45 for the fine size fraction and 24h00 for the coarse size fraction.

The high proportion of soluble components in the slag caused it to disintegrate during leaching. The disintegration rate determined the rate at which soluble and insoluble sulphide components were exposed to the solution. Increasing the starting slag 'block' size and decreasing the agitation rate lowered the disintegration rate.

The dissolution subprocess, which caused disintegration, was rapid under base conditions. Its rate was shown to be limited by the agitation rate at agitation rates lower than the base rate. Its rate was increased by increasing temperature. The dissolution rate equation only accounted adequately for the initial dissolution rate. This was a result of the effect of disintegration and varied resistances of different phases to leaching.

Oxidation of soluble sulphides occurred rapidly under base conditions and was increased substantially by an increase in temperature. Fe^{2+}, a component of the feed slag was found to catalyse the reaction. A rate equation with the reaction orders of Lefers *et al* (1978) adequately modelled the oxidation of the sulphides in solution.

Oxidative leaching was inhibited by the presence of aqueous sulphide and therefore was dependent on the oxidation of aqueous sulphide. The rapid rate of the oxidation of aqueous sulphide under base conditions meant that the impact of this on the end-of-run thiosulphate conversion results was not substantial under these conditions. This would become increasingly significant under conditions less favourable to aqueous sulphide oxidation.

The conversion of slag sulphide to thiosulphate was limited by the oxidative leaching subprocess under base conditions. This subprocess was limiting due to its temperature dependence. The increased rate of removal of aqueous sulphides at higher temperatures would also contribute to reducing the inhibition of oxidative leaching earlier in the experiment. At 60 °C near quantitative conversion of the slag sulphur to thiosulphate and sulphate occurred.

Under conditions where the starting slag size is appreciably larger than the coarse fraction, the disintegration rate becomes limiting to the rate of conversion to thiosulphate. While the base agitation rate did not cause limitation the conversion to thiosulphate, lowering the agitation rate significantly caused this factor to have an increasing effect on the conversion, particularly when slag 'block' starting sizes significantly larger than the coarse fraction are used.

The goal of removing the soluble sulphide components was attained by the leach – oxidation experiments, but that of the slag sulphur conversion to thiosulphate was not attained. If complete conversion of the slag sulphur to thiosulphate is a requirement for the leach – oxidation step, further investigation should only be carried out if operation at 60 °C is feasible. If the removal of the soluble sulphides is the most important criteria, further work into the modelling of the dissolution rate is required for reactor design. Larger scale investigation of the leach – oxidation step is required to properly assess the effect of using slag blocks of larger size than those allowed by the experimental scale of this investigation. Further work for evaluating the treatment of the local slag via the BROSS process would include: investigation of the separation of the solid product of leach – oxidation to recover a lead rich fraction; evaluation of the potential for further biological oxidation of the aqueous product to sulphate; and investigation of treatment options for this sulphate product.

Nomenclature

A	surface area	[m^2]
C_{O_2}	dissolved oxygen concentration at t	[mol/m^3 or kg/m^3]
C_{ST}	total mass concentration of sulphide leached at t	[mol/m^3 or kg/m^3]
C	concentration of solute	[mol/m^3 or kg/m^3]
C_S	sulphide concentration at t	[mol/m^3 or kg/m^3]
$C_{S,MAX}$	maximum concentration of solute in the bulk liquid	[mol/m^3 or kg/m^3]
c	molar or mass concentration	[mol/m^3 or kg/m^3]
D_{AB}	diffusion coefficient	[m^2/s]
$D_{AB,0}$	diffusion constant	[m^2/s]
E_A	activation energy	[J/mol]
k	reaction rate constant	[m^3/(mol^{n+m-1}.s) or m^3/(kg^{n+m-1}.s)]
k_0	frequency factor	[m^3/(mol^{n+m-1}.s) or m^3/(kg^{n+m-1}.s)]
k_L	leach rate constant	[m/s]
K_{SOL}	equilibrium constant	[Pa.m^3/mol]
m	order with respect to sulphide	-
n	order with respect to oxygen	-
P_{O2}	partial pressure of oxygen in the gas stream	[Pa]
R	ideal gas constant	[J/(K.mol)]
r	radius	[m]
T	temperature	[K]
t	Time	[s]
V	volume of solution	[m^3]
δ	boundary layer thickness	[m]
$[O_2]$	equilibrium dissolved oxygen concentration	[mol/m^3]

Abbrieviations

AAS	Atomic Absorption Spectroscopy
EC	European Commission
EDS	Electron Dispersive Spectroscopy
ICP	Inductively Coupled Plasma
ICP-OES	Inductively Coupled Plasma - Optical Emission Spectroscopy
rpm	Revolutions Per Minute
SEM	Scanning Electron Microscope
UCT	University of Cape Town

Table of contents

List of figures

List of tables

1. Introduction

1.1 Background

Secondary lead refiners produce a slag as a waste product of the smelting process. The current practice of disposing the slag to a landfill represents an economic loss to the secondary refiner as well as an environmental hazard. The economic loss occurs in two ways. Firstly, the cost of disposal to a hazardous waste site paid to a waste contractor, secondly, the lead content of the slag represents a loss of lead bullion product (data collected by Pehlken (1997) shows that 2.5% of the total lead exiting the furnaces is lost to the slag).

The slag contains toxic heavy metals, including arsenic, zinc and lead, all of which are leachable in small quantities (Lewis *et al*, 1999). A large soluble sulphide component is also present, which would cause contamination of liquids that come into contact with the slag. These factors make untreated disposal of the slag environmentally hazardous.

This study forms part of a project run in collaboration with a South African Secondary Lead Refiner (henceforth known as the local refiner) with the aim of alleviating the secondary lead slag problem. Lewis *et al* (1999) investigated the optimisation of the smelting operation that produces the slag and made recommendations to the local refiner. Lewis *et al* (1999) found that under South African regulations the slag was regarded as hazardous.

This study focuses on one part of a slag treatment process, which has the potential to alleviate the problems mentioned above. It is a continuation of the work of Pehlken (1997) who investigated several unsuccessful processing possibilities for the recovery of lead from the slag, the results of which are summarised in Section 2.2.3.

The following technical criteria were used to evaluate potential treatment processes reviewed:

1. Production of a less environmentally hazardous slag: i.e. reduce toxic heavy metal components and or highly soluble sulphide components.
2. Recovery of the lead content of the slag.
3. Reduction of the quantity of slag to be disposed.

The composition of secondary lead slags varies appreciably between refiners due to feeds and furnace conditions. Thus, in addition to the criteria above, the selected treatment process must have the potential or have been demonstrated to be able to successfully treat a slag with a similar composition to that of the local refiner. The processes that have been shown to satisfy one or more of the three criteria are presented in Section 2.2.

The BROSS (Bio-Remediation of Sulphidic Slags) process was selected for further investigation in this study as a potential solution to the slag disposal problem. The reasons for this selection were the following:

- It has been demonstrated at pilot plant scale to be capable of satisfying the technical criteria set out above.
- The secondary lead refining operation that generated the slag treated at pilot scale, was similar with respect to furnace feeds and type of furnace to the local refiner.
- It is a low temperature hydrometallurgical process requiring minimal additional reagents. Thus, it has a potential to have lower operating costs than alternative thermal treatment processes.

A description of the BROSS process and results of pilot scale demonstration is given in Section 2.3. Although the biological step of this process was well investigated, the 'chemical pre-oxidation' step was identified as requiring further investigation. This step involves the concurrent leaching and oxidation of the soluble sulphides present in the slag to thiosulphate and a separation of the slag components that remain insoluble. This study sets out to investigate this step with the use of a feed slag from the local refiner. The term 'chemical pre-oxidation' was used to distinguish it from the oxidation of the thiosulphate to sulphate, the second step in the BROSS process. The process investigated: the 'chemical pre-oxidation' step of the BROSS process without the solids separation subprocess, which will be henceforth termed leach – oxidation.

1.2 Objectives

The broad objective of this study was to investigate the application of the leach – oxidation step of the BROSS process to the local slag and the effect that the various subprocesses have on the overall step. Application of this step to the local refiners slag also allows the main objective with respect to the BROSS process for this step to be evaluated for the local slag. This is:

1. The conversion of all the sulphur present in the slag to aqueous oxidation products, thiosulphate and sulphate.

The technical criteria identified the soluble sulphide components present in the slag as environmentally hazardous (see Section 2.2.4). In the BROSS process, the leach – oxidation step was responsible for removing these soluble sulphides from the slag. Thus, an additional objective for leach – oxidation would be:

2. The removal of environmentally hazardous soluble sulphide components from the slag.

In addition, soluble sulphides and other soluble components present in the slag have the following undesirable properties that impact on landfilling: cause rapid slag disintegration when exposed to water; produce a highly alkaline leachate; are hygroscopic and expand in volume when exposed to atmospheric water vapour. The presence of insoluble iron sulphide causes the production of toxic hydrogen sulphide gas when exposed to acids and heat generation (Section 2.2.4). The achievement of the goals (given above) for the leach – oxidation step would result in the removal of these components.

The specific objectives for the investigation of the leach – oxidation step in this study were to:

- Determine the composition of the local slag, with emphasis on components relevant to the leach – oxidation step.

- Determine the effect of certain process conditions, identified as relevant from literature, on the rate of the overall leach – oxidation of the slag.
- Investigate the subprocesses occurring in the leach – oxidation step individually. Specifically this was to:
  - Identify the subprocesses that occur during the leach – oxidation step and identify the sequence of their occurrence, if relevant.
  - Quantify the contribution of each subprocess to determining the rate at which leach – oxidation occurs and to the overall leach – oxidation extraction of sulphur and conversion to thiosulphate under certain selected base conditions.
  - Identify the conditions that significantly affect each of the subprocesses and hence determine under which conditions each of the subprocesses will limit the rate of the overall leach – oxidation process (where relevant).
  - Evaluate the applicability of theoretical rate equations to modelling the dissolution and aqueous sulphide oxidation subprocesses.

The rate at which leach – oxidation occurs, as referred to above, is the rate at which the sulphur is extracted from the slag and converted to thiosulphate and sulphate.

1.3 Approach

Once the BROSS process was selected as a possible solution to the secondary lead slag problem, this investigation set out to perform the following tasks:

- Collection of a representative slag sample from the local refiner.
- Identification of the components relevant to leach – oxidation by quantitative and qualitative analytical techniques.
- Operation of experiments for the investigation of the whole leach – oxidation process. These included repeated experiments under pre-selected base conditions and experiments isolating the effects of certain process conditions on the overall process.
- Operation of experiments for the investigation of the individual subprocesses. These included repeated experiments under pre-selected base conditions and experiments isolating the effects of certain process conditions on the individual subprocesses.
- Evaluation of the fit of rate equations to the leaching and oxidation data and calculate kinetic constants.

In Chapter 2, literature is reviewed on alternative processes that alleviate the slag treatment problem, with emphasis on the selected process, the BROSS process. The subprocesses that were identified as occurring or potentially occurring during leach – oxidation are then reviewed extensively. This is done primarily in terms of the mechanism by which they are expected to occur during leach – oxidation and the conditions that affect their rate of occurrence. Rate equations are also reviewed where appropriate.

In Chapter 3, the identified subprocesses are defined in terms of their occurrence during leach – oxidation. From this a method is determined for examining the subprocesses experimentally. The methods used in the experimental investigation are presented in Chapter 4. This chapter reports the experimental program, the equipment used and the experimental procedure, and includes a discussion on the sources of error associated with the experimental procedure.

In Chapter 5 the experimental results are presented. These are divided into the results of overall leach – oxidation experiments at pre-selected base conditions, results where certain conditions are varied, and the results of experiments investigating the subprocesses individually.

In Chapter 6, the results of each of the sections of Chapter 5 are discussed. In Chapter 7, the results are evaluated as a whole. This is done firstly in terms of the interdependence of the individual subprocesses, and secondly the identification the conditions that most significantly affect their respective rates. Hence, the affect of the rates of these subprocesses, at varied conditions, on the overall leach – oxidation step could be evaluated. This leads to the conclusions and recommendations presented in Chapter 8 and Chapter 9 respectively.

2 Literature Review

2.1 Production of the secondary lead slag

Knowledge of the composition of furnace feeds and theoretical furnace reactions are an important source of information about the composition of the slag.

2.1.1 Furnace feeds

Lead bearing feeds

Lead bearing feeds to the rotary furnace consist primarily of used battery components, typically battery plates, paste and metallics. Feeds that are used intermittently include refining drosses and primary PbS concentrates. These feeds contain lead in the form of PbO, $PbSO_4$, PbS and metallic lead.

Non-lead bearing feeds

Additional furnace feeds are required as reactants for the smelting reactions (equation 2-1 to equation 2-4) and to decrease the viscosity of the slag. Carbon is added to the furnace as coal. It serves as a reductant of PbO and $PbSO_4$. Iron serves as a reductant of PbS and acts as a sulphur collector, fixing sulphur as FeS. Sodium carbonate reduces the melting point of slag, resulting in a reduction in the slag viscosity. It also acts as a sulphur collector, fixing sulphur as Na_2S (Guerrero *et al*, 1997). In addition to the sulphur present in the lead bearing feeds, these components give rise to the formation in the furnace of the secondary lead slag.

2.1.2 Furnace reactions

The primary role of the smelting operation is to convert the lead compounds present to metallic lead via the reduction reactions of equation 2-1 to 2-4.

PbO: $PbO + C \rightarrow Pb^0 + CO$ equation 2-1

$PbSO_4$: $2PbSO_4 + Na_2CO_3 + Fe^0 + 9C \rightarrow 2Pb^0 + FeS.Na_2S + 9CO + CO_2$ equation 2-2

or: $PbSO_4 + 2C \rightarrow PbS + 2CO_2$ equation 2-3

PbS: $PbS + Fe^0 \rightarrow FeS + Pb^0$ equation 2-4

2.1.3 Composition of the slag predicted by furnace reactions

The presence of sulphide and oxide components in the slag result in the formation of two different phases: a sulphide-rich matte phase and an oxide-rich slag phase (Queneau *et al*, 1989). Hence, the secondary lead slag is actually a slag-matte combination. However, in contrast to other smelting practices, the mixing obtained in short rotary furnace smelting [in use at the local refiner (Pehlken, 1997)] means that these phases would be well distributed through the slag.

Matte phase

The formation of the $FeS.Na_2S$ double sulphide compound in a secondary lead rotary furnace is predicted by equation 2-2 from Queneau *et al* (1989). Akkarapattanagoon *et al* (1989) found that there is a strong affinity between the alkali metal sulphide (Na_2S) and heavy metal sulphide (FeS) for the formation of double compounds, confirming that the formation of $Na_2S.FeS$ is favoured. Evidence for

the presence of this double sulphide compound is also presented by Steck *et al* (1929) who compiled a phase diagram for the FeS – Na_2S mixture. Between 53 mass-% and 73 mass-% FeS, all the Na_2S and FeS was attributed to Na_2S.FeS and FeS.

Slag phase

Queneau *et al* (1989) predict from smelting thermodynamics that the slag phase for secondary lead smelting in rotary furnaces should consist principally of Na_2O, FeO and Silica. Na_2O is formed in the furnace as a decomposition product of sodium carbonate in furnaces that do not maintain completely reducing conditions (Queneau *et al*, 1989). Equation 2-5 shows this furnace reaction.

$$Na_2CO_3 \rightarrow Na_2O + CO_2 \qquad \text{equation 2-5}$$

2.2 Alternative approaches to the secondary lead slag problem

2.2.1 Pre-treatment of the furnace feed: Paste desulphurisation

The paste fraction arising from the battery crushing and classification sections of the secondary refining operation has been traditionally routed without further treatment to the furnaces for smelting, as is still the case at the local refiner. Paste desulphurisation is a process that pre-treats this paste fraction prior to its introduction to the furnace. It involves the conversion of the lead sulphate present in the paste to lead carbonate, thus avoiding the production of a sulphidic slag. Sodium sulphate is formed as a waste stream.

This process provides a number of benefits. Firstly, substantial reductions in SO_2 and lead oxide particulate emissions from the furnace are achieved. Secondly, a slag is produced that is reduced in terms of quantity as a result of less furnace fluxes required (Kammer *et al*, 1993) and has virtually none of the soluble sulphide fraction, which causes problems on disposal. This process has reached commercial operation at a number of secondary lead refiners, particularly in countries with strict sulphur dioxide emission controls, for example the United States (Queneau *et al*, 1981). Disadvantages include the requirement for treatment of the sodium sulphate stream via crystallisation and that the implementation of this process requires a major change in operation. This process is further discussed in Section 1 of Appendix A. Further advantages and disadvantages are presented along with processes that have been proposed to extract lead from the lead carbonate product of desulphurisation hydrometallurgically.

2.2.2 Alternative slag treatment processes

Glassification

Shenkler *et al* (1991) investigated the formation of secondary lead smelter slags and mattes into a glassy silica matrix, termed fritting or glassification. The results of this investigation, summarised in Table 2 of Appendix A, indicate that glassification results in the formation of a more benign slag with respect to the TCLP (Toxic Characteristic Leaching Procedure) test for lead.

A number of disadvantages exist for this process in terms of the technical criteria given in Chapter 1 for a potential solution. Firstly, the lead is not recovered but is still disposed to the landfill. Secondly,

this method was reported to be not effective for the matte fraction of the secondary lead slag. This typically forms a significant proportion of secondary lead rotary furnace slag. Thirdly, high temperature processing is required, which would raise operating costs.

Volatilisation of heavy metals

Fuming of a secondary lead slag has been demonstrated by Richards and Oberacker (1992) of the United States Environmental Protection Agency (USEPA) utilising a flame reactor as shown in Figure 1 of Appendix A. Removal and recovery of heavy metals is based on their lower boiling point temperatures.

The high temperatures (>2000^{o}C) at which the flame reactor is operated inevitably mean high operating costs and a high capital expenditure. It is likely that it will only be feasible for central-off site use at large waste management companies, as part of its advantage is that it can be used to render a number of different toxic metallurgical wastes benign. In this case the secondary lead smelter may lose the advantage of the recovery of the lead present in the slag.

Oxidation of a secondary lead matte

Corrick and Sutton (1968) investigated the oxidation of sulphide components in a secondary lead blast furnace matte to sulphates. This was found to occur via the reaction of equation 2 of Appendix A. The authors reported that lead could be recovered from the insoluble lead sulphate formed. They reported that this oxidation reaction could be accomplished by the methods shown in Table 3 of Appendix A.

This is unlikely to be a valid treatment option as the local slag is a combination of slag and matte phases and lead is expected to be predominantly found in the elemental form rather than as lead sulphide.

2.2.3 Treatment processes already investigated on the local refiner's slag

Table 2-1 summarises test work already carried out on the local slag by Pehlken (1997). The main aim of this work was to recover the lead from the slag.

Test	Result obtained
Heavy media separation	Density of common separation liquids was too low. Expensive, high-density liquids are required and the process is slow.
Flotation	No effective concentration in either the froth or tailings was obtained.
Re-melting	No concentration of lead was observable.
Acid leaching	Insufficient lead leached from slag in dilute acids for economic recovery.

Table 2-1 Test work carried out on the local slag by Pehlken (1997)

2.2.4 Undesirable impacts of landfilling the slag

The work done in classifying the local slag as hazardous by virtue of its toxic heavy metal components is summarised in Section 5 of Appendix A. Aqueous sulphide would form if the soluble sulphide components of the slag came into contact with water. Aqueous sulphides are known to have a number

of environmentally undesirable properties. For example, Chen and Morris (1972) report that it is toxic, has a foul odour and imparts strong oxygen-consuming capacity, making it 'an environmental pollutant of considerable importance and concern'.

In addition to the toxic metals and sulphide present in the slag, the following undesirable slag properties can be identified.

- Rapid disintegration of the slag when co-disposed with aqueous waste, causing exposure of the toxic constituents to leaching (Barnes, 1996 and Pehlken, 1997).
- Volume expansion caused when the slag was exposed to atmospheric water vapour, by virtue of the hygroscopic nature of sodium oxide and sodium sulphide (Pehlken, 1997).
- Heat generation on oxidation of ferrous sulphide causes sufficient localised heat generation to ignite elemental sulphur, which is one of its air oxidation products (Queneau *et al*, 1989).
- Production of hydrogen sulphide gas on exposure of ferrous sulphide to acid (Pehlken, 1997).
- Production of highly alkaline leachate in excess of pH 12 on contact with water (Pehlken, 1997).

2.3 The BROSS process

The BROSS process (Bio-Remediation of Sulphidic Slag) was the process that best complied with the process objectives set out in the introduction and therefore was selected for further study. This process was presented by Barnes (1996).

2.3.1 Process objectives

The main objective of Barnes' (1996) study was the evaluation of the potential for bio-oxidation of the sulphides present in the slag to soluble sulphates. The process was found to have potentially the following favourable environmental impacts when implemented on a full scale:

- Recovery of toxic heavy metals, notably lead, which are currently sent to a landfill,
- Reduction of the mass of solids to be landfilled.

The following benefits resulting from the BROSS process would potentially increase refinery efficiency:

- Recovery of lead that would otherwise be lost through disposal of the slag,
- Increase in refinery through-put.

2.3.2 Process background

The BROSS process was developed to treat the slag produced by the H.J. Enthoven & Sons (henceforth known as Enthoven) secondary lead refinery. The Enthoven secondary lead refining operation is similar to that of the local refiner. Both make use of short rotary furnaces and the same furnace feeds are used (Barnes, 1996 and Pehlken, 1997). The composition of the Enthoven slag is given in Appendix B.

The BROSS process takes advantage of the slag's propensity to disintegrate in water. This property has two favourable results. Firstly, a lead rich fraction can be separated from the disintegrated slag, which may be recycled back to the furnaces for increased overall recovery of lead. Secondly, this property exposes the sulphidic component of the slag to extraction via oxidation, thus rendering an insoluble slag product that is more environmentally benign when disposed.

After successful bio-oxidation of the slag sulphides in laboratory scale experiments, a pilot scale plant was built. This was initially a single stage bio-reactor operation. The addition of a 'chemical pre-oxidation' step before the biological oxidation step in a two stage process, was later identified as preferable. This resulted in easier lead separation, higher sulphate production rate and lower acid consumption. The first stage converted the sulphide constituents of the slag to thiosulphate, followed by the further biological oxidation to sulphate in the second stage. The process flow diagram is shown in Figure 2-1.

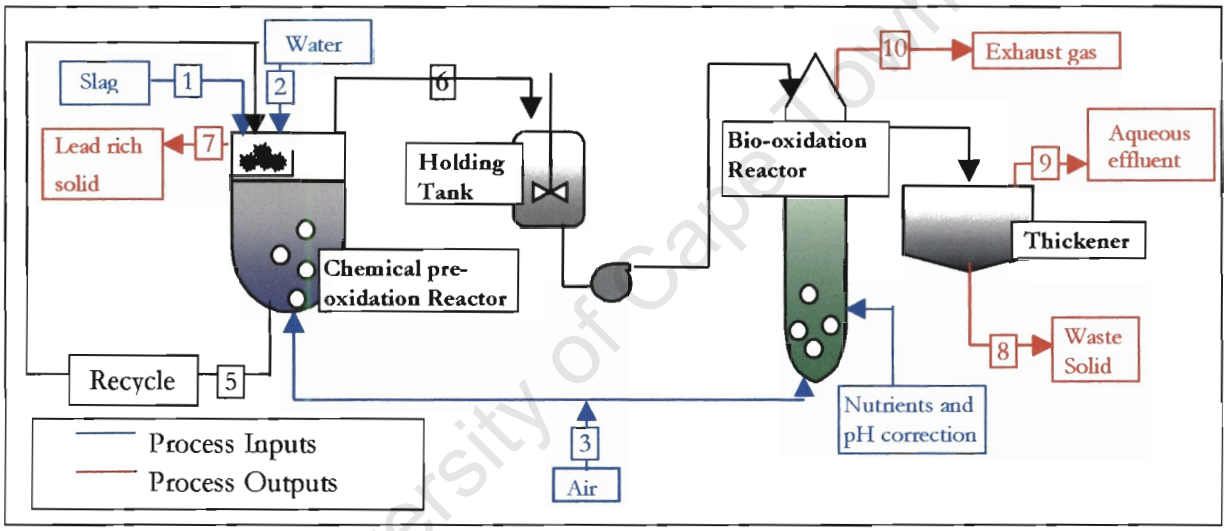

Figure 2-1 Process flow diagram for the two stage BROSS process

2.3.3 Chemical pre-oxidation step

The investigation of this step by Barnes (1996) yielded the following relevant findings.

Disintegration of the slag

Coulson and Richardson (1991) report that disintegration occurs during a leaching operation when the solid contains a relatively large amount of soluble material. The calculated slag composition of Table 2 of Appendix B indicates that soluble sodium compounds of the slag account for over 49 mass-%. Experiments reported by Barnes (1996) to measure the disintegration rate involved suspending roughly litre sized blocks in water and measuring the loss in mass as a function of time. A 203 g block suspended in pumped water completely disintegrated in 4 hours. This was regarded as a feasible disintegration time compared with that required for bio-oxidation; thus this was selected as the approximate size of block required for feeding to the chemical pre-oxidation stage.

Oxidation in air

A sample of the hard black slag was left exposed to atmospheric air. The sample was found by Barnes (1996) to exfoliate and eventually produce a reddish brown powder that was identified as hydrated ferric oxide. Analysis of the solid residue showed that, of the initial sulphur present, 56 % was now found as thiosulphate and 13 % as elemental sulphur, the rest is likely to be remain in sulphide form. This conversion was expected to be a result of FeS oxidation, a reaction known to occur in air.

Oxidation in aqueous solution

In an aqueous solution in the presence of dissolved oxygen, it was found that, not only was the dissolved sodium sulphide converted to thiosulphate, but the sulphide associated with the practically insoluble iron was converted as well. The reaction given by Barnes (1996) for the oxidation of soluble sulphide at raised pH is shown in equation 2-6.

$$2\,S^{2-}_{aq} + 2\,O_2 + H_2O \rightarrow S_2O_3^{2-}{}_{aq} + 2\,OH^- \qquad \text{equation 2-6}$$

Barnes (1996) attributed this unexpectedly high conversion of thiosulphate to the presence of the iron sulphide in the form of soluble $Na_2S.FeS$. Evidence for this compound was found in the green colour of the extract solution under anaerobic conditions (colour of ferrous ions in solution). It was thought that this compound could 'exist transitionally in solution' during the oxidation which would produce thiosulphate via the reaction shown in equation 2-7.

$$4\,Na_2S.FeS + 9\,O_2 + 6\,H_2O \rightarrow 4\,Na_2S_2O_3 + 4\,Fe(OH)_3 \qquad \text{equation 2-7}$$

According to Barnes (1996), the redox – pH diagram predicts that $Na_2S.FeS$ is only formed at a pH of more than 8, which is the condition under which the soluble components of the slag are dissolved. Thus, the conversion of the sulphide associated with the iron at high pH to thiosulphate was attributed to the presence of this compound in solution. However, oxidation in neutral (pH controlled) solutions resulted in the formation of elemental sulphur as an oxidation product of FeS (as found in the case of single stage operation). Barnes (1996) reported a 'near-quantitative conversion' of slag sulphur to thiosulphate in laboratory experiments. The overall mass balance reaction of the chemical pre-oxidation step given by Barnes (1996) is shown in equation 2-8.

$$0.67\,FeS + 0.33\,Na_2S + 0.74\,Na_2CO_3 + 1.17\,O_2 + 1.18\,H_2O \rightarrow 0.50\,Na_2S_2O_3 + 0.67\,Fe(OH)_3 + 0.34\,NaHCO_3 + 0.40\,Na_2CO_3 \qquad \text{equation 2-8}$$

The concentration of reacting species in solution in the chemical pre-oxidation step was given by Barnes (1996), as shown in Figure 2-2, for a run in a pilot scale 5 m^3 air-lift reactor.

Solids separation

A mechanism for separating the insoluble slag components was incorporated into the chemical pre-oxidation reactor. This operation was described as the separation into a "thin suspendable slurry" which was carried over into the biological step and a "dense non-fluidisable thick sludge" (lead rich fraction, recoveries to this fraction shown in Table 2-3). Barnes (1997a) revealed that this separation was caused by the washing of the recycle stream from the reactor over the slag chunks, suspending of

the "thin suspendable slurry" and removing it over the lip of the slag tray. The "dense non-fluidisable thick sludge" was retained in the slag tray.

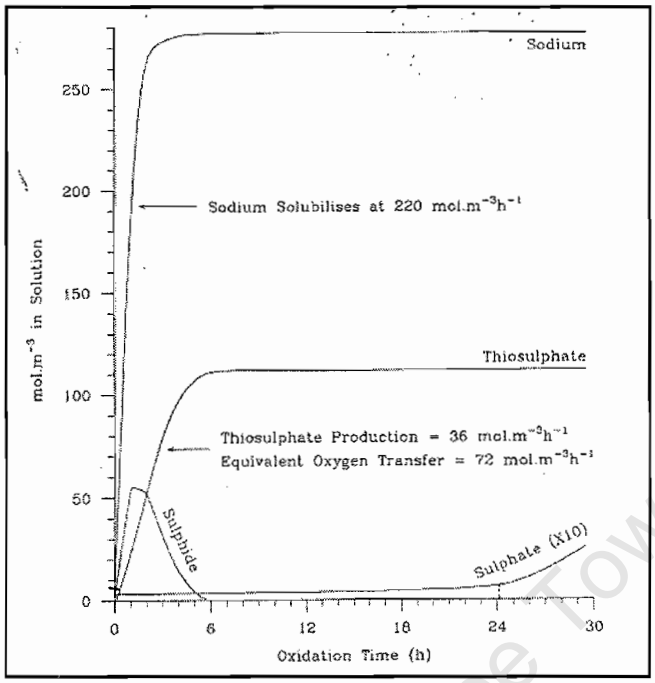

Figure 2-2 Concentration of relevant species in solution for the pre-oxidation step in the 5 m^3 air-lift reactor (reproduced from Barnes, 1996)

2.3.4 Biological oxidation step

The biological oxidation step utilizes sulphur oxidising bacteria to convert thiosulphate to sulphate using a carbonate (present in slag as Na_2CO_3) substrate. This reaction is shown in equation 2-9.

$$S_2O_3^{2-} + 2\,O_2 + H_2O \rightarrow 2\,SO_4^{2-} + 2\,H^+ \qquad \text{equation 2-9}$$

Bio-reactor conditions

The following parameters are important for bio-reactor operation and are affected by the aqueous effluent of the chemical pre-oxidation step.

Nutrients

The carbon substrate that is required by the sulphur oxidising bacteria for growth is carbon dioxide. No addition of this substrate was required, as an appreciable quantity of carbonate was present in the Enthoven slag, from which carbon dioxide is liberated.

pH

The bacteria require a neutral pH for optimal growth. The bacteria could survive pH variations in the range 5 – 9.5. The oxidation rate was lowered when the solution pH deviated from neutrality.

Inhibition caused by the slag concentration

Sulphide oxidation rates were considerably reduced when the slag concentration was increased from 50 g/l to 100 g/l. The explanation given by Barnes (1996) was that the bacteria were inhibited by the increasing ionic strength.

Temperature

The bacteria were found to grow well at 50 °C, but were killed at 55 °C. This parameter is important due to the exothermic nature of the sulphur oxidation. Thus, the bio-reactor needs to be designed to ensure the higher temperature is not reached. The bacteria were tolerant of temperatures as low as 10 °C.

Requirement for acid or alkali addition

An important factor in the operational cost was found to be the sodium to sulphur mole ratio of the feed slag. Deviation from this required either acid addition in the form of sulphuric acid or alkali in the form of sodium hydroxide. A molar ratio of 2 mole sodium to 1 mole sulphur does not require addition of these reagents. A ratio of less than 2 means sodium hydroxide had to be added, and more than 2 required addition of sulphuric acid.

2.3.5 Pilot plant results

The results of two stage operation for a short residence time (>20 hours) are presented in Table 2-2. The feed slag was slurried together with water in the chemical pre-oxidation step at a solid to liquid ratio of 50 g slag /l. This solid to liquid ratio was found to be optimal based on the energy balance for the bio-reactor (temperature must be below 55 °C) and the ionic strength limitation.

	Input stream [g]	Output streams [g]		
Stream Name	Feed slag	Lead rich solid	Waste solid	Aqueous effluent
Stream number (from Figure 2-1)	1	7	8	9
Total mass of solids	1000	270	290	
Sulphide	172	-	14	-
Sulphate	-	-	-	154
Sulphur	-	4	-	-
Sodium	224	6	<0.1	218
Iron	162	39	123	<0.01
Lead	68	61	7	<0.01
Zinc	9.1	0.7	8.4	0.01

Table 2-2 Mass balance over BROSS process pilot plant (Barnes, 1996)

BROSS process product streams

Waste solid

The waste solid fraction (29% of feed slag) consisted almost entirely of the insoluble fluidisable components from the chemical pre-oxidation stage. The major component was reported to be ferric hydroxide (approximately 80%) and a small quantity of heavy metals (less than 7%). This waste is fully oxidised and described by Barnes (1996) as being benign. Barnes (1996) estimated that as much as 80% of this stream could be recycled to the furnace. However, an accumulation of elements present in this fraction such as silicon, barium and aluminium may occur as a result. If this recycle was not possible, Barnes (1996) estimated that about 8000 tons of this stream would have to be sent to landfill each year (maximum annual slag production at Enthoven is 16000 tons per annum).

Aqueous effluent

This stream was reported to contain approximately 40 g/l of sodium sulphate, less than 200mg/l suspended solids and approximately 5 mg/l of heavy metals.

Lead rich solid

This insoluble slag fraction was separated from the "fluidisable" waste solid in the chemical pre-oxidation reactor. The percent recoveries of feed slag elements to this fraction is given in Table 2-3. The most important recovery is that of lead, 90% of which was recovered to this fraction, which accounted for 27% of the mass of the original slag. All percentages are mass percentages.

Total Mass Recovery	Sulphur Recovery	Lead Recovery	Zinc Recovery	Sodium Recovery	Iron Recovery
27%	2%	90%	8%	3%	24%

Table 2-3 Recoveries of feed slag components to lead rich solid stream (Barnes, 1996)

2.3.6 Evaluation of BROSS process results with respect to the technical criteria

Production of a less environmentally hazardous slag

Pilot scale demonstration showed that approximately 90% of the toxic lead component of the slag was removed from the solid waste to be disposed. The soluble sulphide component was extracted from the slag and converted into more environmentally benign sulphate form. Thus, the BROSS process accomplished criterion 2 identified in section 1.2.

Recovery of the lead content of the slag for recovery to the furnace

As reported above, 90% of the lead present in the slag fed to the pilot plant was recovered. This fraction can be recycled back to the furnace, thus increasing overall lead recovery for the secondary refinery.

Reduction of the quantity of slag to be disposed

The pilot plant results indicate that the reduction in mass of solid waste to be disposed lies between 73% and 50%, depending on the amount of the waste solid stream that can be recycled back to the furnace. Thus, a reduction is achieved in the quantity of slag to be disposed. This reduction in slag mass due to the removal of the soluble components must be weighed against the generation of an aqueous waste stream. The quantity of waste solid recycled back to the furnace must be weighed against the problems caused by accumulation of certain components in this recycle loop.

2.3.7 Economic Evaluation

The mild operating conditions and low reagent cost indicates that the BROSS process could potentially have a lower operating cost than thermal slag treatment processes. Barnes (1997b) reported a "Ball park profit estimate" for the BROSS process (based on the Enthoven Smelter producing 16 000 tons slag per annum) of R1.24m per year, including the capital cost of R1.5 m per year (split over 10 years). Although many assumptions were made in obtaining this figure, it does indicate the possibility that the BROSS process may be able to pay for itself, rather than be an additional refinery expense.

2.3.8 Requirement for further investigation

Chemical pre-oxidation reactor

Barnes (1997a) revealed that, while the biological step of the pilot plant was well understood and optimally designed, less design effort and process investigation had been made for the chemical pre-oxidation reactor. The latter reactor was not purpose built for this step and was added to the process only during pilot plant studies when it became clear that a two-stage operation was preferred. The local refiner's slag will need to be treated at an approximate rate of 1416 kg/hr compared to 33 kg/hr treated by the pilot plant. Thus, to avoid excessive capital expenditure in terms of the reactor volume required (if this process is to be implemented at full-scale) a greater understanding of the processes that occur in this reactor is required. Further investigation of this step is the subject of the rest of this study. The step of the BROSS process that is achieved in the chemical pre-oxidation reactor (with the exception of solids separation that was carried out in that reactor in the Enthoven pilot plant) will henceforth be known as the leach – oxidation step.

Disposal of aqueous effluent stream

Barnes (1997a) reported that disposal of the sulphate rich stream was one of the major stumbling blocks to full-scale implementation of the BROSS process at the Enthoven refinery. Barnes (1996) surveyed a number of alternatives to solve this problem. The best solution was seen to be the discharge of the effluent to the local river. It was calculated that this would not raise the river sulphate level above the allowable EC potable water limit of 250 mg/l sulphate.

Local South African regulations are unlikely to allow 40 g/l sulphate in aqueous effluent discharges. This precludes the possibility of disposing this effluent directly to the sewers. Thus, an investigation into the further treatment required for the aqueous effluent is necessary. One possible solution is to

utilize crystallisation; this is a costly operation as noted by Barnes (1996), but does potentially result in a saleable product (sodium sulphate).

Solids separation operation

The separation of the lead rich solid fraction from the "suspendable slurry" is another operation that is likely to benefit from additional investigation. The separation using a simple tray apparatus was shown to achieve a high recovery of lead (90 %) in the non-fluidisable solids (lead rich solid). However, the optimisation of this step may allow an even greater concentration of lead in this product fraction. Also, it is unlikely that a tray would suffice for the greater slag feed rate of a full-scale operation.

2.4 Review of individual processes occurring during leach – oxidation

2.4.1 Leaching of soluble slag components

This section presents the solubilities of the slag components relevant to leach – oxidation, the conditions that affect this leaching process and a theoretically predicted rate equation.

Solubility of slag components

Table 2-4 presents the solubilities of the compounds relevant to leach – oxidation that may be found in the slag.

Compound	Formula	Cold water		Hot water	
		Solubility [mg/l]	Temperature [°C]	Solubility [mg/l]	Temperature [°C]
Sodium Sulphide	Na_2S	1.54×10^5	10 °C	5.73×10^5	90 °C
Sodium Oxide	Na_2O	Forms NaOH in water (Perry and Green, 1984) via the following reaction: $Na_2O + H_2O \rightarrow 2\,NaOH$			
Sodium Hydroxide	NaOH	4.2×10^5	0 °C	3.47×10^6	100 °C
Sodium Carbonate	Na_2CO_3	7.1×10^4	0 °C	4.55×10^5	100 °C
Sodium Chloride	NaCl	3.57×10^5	0 °C	3.98×10^5	100 °C
Sodium Silicates	Na_2SiO_3 Na_4SiO_4 $Na_2SiO_3.9H_2O$	Soluble		Soluble	
Sodium Phosphate	Na_3PO_4	4.5×10^5	0 °C	7.7×10^6	100 °C
Ferrous Sulphide	FeS	6.2	18 °C	Decomposes	
Ferrous Oxide	FeO	Insoluble		Insoluble	
Lead	Pb^0	Insoluble		Insoluble	
Lead (II) Sulphate	$PbSO_4$	2.80×10^2	0 °C	5.6×10^2	40 °C
Silica	SiO_2	Insoluble		Insoluble	

Table 2-4 Equilibrium slag component solubilities (reproduced from Perry and Green, 1984)

Sodium compounds

It can be seen from Table 2-4 that the equilibrium solubilities for the sodium compounds in water are high. It is evident that none of the sodium compounds would reach their solubility limit if the BROSS process slag mass concentration was used (5×10^4 mg/l). Thus, all sodium compounds present in the slag should dissolve completely. This statement assumes that all sodium compounds are exposed to leaching. For all the sodium compounds, the equilibrium solubility is raised by increasing temperature, as indicated by Table 2-4 for hot water (90 °C -100 °C).

Ferrous sulphide

Table 2-4 indicates that ferrous sulphide (FeS) is virtually insoluble under neutral conditions. It is also virtually insoluble under alkaline conditions but soluble under acidic solutions. Thus, the finding by Barnes (1996) that under aerobic conditions, dissolution of the slag initially produces a dark green solution with 20 mg/l of iron is unexpected. The solubility product limit should cause the iron concentration to be significantly less than the 6.2 mg/l of Table 2-4 due to the presence of significant quantities of sulphide during slag dissolution. This is a result of the common ion effect. The reason for this unexpectedly high dissolved iron concentration can be explained by the presence of another compound containing iron and sulphide with a greater solubility than ferrous sulphide. This provides a source of evidence for the existence of the $Na_2S.FeS$ double compound in the Enthoven slag.

$Na_2S.FeS$

Freeman (1925) observed that the smelting of mixed sulphide ores resulted in eutectic mixtures of double sulphides with sodium sulphide. In certain double sulphides, including $Na_2S.FeS$, the sparingly soluble sulphide, in this case FeS, displayed increased solubility compared to when it existed alone. When Freeman (1925) dissolved a small quantity of $Na_2S.FeS$ in water, a green colour resulted. This was assumed to be caused by ferrous iron in solution. Freeman (1925) observed that, after 20 hours, no sulphide was left and a ferric hydrate precipitate had been formed. When dissolved in water in the presence of air, the double sulphide was broken down rapidly into freely soluble sodium sulphide and an insoluble iron sulphide, which made up an extremely fine colloidal suspension.

Conditions affecting the leaching rate of soluble components

Both Coulson and Richardson (1991) and Wakeman (1994) identify the following four process parameters as the most important factors affecting the rate of leaching.

Particle size

Increasing particle size can potentially reduce the leaching rate for two reasons. Firstly, if the extraction rate is limited by the diffusion of solutes out through the remaining insoluble porous structure (pore diffusion), then particle size will be the rate controlling parameter. Decreasing the particle size will reduce the distance that the solute is required to diffuse through, thus increasing the extraction rate.

Secondly, decreasing the particle size increases the specific solid – liquid interfacial area, thus increasing the rate of solute mass transfer. This would be a factor prior to the slag chunks disintegrating. However, once disintegration is complete, the surface area available for leaching is expected to be independent of the starting size.

Solvent

The use of water for the BROSS process is an obvious choice. Among its numerous advantages is the fact that it allows the separation and removal of the sulphide components (via leaching) from the lead component, which remains insoluble.

Temperature

The temperature of the solvent may affect the overall quantity of slag extracted as increased temperature leads to higher solubility of most compounds. The rate of extraction is also increased by

Temperature

The temperature of the solvent may affect the overall quantity of slag extracted as increased temperature leads to higher solubility of most compounds. The rate of extraction is also increased by raising the solution temperature, due to an increase in the value of the diffusion coefficient. The temperature dependence of the diffusion coefficient is given by Jackson (1986) in equation 2-10.

$$D_{AB} = D_{AB,0} e^{\frac{-E_A}{RT}}$$ equation 2-10

Where:			
	D_{AB}	diffusion coefficient	[m²/s]
	$D_{AB,0}$	diffusion constant	[m²/s]
	E_A	activation energy	[J/mol]
	R	gas constant	[J/(K.mol)]
	T	temperature	[K]

Jackson (1986) reported that diffusion processes have low activation energies (approximately 20 kJ/mole) in comparison with chemical reaction activation energies (typically > 40 kJ/mole). This results in the increase of the diffusion coefficient with increasing temperature being smaller than the increase in the chemical reaction constant. This allows the identification of a diffusion-controlled process.

Agitation of the fluid

The local turbulence caused by agitation of the solvent increases the rate of convective mass transfer from the surface of the particles to the bulk solution. This is as a result of the reduction of the boundary layer thickness surrounding the slag particles. A decrease in boundary layer thickness reduces the length of the diffusion path that provides resistance to mass transfer. According to Jackson (1986), vigorous agitation can increase the leaching rate by up to 50 times. In the absence of agitation, the boundary layer thickness was reported as being typically about 0.5 mm. However, in a vigorously stirred solution this may be as little as 0.01 mm.

Leaching rate equation

The rate of mass transfer through the diffusion boundary layer is given by Fick's first law in equation 2-11.

$$\frac{dn}{dt} = -D_{AB} A \frac{dc}{dr}$$ equation 2-11

Where:			
	D_{AB}	diffusion coefficient	[m²/s]
	A	surface area available for mass transfer	[m²]
	c	molar or mass concentration	[mol/m³ or kg/m³]
	r	radius	[m]
	n	moles or mass	[mol or kg]
	t	time	[s]

If a linear concentration profile for the diffusion layer surrounding the particle is assumed, and the volume of the solution remains constant, then equation 2-12 can be derived for the rate of accumulation of leached solute in the bulk liquid phase.

$$\frac{dC}{dt} = \frac{D_{AB}A}{\delta.V}(C_{S,MAX} - C) \qquad \text{equation 2-12}$$

Where	C	concentration of solute in the bulk liquid at t	[mol/m³ or kg/m³]
	$C_{S,MAX}$	maximum concentration of solute in the bulk liquid	[mol/m³ or kg/m³]
	δ	boundary layer thickness	[m]
	V	volume of solution	[m³]

The error in assuming a linear concentration gradient is minimised as the boundary layer thickness is reduced. However, according to Jackson (1986), at the high agitation rates that make this possible, the direct proportionality dependence of the rate on the diffusion coefficient often does not hold. This is particularly the case when turbulent flow around the particles is induced, but also for some cases of laminar flow. Therefore, a leach rate constant is often used to encompass the diffusion, area and boundary thickness terms in equation 2-12. Another advantage of this grouping is that often these terms often cannot be determined separately, so the mass transfer coefficient encompasses these effects and is determined experimentally. Thus, equation 2-12 can be represented by equation 2-13, which is general as it applies to all flow conditions.

$$\frac{dC}{dt} = k_L(C_{S,MAX} - C) \qquad \text{equation 2-13}$$

Where: k_L leach rate constant [m/s]

The maximum sulphide concentration term in equation 2-13 is usually the equilibrium solubility of the component of interest at the solution temperature. However, for this study, the component that is of interest, sulphide, would not attain its maximum equilibrium solubility in the leaching solution at the slag mass concentration of the BROSS process (50 g/l) even in the absence of oxidation. For the integrated form of equation 2-13 to hold (shown below as equation 2-14), at infinite time $C_{S,MAX}$ would have to equal C_S. Thus, for the leach – oxidation step, $C_{S,MAX}$ must be equal to the maximum sulphide solution concentration when all possible soluble sulphide has leached, and not the maximum solubility of this component in water.

$$\ln\left(\frac{C_{S,MAX}}{C_{S,MAX} - C}\right) = k_L t \qquad \text{equation 2-14}$$

The equation predicting the sulphide leaching rate (where $C = C_S$, the concentration of sulphide in the solution), assumes that sulphide is not being depleted from the solution, as is the case during leach – oxidation, via oxidation. Therefore when sulphide is depleted by oxidation, $C_{S,MAX}$ would not equal C_S at infinite time and the equation would still not hold. Thus, in place of the solution sulphide concentration, C_S, the term used will be the sulphide concentration as if no oxidation had taken place, C_{ST}. Thus, the leaching equation that should be used is given in equation 2-15. In the absence of oxidation C_{ST} is equal to C_S.

$$\frac{dC_{ST}}{dt} = k_L(C_{S,MAX} - C_{ST}) \qquad \text{equation 2-15}$$

Where: C_{ST} total mass concentration of sulphide that has leached at t [mol/m³ or kg/m³]

An important assumption in this first order equation is that all of the soluble sulphide that can potentially leach, i.e. $C_{S,MAX}$, is available and exposed to leaching from the onset. Unless disintegration of the slag is rapid, this assumption would not hold.

2.4.2 Oxidation of soluble sulphide by dissolved oxygen

Sulphide species present

In the leach – oxidation step, sulphide in solution is a result of the dissolution of the soluble sulphide components of the slag. These components potentially include the $Na_2S.FeS$ double sulphide and Na_2S if this compound is found separately. The form of the sulphide ion found in solution has been found to be highly dependent on the pH of the solution. Table 2-5 gives the calculated pH regions of predominance of each of the three forms of the sulphide ion, at 25 °C.

Sulphide species	pH range of predominance
H_2S	0 – 7
HS^-	7 – 14
S^{2-}	> 14

Table 2-5 pH dependence of sulphide species (Garrels and Naester, 1958)

In this investigation, the form of the sulphide ion present under leach – oxidation conditions is of interest. Barnes (1996) reported that leach – oxidation of the Enthoven slag occurred at pH > 11 and Pehlken (1997) reported that the local slag forms a solution of approximately pH 12. Thus, it is evident that the predominant sulphide species in solution will be the HS^- ion.

The dependence of the rate and products of sulphide oxidation on the pH of the reaction solution is well documented and is discussed further in the remainder of Section 2.4.2. This pH dependence is thought to result primarily from the form of sulphide ion present (Zhang and Millero, 1993).

Products of sulphide oxidation reaction

Effect of pH on oxidation product distribution

The most common oxidation products found in the pH region of HS^- predominance are thiosulphate, sulphite and sulphate. These were the main observed products in the investigations of Chen and Morris (1972), Cline and Richards (1969), Alferova and Titova (1969) and O'Brien and Birkner (1977). Elemental sulphur was also observed by investigators. However, Chen and Morris (1972) reports that sulphur is only formed in appreciable concentrations at pH less than 8, above which it is thermodynamically not favoured to form. Lefers *et al* (1978) preclude the possibility of sulphur and polysulphides forming at pH values greater than 9.

At a solution pH greater than 8.5, Chen and Morris (1972) found that thiosulphate is the principal oxidation product, regardless of sulphide to oxygen ratio. No appreciable conversion to sulphate was found to occur within the period of observation. The other oxidation product formed was sulphite. The relative proportion of thiosulphate compared to sulphite formed became larger with increasing pH. Alferova and Titova (1969) also found that thiosulphate is the principal oxidation product for the pH range 7 – 13.75. However, sulphite was observed as an intermediate species which was oxidised completely to sulphate within the observed reaction period of 7 h, at which time the sulphur species present were 68% thiosulphate and 32% sulphate for a starting pH of 11.38. This difference in

results may have been a result of the high initial sulphide concentration (1200 mg/l), which is approximately 1000 times higher than the other studies presented here.

At pH 12.1, Avrahmi and Golding (1968) reported the products of oxidation after 35 h are 30 % sulphate and 40 % thiosulphate, based on sulphide consumed. The rest of the initial sulphur was unaccounted for, except that occasionally a milky precipitate was detected which was presumed to be colloidal sulphur. O'Brien and Birkner (1977) studied product distribution between pH 8.1 to 10.7. Over this range the thiosulphate increased from 34% to 46% of initial sulphide, but sulphite decreased from a maximum of 22.3 % at pH 9.8 to 17.8 % at pH 10.7.

These experimental observations are confirmed thermodynamically by the Eh-pH diagrams of Figure 2-3 and Figure 2-4. Figure 2-3 indicates the sulphur species stable at equilibrium, under various conditions of pH and redox potential, while Figure 2-4 indicates the metastable oxidation product species. Metastable species are those which are not the final stable equilibrium species, but are stable under the prevalent conditions for a relatively long period of time before being converted to the equilibrium stable species. Peters (1976) describes the metastable Eh – pH plot as "an artificial way to bring the descriptive thermodynamics into agreement with observations that contain only the rapidly obtained equilibria".

In Figure 2-3 it can be seen that elemental sulphur will only be a predominant oxidation species for pH values less than 8, as was determined experimentally by Chen and Morris (1972). Comparison of Figure 2-3 and Figure 2-4 indicate that at pH values above 8, the equilibrium stable oxidation species of sulphide is sulphate. However, the metastable oxidation species are thiosulphate and sulphite.

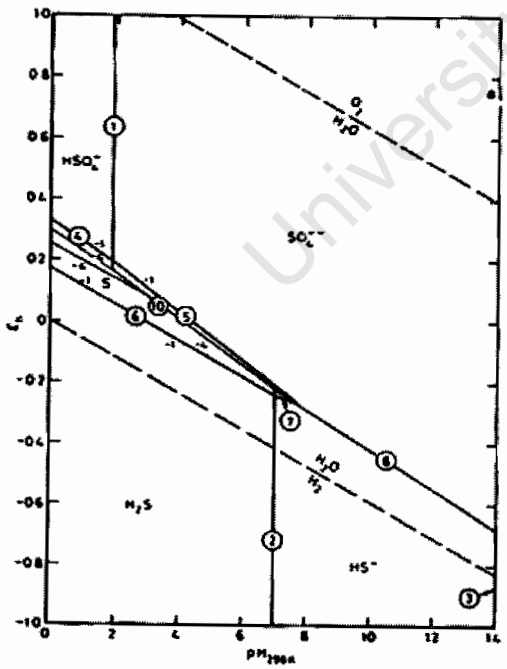

Figure 2-3 Equilibrium Eh – pH diagram for sulphur water at 25 °C (reproduced from Ferreira, 1975)

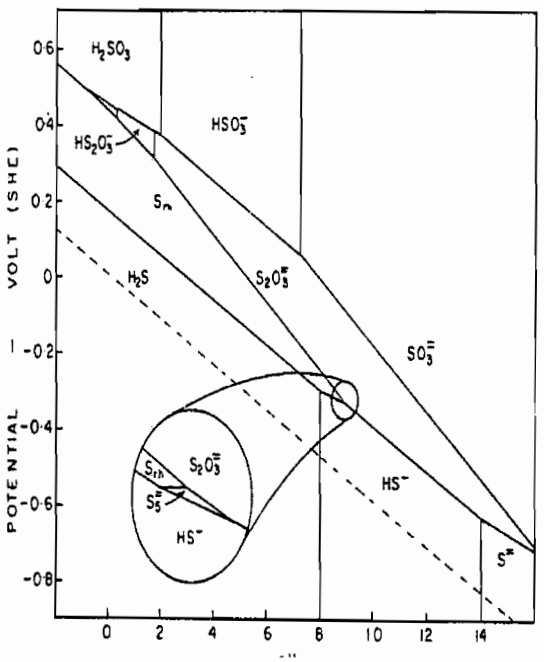

Figure 2-4 Metastable Eh – pH diagram for sulphur water at 25 °C (reproduced from Peters, 1976)

Effect of catalysis on product distribution

Cline and Richards (1969) found that, in the presence of Fe^{2+} ions, the majority of the sulphide (82 %) was converted to thiosulphate, the rest being attributed to elemental sulphur and sulphate, but not to sulphite, a product found in experiments without Fe^{2+} catalysis. Only 30 % – 35 % of the initial sulphide was converted to thiosulphate in experiments containing no Fe^{2+} catalyst.

Effect of redox potential on product distribution

The metastable Eh – pH diagram (Figure 2-4) indicates that the solution redox potential in the basic pH region plays an important role in determining the distribution of the metastable thiosulphate and sulphite oxidation products. A lower solution redox potential favours thiosulphate rather than sulphite. The greater oxidation number of the sulphur atom of sulphite (+8) compared to thiosulphate (+4) explains this finding.

Influence of reaction time on oxidation product distribution

In low pH solutions, the oxidation of sulphide to sulphite is a relatively slow process compared to the further oxidation of sulphite to sulphate. Thus, sulphite remains at low concentration and sulphate is the main oxidation product. However, at high pH, the oxidation of sulphide to the intermediate oxidation compounds, sulphite and thiosulphate, is relatively fast compared to the removal of these as the equilibrium oxidation product, sulphate, and their concentrations can build up significantly (Zhang and Millero, 1993).

The oxidation of thiosulphate to sulphate was found to be very slow. Thiosulphate exists in solution as a relatively stable species for a number of days before being converted. Zhang and Millero (1993) found that in the absence of bacteria, little thiosulphate oxidation occurs over the first 80 hours of the reaction, while Avrahmi and Golding (1968) report a half life for thiosulphate in solution of 8 days. The reaction of sulphite to sulphate is reported to be comparatively fast by Avrahmi and Golding (1968). However, Chen and Morris (1972) report that the rate of oxidation of sulphite in a sulphide containing solution is inhibited, proceeding much slower than in the absence of sulphide.

Reaction scheme for sulphide oxidation

Many authors have noted that the mechanism for sulphide oxidation at high pH values is complex [Chen and Morris (1972), Lefers *et al* (1978), Zhang and Millero (1993)]. For this reason, many investigators examined the reaction only with respect to the rate at which sulphide is depleted, without determining the reactions by which the oxidation products are formed. As the reaction was mostly being studied for environmental reasons, the rate of sulphide depletion that was of prime importance. The reaction schemes of the authors who did attempt this analysis in the pH region where HS^- is dominant are presented in this section.

Avarahmi and Golding (1968) investigated the reaction over pH range 11 – 13 and initial sulphide concentration of 10^{-3} M to 10^{-4} M and proposed the reaction scheme shown in equation 2-16.

1. $HS^- + 3/2\ O_2 \rightarrow SO_3^{2-} + H^+$ (rate determining step)
2. $SO_3^{2-} + 1/2\ O_2 \rightarrow SO_4^{2-}$ (rapid)
3. $SO_3^{2-} + HS^- + 1/2\ O_2 \rightarrow S_2O_3^{2-} + OH^-$ (rapid)

4. $S_2O_3^{2-} + 1/2\ O_2 \rightarrow SO_4^{2-} + S^0$ (very slow) equation 2-16

In this model, sulphite is the hypothesised intermediate between sulphide and thiosulphate, and the initial oxidation to sulphite (reaction 1) is the rate determining step. According to the authors, the sulphite is then instantaneously removed as either thiosulphate, via reaction 2, or sulphate via reaction 3. From the previous section it is clear that, especially at high pH values, sulphite is present in the solution for long periods of time and not instantaneously removed, contradicting the relative reaction rates described in this investigation.

O'Brien and Birkner (1977) proposed another reaction scheme for the sulphide oxidation reaction (equation 2-17). This was determined from experiments in a mildly alkaline solution (pH 7.55), but the dominant sulphide species, HS^-, was the same as at higher pH values.

1. $S^- + 3/2\ O_2 \rightarrow SO_3^{2-}$
2. $SO_3^{2-} + 1/2\ O_2 \rightarrow SO_4^{2-}$
3. $2\ S^- + 3/2\ O_2 \rightarrow S_2O_3^{2-}$
4. $S^- + 2\ O_2 \rightarrow SO_4^{2-}$ equation 2-17

By this mechanism, sulphide can either be oxidised to sulphite (reaction 1), thiosulphate (reaction 3) or straight to sulphate (reaction 4). Sulphite is further oxidised to sulphate via reaction 2. However, the further oxidation of thiosulphate to sulphate is discounted as insignificant over the typical reaction period observed (500 minutes). O'Brien and Birkner (1977) report that this reaction model was hypothesized based on an exhaustive process of fitting the model to experimental data, "many different combinations of simple bimolecular reactions were tested. Parallel and consecutive reaction sequences were investigated".

The reaction schemes of equation 2-16 and equation 2-17 differ in that O'Brien and Birkner (1977) do not account for the reaction of sulphide with sulphite. Teder and Wilhelmsson (1975) found that this reaction did not occur at pH values greater than 8 in a solution of ionic strength of 3 M and pH 7 in the case of a lower 0.5 M ionic strength solution. Heunisch (1977) also found that, at pH values above 10.68, no thiosulphate product was observed, indicating that the reaction does not proceed.

This finding corresponded to the reaction scheme of Cline and Richards (1969) shown in equation 2-18. They investigated sulphide oxidation at pH 7.5 – 7.8 in sea water.

1. $2HS^- + O_2 \rightarrow S^o + 2OH^-$
2. $2HS^- + 2O_2 \rightarrow S_2O_3^{-2} + H_2O$
3. $2HS^- + 3O_2 \rightarrow 2SO_3^{-2} + 2H^+$
4. $HS^- + 2O_2 \rightarrow SO_4^{-2} + H^-$ equation 2-18

Other studies showed that, at higher pH values (>9), reaction 1 does not occur and reaction 4 occurs extremely slowly. An important finding relevant to this investigation, by Cline and Richards (1969), was that in the presence of Fe^{2+} (a catalyst), sulphide was directly oxidised to thiosulphate by reaction 2 of equation 2-22 and reaction 3 did not occur significantly.

From the reaction schemes proposed in this section, it appears that, at high pH values, the dominant reactions are the sulphide oxidation reactions to thiosulphate and sulphite (reactions 2 and 3 of Cline and Richards (1969) and 3 and 1 of O'Brien and Birkner (1977) respectively). However, in the presence

of Fe^{2+}, sulphide was found to oxidize directly to thiosulphate, and the oxidation reaction to sulphite was suppressed (Cline and Richards, 1969).

Reaction kinetics

The complex sulphide oxidation reaction scheme resulted in virtually all authors fitting a kinetic model to the depletion rate of sulphide rather than the production rate of oxidation products. These authors (listed in Table 2-6) were successful in fitting their experimental data to an exponential rate law equation in the form of equation 2-19. Wilmot *et al* (1988) also successfully applied a Michaelis-Menton rate law to their data.

$$\frac{dC_S}{dt} = -k \cdot C_S{}^m C_{O_2}{}^n \qquad \text{equation 2-19}$$

Where:			
	k	rate constant	$[m^3/(mol^{n+m-1}.s)$ or $m^3/(kg^{n+m-1}.s)]$
	C_S	sulphide concentration at t	$[mol/m^3$ or $kg/m^3]$
	C_{O_2}	dissolved oxygen concentration at t	$[mol/m^3$ or $kg/m^3]$
	m	order with respect to sulphide	-
	n	order with respect to oxygen	-

The authors listed in Table 2-6 calculated the reaction orders using either an integration method or initial rate method. For the integration method, orders are assumed and it is determined whether a linear fit is obtained. For the initial rate method, the orders are calculated by evaluating the initial rate at a certain known initial concentrations. When two reactants affect the rate of the reaction, as is the case for the sulphide oxidation reaction, the orders can be calculated by holding the concentration of one species constant while varying the concentration of the other species. This method examines the effect of each individual reactant on the reaction rate independently and therefore is better for complex reactions where the orders are not integer values, as is the case for the sulphide oxidation reaction.

Table 2-6 gives published reaction orders determined using the rate law of equation 2-19 and the conditions under which they were obtained.

Source	Medium	pH	Temperature [°C]	Sulphide concentration [mg/l]	Oxygen concentration [mg/l]	Reaction orders		Technique
						m	*n*	
O'Brien and Birkner (1977)	Buffered Na_2S solution	4.1	25	0.32 – 3.2	32	1		Integration
		7.55	25	0.70 – 3.9	6.6 – 3.4	1.02	0.80	Initial Rate
		10	25	0.32 – 3.2	32	1		Integration
Chen and Morris (1972)	Buffered Na_2S solution	6.9 – 11.75	25°C	1.6 – 6.4	5.1 – 26.5	1.34	0.56	Initial Rate
Lefers *et al* (1978)	Buffered Na_2S solution	9.7	48.5			1.61	0.52	Initial Rate
		12	48.5	70 - 290	27	1.47	0.55	Initial Rate
Wilmot *et al* (1988)	Wastewater	7.0	20 ± 2 °C	1.0	12 – 20	0.6 – 0.8	0.12 - 0.32	Initial Rate
				6.0		1.0 – 1.2		Initial Rate

Table 2-6 Published reaction orders for the sulphide oxidation reaction exponential rate law

Table 2-6 shows that the investigators did not achieve agreement on the calculated values of the reaction orders. This is indicative of the variation in the reaction mechanism, as was found in the previous section. A major factor causing this variation in mechanism was shown to be pH. However, the orders determined by Chen and Morris (1972) remained virtually constant over the pH range investigated (6.9 – 11.75). In the case of sulphide this was 1.34 and for oxygen this was 0.56. These values are in reasonable agreement with the pH 12 orders of Lefers *et al* (1978), which were also determined by the initial rate method. Lefers *et al* (1978) found that the orders did not remain constant for a changing pH, as shown in Table 2-6. At pH 12, Lefers *et al* (1978) calculated a sulphide order of 1.47 and an oxygen order of 0.55. The reaction orders are independent of temperature, thus the different temperatures at which the orders were evaluated should not affect their values. Thus, at the high pH (> 11) the orders of Chen and Morris (1972) or Lefers *et al* (1978) are the most likely to hold of those reviewed.

Parameters affecting the sulphide oxidation rate

pH

In the sections above it was shown that pH plays a large role in the product distribution, reaction mechanism, reactant orders and the species of sulphide present. Therefore it is not surprising that the rate of the sulphide oxidation reaction is highly dependant on the solution pH. This dependence is best illustrated by Figure 2-5, in which the rate constant (determined by the rate of oxygen uptake) is plotted against pH (Chen and Morris, 1972).

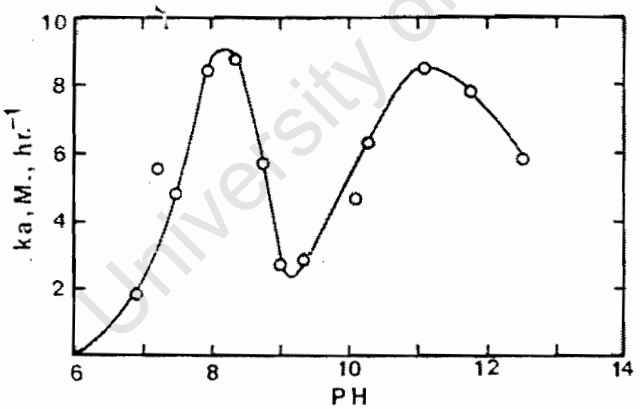

Figure 2-5 Dependence of rate constant on pH (reproduced from Chen and Morris, 1972)

Figure 2-5 shows that the dependence is complex. In the HS- region a maximum rate constant is reached at pH 8 and another at pH 11, followed by a decrease as the pH is raised above 11.

Temperature

The reaction rate law term that is a function of temperature is the rate constant. The rate constant is predicted to increase exponentially with an increase in temperature by the Arhennius law, shown in equation 2-20.

$$k = k_0 e^{\frac{-E_A}{R.T}}$$

equation 2-20

Where:			
	k	reaction rate constant	[$m^3/(mol^{n+m-1}.s)$ or $m^3/(kg^{n+m-1}.s)$]
	k_0	frequency factor	[$m^3/(mol^{n+m-1}.s)$ or $m^3/(kg^{n+m-1}.s)$]
	E_A	reaction Activation Energy	[J/mol]
	R	ideal Gas constant	[J/(K.mol)]
	T	reaction temperature	[K]

Table 2-7 gives the rate constants, published for the sulphide oxidation reaction, for rate law equations in the form of equation 2-19 in the units they are reported. Table 5.4-10 of Section 5.4.3 gives the results of the conversion of these rate constants into a unit by which they can be compared to the experimental results.

Author	Experimental Conditions			Value of rate constant	Units of rate constant
	pH	Temperature	Catalyst		
Lefers *et al* (1978)	12	48.5 °C	None	0.103	$M^{-1.02}.l^{1.02}.s^{-1}$
Chen and Morris (1972)	11.10	25 °C	None	22.20	$M^{-0.9}.h^{-1}$
	11.75	25 °C	None	19.42	
	12.50	25 °C	None	15.45	
O'Brien and Birkner (1977)	7.55	25 °C	None	86.4	$M^{-1}.h^{-1}$
Zhang and Millero (1993)	8.0	25 °C	None	3.0	$M^{-1}.h^{-1}$
	8.0	25 °C	Fe^{2+}	179	
	10.0	25 °C	None	4.2	

Table 2-7 Published literature rate constants for the sulphide oxidation reaction

Catalysis

Zhang and Millero (1993) report that Fe^{2+} is an effective catalytic agent in the oxidation of sulphide. The effect of Fe^{2+} catalysis on the rate constant can be seen from the pH 8 results of Zhang and Millero (1993) in Table 2-7, where the rate constant is increased approximately 60 times by the presence of Fe^{2+}. Cline and Richards (1969) also observed Fe^{2+} catalysis, but could not determine whether this catalysis occurred solely heterogeneously (solid phase catalysis) or homogeneously (aqueous phase catalysis), as the initially dissolved Fe^{2+} ions were found in the solid form at the end of the experiment. Cline and Richards (1969) found evidence was that both types of catalysis might occur, as the degree of catalysis was found to be related to the total Fe^{2+} concentration (aqueous and solid phase). Cline and Richards (1969) also observed that Fe^{2+} catalysis did not cause the reaction orders to change.

2.4.3 Oxidative leaching of insoluble slag sulphides

There is some evidence that, during the leach – oxidation of a secondary lead slag, oxidation of insoluble sulphides occurs in addition to oxidation of sulphides present in the aqueous phase. This oxidation of the insoluble sulphides is termed oxidative leaching and occurs by virtue of the redox potential difference between sites of the solid surface and the aqueous solution in contact with it. Barnes' (1996) slag composition shown in Appendix B shows that the insoluble sulphide present in the slag is expected to be virtually all ferrous sulphide (FeS).

Thermodynamic considerations for oxidative leaching of insoluble FeS

Air is used to oxidise the soluble sulphide components of the slag, but would also act as an oxidising agent for the insoluble sulphide components. The property of air to act as an oxidising agent in solution is shown by the cathodic reaction of equation 2-21.

$$O_2 + 4H^+ + 4e^- \Leftrightarrow 2H_2O \qquad \text{equation 2-21}$$

The ferrous sulphides may therefore be oxidised via an anodic process in the presence of air as an oxidising agent. This reaction will only occur to a significant degree if the redox potential of the solution is sufficiently higher than that of the ferrous sulphide. Jackson (1986) reports that the generally accepted value for this redox potential difference is at least 0.2 V.

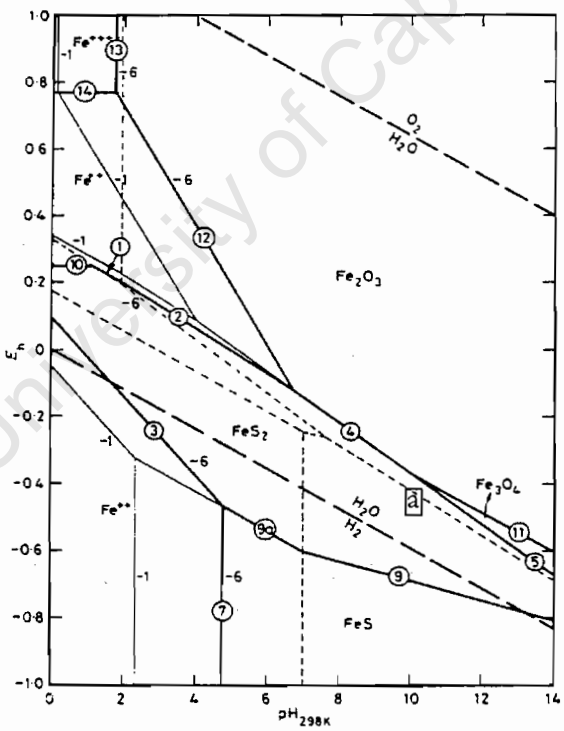

Figure 2-6 Fe-S-H_2O Eh – pH diagram at 25 °C and 1 atmosphere pressure (reproduced from Ferreira, 1975)

Figure 2-6 shows the regions of redox potential and pH where the sulphides and oxides of iron are most thermodynamically favoured. The area between the dashed equipotential O_2/H_2O and H_2O/H_2 lines shows the region of water stability. Therefore, under standard conditions, the redox potential of an aqueous solution would lie between these lines. The dashed equipotential O_2/H_2O line indicates the

standard redox potential (1 M O_2, 25 °C) as a function of pH for the reaction of equation 2-21 (Jackson, 1986). The redox potential of the solution would be significantly below this line due to it being determined at 1 M dissolved oxygen, which is substantially higher than could be achieved by the solubility of air at 1 atmosphere pressure.

While the redox potential of the solution would be significantly lower than indicated by the O_2/H_2O line, it is likely that the presence of dissolved oxygen would raise the redox potential of the solution sufficiently to exceed the lines labeled (4) or (11). Aqueous sulphide is known to be oxidised during leach – oxidation. The dashed line labeled [a] on the diagram shows the boundary between the thermodynamically favoured regions for sulphide and sulphate (the latter is favoured in the region above [a] under equilibrium conditions). Comparison of the dashed line labeled [a] to the lines labeled (4) or (11) indicates that the solution would not have to have an appreciably higher redox potential to oxidise the FeS in addition to the aqueous sulphide. Rather than sulphate, the metastable Eh – pH diagram for sulphur – water, Figure 2-4, indicated that thiosulphate is the favoured metastable oxidation product of sulphide in this region.

The presence of sulphide, a reduced species, in the reaction solution would have the effect of lowering its redox potential as shown in Figure 2-6. Thus, the FeS oxidative leaching reaction may be inhibited until this aqueous sulphide component is removed.

Thus, Figure 2-6 shows that if the redox of the leach – oxidation solution is raised sufficiently by means of equation 2-21, oxidative leaching reaction of FeS is likely to become thermodynamically favoured. Whether it occurs significantly must be determined experimentally.

Products of oxidative leaching of FeS

Alferova and Titova (1969) confirm that the metastable sulphide oxidation species, thiosulphate, is the main sulphur product of the FeS oxidative leaching reaction. They also observed the formation of elemental sulphur at neutral pH values. However, at pH 12, virtually all the sulphur was reported to be thiosulphate. Majima and Peters (1966) also observed that, in an alkaline solution, the 'unstable' (metastable) forms of sulphur that are not shown on the equilibrium Eh – pH diagram are the oxidation products. This was primarily thiosulphate, but also possibly polythionates ($S_xO_6^{2-}$, where x = 2 to 6). On 'prolonged oxidation' these were reported to be converted to sulphate.

Peters (1976) found that the iron oxidation product is likely to be $Fe(OH)_3$. This compound was reported to able be used interchangeably with the Fe_2O_3 (ferric oxide) form of Fe^{3+} on Figure 2-6.

Oxidative leaching reaction for FeS

At high pH, as occurs in the leach – oxidation step, Barnes (1996) predicted that it was likely that the FeS part of the $Na_2S.FeS$ double compound is oxidised as shown in equation 2-11. At neutral pH Barnes (1996) predicted that FeS may oxidise via equation 2-22.

$$4\,FeS + 3\,O_2 + 6\,H_2O \rightarrow 4\,Fe(OH)_3 + 4\,S^0 \qquad \text{equation 2-22}$$

Peters (1976) gives a generic oxidative leaching reaction for FeS_x that can be easily converted to show the reaction for both FeS and FeS_2. The reaction for the oxidative leaching of FeS under non-acid conditions is shown in equation 2-23.

$$FeS + 7H_2O + 9\ Ox \rightarrow Fe(OH)_3 + SO_4^{-2} + 11H^+ + 9\ Ox^- \qquad \text{equation 2-23}$$

Ox stands for the oxidising agent, which in this case is oxygen. Addition of the balanced reduction half reaction for oxygen (equation 2-24) to equation 2-23 results in equation 2-25.

$$9/4\ O_2 + 9H^+ + 9e^- \rightarrow 9/2\ H_2O \qquad \text{equation 2-24}$$

$$FeS + 5/2\ H_2O + 9/4\ O_2 \rightarrow Fe(OH)_3 + SO_4^{-2} + 2H^+ \qquad \text{equation 2-25}$$

Modifying equation 2-28 in line with the predominant metastable sulphur oxidation product observed by Alferova and Titova (1969) and Majima and Peters (1966), namely thiosulphate, results in equation 2-26. This is the expected FeS oxidative leaching reaction.

$$FeS + 2\ H_2O + 5/4\ O_2 \rightarrow Fe(OH)_3 + \tfrac{1}{2}\ S_2O_3^{2-} + H^+ \qquad \text{equation 2-26}$$

If the sulphur oxidation product of equation 2-22 is changed to the high pH product, thiosulphate, it can be converted to a form identical to equation 2-26. This was done by substitution of a thiosulphate ion for the elemental sulphur and balancing the charge with the addition of an H^+ ion, together with corresponding addition of H_2O and O_2 molecules to the left hand side of equation 2-22 to balance the hydrogen and oxygen elements.

Kinetics of the FeS oxidative leaching reaction

Thermodynamic data only indicates the tendency for a reaction to occur. Whether this reaction actually occurs to a significant degree depends on its kinetic rate. Four individual stages can be identified in the case of oxidative leaching utilising a gaseous reactant, where pore diffusion is assumed negligible. This is a reasonable assumption for the secondary lead slag as it was shown to disintegrate rapidly (Barnes, 1996).

Any of these stages (discussed below) may the rate controlling step. Jackson (1986) reports that in most cases it is found that the diffusion of the reactant to the surface of the particle controls the rate.

Stage 1: Transfer of gaseous oxygen to the aqueous phase

In leach – oxidation this stage is necessary for the oxidation of both the soluble sulphide and insoluble sulphide components. Equation 2-27 shows the process occurring.

$$O_2(g) \Leftrightarrow O_2(aq) \qquad \text{equation 2-27}$$

Jackson (1986) reports that the equilibrium constant for this process is given by equation 2-28 and can be used for the transfer of oxygen from atmospheric air.

$$K_{SOL} = \frac{[O_2]}{P_{O_2}} \qquad \text{equation 2-28}$$

Where:

$[O_2]$	equilibrium dissolved oxygen concentration	[mol/m³]
P_{O2}	partial pressure of oxygen in the gas stream	[Pa]
K_{SOL}	equilibrium constant	[Pa.m³/mol]

The difference between the equilibrium dissolved oxygen concentration and the actual dissolved oxygen concentration provides the driving force for transport of oxygen across the gas – liquid interface to the aqueous phase. The equilibrium dissolved oxygen concentration of atmospheric oxygen in water at 25 °C at atmospheric pressure is 8.26 mg/l. Raising the oxygen partial pressure of the gas phase causes a corresponding increase in the equilibrium dissolved oxygen concentration. For example, if pure oxygen was used, the equilibrium solubility is 40.3 mg/l under the same conditions. High pressures are often used for leaching to increase the oxygen partial pressure (for example autoclaves), but this is unlikely to be practical in leach – oxidation. Factors that reduce the equilibrium concentration of oxygen in solution include the presence of solutes in solution and raising the temperature of the solution.

Factors that increase the rate of oxygen mass transfer by increasing the area of the gas – liquid interface are a higher gas flow rate and increased bubble dispersion. The latter can be achieved by increasing the agitation rate in a stirred tank reactor. Jackson (1986) warns that, while adequate oxygen mass transfer can be achieved in laboratory scale tests, often it is not as efficient on an industrial scale. Hence this process may become rate controlling on scale-up.

Stage 2: Transport of dissolved oxygen to the particle surface

Provided the bulk of the fluid is well mixed, all the resistance to mass transfer should occur in the diffusion of oxygen through the stagnant film surrounding the particles. Jackson (1986) reports that for the case of oxygen transfer, solubility at atmospheric pressures is so low that this diffusion resistance is likely to be the rate limiting step of the oxidative leaching process.

Stage 3: Surface reaction

Electrochemical reactions (of which oxidative leaching is an example) cannot be described adequately by a chemical reaction rate equation. The mechanism for these reactions is known to be complex (Jackson, 1986). Sites on the mineral surface which have a slightly more positive potential promote the reduction reaction of the oxygen oxidant, while areas of the iron sulphide surface that have more negative potentials dissolve anodically as the electrons from the oxidation half reaction are transferred to the oxidant. The mechanism is further complicated by adsorption and desorption steps. An increase in temperature is known to increase the rate of the surface reaction exponentially, similarly to chemical reactions.

Stage 4: Transport of the reactant away from the surface

As in Stage 2, this is a diffusion controlled process. Jackson (1986) reports that this stage is not often rate determining, but may be significant if an insoluble product causes hindering of the aqueous products as they leave the solid surface via diffusion.

Conditions affecting the FeS oxidative leaching rate

pH

Majima and Peters (1966) investigated the oxidation rate of FeS with pure oxygen at high pressure (100 psia O_2) and high temperature (120 °C). They found that the rate of oxidation increases with increasing pH values. At pH 14, the initial rate of oxidation was significantly faster than at pH 11.1. However, after 30 min, the rates equalised. The explanation given for this is that, under the higher pH condition, the higher initial rate is retarded after a short period of time by a layer of hydroxide or oxide oxidation products.

Alferova and Titova (1969) compared the oxidative leaching rate of FeS to the oxidation rates of soluble sulphide forms (H_2S and HS^-). They found that between pH values of 6 – 10 the oxidation rate of the iron sulphide was up to 20 times greater than that of the soluble sulphides.

Particle size

An investigation of the effect of particle size on FeS oxidative leaching by Bayrakcelen *et al* (1990) yielded the result that a decreased starting particle size caused an increase in the initial rate of extraction due to the correspondingly greater surface area. This is the expected result for a surface reaction. The shrinking core model (Levenspiel, 1972) was successfully used by Bayrakcelen *et al* (1990) to model the this reaction. However, the reported rapid disintegration of the slag during leach – oxidation step indicates that the traditional fluid-particle reaction models of Levenspiel (1972) are unlikely to apply.

Temperature

Bayrakcelen *et al* (1990) found that increasing the reaction temperature from 12 °C to 40 °C resulted in an increase in the FeS oxidative leaching extraction of approximately 20% (based on iron extracted). Increasing the temperature increases the diffusivity of the species being transported through the liquid phase to the solid surface. However, its greatest effect is on the surface reaction rate through the rate constant, which is typically an exponential function of temperature.

Agitation

Bayrakcelen *et al* (1990) observed that an increase in the stirring rate from 5 to 25 revolutions per second resulted in an increase in extraction of iron from FeS in excess of 10%. A significant increase in the leaching rate, in response to an increase in agitation, normally indicates that mass transfer to the solid surface is the controlling step of the process. However, where the agitation also increases the gas bubble break up, a change in the extraction rate may also indicate that gas – liquid transfer limits the rate of the oxidative leaching process.

3 Theory

A number of subprocesses must occur to convert a single 'package' of slag sulphur from a solid bound up in a block of slag to a soluble oxidation product. Chapter 2 identified the subprocesses that potentially occur during leach – oxidation. Firstly, a leaching process occurs. Secondly, oxidation of the aqueous sulphides is known to occur. Thirdly, oxidative leaching of the insoluble sulphides may occur.

3.1 Leaching of soluble components

The process termed 'leaching of the soluble components', is defined here as being the process by which the soluble components are converted from being bound up in a block of slag to being present in the aqueous phase. This definition encompasses two steps: firstly, the step by which the soluble component, bound up in the slag block, is exposed to the dissolving action of the solvent; secondly, the dissolution step, during which the exposed solid is dissolved by the aqueous solvent.

Barnes (1996) found that the Enthoven slag disintegrated rapidly on contact with agitated water, a property that was identified as important to the success of BROSS process treatment. Pehlken (1997) found that the local slag also disintegrated in water. These observations were explained by Coulson and Richardson (1991), who reported that if a solid contains a high proportion of soluble components it disintegrates. Thus, the rate of first leaching step, the exposure of the soluble components to the solvent, will be determined by the rate at which the slag disintegrates. Disintegration is not a distinct subprocess of leach – oxidation due to the fact that it is caused by the dissolution subprocess. Therefore leaching of the slag is a result of the parallel actions of dissolution and disintegration. In an investigation of the leach – oxidation process it is still relevant to investigate the rate at which disintegration occurs. This is because it is necessary to determine the effect of its rate on the rate of the conversion of slag sulphur to thiosulphate.

3.1.1 Investigation of the dissolution subprocess

It is impossible to investigate disintegration independently of the dissolution subprocess, but it is possible to investigate the dissolution subprocess and overall leach – oxidation step independently of the occurrence of disintegration. This can be done by using a very finely divided slag starting particle size, rather than slag 'blocks'. If the slag particles are sufficiently reduced in size, an assumption can be made that the components of the slag are exposed to the solution from the start of the experiment, therefore eliminating the effect of disintegration. This size fraction was termed the fine fraction. Its size is defined in Section 4.1.1.

To investigate the dissolution of sulphide in isolation from the other subprocesses, it is necessary to eliminate the aqueous sulphide oxidation subprocess that removes sulphide from the solution. This is because the sulphide leaching rate is measured by the change in sulphide concentration in the solution. This would be achieved by excluding all oxygen from the reactor solution.

3.1.2 Investigation of disintegration

It is impossible to investigate the disintegration subprocess independently of the dissolution subprocess. However, comparison between the results of leach – oxidation treatment of the fine

fraction to those of a 'block' form, shows the effect that disintegration has on the rate of the overall process. A measure of the effect that certain conditions have on the disintegration rate was found by comparing the results obtained under varied conditions duplicated on both the fine fraction and 'block' starting size. The effect of variation of conditions on the disintegration rate is expected to be similar to the effect on the dissolution subprocess, due to this subprocess causing disintegration. The 'block' starting size is termed the coarse fraction. Its size is defined in Section 4.1.1.

Despite the fact that it is not an independent process, the disintegration rate may have a significant impact on the rate at which the slag sulphides are converted to thiosulphate. On a full or pilot scale operation, the starting slag condition is likely to be 'blocks' of considerably greater starting size than the coarse fraction, due to the cost of comminution. The coarse fraction was limited in size by the scale of the laboratory equipment used. Thus, the actual effect that the rate of disintegration of larger slag blocks would have on full-scale treatment may not be evident from the comparison between the coarse and fine fraction results. A separate set of experiments was therefore required to determine the disintegration rate of slag 'blocks' of larger diameter than the coarse fraction.

3.2 Oxidation of aqueous sulphides

A third slag starting condition, where all the soluble sulphides have already been pre-extracted from the slag into the solution, allowed the independent investigation of the oxidation of aqueous sulphide subprocess. Elimination of the leaching subprocesses in this way means that the change in the aqueous sulphide concentration would be due to oxidation alone. This slag starting condition is termed a pre-leached solution. The procedure under which it is generated is given in Section 4.3.3. It was obtained from the product of the dissolution experiments, where the oxidation of the aqueous sulphides was inhibited.

3.3 Oxidation of insoluble sulphides

In addition to the oxidation of aqueous sulphides, another mechanism was required to account for the sulphides that remain insoluble, but were found by Barnes (1996) to also be oxidised to a thiosulphate product. Thus, experimental investigation was required to investigate whether direct oxidative leaching of the insoluble sulphides was responsible for this observation.

As thiosulphate is the oxidation product of both the soluble and insoluble sulphides, its production rate would not give the rates of either the aqueous or insoluble sulphide oxidation explicitly if these both occurred simultaneously. Thus, oxidative leaching of the insoluble sulphides is much harder to quantify as no aqueous reactant or product could be independently measured. Firstly, deductions that indicate that two mechanisms are responsible for thiosulphate production may be able to be drawn from the trend in the production rate during leach – oxidation. Secondly, experiments were required to separate out the two forms of sulphide oxidation. Comparing the oxidation results of a pre-leached solution from which the insoluble components had been removed, to the results of one where the insoluble components had not been removed would achieve this.

4 Experimental methods

4.1 Experimental program

An experimental program was planned and undertaken in order to achieve the objectives outlined in Chapter 1. This entailed an experimental investigation of the overall leach – oxidation step and of the subprocesses that make up this step.

4.1.1 Program for leach - oxidation experiments

Base condition experiments

Table 4-1 details the processing conditions that were chosen as the base conditions for the laboratory scale experiments undertaken.

Slag mass concentration	50 g/l
Reactor type	1.5 litre and 4 litre stirred tank reactors
Air flowrate	1.33 litre air per litre of solution per minute
Temperature	20 ±2 °C
Agitation rate	600 rpm
Slag starting size	coarse fraction and fine fraction

Table 4-1 Base conditions for the experiments undertaken in this study

The only condition that was exactly the same between the base conditions and the BROSS process pilot plant conditions was the slag mass concentration. All other BROSS process pilot plant conditions were either impractical on a laboratory scale or not reported. Reasons for the selection of these base conditions are presented later in this section.

The two slag types selected for experimental investigation were from the N 20 ton furnace and O 20 ton furnace of the local refiner. These will henceforth be referred to as slag N and slag O respectively. The two starting slag sizes used were the fine fraction and coarse fraction. The fine fraction was prepared by milling the slag for two minutes in a Sieb Technik Mill, the average passing mass fraction achieved for a 100 µm sieve was 94 mass-%. The coarse fraction was prepared by crushing the slag and sieving it to a particle size range of 8.0 - 11.2 mm.

A number of base condition runs were undertaken in order to determine the reproducibility of the results obtained. These experiments are shown in Table 4-2.

Slag type	Slag starting size	Number of Experiments
N	Fine fraction	3
	Coarse fraction	6
O	Fine fraction	3
	Coarse fraction	3

Table 4-2 Leach – oxidation experiments run under base conditions

Experiments in which conditions were varied

On the basis of the conditions identified in Chapter 2 that affect the subprocesses making up the leach – oxidation step, the variables shown in Table 4-1 were selected for experimental investigation. Varying the investigated experimental variable, when all others are held constant, allowed the effect of that variable on the leach – oxidation process to be determined independently. Table 4-1 also shows the extent to which the experimental variables were varied in each experiment.

Experimental Variable	Slag type	Slag starting size	Extent of Variation			
Temperature	N	Coarse fraction	**20 °C**	40 °C	60 °C	80 °C
		Fine fraction	**20 °C**	40 °C	60 °C	-
	O	Coarse fraction	**20 °C**	40 °C	60 °C	80 °C
		Fine fraction	**20 °C**	40 °C	60 °C	-
Agitation	N	Coarse fraction	0 rpm	200 rpm	**600 rpm**	1200 rpm
		Fine fraction	-	200 rpm	**600 rpm**	1200 rpm
Solid – liquid Ratio	N	Coarse fraction	25 g/l	**50 g/l**	100 g/l	133 g/l
		Fine fraction	-	**50 g/l**	100 g/l	133 g/l
Air flow rate	O	Fine fraction	**5.3 l/min**	10.6 l/min	-	-
Slag particle size	N	Varied	0.6 – 1.0 mm	1.4 – 2.0 mm	4.0 – 4.75 mm	**8.0 - 11.2 mm**
	O	Varied	0.6 – 1.0 mm	1.4 – 2.0 mm	4.0 – 4.75 mm	**8.0 - 11.2 mm**

Table 4-1 Experiments investigating the effect of certain process conditions on leach – oxidation (base conditions in bold)

Selection of base conditions and extent of variation

Temperature

The ambient temperature was at or slightly below 20 °C. Therefore, this temperature was chosen to be the base condition temperature. Runs at temperatures above 60 °C were problematic due to excessive evaporation from the reactor vessel. Completely sealing the reactor was not possible due to the air vent requirement.

Agitation

An agitation rate of 600 rpm was used as the base case condition. Nagata (1974) predicts that, for the geometry of the reactors used in this experimental program, this agitation rate should be able to suspend a finely divided solid as well as accomplish sufficient bubble dispersion so as not to appreciably limit oxygen transfer. One stirrer motor was capable of operation at 1200 rpm and this was used to determine whether agitation at the base agitation rate limited leaching or gas transfer. A lower agitation rate of 200 rpm was used, as well as one run being operated with no agitation. A lower rate of agitation than the base rate (200 rpm compared to 600 rpm) was investigated as it is unlikely that a scaled up operation could achieve the same agitation rate as the base rate.

determine the effect of varied sulphide concentrations in the reactor solution. Secondly, if further biological treatment was not undertaken, there are several potential advantages for a greater slag mass concentration than 50 g/l, for example in water savings. An upper limit of 133 g/l was imposed due to the scale of the reactor, due to the air inlet being obstructed if more slag was fed to the reactor at the start of the experiment.

Air flowrate

An air flowrate of 1.33 (l air)(l solution)$^{-1}$(min)$^{-1}$ was used as the base condition. This translated to a rate of 2.0 l/min for the 1.5 litre reactors and 5.3 l/min for the 4 litre reactor. Nagata (1975) predicts that operation at this high air flow rate would not limit the transfer of oxygen from the air stream to the reactor solution. To verify this, an experiment was run with a flow rate of double the base case flow rate as shown in Table 4-3.

Slag particle size

The scale of laboratory reactors meant that slag blocks of greater size than the coarse fraction could not be accommodated. The experiments that investigated this variable utilised three size fractions between the coarse and fine fraction particle sizes. These fractions were sieved so that they were distinct from each other.

4.1.2 Program for experiments investigating the individual subprocesses

Disintegration

Four slag disintegration experiments were run to determine how this factor affects the rate of the overall leach – oxidation process. The conditions under which these experiments were run are shown in Table 4-4.

Experiment no.	Slag type	Agitation rate	Slag mass [g]
1	N	600 rpm	313.5
2	O	600 rpm	398.4
3	N	0 rpm	280.7
4	N	600 rpm	1132.0

Table 4-4 Conditions under which disintegration experiments were run

These different conditions allowed three different comparisons to be made. Firstly, between the two slag types, secondly, an agitated and non-agitated solution and thirdly, differing mass of the slag block.

Dissolution

Dissolution experiments were undertaken by dissolving the slag in water under nitrogen. The procedure for these experiments is given in Section 4.3.3.

Base condition experiments

Base conditions for the dissolution experiments were identical to those shown in Table 4-1 with the exception that nitrogen was bubbled through the reactor in place of air. Table 4-5 shows the dissolution experiments that were run under base conditions.

Slag type	Slag starting size	No. of experiments
N	Coarse fraction	1
	Fine fraction	3
O	Fine fraction	3

Table 4-5 Experiments investigating the dissolution process under base case conditions

Experiments where conditions were varied

The conditions that were identified in Chapter 2 that affect the leaching rate were investigated experimentally, with the exception of particle size, to determine their effect on the dissolution rate. The experiments that were carried out are shown in Table 4-6.

Experimental variable	Slag type	Slag starting size	Extent of variation		
Temperature	N	Fine fraction	20 °C	40 °C	60 °C
Agitation	N	Fine fraction	200 rpm	600 rpm	1200 rpm
Solid to liquid ratio	N	Fine fraction	10 g/l	50 g/l	100 g/l
	O	Fine fraction	10 g/l	50 g/l	

Table 4-6 Experiments investigating the effect of certain process conditions on dissolution

Oxidation of soluble sulphide

Experiments that investigated the soluble sulphide oxidation process were carried out on a pre-leached solution. The procedure for these experiments is given in Section 4.3.3.

Base condition experiments

Base conditions for the oxidation of soluble sulphide experiments were identical to those shown in Table 4-1, with the exception that the slag starting condition was a pre-leached solution. The experiments run under base conditions are shown in Table 4-7.

Slag type	Slag starting condition	No. of experiments
N	Pre-leached solution	4
O	Pre-leached solution	4

Table 4-7 Experiments investigating the oxidation process under base case conditions

Experiments where conditions were varied

Certain conditions that were identified in Chapter 2, that affect the leaching rate, were investigated experimentally to determine their effect on the aqueous sulphide oxidation rate. The controllable experimental variables that were investigated are shown in Table 4-8.

Experimental variable	Slag type	Slag starting condition	Extent of variation		
Temperature	N	Pre-leached solution	20 °C	40 °C	60 °C
Solid to liquid ratio	N	Pre-leached solution	10 g/l	50 g/l	100 g/l

Table 4-8 Experiments investigating the effect of certain process conditions on oxidation

Oxidative leaching of insoluble sulphides

Experiments were run to determine whether oxidative leaching of the insoluble sulphides does occur during leach – oxidation. As mentioned in Section 3.4, this was achieved by comparing oxidation experiments where the insoluble components were removed prior to starting the run, and oxidation experiments where the insoluble components were not removed. Table 4-9 shows these experiments.

Slag type	Slag starting condition	No. of experiments
N	Pre-leached **Filtered** solution	1
	Pre-leached **Unfiltered** solution	1
O	Pre-leached **Filtered** solution	1
	Pre-leached **Unfiltered** solution	1

Table 4-9 Experiments comparing the oxidation of filtered and unfiltered pre-leached solutions

4.2 Experimental apparatus

4.2.1 Disintegration experiments

The apparatus used for the disintegration experiments is shown in Figure 4-1. The slag block was supported on a sieve with 9 mm perforations. The impeller was located 100 mm above the slag block and agitated the surrounding water. The impeller was the same as that used for the 4 litre reactor leach – oxidation experiments. The geometry of this reactor is given in Table 4-10.

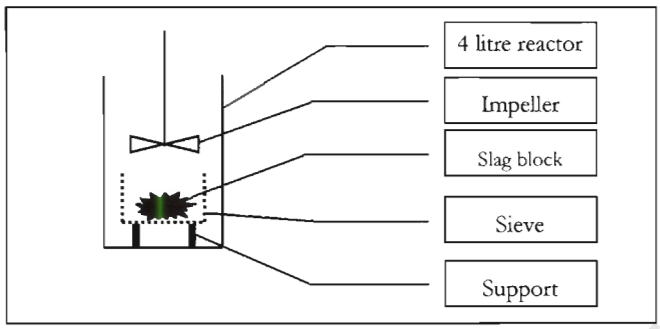

Figure 4-1 Experimental apparatus for disintegration experiments

4.2.2 Leach – oxidation experiments, leaching and oxidation subprocess experiments

Reactor type

Leach – oxidation experiments and experiments investigating the subprocesses were carried out in cylindrical stirred tank reactors of two different volumes, 1.5 litres and 4 litres. The 4 litre reactor was required in addition to the 1.5 litre reactors as the smaller reactors could not accommodate the dissolved oxygen probe. Thus, the dissolved oxygen could only be measured in the reactor solution of the 4 litre reactor. The four 1.5 litre reactors were required due to time constraints not allowing for all the experiments to be carried out in the single 4 litre reactor.

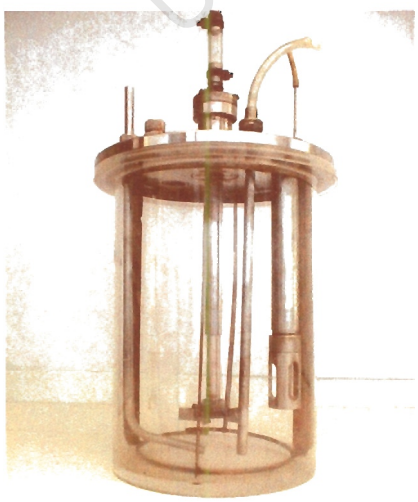

Figure 4-2 4 litre reactor

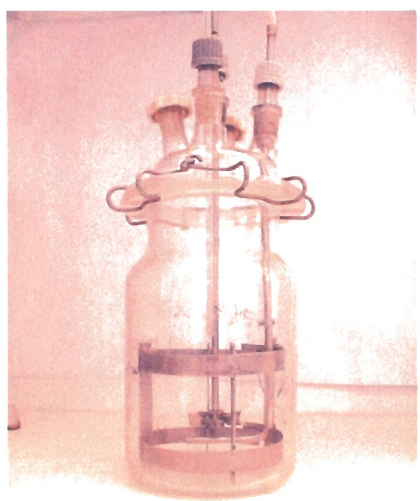

Figure 4-3 1.5 litre reactor

Reactor dimensions

Two important reactor characteristics were required. These were the provision of sufficient gas-liquid mass transfer and solids suspension. Often the reactor dimensional parameters were selected as a best compromise between the optimal dimensions for these two factors.

For gas transfer in a flat-bottomed cylindrical vessel, Nagata (1975) reported that the optimal impeller to vessel diameter ratio is 1/3, while for solids suspension this was 0.45. As a compromise between these, a ratio of 0.375 was selected. The clearance of the impeller off the bottom of the reactor is reported to be normally H/3, (where H is the height of the tank) for optimal gas transfer. For the best suspension of solids it should be closer to the bottom of the tank, at approximately H/6 (Nagata, 1975). As a compromise between these two ratios, the height of the impeller above the reactor bottom was selected to be H/4.5. A baffle width of approximately one tenth of the tank diameter was used as recommended by Nagata (1975).

A Rushton turbine, which is recommended for bubble dispersion in gas-liquid contacting reactors, was initially used. However, this type of impeller failed to provide the necessary suspension of the solid particles. Therefore a 6 bladed 45°-pitched turbine impeller was selected. Nagata (1975) reports that this impeller should provide the necessary axial flow in a reactor of typical dimensions to suspend solid particles while also providing reasonable mass transfer characteristics. Table 4-1 shows the dimensions of the 1.5 and 4 litre reactors and impellers.

Dimension	4 litre Reactor	1.5 Litre Reactor
Height (H)	173 mm	115 mm
Vessel diameter (D)	176 mm	120 mm
Impeller diameter (d)	65 mm	45 mm
Baffle width (B_w)	15 mm	10 mm
Clearance (C)	38 mm	25 mm
Impeller type	6 bladed 45°-pitched turbine	6 bladed 45°-pitched turbine

Table 4-1 Dimensions of the 1.5 and 4 litre reactors

Dimensional consistency was fixed between the 1.5 and 4 litre reactors with respect to the following ratios: H/D, d/D and B_w/D.

4.1 Experimental procedure

4.1.1 Collection of a representative slag sample

Slag samples were collected at a local secondary lead refiner. The remainder of Section 4.3.1 details the method by which the slag was collected, highlighting each level of slag sampling and the procedure followed to ensure that the slag was representative of the slag produced at the local refiner.

Furnaces selected for sampling

The limit on time available for the experimental program meant that the slags of only two of the four furnaces could be extensively studied. Both the plant's 20 ton furnaces were selected (N and O). Collectively these two furnaces produce more than half of the total slag produced by the refiner.

Variability of slag composition between batches for the same furnace

The slag from one furnace batch of each furnace was selected for the leach – oxidation treatment. This was done on the premise that it was preferable to perform rigorous test work on one slag batch, rather than a less rigorous experimental investigation on more than one slag batch from each furnace. The significance of variability of slag composition between batches is presented in section 5.1.1. The batches of slag from which the samples were taken were assumed to be from a typical furnace cycle with a typical furnace feed.

Proportion of slag batch from which the sample was obtained

Three slag pans were tapped from the furnace at the end of each selected batch cycle. Due to the labour required in breaking up the 2 ton blocks of each slag pan sufficiently for the next step, only one slag pan block could be selected for sampling for practical reasons. In order to counter any change in composition over the time taken to tap all the slag, the second slag pan filled was selected as the most likely to have a representative composition if variation did occur.

Sample size taken from the slag pan

The 2 ton slag blocks were broken up into 'chunks' of approximately 1 to 10 kg. Approximately 10 of the 'chunks' were selected to make up a sub-sample of approximately 20 kg. These 'chunks' were selected at random from different locations in the pile of broken up slag. This procedure was followed for the second slag pan of both furnaces.

Experimental samples

The two 20 kg samples were crushed in a jaw crusher to a particle size of approximately 10 mm diameter. From these samples, further samples were taken for use in experiments by taking ten or more sub-samples from random points from the container holding the slag. A more rigorous grid method was not feasible due to the need to protect the slag as much as possible from oxidation. The subsamples were sieved to a size fraction of 8.0 - 11.2 mm, and 50 g or 200 g of this was used in coarse fraction starting size experiments (for 1.5 litre and 4 litre reactors respectively). The samples for experiments requiring the fine fraction starting size were ground for 2 minutes in a Sieb Technik Mill.

4.3.2 Leach – oxidation experiments

The water used in the experiments was partially de-ionised in a Milli – RO®4 water purification system prior to introduction into the reactor. The air feed was obtained from a compressed air line introduced below the impellers as shown in Figure 4-2 and Figure 4-3. Fluctuations in supply line pressure were evened out by the use of gas regulators and the flow rate was monitored by air flow meters. The air feed was passed through the reactor under agitation for thirty minutes prior to addition of the slag to ensure the reactor water was saturated.

The slag was then introduced into the reactor to start the experiment. More reactor solution samples were taken at the beginning of the run where the leaching and oxidation rates were observed to be the highest. Liquid samples were withdrawn through a sampling tube, suspended midway into the reaction solution, by means of a 20 ml syringe. The samples were immediately filtered through a 0.45 µm Millipore® filter to remove any solid material that could still leach into solution.

Leach – oxidation experimental runs were operated for 48 hours, except in the case of two extended 96 hour runs. After final reactor solution samples were taken, the reactor solution was filtered through an air pressure filter. The filter cake was dried in an oven at approximately 110 °C and retained for mass and elemental analysis.

4.3.3 Experiments investigating the individual subprocesses

<u>Disintegration experiments</u>

The run lengths of the disintegration experiments were 24 hours. The state of disintegration at different times in the experiment was determined by calculating the percentage of the original slag mass being retained by the sieve. This mass was obtained by weighing the slag block together with the pre-weighed sieve. 100 % disintegration of the slag block was defined to be when the sieve no longer retained the slag block, i.e. the block width was less than the 9 mm sieve apertures in at least one dimension. The experiments were run so that they would simulate the leaching conditions in the 4 litre reactor as far as possible.

<u>Dissolution experiments</u>

Dissolution experiments were operated in the same way to leach – oxidation experiments, except that nitrogen was sparged through the reactor instead of air to inhibit the oxidation of the leached sulphide. A nitrogen flow rate of approximately 0.25 l/min and 1 l/min was maintained to the 1.5 litre and 4 litre reactors respectively. A higher flow rate would have been preferable. However, the bottled nitrogen supply was limited. The dissolution experiment run length was 24 hours. The same sources of potential error would be found in experimental sampling and analytical error for dissolution experiments as per Section 4.3.5.

<u>Oxidation experiments</u>

As discussed previously, the starting condition for these experiments was a pre-leached solution, the product of the dissolution experiments. Apart from the starting condition, base conditions were the

same as for the leach – oxidation experiments. The oxidation experiment run length was 24 hours. The same sources of potential error would be found in experimental sampling and analytical error for dissolution experiments as per Section 4.3.5.

4.3.4 Analytical techniques

Online analysis

Dissolved oxygen

The 4 litre reactor accommodated the use of a YSI 5700 series dissolved oxygen probe suspended 'on-line' into the reactor solution. Continuous readings were not possible due to the probe's membrane being eroded by sulphides and strong alkalis present in the solution. The dissolved oxygen meter was calibrated before each run by a zero oxygen sodium sulphite solution and air saturated water (the equilibrium dissolved oxygen concentration of water is known as a function of temperature).

Analysis of liquid samples

Sulphide

Immediately after filtering, a 5ml aliquot was diluted 1:1 with Sulphide Anti-Oxidant Buffer (SAOB) as per manufacturer's instructions and analysed for sulphide using an Orion Model 9619 combination silver/sulphide probe. The probe was calibrated before each run. The sample temperature was required to be the same as the temperature at which the probe was calibrated, otherwise a 4 % error was recorded per 1 °C difference. This error would not be appreciable during all experiments where the temperature was maintained at 20 °C (all experiments except temperature variation experiments). This temperature approximated the ambient temperature, therefore the short time between drawing the sample and analysis would not have caused a significant temperature change. For higher temperature experiments (40 °C and 60 °C) the difference between the actual sample temperature and the estimated temperature at which the probe was calibrated would have caused an error in these results.

pH, temperature and redox potential

Undiluted samples were analysed by a pre-calibrated Metrohm 744 combination pH – temperature probe. The sample pH and temperature were recorded along with the redox potential estimate that the probe provides. A more accurate estimate of the solution redox potential was attempted using a redox probe, but calibration problems meant that readings were not meaningful.

Anion analysis

The remaining sample was diluted 1:200 with de-ionised, de-oxygenated water for anion analysis on a Dionex Series 2000 Ion Chromatograph. The chromatograph was calibrated daily with specially prepared standards for thiosulphate, sulphate and chlorine.

Dissolved metal analysis

Atomic Absorption Spectroscopy (AAS) was performed on the liquid samples of selected experimental runs to determine their sodium and iron content. The dilutions were 1:200 and 1:10 respectively for sodium and iron, in order to achieve concentrations in a range that is best detected by AAS analysis.

Anion analysis

The remaining sample was diluted 1:200 with de-ionised, de-oxygenated water for anion analysis on a Dionex Series 2000 Ion Chromatograph. The chromatograph was calibrated daily with specially prepared standards for thiosulphate, sulphate and chlorine.

Dissolved metal analysis

Atomic Absorption Spectroscopy (AAS) was performed on the liquid samples of selected experimental runs to determine their sodium and iron content. The dilutions were 1:200 and 1:10 respectively for sodium and iron, in order to achieve concentrations in a range that is best detected by AAS analysis. Samples from preliminary runs were also analysed for lead and zinc. These concentrations were below the reliable detection range when the samples were sufficiently dilute for AAS analysis of other elements, and therefore were not subsequently analysed.

Analysis of solid samples

A representatively collected sample from both the crushed fresh feed slag and filtered insoluble product was powdered and 0.1g and 0.15g samples were taken for AAS elemental analysis and sulphur analysis respectively. Elemental analysis of the digested solid was done for lead, zinc, iron and sodium by AAS. The sulphur content was determined by using a Leco sulphur analyser. The analysis of the feed slag for characterisation purposes is given in Appendix C.

4.1.1 Sources of error

Sources of slag sampling error

The procedure in the collection of a representative slag sample was given in Section 4.3.1. The potential sources of error associated with each level of slag sampling were also discussed in that section.

Sources of experimental sampling error

Position of sampling point within the reactor

The sampling tube was located at one third of the liquid height from the bottom of the reactor. High agitation rates were typically used during the reactor run (600 rpm), thus, the solution was well mixed and the liquid sample was likely to be representative of the reactor solution at the time of sampling.

Number of samples taken

One liquid sample was withdrawn for analysis at each sampling time during the run. Two liquid samples were withdrawn at the end of the run and were analysed separately for the sulphide oxidation products. Comparison of these results gives a measure of the combined sampling and analytical error.

Filtration of samples

Filtration is unlikely to inherently alter the concentrations of the solution. However, the time taken to complete this task prior to the addition of an anti-oxidant and sulphide analysis, may have resulted in the increased oxidation of the sample compared to the reactor solution at the time of sampling. This error was reduced due to the filtration being done immediately upon extraction of the sample.

Temperature of sample

The error associated with temperature on sulphide analysis of high temperature experiments was discussed in Section 4.3.4.

Dilution of samples

An error would have been associated with sample dilution. The apparatus used for this was a 10 ml dispenser and 0.1, 1 and 5 ml pipetmen. These were calibrated between runs. Samples were diluted with partially de-ionised water to reduced contamination.

Degradation of samples prior to analysis

Sulphide was analysed immediately. However, this was not possible for samples analysed by Atomic Absorption Spectroscopy (AAS) and Ion Chromatography. Samples that could not be analysed immediately were refrigerated. These were discarded if analysis was not done within 48 hours. Thiosulphate is reported to be metastable in solution (refer to Section 2.4.2) and therefore its sample concentration should not be significantly affected by delays in analysis shorter than this. The measured thiosulphate concentration may be increased by sulphide oxidation in the sample prior to analysis, particularly if dilution rendered the sulphide anti-oxidant buffer less effective. The low liquid sample sulphide concentrations after two hours into the experiment would mean that this impact is not appreciable, as thiosulphate samples were not taken before 2 hours.

Sampling of insoluble product for analysis

Two independently collected samples of each insoluble leach – oxidation product were analysed. The samples were taken by powdering the insoluble product and mixing it, followed by the collection of at least 5 different sub-samples from different randomly chosen locations.

Sources of analytical error

Analytical error was reduced by ensuring that the samples were diluted to the correct concentration range (i.e. that for which the analytical equipment was calibrated). Repeat analyses of the same sample were often undertaken. Standards of known concentration were included with the experimental samples to detect systematic analytical errors. For both of these cases, if significant variation was found, the batch of samples was re-analysed.

Quantification of the error associated with the sampling of the slag is difficult to determine rigorously. It would be meaningless to quantify the error associated with experimental sampling and analysis if the major potential source of error was not accounted for. Thus, the quantification of the overall error associated with the experimental results was not attempted.

5 Experimental results

5.1 Characterisation of the slag

5.1.1 Quantitative analysis

Variability in slag composition

The slag exhibits a significant variability in composition from one batch to another. The high values of the standard deviation and the range between maximum and minimum values in Table 5.1-1 gives a measure of this variability of the major slag components. Sampling error would also be expected to play a significant role in the observed variability.

	Pb [mass-%]	Na [mass-%]	Fe [mass-%]	S [mass-%]
Average	5.95	14.96	21.58	14.36
Maximum value	46.60	49.68	42.10	37.39
Minimum value	0.64	2.30	1.40	0.66
Standard deviation	6.23	7.55	8.51	7.32

Table 5.1-1 Results of ICP analysis of selected elements on 152 slags at the local refiner from Jan 19 to July 23 1998

Table 5.1-2 shows the elemental analysis of two slags from AAS and ICP analyses at the University of Cape Town (UCT) and ICP analysis at the local refiner. One slag was from the O 20 ton furnace and one was from the N 20 ton furnace. Also indicated is the number of independent samples taken from each slag in each of the analyses.

	Elemental composition of an O 20 ton furnace slag			Elemental composition slag of N 20 ton furnace slag		
Analysis	AAS (UCT) [mass-%]	ICP – OES (UCT) [mass-%]	ICP (refinery) [mass-%]	AAS (UCT) [mass-%]	ICP – OES (UCT) [mass-%]	ICP (refinery) [mass-%]
No. of samples analysed per slag	3	3	5	3	3	3
Sn	0.92	1.97	-	1.17	2.15	-
Zn	1.04	1.05	-	0.74	0.61	-
Pb	1.83	1.14	3.8	1.52	1.51	1.9
Si	-	2.11	-	-	1.86	-
Fe	22.70	25.30	27.82	18.33	21.44	15.3
Mg	0.12	0.11	-	0.27	0.27	-
Cu	0.54	0.76	-	0.45	0.66	-
Na	10.92	9.28	12.1	10.12	8.84	16.1
Sb	0.35	-		0.25	-	-
S	-	-	18.6	-	-	3.2
Total slag accounted for	38.42	41.71	65.2	32.94	36.33	41.5

Table 5.1-2 Comparison of elemental analyses of two slags by AAS and ICP analyses at the University of Cape Town with ICP analysis at the local refiner

The two slags that were analysed in Table 5.1-2 were not those used for the leach – oxidation experiments, as a fresh, unoxidised slag was required. These slags did come from the same furnaces as those used in the experimental program and provide a useful comparison between the results of different analytical technique (the UCT AAS and ICP-OES analysis was on the same digested sample) and slag sampling (comparison to local refinery ICP results). The composition of the slags used for the experiments, determined by AAS analysis, is given in Table 5.1-3 and Table 5.1-4. Only sulphur, sodium, iron, zinc and lead were analysed for, as these have the most significant bearing on the leach – oxidation experiments. A comparison of the ICP and AAS techniques is given in Appendix C.

	S [mass-%]	Na [mass-%]	Fe [mass-%]	Pb [mass-%]	Zn [mass-%]
Average	20.4%	13.9%	20.4%	10.0%	1.6%
Maximum value	20.8%	17.0%	22.6%	13.2%	1.7%
Minimum value	19.9%	11.4%	17.1%	7.4%	1.3%
Standard deviation	0.004	0.023	0.024	0.029	0.002

Table 5.1-3 Composition of the slag from N 20 ton furnace used in leach – oxidation experiments (8 slag samples analysed)

	S [mass-%]	Na [mass-%]	Fe [mass-%]	Pb [mass-%]	Zn [mass-%]
Average	17.1%	15.1%	19.9%	2.9%	1.9%
Maximum value	17.6%	21.1%	20.1%	3.1%	1.9%
Minimum value	16.5%	12.2%	19.4%	2.8%	1.7%
Standard deviation	0.005	0.040	0.003	0.002	0.001

Table 5.1-4 Composition of the slag from O 20 ton furnace used in leach – oxidation experiments (8 slag samples analysed)

Comparison of Table 5-3 and Table 5-4 to Table 5-1 provides a measure of how representative the slags chosen for treatment are of the overall slags produced. Data more recent than August 1998 is not available. The slags selected for treatment were collected in March 1999. The slags selected both have a greater sulphur composition than the average of the historical data, particularly for the slag from the N 20 ton furnace. The sulphur composition of the selected slags both fell within one standard deviation of the average given in Table 5-1. The iron and sodium compositions were consistent with the historical average values. Although the lead content of the N 20 ton furnace was significantly higher than average, and that of the O 20 ton furnace was lower, both values fell within one standard deviation of the average given in Table 5-1.

5.1.2 Qualitative analysis

For an investigation of the leach – oxidation treatment process, it is necessary to not only know the elemental composition of the slag, but also in which compounds the major elements of sulphur, iron and sodium are found. Properties of these compounds determine the leaching and oxidation behaviour of the slag. Slag compounds that have been predicted from knowledge of secondary lead rotary furnace reactions were reported in Section 2.1. However, the determination of which compounds are present via direct analysis, remains necessary. This is because the compounds formed are dependent on actual

thermodynamic conditions, which may be different to those predicted theoretically. The analytical procedures for the results presented below are given in Appendix C.

X-ray diffraction analysis

X-ray diffraction (XRD) analysis was carried out on samples of slag from both N and O 20 ton furnaces.

Matte phase compounds

XRD analysis did not detect the major sulphide compounds expected to be present in the slag. The reason for this was expected to be the lack of crystallinity of the matte phase.

Slag phase compounds

Several possible slag phase oxides, hydrates, hydroxides and silicates were detected. Sodium hydroxide (NaOH) and ferrihydrite (FeO(OH)) were detected. A number of different silicate species matched the detected diffraction angles. Combinations of sodium aluminium silicates dominated those detected. Other elements that were found in these silicate matrices include magnesium, calcium and zinc.

Lead and zinc compounds

By identifying the compounds in which these elements are found, an estimate can be made of the extent to which the lead and zinc components of the slag are leachable under leach – oxidation conditions. The lead compound that was most often detected by XRD analysis was $PbSO_4$. Lead in platinum alloys was also detected. Zinc alloys were found present as zinc sulphide ZnS, zinc hydroxide ($Zn(OH)_2$) and in a sodium zinc silicate.

SEM analysis

Backscatter SEM (Scanning Electron Microscope) images of slag samples from the O 20 ton and N 20 ton furnaces were taken and phases of typical appearance were analysed by EDS (Electron Dispersive Spectroscopy). It is not possible to detect individual compounds using this analysis, but the elemental composition of a certain phase can be ascertained. Background interference was still evident even though topographical images were examined in order to select flat spots for analysis. Elements were assigned to compounds based on which compounds were expected from literature, thermodynamically predicted compounds and XRD analysis. This assignation was evaluated by how well these compounds accounted for the quantitative elemental composition for that particular spot given by EDS analysis. Two examples of this analysis is given in this section, the remaining analysis is given in Appendix D.

Matte phase

The matte phase spots that were analysed by EDS all fell within the FeS – Na_2S phase diagram region between 55 and 73 mass-% FeS. Thus, the sodium, iron and sulphur were assigned to Na_2S.FeS and FeS (see Section 2.1.3). SEM analysis cannot prove or disprove the presence of the Na_2S.FeS double compound, as the elements could just as easily be assigned to individual Na_2S and FeS compounds. However, the evidence presented in Section 2.1.3 suggests that a double compound is formed.

Photo number 4 shown in Figure 5.1-1 (at end of Section 5.1) was taken of a prepared slag sample from the O 20 ton furnace. It illustrates the heterogeneity of the slag. The lighter and darker parts

indicate different phases. The lighter regions are the higher molecular weight matte phases and the darker regions are the lower molecular weight slag phase.

The lighter spot, indicated as spot number 1 on the photo, is a matte phase and was analysed to have the following elemental composition:

Element		Mass-%	Mole-%
Sulphur	S	36.45	37.27
Sodium	Na	14.52	20.70
Iron	Fe	39.21	23.02
Oxygen	O	8.89	18.21

Table 5.1-5 Elemental analysis for spot number 1 on photo number 4

This composition indicates that this spot has a FeS composition of 57 mass-% (relative to the sum of Na_2S and FeS) and thus falls within the region of $FeS.Na_2S$ and FeS as predicted by Steck *et al* (1929). Thus, the elements of Table 5.1-5 were assigned to the compounds given in Table 5.1-6.

Compound	Mole-%
FeS	33
$FeS.Na_2S$	25
O	42

Table 5.1-6 Elemental assignation to compounds for spot number 1 on photo number 4

The assignation in Table 5.1-6 accounted stoicheometrically for all the iron, sodium and sulphur present in the elemental EDS analysis of Table 5.1-5. An excess of oxygen was present which could not be assigned to any of the other elements. The explanation for this lies in the hygroscopic nature of certain components of the slag. The matte phase compound that displays this characteristic is sodium sulphide (Bush, 1994). Thus, the oxygen was assumed to be associated with water (hydrogen cannot be detected by EDS analysis), which is adsorbed from the atmosphere onto the slag's surface. The significant amount of water present is explained by the fact that elemental analysis using this technique is limited to the surface layers of the slag sample.

Slag phase

An example of a slag phase region is the spot marked number 2 on photo number 4. The EDS elemental composition is given in Table 5.1-7.

Element		Mass-%	Mole-%
Sulphur	S	1.51	1.06
Sodium	Na	13.67	13.42
Iron	Fe	9.42	3.81
Silica	Si	23.09	18.56
Oxygen	O	35.92	50.69
Calcium	Ca	2.82	1.59
Magnesium	Mg	3.09	2.87
Aluminium	Al	8.56	7.16

Table 5.1-7 Elemental analysis for spot number 2 on photo number 4

The presence of this excess oxygen in the slag phase can be explained in a similar manner to the matte phase, the deliquescent compound in this case being Na_2O. Queneau *et al* (1989) assign the major slag phase elements to Na_2O, FeO and SiO_2. The slag phase elements detected by EDS analyses can be assigned to these compounds as is shown in Table 5.1-8. The minor elements, calcium, magnesium and aluminum, were assigned to the compounds assumed to be present in a similar secondary lead smelter slag (Barnes, 1996).

Compound	Mole -%
FeO	6
Na_2O	15
SiO_2	29
O	28
$CaSiO_2$	5
$MgSiO_2$	8
$CaSi_2O_3$	8
$Na_2S.FeS$	1

Table 5.1-8 First elemental assignation to compounds for spot number 2 on photo number 4

XRD analysis detected the presence of sodium silicate. The elements of Table 5.1-7 could also be successfully assigned as shown in Table 5.1-9, in which sodium was assigned to sodium silicate.

Compound	Mole- %
FeO	8
Na_2SiO_2	19
SiO_2	19
O	29
$CaSiO_2$	6
$MgSiO_2$	10
$CaSl_2O_3$	10
$Na_2S.FeS$	1

Table 5.1-9 Second elemental assignation to compounds for spot no.2 on photo no. 4

Significant pure component elemental phases observed in the slag

The bright spot labeled 3 on photo number 1 was found to be a metallic iron inclusion (85 wt % Fe) as well as a small amount of tin (2.8 wt %) surrounded by a FeS rich matte region. A number of elemental lead inclusions were also observed in the slag. Inclusions rich in carbon (70%) were observed, these are likely to be unburned coal particles.

5.1.3 Indirect techniques

Mass balance over furnace

In addition to analysing the slag directly, the elemental composition of the slag can be established by carrying out a mass balance over the furnace for one batch cycle. Generic compositions of the furnace feeds are known and the bullion lead product is regularly analysed. Recording of the quantities of feed

used and products generated allowed a mass balance to be carried out. This method is also useful for determining the feed materials from which the various components of the slag originate.

The results of mass balances across one furnace cycle of each of the 20 ton furnaces (O 20 ton and N 20 ton) is given in Appendix E. Table 5.1-10 gives an aggregated mass balance for one batch cycle of the O 20 ton furnace. The furnace feeds are not weighed on the plant, but are added to the furnace in skips and the mass is calculated from the estimated bulk density of that feed.

Furnace Inputs	
Element	Mass [kg]
Pb	13,141
Fe	1,471
Na	1,280
S	1,039
C	1,856
Ag	-
As	25
Cu	42
Ni	-
Sb	101
Sn	4
Zn	81
Si	63
Al	17
O	4,268
H	
N	
Total	24112.9

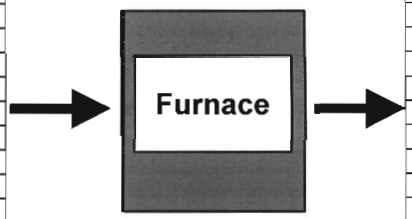

Furnace outputs		Error based on output mass
Element	Mass [kg]	[%]
Pb	15,425	16%
Fe	1,468	0%
Na	840	52%
S	1,275	19%
C	1,551	20%
Ag	-	
As	4	525%
Cu	47	11%
Ni	-	
Sb	176	43%
Sn	1	300%
Zn	76	7%
Si	131	52%
Al	106.1	84%
O	4,629	8%
H		
N		
Total	25728.8	6%

Table 5.1-10 Mass balance for one batch cycle of the O 20 ton furnace

Carbonate analysis

Wet chemical means were used to determine whether carbonate was present in the local slag. The method used are given in Appendix C. Barium carbonate was not observed to precipitate from aqueous slag extracts on addition of barium chloride. Carbon dioxide was not evolved on addition of an acid.

Phosphate and chlorine analysis

An aqueous extract was analysed by ion chromatograph for phosphates and chloride, both of which were expected to be present in a soluble form. Table 5.1-11 gives the mass percentage of these components in the slag, assuming that they totally dissolve.

	Concentration [g/l]	Mass % of Slag
Total Slag Dissolved	100.1	100 %
Chlorine	2.7	2.7 %
Phosphate	0.3	0.3 %

Table 5.1-11 Determination of chlorine and phosphate present in the slag from ion chromatograph analysis

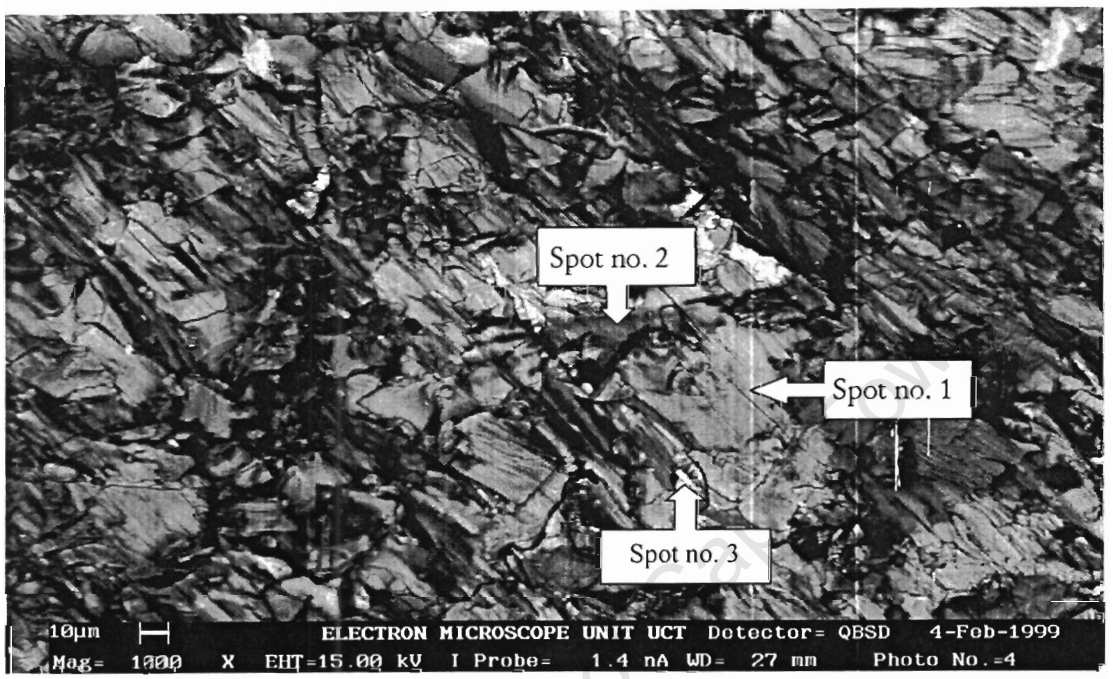

Figure 5.1-1 SEM backscatter photo number 4

5.2 Leach – oxidation of the slag under base conditions

5.2.1 Presentation of leach – oxidation experiment results

Table 5.2-1 is an example of the generic results table, which is used to summarise the end-of-run (48 hour) overall mass extraction and sulphur extraction results for a set of leach – oxidation experiments. These tabulated results indicate the degree to which the leach – oxidation experiment accomplished the goal of extracting the sulphur from the slag and converting it to thiosulphate and sulphate oxidation products. The first column indicates the overall extraction of the feed slag components to the aqueous phase. The following three columns give the percent of the feed slag sulphur reporting to the respective product phases at the end of the experiment. The method for calculating these from the analytical results is given in Appendix F. The last column sums the percentages of the feed slag sulphur reporting to the three product phases, thus completing the sulphur mass balance for feed and products. Failure of the product sulphur to account fully for all the feed sulphur can be ascribed to slag sampling error, experimental sampling error and analytical error (discussed in Section 3.3). Another possible reason could be that not all product aqueous phase species are accounted for in this mass balance. In all experiments the aqueous sulphide present in the reaction solution was reduced to zero by the end of the 48 h experiment and therefore this component does not require inclusion into the table.

The rate of production of oxidised sulphur species and presence of aqueous sulphide during the experiment is presented in the form of graphs of thiosulphate, sulphate (where significant) and sulphide plotted against time for the duration of the experiment. Sodium end-of-run extraction tables and during-run concentration versus time graphs are also presented where relevant to illustrate leaching behaviour.

The results of analysis of liquid samples during the leach – oxidation experiment and end-of-run analysis of liquid and insoluble solids are given in Appendix G.

5.2.2 End-of-run experimental results

Table 5.2-1 summarises the end-of-run fine fraction sulphur extraction results of six separate experiments on slag N and three separate experiments on slag O under base conditions.

Slag type	Reactor used	Run number	Overall percent of feed slag remaining insoluble	Feed slag sulphur remaining in insoluble phase	Recovery of feed slag sulphur to aqueous phase oxidised sulphur species (mass basis)		Sulphur accounted for by product phases as percent of feed slag sulphur
					Conversion to thiosulphate	Conversion to sulphate	
N	1.5 l	1	75.6%	33.1%	58.0%	0.2%	91.3%
	1.5 l	2	74.2%	32.5%	60.3%	0.1%	92.9%
	1.5 l	3	78.5%	39.1%	55.8%	0.1%	95.0%
	1.5 l	4	79.2%	38.6%	59.5%	0.0%	98.1%
	1.5 l – Ext. run *	5			54.6%	0.1%	
	4 l	6	80.6%	39.1%	59.6%	0.0%	98.7%
O	1.5 l	7	77.6%	52.9%	53.4%	0.4%	106.7%
	1.5 l – Ext. run *	8			55.7%	0.3%	
	4 l	9	78.8%	37.4%	58.3%	0.5%	96.2%

Table 5.2-1 Recovery of sulphur present in the slag to product phases: leach – oxidation of the fine fraction under base conditions

*48 hour liquid sample of the extended experiment (Ext. run) was used to calculate conversion to thiosulphate and sulphate.

Table 5.2-2 summarises the end-of-run coarse fraction sulphur extraction results of four separate experiments on slag N and two separate experiments on slag O under base conditions.

Slag Type	Reactor Used	Run number	Overall percent of feed slag remaining insoluble	Feed slag sulphur remaining in insoluble phase	Recovery of feed slag sulphur to aqueous phase oxidised sulphur species (mass basis)		Sulphur accounted for by product phases as percent of feed slag sulphur
					Conversion to thiosulphate	Conversion to sulphate	
N	1.5 l	10	78.6%	46.1%	38.9%	0.0%	85.0%
	1.5 l	11	81.8%	47.7%	43.4%	0.0%	91.1%
	1.5 l	12	83.3%	40.0%	43.0%	0.0%	83.0%
	1.5 l	13	84.9%	47.7%	39.6%	0.0%	87.3%
O	1.5 l	14	80.7%	39.3%	52.1%	0.3%	91.7%
	1.5 l	15	84.8%	44.4%	46.3%	0.0%	90.7%

Table 5.2-2 Recovery of sulphur present in the slag to product phases: leach – oxidation of the coarse fraction under base conditions

Table 5.2-1 and Table 5.2-2 indicate the success that leach – oxidation achieves under base conditions in terms of sulphur extraction for the fine fraction and the coarse fraction respectively. In addition, they compare the results obtained from the 1.5 litre and 4 litre reactors. This comparison is assessed in Section 5.2.9.

Reproducibility of base condition experiments

The five repeated leach – oxidation experiments run on slag N, from Table 5.2-1, were analysed statistically. This was done to obtain a measure of the between experiment variability in the results

obtained under identical conditions. The results are not reproduced identically as a result of sampling and analytical error.

		Overall percent of slag remaining insoluble	Sulphur remaining in insoluble phase	Conversion to thiosulphate	Conversion to sulphate
Number of experiments		4	4	5	5
Average		76.9%	35.8%	57.6%	0.1%
Standard deviation		2.3%	3.5%	2.4%	0.1%
Range	Maximum	79.2%	39.1%	60.3%	0.2%
	Minimum	74.2%	32.5%	54.6%	0.0%

Table 5.2-3 Statistical analysis of base condition results for the fine fraction of slag N

Four repeated coarse fraction experiments were also run under base conditions on slag N. These results were treated similarly to the fine fraction results of Table 5.2-3, as shown in Table 5.2-4.

		Overall percent of feed slag remaining insoluble	Sulphur remaining in insoluble phase	Conversion to thiosulphate	Conversion to sulphate
No. of experiments		4	4	4	4
Average		82.1%	45.4%	41.2%	0.0%
Standard deviation		2.7%	3.7%	2.3%	0.0%
Range	Maximum	84.9%	47.7%	43.4%	0.0%
	Minimum	78.6%	40.0%	38.9%	0.0%

Table 5.2-4 Statistical analysis of base condition results for the coarse fraction of slag N

Comparison of fine fraction and coarse fraction results

Comparison between the average extraction and conversion values for the fine fraction (Table 5.2-3) and coarse fraction (Table 5.2-4) shows significant differences. Reducing the slag particle size from the coarse fraction to the fine fraction causes a 5.2 % increase in the overall amount of slag extracted, a 9.6 % decrease in the sulphur remaining insoluble and a 16.4 % increase in conversion to thiosulphate. The fine fraction experiments show a small increase in the conversion to sulphate.

5.2.3 Sulphur species in solution during the experiment

Figure 5.2-1(a) shows the sulphur species in solution during experiment number 1 over the entire 48 h of the experiment. This graph does not show the sulphide concentration trend adequately, due to the sharp initial rise and fall in sulphide concentration followed by a relatively very small or zero value after 8 h. Figure 5.2-1(b) shows the same sulphide concentration graph on a more meaningful scale (the first 8.5 h). Subsequent graphs that compare the concentrations of sulphur species between different experiments will either just contain thiosulphate over the entire experiment or sulphide over the first 8.5 h where these are relevant.

In Figure 5.2-1(a) a typical relationship between the sulphur species is shown, where the sulphide concentration initially has a sharp increase, and reaches a maximum at approximately 10 minutes.

Figure 5.2-1(b) shows that this is followed by a sharp decrease, achieving a concentration of approximately 2 % of the 10 min value after 2 h. A further, more gradual decrease is then observed. The sulphide concentration reached zero for this experiment between 8 h and 18 h. The thiosulphate production rate decreases gradually until termination of the experiment at 48 h. The rate of thiosulphate production does not decrease to zero once the sulphide concentration becomes zero. Note also that the sulphide and thiosulphate concentrations are plotted on different scales, the maximum thiosulphate concentration being virtually two orders of magnitude greater than the maximum sulphide concentration.

The sulphate concentration remains very low throughout this experiment and all other leach – oxidation experiments, the exception being the high temperature experiments. Inconsistencies in sulphate results can be attributed to the low sample concentrations, a high sample dilution being required to comply with the upper conductivity constraint imposed by the ion chromatograph analysis.

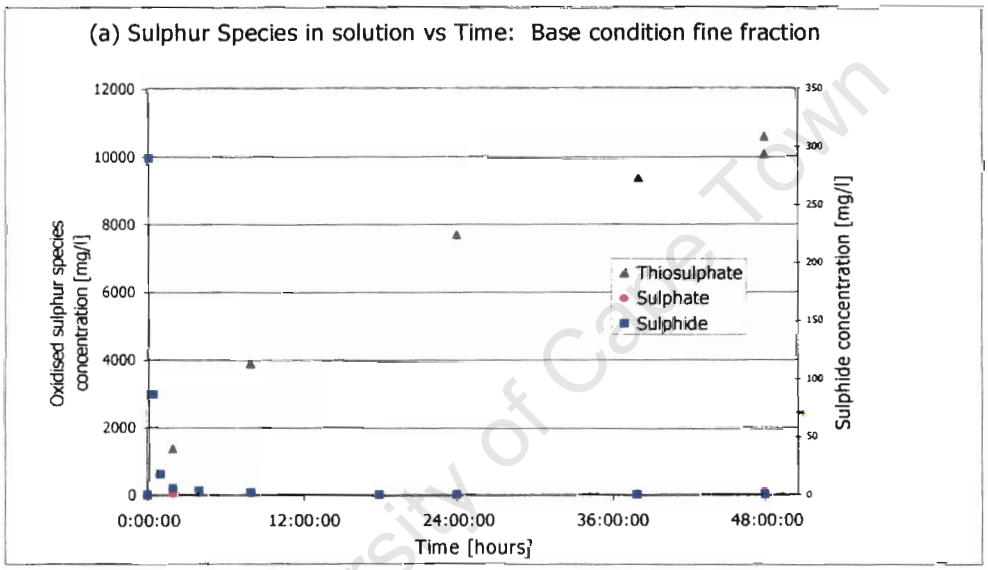

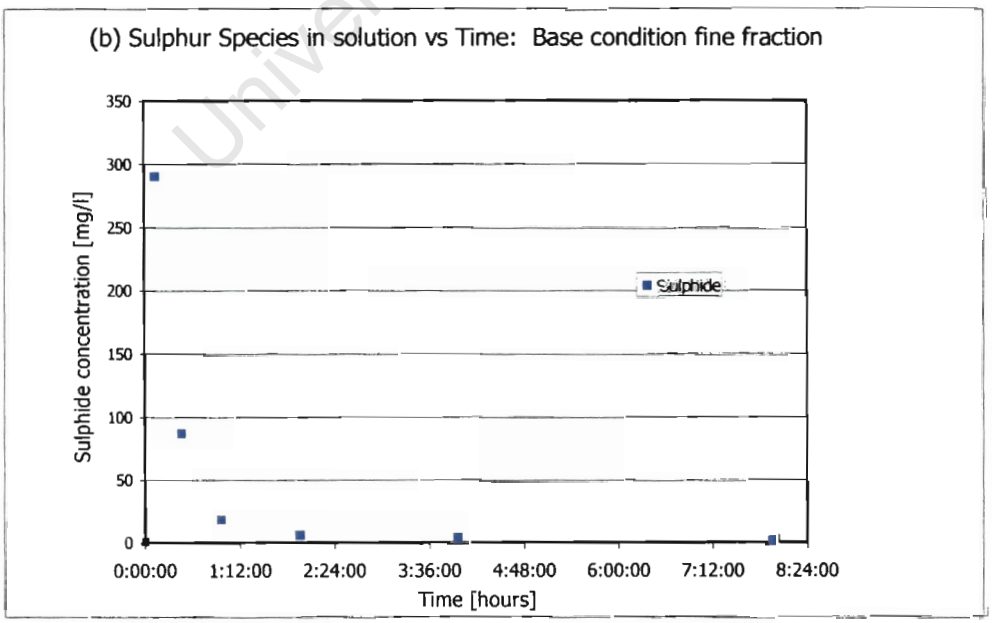

Figure 5.2-1 (a) and (b) Thiosulphate and sulphide concentration graphs for the fine fraction of slag N under base conditions

Figure 1 (a) and (b) of Appendix H-1 compare the sulphide and thiosulphate concentrations respectively for experiments 1 to 5. Note that, unlike the values of Table 5.2-1 and Table 5.2-2, which were based on percentages of the sulphur in each slag sample fed to each of the experiments, these concentration graphs are not directly comparable to each other. The reason for this is that there would be differences in the quantity of sulphur in each slag sample fed to each of the experiments due to slag sampling error.

It is evident that the concentration trends in the sulphide and thiosulphate graphs of Figure 1 (a) and (b) of Appendix H-1 are similar for experiments 1 to 5. Appendix H-1 also gives the equivalent graphs for the coarse fraction in Figure 2 (a) and (b).

Figure 5.2-2 (a) and (b) compare the sulphur species in solution for typical fine fraction and coarse fraction experiments 1 and 12 respectively. Figure 5.2-2(a) shows that the conversion to thiosulphate remains higher throughout the experiment for the fine fraction. It is evident that the thiosulphate production rate is greater towards the end of the experiment for the coarse fraction and that the difference in thiosulphate concentration is decreasing.

The 10 minute sulphide concentration readings shown on Figure 5.2-2(b) indicates that the initial sulphide leaching rate of the fine fraction significantly exceeds that of the coarse fraction. The fine fraction experiments 1 to 5 reached a zero value before 18h45, with experiment 5 reaching zero before 8 h. The coarse fraction experiments (9 to 13 in Appendix G) all reached zero before 24 h, with the exception of experiment 12, for which a zero sulphide concentration value was only measured at 36 h.

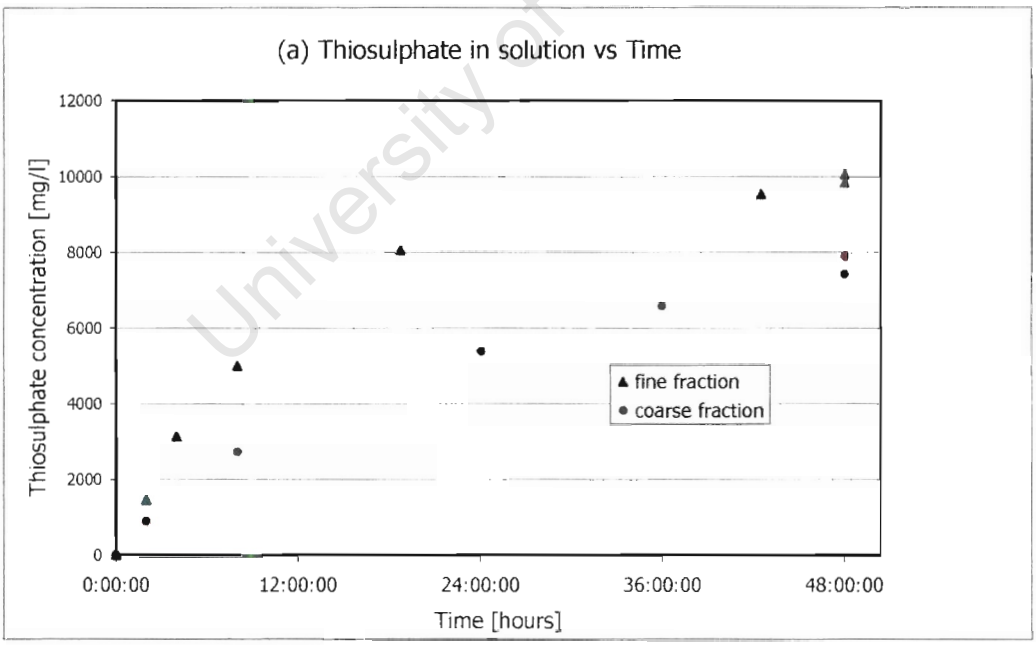

Figure 5.2-2 (a) Comparison of fine fraction and coarse fraction thiosulphate concentration graphs for leach – oxidation of slag N under base conditions.

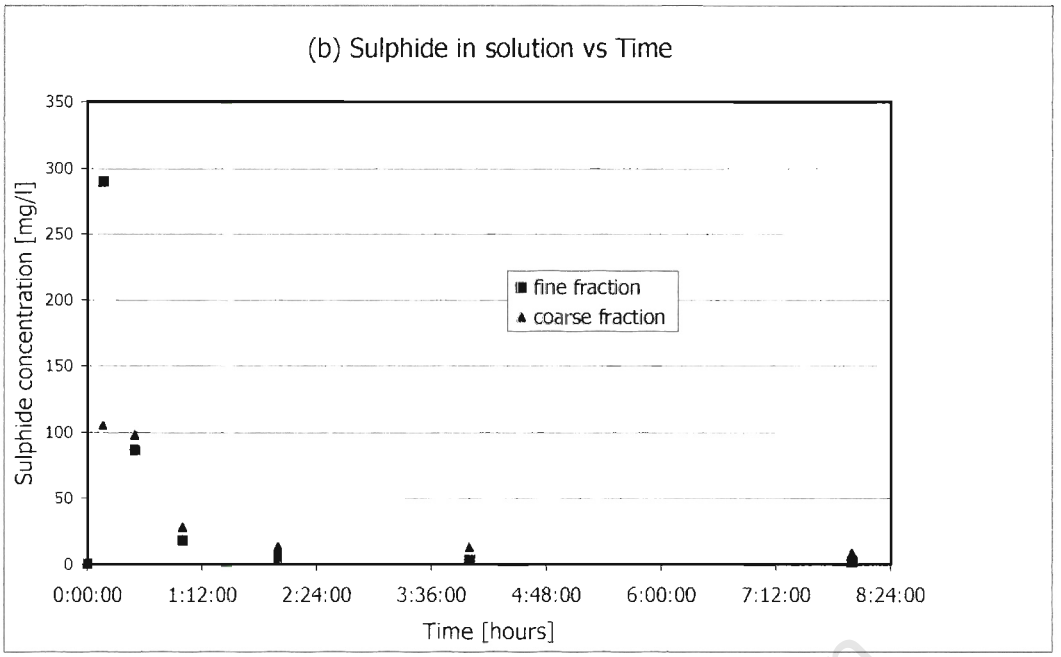

Figure 5.2-3 (b) Comparison of fine fraction and coarse fraction sulphide concentration graphs for leach – oxidation of slag N under base conditions.

5.2.4 Sodium leaching

Table 5.2-5 and Table 5.2-6 show the percent of the sodium present in the feed slag reporting to the aqueous phase during the leach-oxidation of the fine fraction. Analysis of the insoluble product for sodium, to complete the mass balance, revealed a systematic error. Silica from the glass digestion containers, used for the analysis of the insoluble product, was found to leach into the digested sample. Thus, these results are not reported. Although the mass balance cannot be confirmed, Table 5.2-5 and Table 5.2-6 indicate that a significant proportion of the sodium present in the feed slag remains in the insoluble product phase. Comparison of Table 5.2-5 and Table 5.2-6 shows that sodium extraction to the aqueous phase from the fine fraction was greater than the extraction from the coarse fraction.

Slag Type	Reactor Used	Run number	Feed slag sodium extracted to aqueous phase
N	1.5 l	3	85.3%
	1.5 l	4	77.6%
O	1.5 l	7	82.2%

Table 5.2-5 Recovery of sodium present in the feed slag to the aqueous phase

Slag Type	Reactor Used	Run number	Feed slag sodium extracted to liquid phase
N	1.5 l	10	66.9%
O	1.5 l	14	71.5%

Table 5.2-6 Recovery of sodium present in the slag to aqueous phase during leach – oxidation of the coarse fraction

Figure 5.2-4 shows the sodium leaching graphs for experiments 4 and 10. A rapid initial leaching rate is evident for the first hour of the experiment followed by a progressively more gradual increase in sodium concentration until the end of the experiment. Figure 5.2-4 also shows the comparison between sodium leaching from the fine fraction and the coarse fraction. The initial sodium leaching rate is higher for the fine fraction and the concentration remains higher for this fraction throughout the experiment.

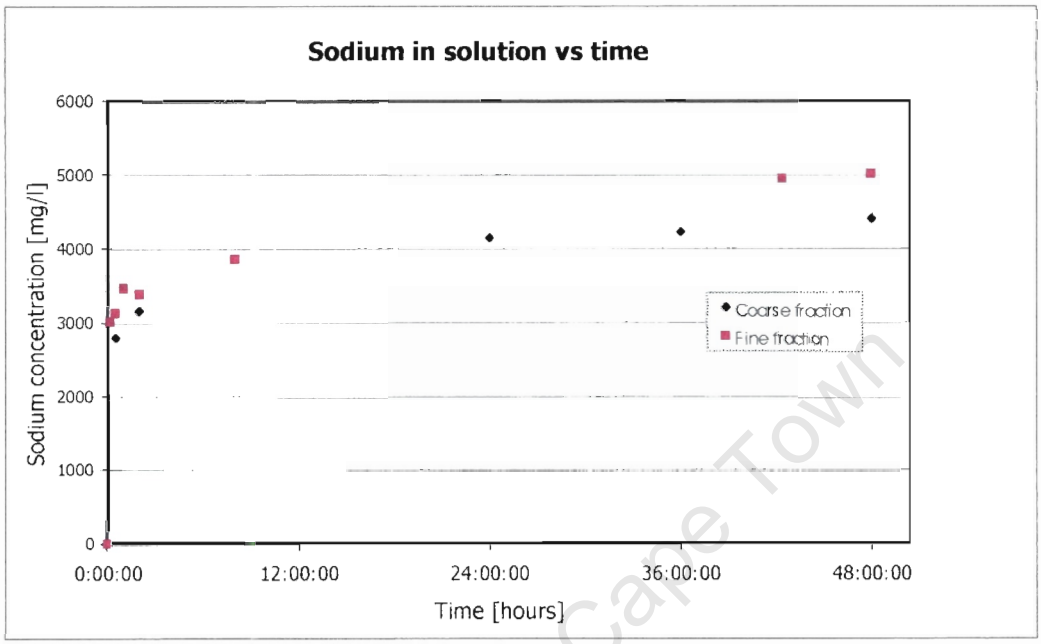

Figure 5.2-4 Sodium concentration in solution during the leach – oxidation experiment for fine fraction and coarse fraction of slag N

5.2.5 Iron leaching

Figure 5.2-5 shows the leaching of iron from the slag for experiments 4 and 10. Analysis of the end-of-run reaction solution showed that a low concentration of iron was recovered to the aqueous product phase (0.6 mg/l for experiment 4). Analysis of the insoluble product confirmed that the iron remains in the insoluble product fraction at the end of the experiment. Figure 5.2-5 shows that the iron concentration reaches a maximum value early in the experiment, followed by a rapid decrease. A maximum iron concentration of 23 mg/l was found for experiment 4 after 30 minutes. At this time, the sulphide concentration of the solution was 82.4 mg/l. The maximum solubility in 18 °C water for ferrous sulphide is 6.2 mg/l (Section 2.4.1). The iron and sulphur present in solution at this time exceeds this value. Figure 5.2-5 also shows that, similarly to the sulphide and sodium cases, the initial leaching rate of iron is greater for the fine fraction, and a higher maximum concentration is reached.

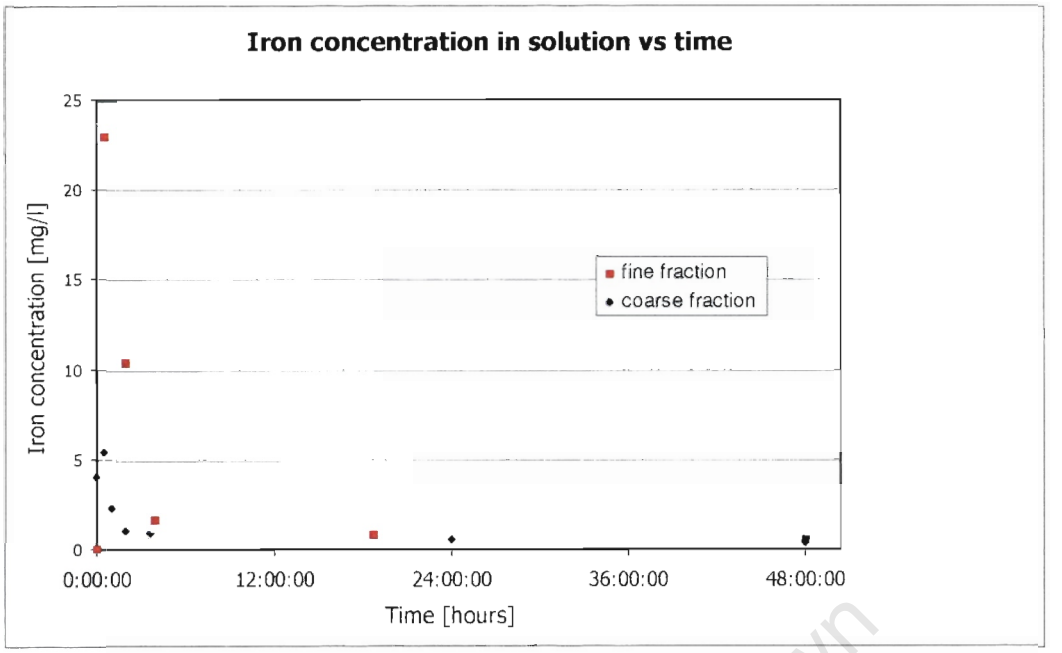

Figure 5.2-5 Iron concentration in solution during a typical leach – oxidation experiment for the fine fraction and the coarse fraction of slag N

5.2.6 pH change during leach - oxidation

Figure 5.2-6 shows that the pH of the reactor solution decreases from a value between 12.5 and 13.0 to a value between 11.5 and 12.0 during the course of the leach – oxidation experiment. The greatest decrease occurs during the first 24 hours.

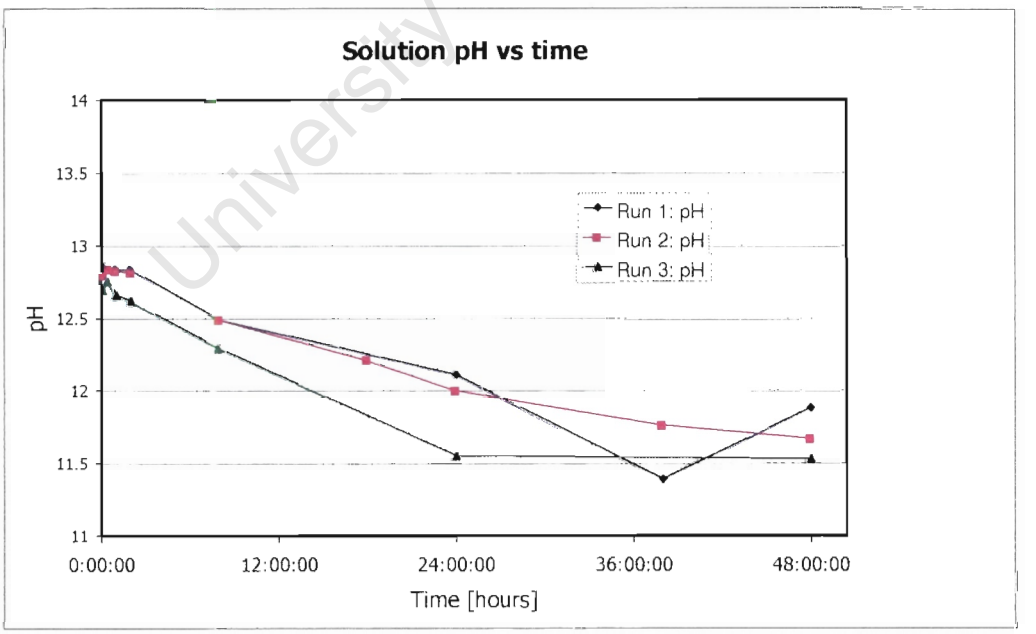

Figure 5.2-6 pH during base condition leach – oxidation experiments 1 to 3 for the fine fraction of slag N

5.2.7 Observations during a leach – oxidation experiment

Observations were recorded of the colour of the filtered and unfiltered solution during the leach – oxidation experiment. This provides additional evidence for the species present in the solution at various times. During the first four hours, the filtered solution was green; this became progressively paler (often a pale yellow) and typically became clear after 8 hours. The unfiltered solution remained black for the first 24 hours, after which it became progressively more brown. The final colour was dark brown for the base condition experiments, but was reddish brown for the high temperature experiments as described in Section 5.3.1. A dense finely divided solid caused the colour of the unfiltered solution. A picture of the insoluble product is shown in Appendix I.

5.2.8 Comparison between the slag types N and O

The end-of-run conversions to thiosulphate for the coarse fraction experiments of slag O (experiment 14 and 15) both exceed the average slag N conversion in excess of 2 standard deviations. As expected, the sulphur extraction from these slag O experiments was also correspondingly greater that that of slag N. However, this trend was not evident from the results of the fine fraction experiments. Comparison of the species in solution during the experiment is not valid, as slag types N and O contain differing sulphur compositions.

5.2.9 Comparison of reactors of differing volumes

Comparison between the results obtained under the same conditions of the 1.5 litre and 4 litre reactors is shown in Table 5.2-1. In the case of slag N, the overall slag remaining insoluble for the 4 litre reactor (experiment 6) exceeded all the 1.5 litre results. The sulphur extraction to the aqueous phase for experiment 6 was exceeded by all the 1.5 litre reactor results except one, which was matched. The conversion to thiosulphate for experiment 6 was similar to the 1.5 litre results. Too few results were obtained for slag O to make a significant comparison.

5.3 Investigation of conditions that affect the leach – oxidation process

5.3.1 Temperature

Table 5.3-1 and Table 5.3-3 show the effect of varying the temperature on results obtained from leach – oxidation experiments run at on fine fraction and coarse fraction samples of slag N and O respectively.

Slag Type	Temperature [°C]	Overall percent of feed slag remaining insoluble	Feed slag sulphur remaining in insoluble phase	Recovery of feed slag sulphur to aqueous phase oxidised sulphur species (mass basis)		Sulphur accounted for by product phases as percent of feed slag sulphur
				Conversion to thiosulphate	Conversion to sulphate	
N	20	78.5%	39.0%	55.8%	0.1%	95.0%
	40	74.8%	24.7%	75.2%	0.4%	100.3%
	60	71.5%	3.7%	112.8%	0.8%	117.2%
O	20	77.6%	52.9%	53.4%	0.4%	106.6%
	40	70.5%	18.0%	84.8%	0.8%	103.6%
	60	69.0%	7.9%	105.4%	6.5%	119.7%

Table 5.3-1 Recovery of sulphur present in the slag to product phases of the fine fraction

Insoluble product

The end-of-run results of Table 5.3-1 and Table 5.3-3 show that operation at elevated temperature increases the overall extraction of slag to the aqueous phase. A substantial decrease in sulphur remaining in the insoluble product was evident for both types of slag. The preferential extraction of sulphur out of the slag at elevated temperatures was best shown in Table 5.3-2 for the fine fraction.

Slag Type	Parameter value [°C]	Overall percent of feed slag remaining insoluble	Sulphur composition of insoluble phase
N	20	78.5%	10.1%
	40	74.8%	6.7%
	60	71.5%	1.2%
O	20	77.6%	12.7%
	40	70.5%	4.9%
	60	69.0%	2.2%

Table 5.3-2 End-of-run sulphur composition of the insoluble phase at varied temperatures for the fine fraction

Comparison of Table 5.3-1 and Table 5.3-3 shows that increasing the temperature from 20 °C to 60 °C had a greater effect on sulphur extraction for the fine fraction (35 % increase) than the coarse fraction (26.8 % increase). The insoluble product was a lighter, more reddish brown colour for the higher temperature experiments than under base condition experiments.

Slag Type	Parameter value [°C]	Overall percent of feed slag remaining insoluble	Feed slag sulphur remaining in insoluble phase	Recovery of feed slag sulphur to aqueous phase oxidised sulphur species (mass basis)		Sulphur accounted for by product phases as percent of feed slag sulphur
				Conversion to thiosulphate	Conversion to sulphate	
N	20	84.9%	47.7%	39.6%	0.0%	87.3%
	40	89.9%	57.6%	36.4%	0.0%	94.0%
	60	73.7%	20.9%	77.7%	0.5%	99.1%
	80	71.1%	11.4%	89.1%	0.6%	101.1%
O	20	84.8%	44.4%	46.3%	0.0%	90.7%
	40	81.2%	30.9%	57.5%	0.2%	88.6%
	60	78.3%	36.0%	65.6%	0.6%	102.2%
	80	64.2%	8.0%	88.7%	9.0%	105.6%

Table 5.3-3 Recovery of sulphur present in the slag to product phases of the coarse fraction

Soluble product

Table 5.3-1 and Table 5.3-3 show that the conversion to thiosulphate increases substantially as the operating temperature is increased. The end-of-run fine fraction results (Table 5.3-1) show a doubling of the conversion to thiosulphate by increasing the temperature from 20 °C to 60 °C for both slag types. The coarse fraction results (Table 5.3-3) showed a smaller increase in conversion for the same temperature increase, corresponding to the smaller increase in sulphur extraction from the insoluble product.

The recovery to thiosulphate in Table 5.3-1 in excess of 100% of the slag feed sulphur indicates an experimental error. Either the value for the slag feed sulphur was over estimated (due to sampling error or analytical error) or the thiosulphate concentration reading was too high. The latter is possible as the sample thiosulphate concentrations fell outside of the expected concentration range for which the equipment was calibrated.

Table 5.3-1 shows that for slag N, a steady increase in conversion to sulphate occurred with increasing temperature, although the conversion remains low. However, for slag O, a substantial increase was evident in sulphate conversion for the 60 °C fine fraction and 80 °C coarse fraction experiments. No other experiments in the experimental program showed this substantial increase in sulphate conversion.

Figure 5.3-1(a) and (b) show the graphs of the oxidised sulphur species and sulphide respectively at different temperatures for the fine fraction of slag O. Comparison between the 8 h thiosulphate concentration readings, shown in Figure 5.3-1(a), reflect the same trend in variation between temperatures as shown the end-of-run 48 h conversions in Table 5.3-3, i.e. a substantially increased thiosulphate conversion with increasing temperature. Less variation in thiosulphate conversion is evident from the 2 h readings, particularly between the 20 °C and 40 °C readings. Figure 5.3-1(a) also shows that the thiosulphate production rate for the 60 °C run is lower between 24 h and 48 h relative to the first 24 h.

Figure 5.3-1(b) shows that the 10 min sulphide concentration decreases with increasing temperature. For both the elevated temperature experiments, 40 °C and 60 °C, the sulphide concentration reached zero before 8 h.

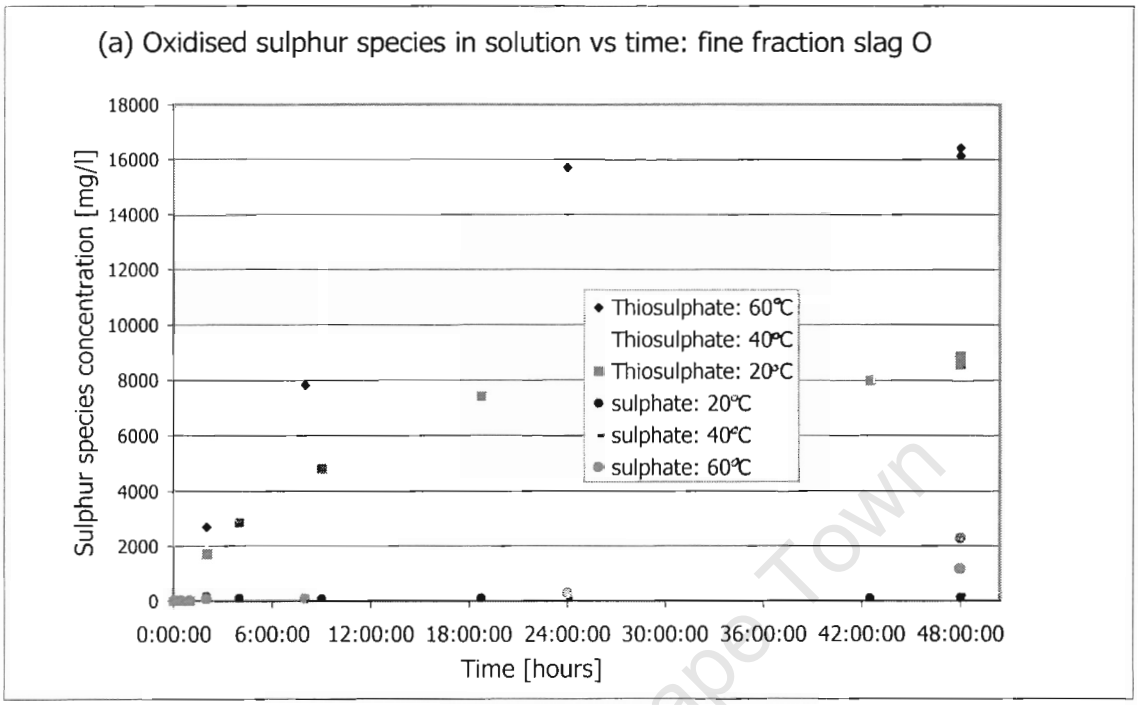

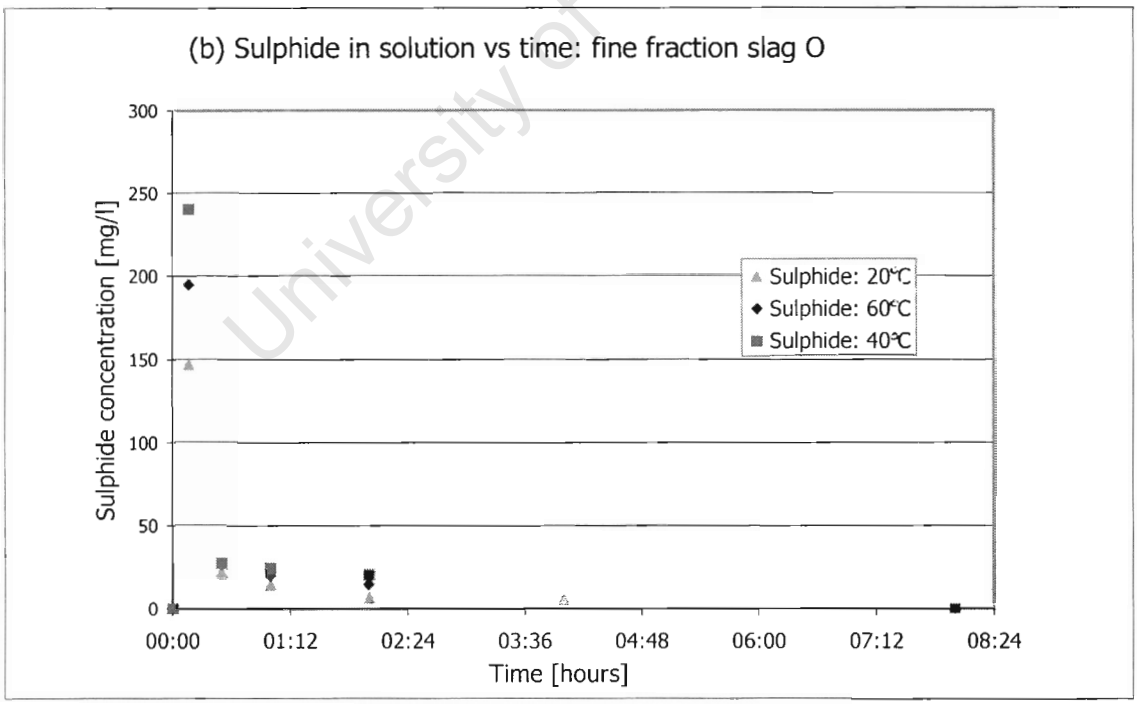

Figure 5.3-1 (a) and (b) Oxidised sulphur species (a), and sulphide (b), concentration graphs for the fine fraction of slag O: variation of temperature

Slag Type	Agitation rate	Overall percent of feed slag remaining insoluble	Feed slag sulphur remaining in insoluble phase	Recovery of feed slag sulphur to aqueous phase oxidised sulphur species (mass basis)		Sulphur accounted for by product phases as percent of feed slag sulphur
				Conversion to thiosulphate	Conversion to sulphate	
N	200 rpm	80.4%	43.2%	48.2%	0.0%	91.4%
	600 rpm	78.5%	39.0%	55.8%	0.1%	95.0%
	1200 rpm	75.5%	37.0%	57.5%	0.1%	94.7%

Table 5.3-4 Recovery of sulphur present in the slag to product phases of the fine fraction: variation of agitation rate

Insoluble products

Table 5.3-4 shows that for the fine fraction there is a steady increase in the overall quantity of slag extracted to the aqueous phase with increased agitation rate. Table 5.3-6 shows that, for the coarse fraction experiments, the substantial increase in overall extraction occurs for the increase from 600 rpm to 1200 rpm. In terms of sulphur extraction, the increase is greater from 200 rpm to 600 rpm than from 600 rpm to 1200 rpm for the fine fraction experiments. The coarse fraction results follow the same trend, although the increase in sulphur extraction for the coarse fraction, corresponding to a stirring rate increase from 600 rpm to 1200 rpm, is higher. For the fine fraction, increasing the stirring rate from 200 rpm to 1200 rpm resulted in a 5 % increase in overall extraction and a 6 % increase in sulphur extraction. For the coarse fraction, the same agitation increase caused a 9 % increase in overall extraction and 14 % increase in sulphur extraction.

Slag Type	Stirring rate	Overall percent of feed slag remaining insoluble	Sulphur composition of insoluble phase
N	200 rpm	79.1%	10.6%
	600 rpm	78.5%	10.1%
	1200 rpm	75.5%	10.0%

Table 5.3-5 Sulphur composition of the insoluble phase at varied stirring rates for the fine fraction

Comparison of the increase in overall extraction with the sulphur composition of the resulting insoluble phase in Table 5.3-5 for the fine fraction shows that the removal of sulphur from the slag does not occur selectively with increased agitation.

Slag Type	Agitation rate	Overall percent of feed slag remaining insoluble	Feed slag sulphur remaining in insoluble phase	Recovery of feed slag sulphur to aqueous phase oxidised sulphur species (mass basis)		Sulphur accounted for by product phases as percent of feed slag sulphur
				Conversion to thiosulphate	Conversion to sulphate	
N	0 rpm	91.8%	66.7%	20.1%	0.0%	86.9%
	200 rpm	82.5%	54.2%	34.1%	0.0%	88.3%
	600 rpm	84.8%	44.4%	46.3%	0.0%	90.7%
	1200 rpm	73.3%	39.8%	46.8%	0.0%	86.6%

Table 5.3-6 Recovery of sulphur present in the slag to product phases of the coarse fraction: variation of agitation rate

Soluble products

The trend observed in the increase in sulphur extraction with increased agitation rate is echoed by the trend in the conversion to thiosulphate.

Comparison of the thiosulphate production graphs in Figure 5.3-2(a) for the fine fraction shows that the 600 rpm and 1200 rpm graphs are generally closer over the experiment than the 200 rpm graph.

The 10 min sulphide concentrations of Figure 5.3-2(b) appear to show that the 600 rpm experiment had the highest maximum and the 1200 rpm experiment had the lowest maximum. The 600 rpm and 1200 rpm experiments both obtained a zero sulphide concentration by 18h45. However, the 200 rpm experiment still had not obtained a zero value by 24 h.

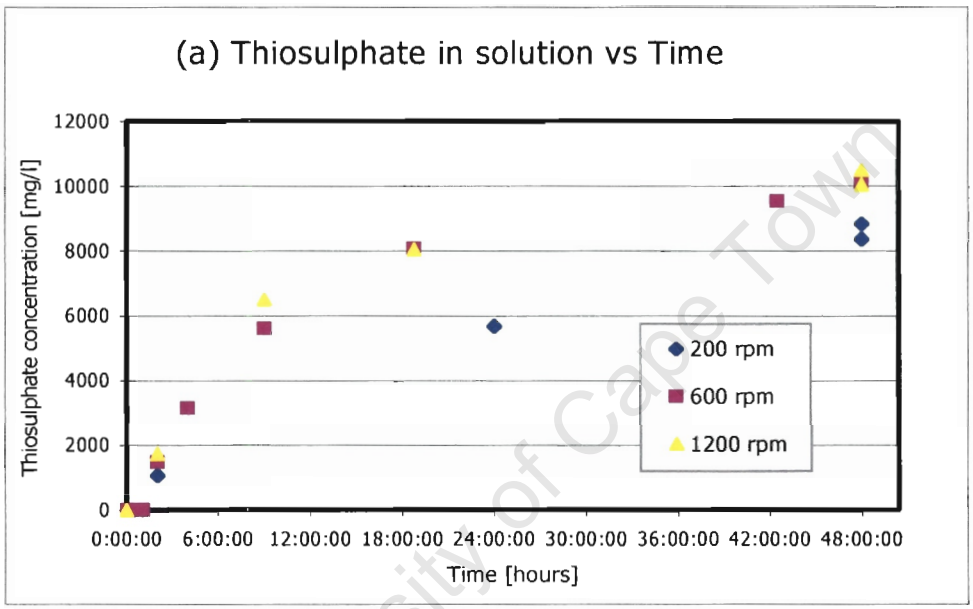

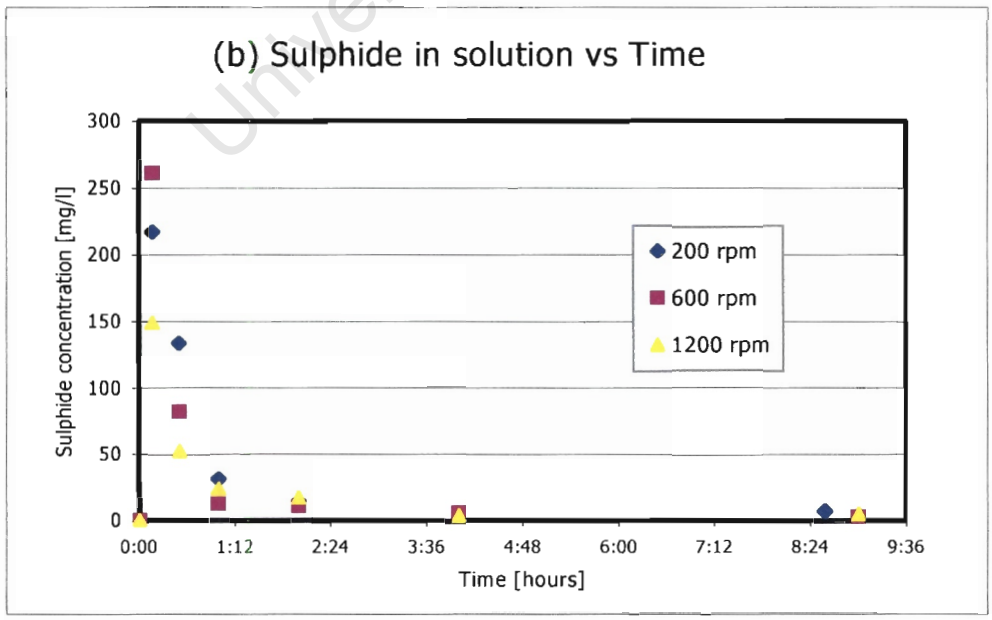

Figure 5.3-2(a) and (b) Thiosulphate and sulphide concentration curves for varied agitation of the fine fraction

Comparison of the sodium concentration graphs of Figure 5.3-3 for the fine fraction shows that the sodium leaching of the 600 rpm and 1200 rpm experiments are closer than the 200 rpm experiment. The sodium leaching rate of the 200 rpm experiment is significantly lower that the 600 rpm and 1200 rpm experiments after the initial rapid increase in sodium concentration. The equivalent graph for the coarse fraction agitation experiments is given in Figure 1 of Appendix H-2.

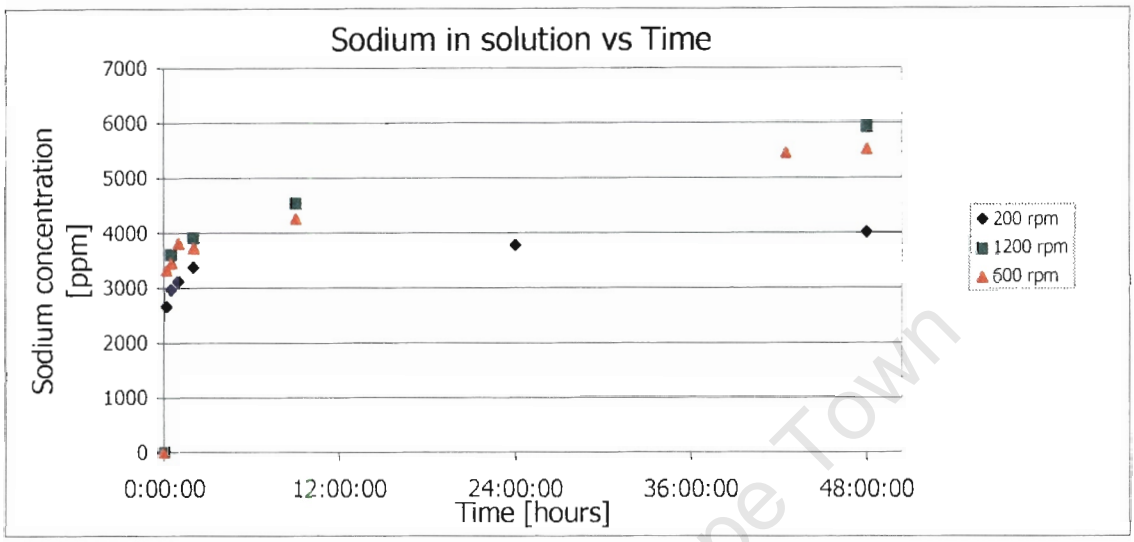

Figure 5.3-3 Sodium concentration dependence on agitation rate for the fine fraction

5.3.3 Solid to liquid ratio

Table 5.3-7 and Table 5.3-8 summarise the effect of varying the solid to liquid ratio on the end-of-run results for the fine fraction and the coarse fraction respectively. The solid to liquid ratio was varied by changing the mass concentration of slag in the reactor solution.

Slag Type	Mass concentration of slag	Overall percent of feed slag remaining insoluble	Feed slag sulphur remaining in insoluble phase	Recovery of feed slag sulphur to aqueous phase oxidised sulphur species (mass basis)		Sulphur accounted for by product phases as percent of feed slag sulphur
				Conversion to thiosulphate	Conversion to sulphate	
N	50 g/l	79.2%	34.6%	59.5%	0.0%	94.1%
	100 g/l	77.8%	31.3%	63.9%	0.2%	95.4%
	133 g/l	76.1%	31.0%	64.9%	0.1%	96.0%

Table 5.3-7 Recovery of sulphur present in the slag to product phases of the fine fraction

Insoluble products

The results of both fine fraction and coarse fraction experiments show an increase in the end-of-run sulphur extraction from the insoluble phase as the solid to liquid ratio is increased. The sulphur extraction increase is higher for the increase in solid to liquid ratio from 50 g/l to 100 g/l than for the increase from 100 g/l to 133 g/l. A significant increase is also evident from 25 g/l to 50 g/l for the coarse fraction.

However, no significant increase in extraction of sulphur occurs for either starting size when increasing the mass concentration from 100 g/l to 133 g/l. The fine fraction shows a small but steady increase in overall slag extraction and approximately a 3 % increase in sulphur extraction for an increase in mass concentration of 50 g/l to 133 g/l. For the corresponding mass concentration increase, the coarse fraction does not show any detectable trend in the overall slag extraction, but an increase in sulphur extraction of approximately 5 %.

Slag Type	Mass concentration of slag	Overall percent of feed slag remaining insoluble	Feed slag sulphur remaining in insoluble phase	Recovery of feed slag sulphur to aqueous phase oxidised sulphur species (mass basis)		Sulphur accounted for by product phases as percent of feed slag sulphur
				Conversion to thiosulphate	Conversion to sulphate	
N	25 g/l	83.1%	54.6%	38.3%	0.0%	92.9%
	50 g/l	81.8%	52.6%	43.4%	0.0%	96.0%
	100 g/l	84.0%	47.6%	44.2%	0.0%	91.8%
	133 g/l	82.9%	47.5%	48.5%	0.0%	96.0%

Table 5.3-8 Recovery of sulphur present in the slag to product phases of slag in the coarse fraction

Soluble products

The trend observed in the increase in sulphur extraction with increased solid to liquid ratio is echoed by the trend in the conversion to thiosulphate for the fine fraction. However, for the coarse fraction, a greater increase in conversion occurs between 100 mg/l and 133 g/l, despite no increase being evident in sulphur extraction. The poor mass balance for the 100 g/l experiment indicates the likelihood of error in this result.

Figure 5.3-4 shows that the initial thiosulphate concentration increase is greater for the 100 g/l and 133 g/l mass concentration experiments than the 50 g/l experiment. The thiosulphate production rate does fall appreciably towards the end of the experiment, which was the case with the 50 g/l experiment. The only one thiosulphate concentration measurement for the 133 g/l experiment was successfully made at 48 h, the second unsuccessful reading is represented by the point (48 h, 0 mg/l).

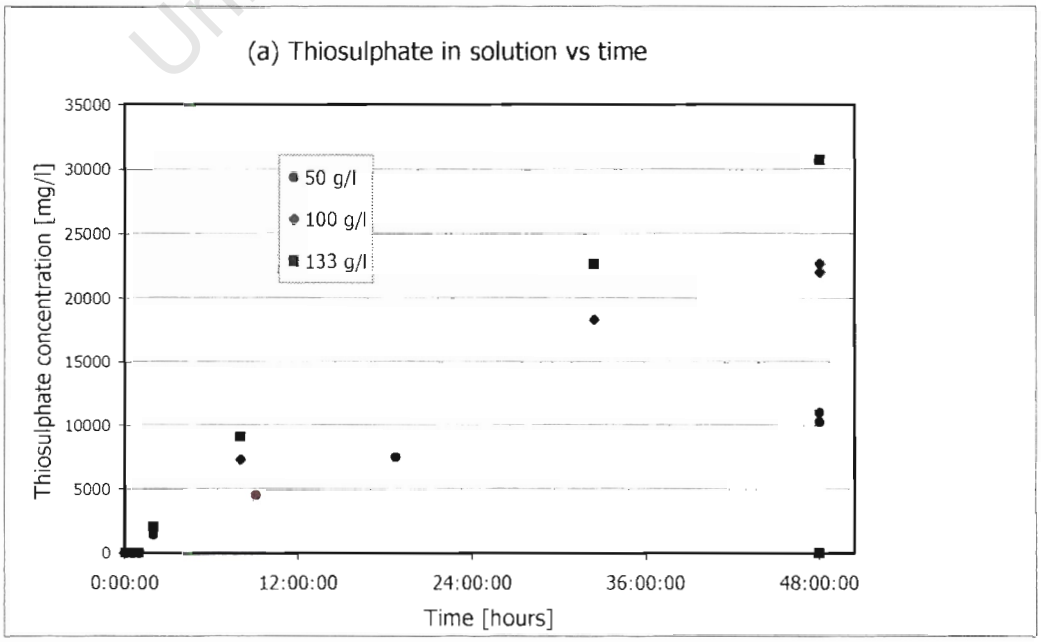

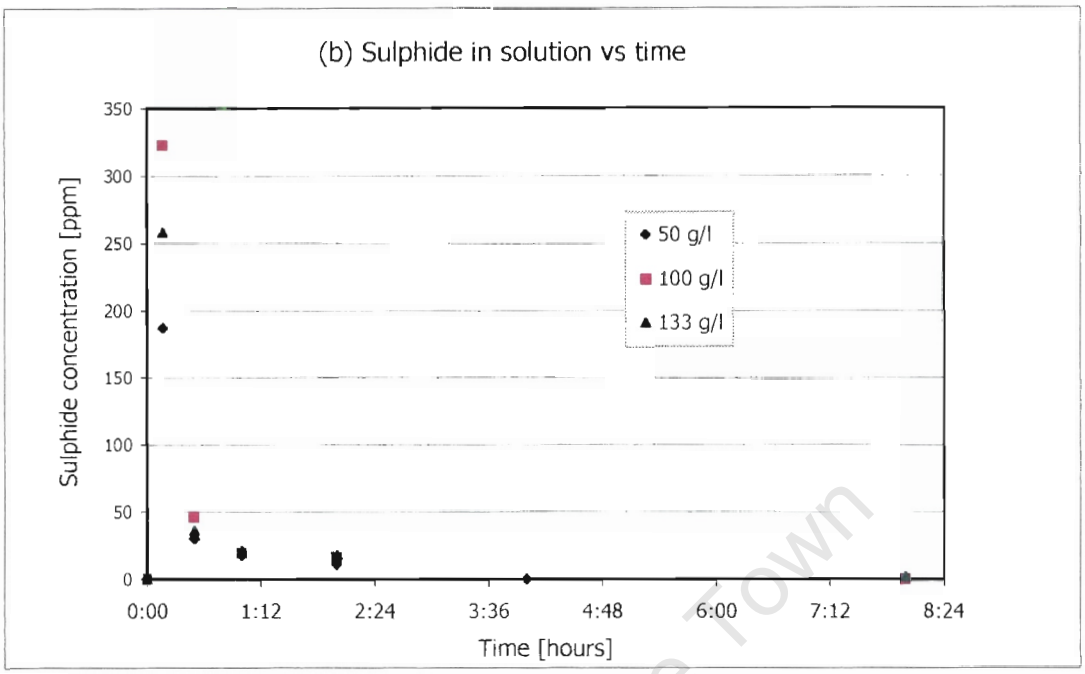

Figure 5.3-4 (a) and (b) Thiosulphate and sulphide concentration curves for experiments of different solid to liquid ratio for the fine fraction of slag N

The 10 min sample sulphide concentration for the 100 g/l experiment exceeded the reading for the 50 g/l sample appreciably. However, the difference between these two concentrations was not double, as may be expected from the difference in the respective experiments' mass concentrations. A sulphide concentration of zero was obtained for the 50 g/l experiment at 8 h, at which time the sulphide concentrations for the 100 mg/l and 133 mg/l experiments were 0.6 and 2.4 mg/l respectively. The 100 mg/l experiment's sulphide concentration was zero at 24 h, while that of the 133 g/l experiment only was found to be zero only at 32h25.

5.3.4 Particle starting size

Table 5.3-9 shows the effect of particle starting size on end-of-run results for slag O and slag N.

Slag Type	Particle Size	Overall percent of feed slag remaining insoluble	Feed slag sulphur remaining in insoluble phase	Recovery of feed slag sulphur to aqueous phase oxidised sulphur species (mass basis)		Sulphur accounted for by product phases as percent of feed slag sulphur
				Conversion to thiosulphate	Conversion to sulphate	
N	11.2 - 8.0 mm	83.3%	45.7%	43.9%	0.0%	89.7%
	4.0 - 4.75 mm	84.5%	48.5%	47.2%	0.2%	95.9%
	1.4 - 2.0 mm	81.3%	39.0%	46.3%	0.2%	85.5%
	0.6 - 1.0 mm	78.4%	37.3%	49.6%	0.3%	87.2%
	Fine fraction *	76.9%	35.8%	57.6%	0.1%	
O	11.2 - 8.0 mm	80.7%	39.3%	45.5%	0.3%	85.1%
	4.0 - 4.75 mm	79.7%	40.2%	47.2%	0.4%	87.7%
	1.4 - 2.0 mm	79.0%	38.5%	48.6%	0.4%	87.5%
	0.6 - 1.0 mm	75.8%	38.0%	52.2%	0.6%	90.8%
	Fine fraction *	78.8%	37.4%	58.3%	0.5%	96.2%

Table 5.3-9 Recovery of sulphur present in the slag to product phases (* averaged fine fraction results from Table 5.2-1 and Table 5.2-2 for slag N and O respectively)

Insoluble product

Table 5.3-9 shows that a decrease in the feed slag particle size generally causes an increased overall slag extraction and sulphur extraction for both slag types. The 4.0 – 4.75 mm size fraction was an exception to this trend.

Soluble product

The end-of-run thiosulphate conversion trend generally reflected the sulphur extraction trend, showing an increase as the particle size was decreased. A calculation of the surface area difference between the largest size fraction (average diameter of 9.6 mm) and the smallest size fraction (average diameter of 0.8 mm), shows that the smaller fraction has a surface area of approximately 12 times that of the larger fraction for the same mass (assuming spherical slag blocks). This increase in surface area was shown in Table 5.3-9 to result in an 5.7 % increase in thiosulphate conversion for slag N and a 6.7 % increase for slag O. A greater increase in conversion is evident from between the 0.6 – 1.0 mm fraction to the fine fraction. The corresponding increase in surface area between these fractions is 16 times if the average fine fraction particle size is estimated as 50 µm.

Figure 5.3-5 indicates that the variation between the thiosulphate concentrations of the different size fraction experiments did not increase significantly after the 8 h sample if the end-of-run readings are averaged.

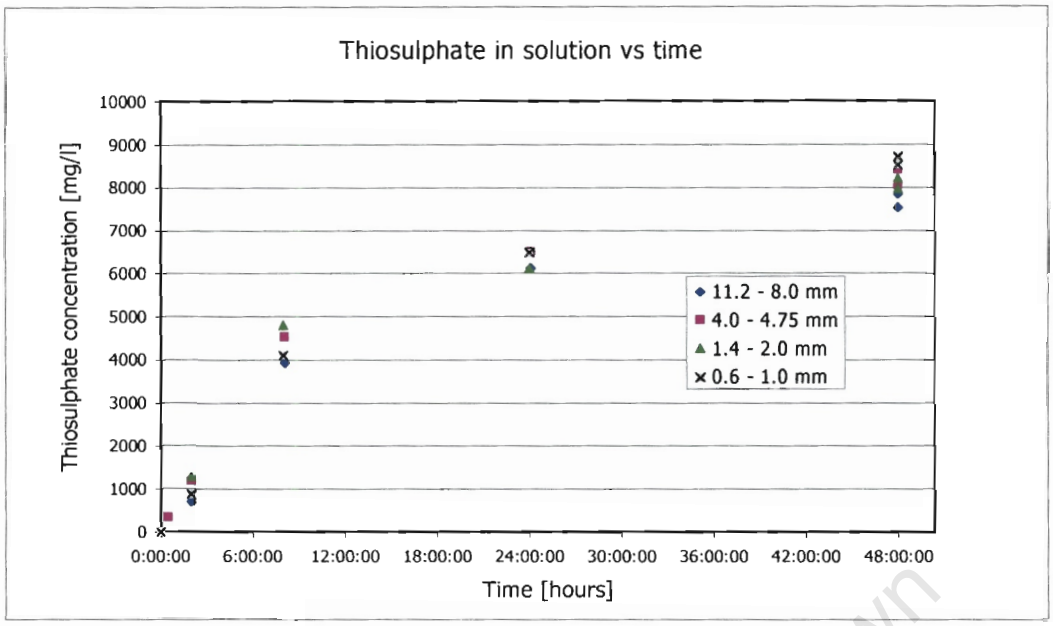

Figure 5.3-5 Thiosulphate concentration curves for slag particles of differing starting particle size for slag N

5.3.5 Air flowrate

Table 5.3-10 shows that doubling the air flowrate does not cause a significant increase in the extraction of sulphur from the slag. This is verified by the small increase in thiosulphate conversion.

Slag Type	Air flowrate	Overall percent of feed slag remaining insoluble	Feed slag sulphur remaining in insoluble phase	Recovery of feed slag sulphur to aqueous phase oxidised sulphur species (mass basis)		Sulphur accounted for by product phases as percent of feed slag sulphur
				Conversion to thiosulphate	Conversion to sulphate	
O	5.3 l/min	78.8%	37.4%	61.0%	0.5%	98.9%
	10.6 l/min	81.9%	36.9%	62.9%	0.3%	100.1%

Table 5.3-10 Recovery of sulphur present in the slag to product phases

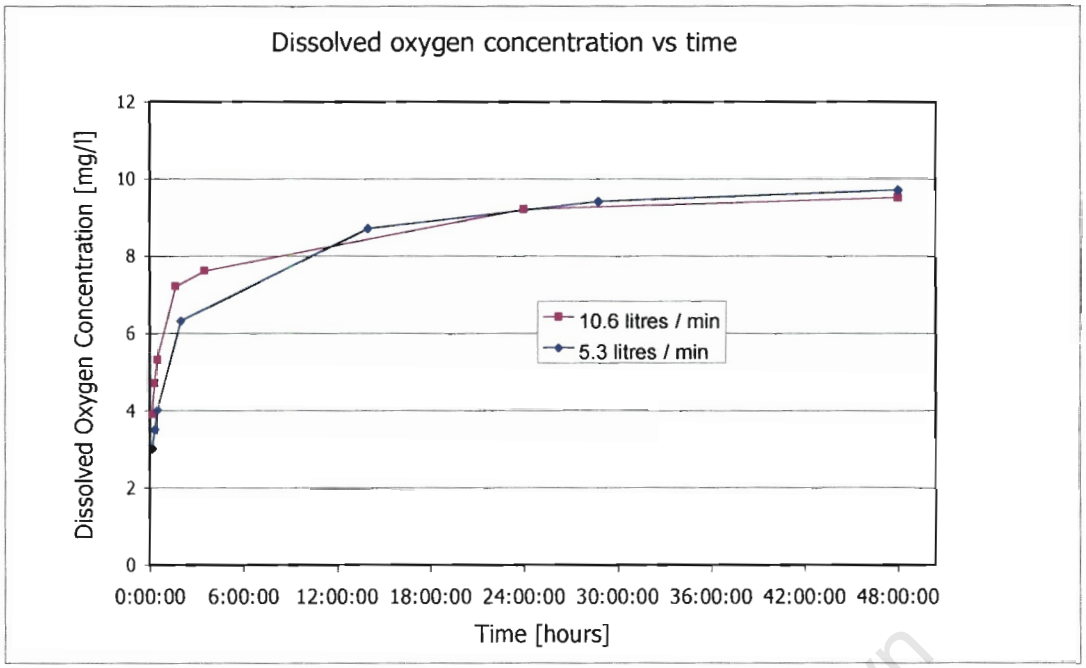

Figure 5.3-6 Dissolved oxygen concentration of reaction solution during experimental air flowrate experiments

Figure 5.3-6 shows that the dissolved oxygen concentration in solution is higher over the first 12 hours for the higher air flowrate experiment. However, this increase is not proportional to the increase in airflow rate between the experiments. The dissolved oxygen concentration reaches a similar maximum for both experiments at the termination of the experiment.

Figure 5.3-7 shows that the thiosulphate concentrations were not significantly increased for the higher air flowrate experiment compared to the base condition flow rate experiment

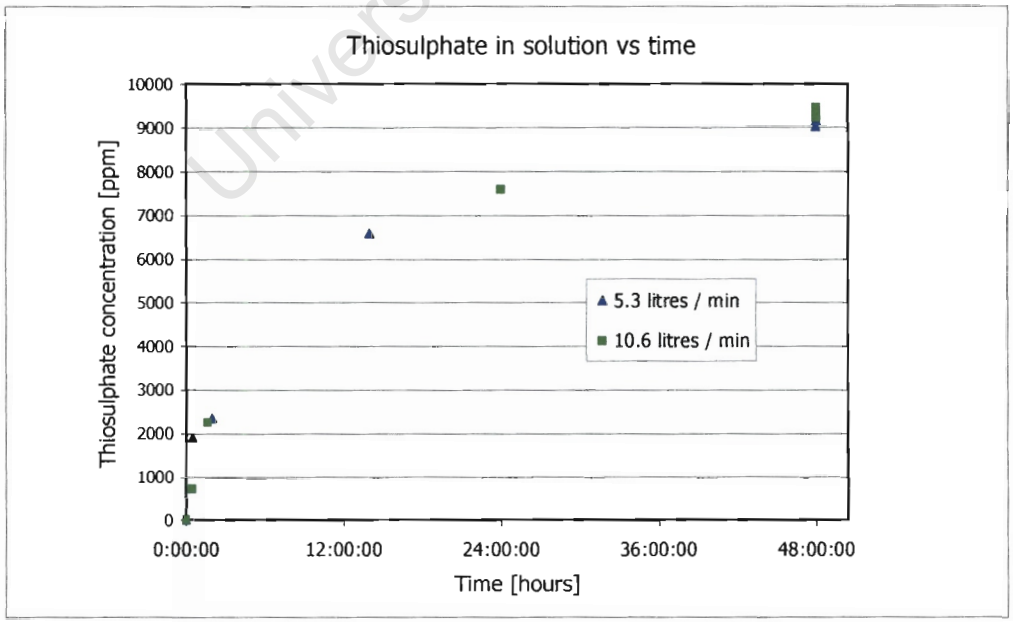

Figure 5.3-7 Thiosulphate concentration in solution as a function of time: variation of airflow rate

5.3.6 Experimental run length

Table 5.3-11 gives the thiosulphate readings for the 48 h and 96 h samples of extended length experiments for slag N and O. Typical insoluble product recoveries and sulphur percent extraction for experiments terminated after 48 hours are given in Table 5.2-1 for comparison to the end-of-run values for the 96 h experiment.

Slag Type	Run length	Overall percent of feed slag remaining insoluble	Feed slag sulphur remaining in insoluble phase	Recovery of feed slag sulphur to aqueous phase oxidised sulphur species (mass basis)		Sulphur accounted for by product phases as percent of feed slag sulphur
				Conversion to thiosulphate	Conversion to sulphate	
N	48 hour			55.7%	0.3%	
	96 hour	71.1%	28.8%	62.0%	0.6%	91.4%
O	48 hour			54.6%	0.1%	
	96 hour	71.5%	30.8%	66.0%	0.2%	96.9%

Table 5.3-11 Recovery of sulphur present in the slag to product phases for one extended fine fraction experiment of each slag type.

Table 5.3-11 shows that doubling the run time results in only a 6.3 % and 8.6 % increase in thiosulphate recovery for slag types N and O respectively. A greater overall conversion to thiosulphate was achieved for slag O.

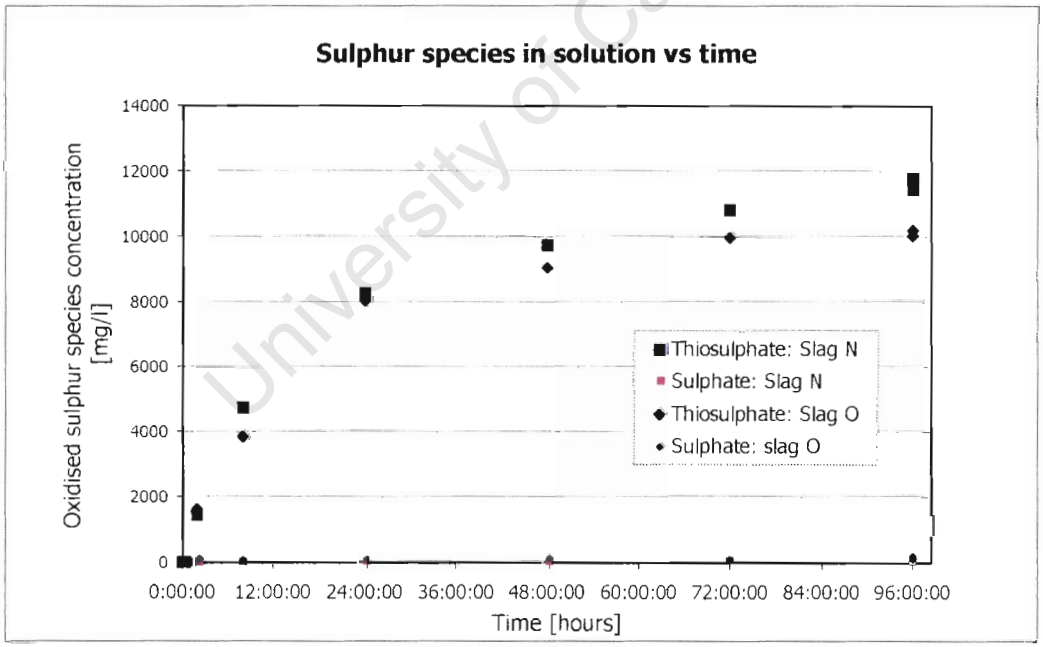

Figure 5.3-8 Thiosulphate concentration as a function of time for base condition extended time experiments

Figure 5.3-8 shows the thiosulphate production graph for extended experiments. Note that the thiosulphate concentrations for slag types N and O are not directly comparable because of the increased sulphur content of slag N. The thiosulphate production rate for slag N is greater for slag O than slag N over the final 48 hours. The thiosulphate production rate of slag O shows little increase over the final 24 hours.

5.4 Investigation of the subprocesses that occur during leach – oxidation

5.4.1 Disintegration rate

Figure 5.4-1 shows graphically the results of the four different disintegration experiments operated as described in Section 4.3.3. The experimental results are shown in full in Table 1 to Table 4 of Appendix G. It must be noted that 100 % disintegration given by the results is not a form where all the components are exposed to the action of the solution, but means that the remaining slag is sufficiently reduced in size to pass through a 9 mm square aperture. This size is equivalent to the coarse fraction size.

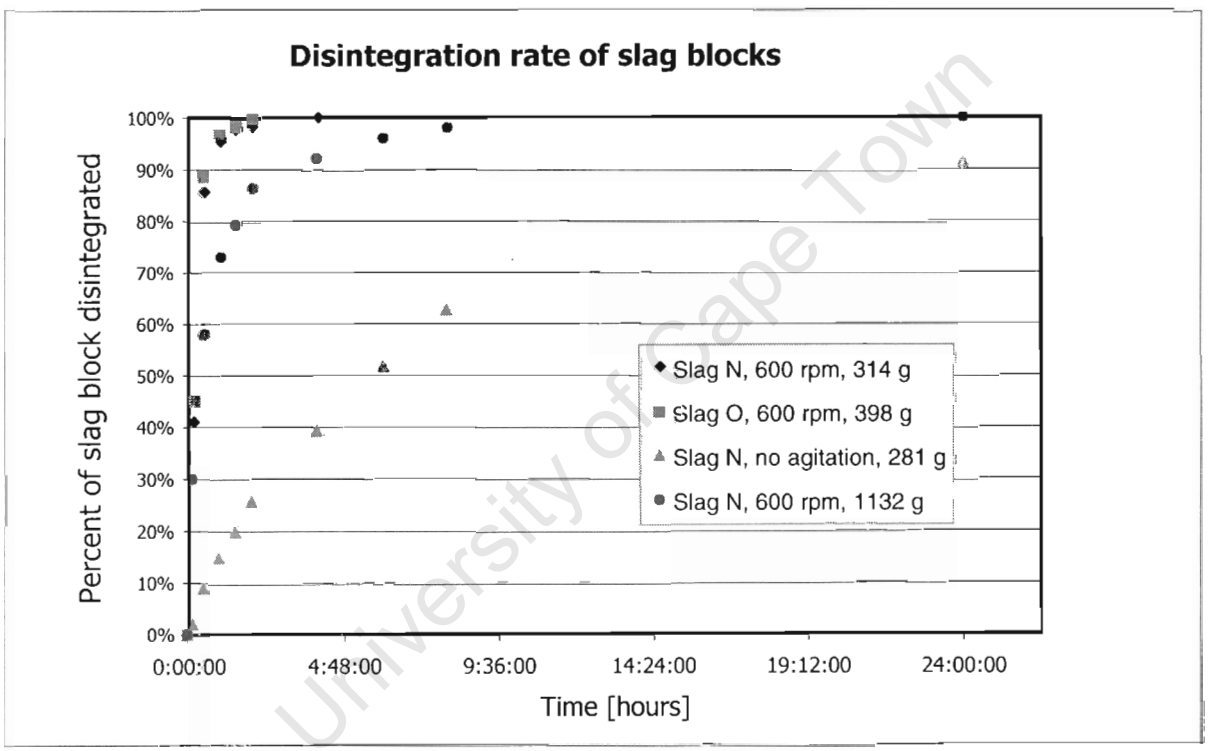

Figure 5.4-1 Disintegration rate graph for slag blocks under different conditions

Effect of agitation

It is apparent from Figure 5.4-1 that agitation substantially increases the disintegration rate. After 60 minutes, the non-agitated experiment (slag N) was 15 % disintegrated, while the agitated experiment (600 rpm, slag N) was 95 % disintegrated. No slag was retained in the sieve for the agitated experiment after 4 hours, while the non-agitated experiment was 91 % disintegrated after 24 h when the experiment was terminated.

Effect of slag mass

The disintegration rate of a slag block was lowered as its mass (hence volume) was increased. This is shown in Figure 5.4-1 by comparing the disintegration of the 313.5 g block of slag N to the 1132.0 g block of slag N. The 313.5 g block was 95 % disintegrated after 60 min at which time the 1132.0 g was 73 % disintegrated. The sieve retained no slag at 4 hours and 24 hours for the 313.5 g block and the 1132.0 g block respectively.

Effect of slag type

Both slag types N and O were rapidly disintegrated in a solution agitated at 600 rpm, achieving 95 % and 97 % disintegration respectively after 60 min. No slag was retained by the sieve after 4 h and 2 h for slag N and O respectively. Slag O was found to have a slightly greater degree of disintegration than slag N at all times during the experiments.

5.4.2 Dissolution

Presentation of dissolution experimental results

The results of these experiments are presented in a graphical and tabular form. The graphs are presented as sulphide or sodium aqueous concentration against experimental run time. The tabulated results include: the measured maximum sulphide concentration; the calculated maximum sulphide concentration reached at the end of the experiment; the fraction of feed slag sulphur that the calculated maximum accounts for; and the calculated initial leach rate constant. An example of graphs from which the initial leach rate constant was calculated is presented in Appendix H-4.

Analysis of dissolution rate data

Besides analysing the effect that various conditions have on this subprocess, an aim of the dissolution rate data analysis was to determine if the first order leach rate equation (equation 2-13) adequately models the dissolution rate of the leachable sulphide. To test the validity, it was necessary to calculate the following constants in equation 2-13: the maximum amount of sulphide that could dissolve from the slag and the leach rate constant. Equation 2-13 is repeated below (terms as defined in chapter 2).

$$\frac{dC}{dt} = k_L(C_{S,MAX} - C) \qquad \text{equation 2-1}$$

Significant depletion of aqueous sulphide during the course of the leaching experiment meant that calculation of the maximum soluble sulphide from the final sulphide concentration was not possible. Instead, this value was calculated from the total sulphur species in solution. This calculation assumes that thiosulphate and sulphate were only produced by oxidation of soluble sulphide during a dissolution experiment.

To determine a leaching constant, the integrated form of equation 2-13 must be used. This is given in equation 2-14. If equation 2-13 explains the dissolution rate data adequately, a plot of the term on the left hand side of equation 2-14 versus time should be linear. The leach rate constant would then be the calculated gradient of this plot. It was found that after 10 min the plotted values no longer followed a linear trend. This was likely to be the result of the increased significance of sulphide depletion via oxidation after this time. Therefore only the initial three sulphide values (0, 5 and 10 min) were used in evaluating the sulphide leach rate constant. As a result of equation 2-13 only being valid for the initial leaching rate (up to 10 min) the leach rate constants calculated for this period will be known as initial leach rate constants. These initial leach rate constants are used in this section to compare the initial sulphide leaching rates under various conditions. An example of the plots of the term on the left hand side of equation 2-16 versus time and the linear fit is given by Figure 1 in Appendix H-4. A sample calculation of the initial sulphide leach rate constant from this plot is also given in Appendix H-4. The sample calculation shows that from the first 10 min of dissolution base experiment 2, a leach rate constant of 76.9 d^{-1} was obtained with a regression coefficient of 0.967 and a relative error of 0.032. The equation for the calculation of the relative error is given in Appendix H-4.

Dissolution of slag under base conditions

Sulphide dissolution

The sulphide leaching trend is shown in the sulphide concentration graph of Figure 5.4-2 obtained under dissolution base conditions for the fine fraction of slag N. The equivalent graph for slag O is given in Figure 1 in Appendix H-3. The sulphide concentration initially increased sharply. Typically the maximum measured sulphide concentration was reached at 60 min. This was followed by gradual decline in the concentration until the dissolution experiment was terminated after 24 h.

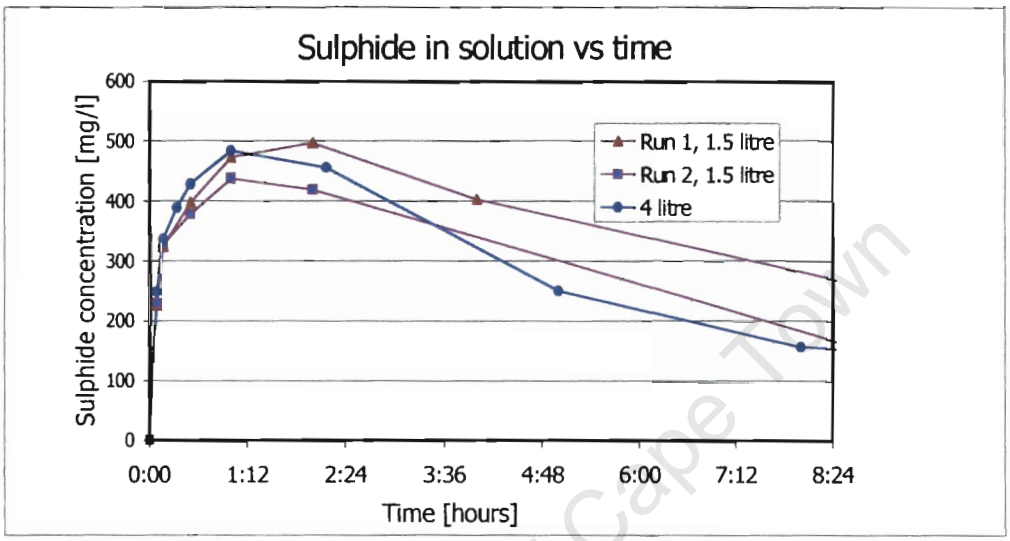

Figure 5.4-2 Sulphide in solution during leaching experiments: the fine fraction of slag N, 1.5 and 4 litre reactor

Table 5.4-1 shows that the maximum measured sulphide reading typically only accounted for approximately 60 % of the calculated maximum soluble sulphide leached. Table 5.4-1 also shows that the calculated maximum soluble sulphide accounts for only a small fraction of the total sulphur in the feed slag. Comparison of these results with the average slag sulphur extraction from base condition leach – oxidation experiments (64.2 % for the fine fraction of slag N from the 1.5 litre reactor) shows that dissolution of the soluble sulphides only accounts for approximately 12 % of the total sulphur extracted.

Slag type	Slag starting condition	Reactor	Run number	Maximum measured sulphide concentration [mg/l]	Calculated maximum amount of sulphide dissolved [mg/l]	Percent of feed slag sulphur accounted for by calculated maximum amount of sulphide dissolved	Calculated sulphide leach rate constant [d^{-1}]
N	Fine fraction	1.5 litre	1	496.4	778.5	7.6%	77.5
			2	437.2	794.0	7.8%	76.9
		4 litre	3	477.0	790.3	7.8%	79.8
	Coarse fraction	4 litre	4	380.4	732.8	7.2%	56.2
O	Fine fraction	1.5 litre	5	474.6	740.3	8.7%	84.3
			6	394.6	746.3	8.7%	80.2
			7	434.0	720.5	8.4%	88.6

Table 5.4-1 Leaching of sulphide from the slag: base condition experiments

Sodium dissolution

Figure 5.4-3, for the fine fraction of slag N, shows a typical sharp initial increase in the sodium concentration, similar to the increase observed in the initial sulphide concentration. The equivalent graph for slag O is given in Figure 2 of Appendix H-3. The sodium concentration shows a small relative increase over the final 23 h of the experiment.

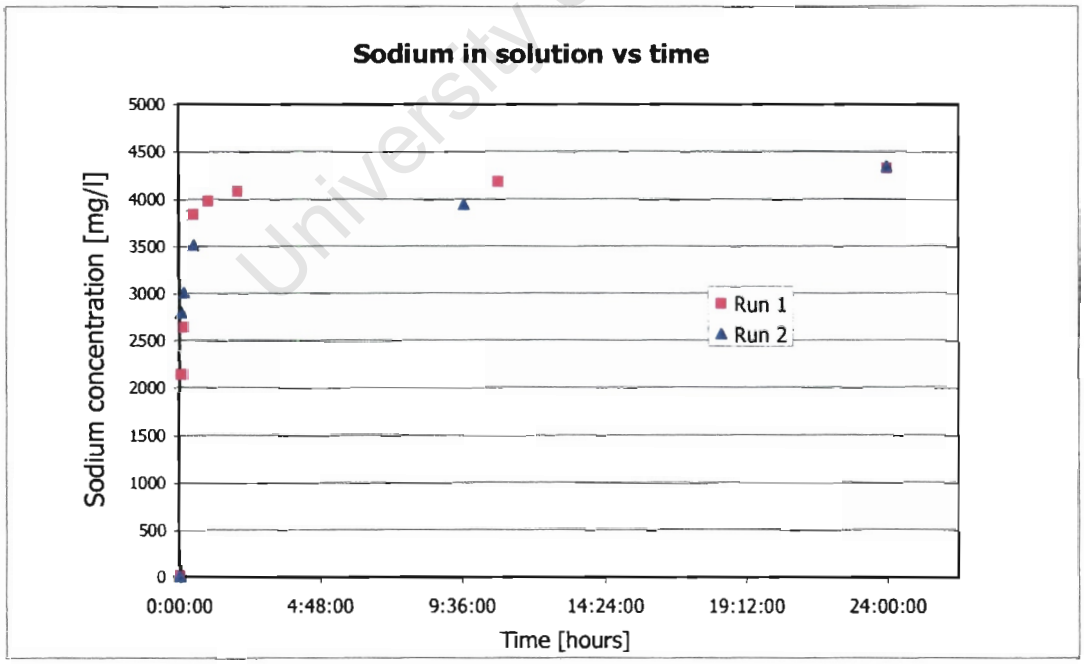

Figure 5.4-3 Sodium in solution during leaching experiments: the fine fraction of slag N

Figure 2 of Appendix H-4 shows the fit obtained by sodium leaching to the first order leaching equation. A fit with a linear regression coefficient of 0.97 was obtained from sodium concentration values for the fist 30 minutes, after this time the plot is not linear.

Comparison of reactors of differing volumes

Figure 5.4-2 allows comparison between the 1.5 litre and 4 litre reactors. No significant differences between the dissolution trends were evident for the initial increase during the first 60 minutes. The rates of decline in the sulphide concentration after the experiments reach their respective maximum measured sulphide concentrations was greater for the 4 litre reactor.

Comparison between slag N and slag O

Table 5.4-1 indicates that the maximum measured and calculated sulphide concentrations were typically lower for slag O. However, Table 5.4-1 also shows that the percent of sulphur in the feed slag that dissolves from Slag O was greater than slag N. The initial leach rate constants calculated for these base condition experiments were higher for slag O than slag N.

Comparison between dissolution from the coarse fraction and the fine fraction

Figure 5.4-4 shows the comparison between the results of coarse fraction and fine fraction dissolution experiments. The fine fraction had a significantly greater initial dissolution rate and reaches a greater maximum value. The rate of decrease of the sulphide concentration after the maximum value was greater for the fine fraction than the coarse fraction.

Table 5.4-1 shows that the maximum soluble sulphide calculated for the coarse fraction was not considerably less than that of the fine fraction. However, the initial leach rate constant of the coarse fraction was significantly lower than for the fine fraction.

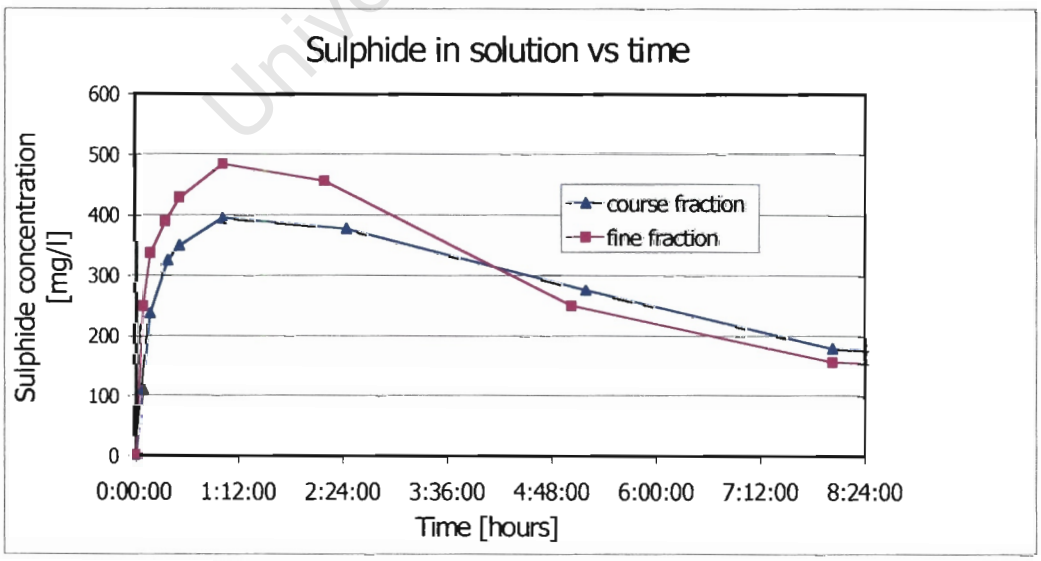

Figure 5.4-4 Sulphide in solution during leaching experiments: fine fraction and coarse fraction slag N, 4 litre reactor

Investigation of conditions affecting the dissolution subprocess

Temperature

Figure 5.4-5 shows that the initial dissolution rate was significantly increased by an increase in temperature. Figure 5.4-5 also shows that the depletion of sulphide occurred rapidly after the 10 min sample was taken. For this reason the experiments were cut off at 2h45, well before the typical leach experiment of 24 h. This was done to prevent the sulphide concentration from dropping too low. This was necessary due to preventing significant oxidative leaching from occurring.

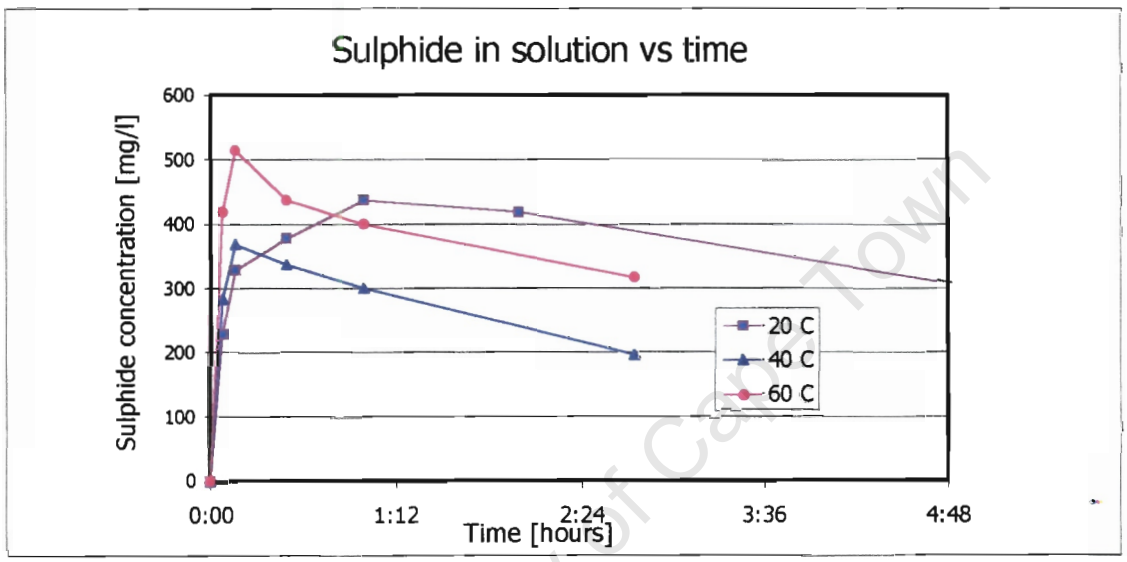

Figure 5.4-5 Sulphide in solution during temperature variation leaching experiments: the fine fraction of slag N

Table 5.4-2 shows that an increased amount of soluble sulphide was extracted at the higher temperatures despite the shorter run time. The 60 °C value significantly exceeds the extractions obtained at 20 °C and 40 °C.

Slag type	Slag starting condition	Temperature [°C]	Maximum measured sulphide concentration [mg/l]	Calculated maximum amount of sulphide leached [mg/l]	Percent of feed slag sulphur accounted for by calculated maximum amount of sulphide leached	Calculated sulphide leaching rate constant [d^{-1}]
N	fine fraction	20	496.4	778.5	7.6%	77.5
		40	369.0	760.4	7.5%	95.6
		60	515.0	820.9	8.1%	142.1

Table 5.4-2 Leaching of sulphide from the slag: temperature experiments

Literature predicts that the diffusion coefficient, which is a term encompassed by the leach rate constant (shown by comparison of equation 2-14 and 2-15), follows an Arrhenius type increase with

increasing temperature. Figure 3 of Appendix H-4 gives the graph of the natural logarithm of the rate constant versus the inverse of temperature. Table 2 of Appendix H-4 gives the data required for this graph. The regression coefficient for the plot was 0.96, and the evaluation of the best linear fit gradient yielded an Arrhenius exponential term of 1.5.

Agitation rate

Figure 5.4-6 shows sulphide concentration graphs for experiments operated under different agitation rates. It shows the significant increase in the sulphide dissolution rate with increased agitation. Table 5.4-3 shows the effect of agitation on the soluble sulphide extracted from the slag and on the initial leach rate constant. The increased dissolution rates evident from Figure 5.4-6 with increasing agitation are reflected in the appreciable increases in the initial leach rate constant. The increase in leach rate constant is greater for the increase from 200 rpm to 600 rpm than the increase from 600 rpm to 1200 rpm. The increase in the soluble sulphide extracted was appreciable for the increase in agitation from 600 rpm to 1200 rpm, but the increase in the soluble sulphide extracted from 600 rpm to 1200 rpm was small.

Slag type	Slag starting condition	Agitation rate [rpm]	Maximum measured sulphide concentration [mg/l]	Calculated maximum amount of sulphide leached [mg/l]	Percent of feed slag sulphur accounted for by calculated maximum amount of sulphide leached	Calculated sulphide leaching rate constant [d^{-1}]
N	fine fraction	200	327.6	671.8	6.6%	53.0
		600	496.4	778.5	7.6%	77.5
		1200	552.0	787.8	7.7%	97.0

Table 5.4-3 Leaching of sulphide from the slag: agitation experiments

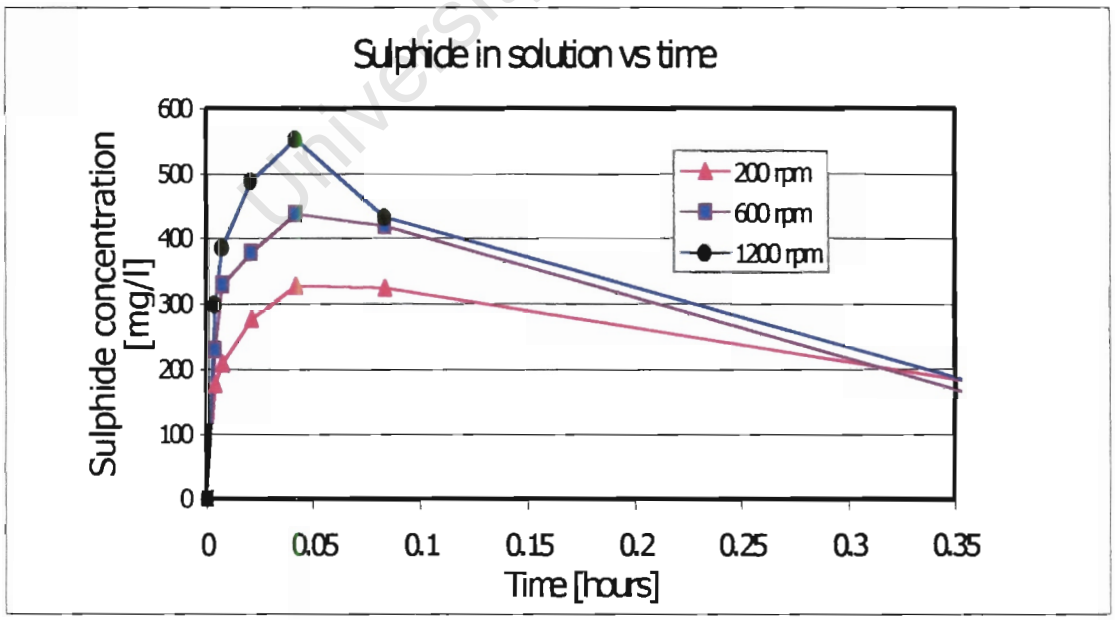

Figure 5.4-6 Sulphide in solution during agitation variation leaching experiments: the fine fraction of slag N

Solid to liquid ratio

Figure 5.4-7 shows sulphide concentration graphs for experiments operated under differing solid to liquid ratios. Table 5.4-4 shows the effect of solid to liquid ratio on the soluble sulphide extracted from the slag and on the initial leach rate constant. The appreciable sulphide dissolution rate increase with increasing solid to ratio, that is evident from Figure 5.4-7, was not accompanied by an appreciable increase in the leach rate constant. Table 5.4-4 also shows that, while the fraction of slag sulphur extracted is not really affected by the increase from 10 g/l to 50 g/l, the extraction is lower for the 100 g/l case.

Slag type	Slag starting condition	Mass concentration of slag	Maximum measured sulphide concentration [mg/l]	Calculated maximum amount of sulphide leached [mg/l]	Percent of feed slag sulphur accounted for by calculated maximum amount of sulphide leached	Calculated sulphide leaching rate constant [d^{-1}]
N	Fine fraction	10 g/l	119.0	146.0	7.2%	75.2
		50 g/l	496.4	778.5	7.6%	77.5
		100 g/l	843.2	1387.8	6.8%	81.21

Table 5.4-4 Leaching of sulphide from the slag: solid to liquid ratio experiments

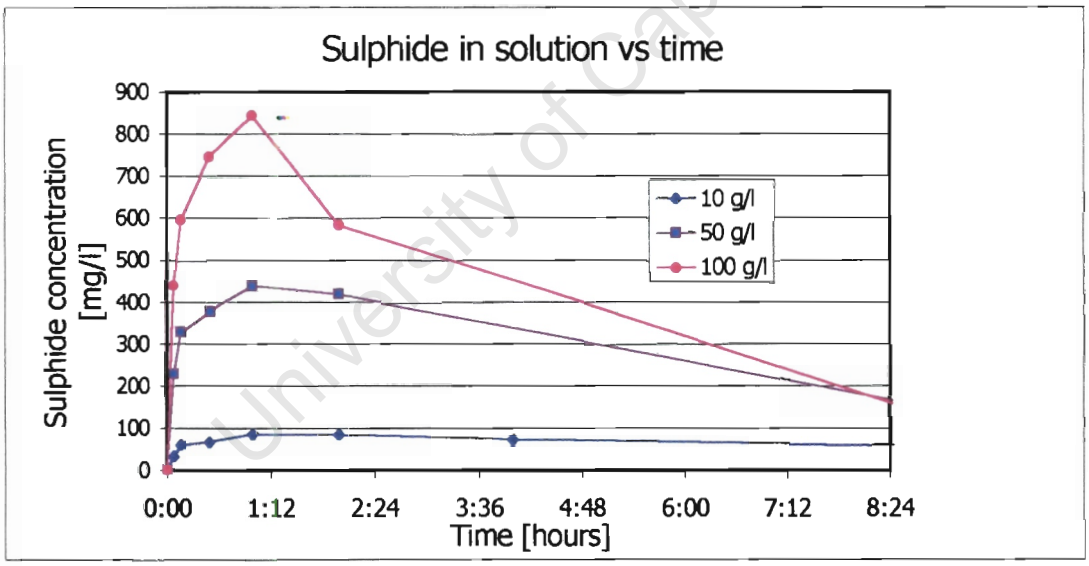

Figure 5.4-7 Sulphide in solution during solid to liquid ratio variation leaching experiments: the fine fraction of slag N

5.4.3 Oxidation of aqueous sulphides

Analysis of oxidation rate data

The best way of comparing the results of oxidation experiments was found to be the evaluation of oxidation rate constants. This is because sulphide concentration graphs often did not show differences clearly due to different initial sulphide concentrations and rapid initial depletion rates.

The oxidation rate constant was evaluated by integrating the aqueous oxidation rate equation (equation 2-19) with respect to the sulphide concentration so that a linearised form was obtained. This is shown in equation 5.4-1. The experimentally obtained sulphide and oxygen concentrations at various times were then substituted into this equation. If the reaction orders with respect to sulphide and oxygen, obtained from literature, were correct for these experiments, a linear plot would be obtained with a gradient equal to the oxidation rate constant. A sample calculation is given in Appendix H-5.

$$\frac{-1}{C_{O_2}^{\ n}} \times \frac{C_S^{\ -m+1}}{-m+1} = kt \qquad \text{equation 5.4-2}$$

The reaction orders of Table 2-6 were all tested using the method of the previous paragraph. The best linear fit was obtained by the orders of Lefers *et al* (1978). These orders, with respect to sulphide and oxygen, were 1.47 and 0.55 respectively. The conditions under which these orders were evaluated by Lefers *et al* (1978) resembled the conditions of the experiments in this study. The initial sulphide concentration was 70 mg/l to 290 mg/l, pH of 12. The temperature at which they were evaluated was 48.5 °C.

Oxidation of aqueous slag sulphide under base case conditions

Figure 5.4-2 shows the depletion of sulphide during oxidation experiment number 4. The initial rapid depletion of sulphide is typical of all the oxidation experiments. This initial rapid depletion was followed by a substantial decrease in the depletion rate at low sulphide concentrations. From an initial sulphide concentration of 210 mg/l, the sulphide concentration reached a value of 0.1 mg/l after 6h46. Other base case experiments typically reached a zero sulphide concentration before 8 h. However, this experiment had a significantly greater initial sulphide concentration than other experiments.

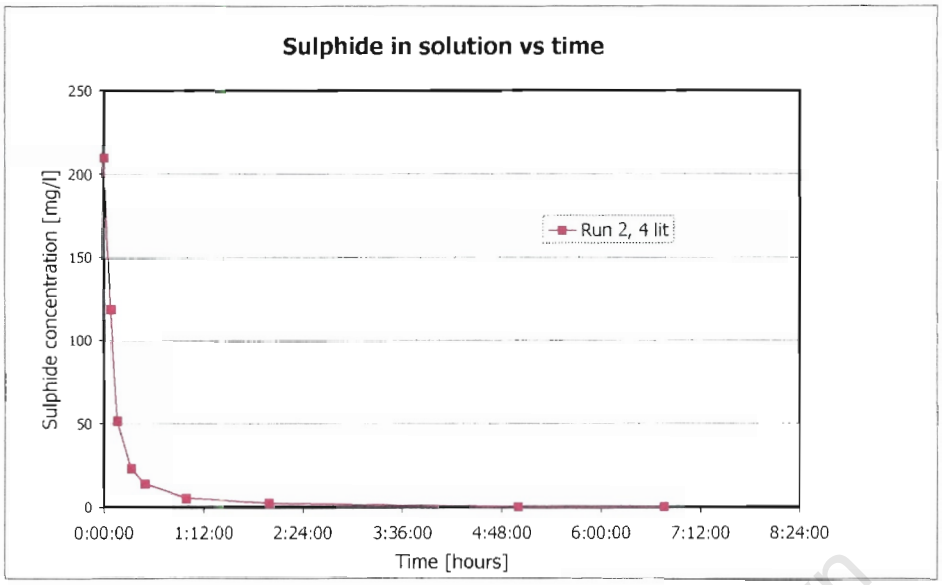

Figure 5.4-8 Sulphide in solution during oxidation experiment number 2 (4 litre slag N)

Figure 5.4-9 shows the dissolved oxygen concentration graph during the experiment. After a rapid initial increase during the first hour, the dissolved oxygen concentration increased more gradually towards the maximum equilibrium dissolved oxygen concentration (9.2 mg/l in fresh water at 20 °C).

Figure 5.4-9 shows that the dissolved oxygen concentration increase closely follows a logarithmic fit. This fitted equation may be used to estimate the dissolved oxygen concentration for the 1.5 litre reactor experiments where measurement was not possible.

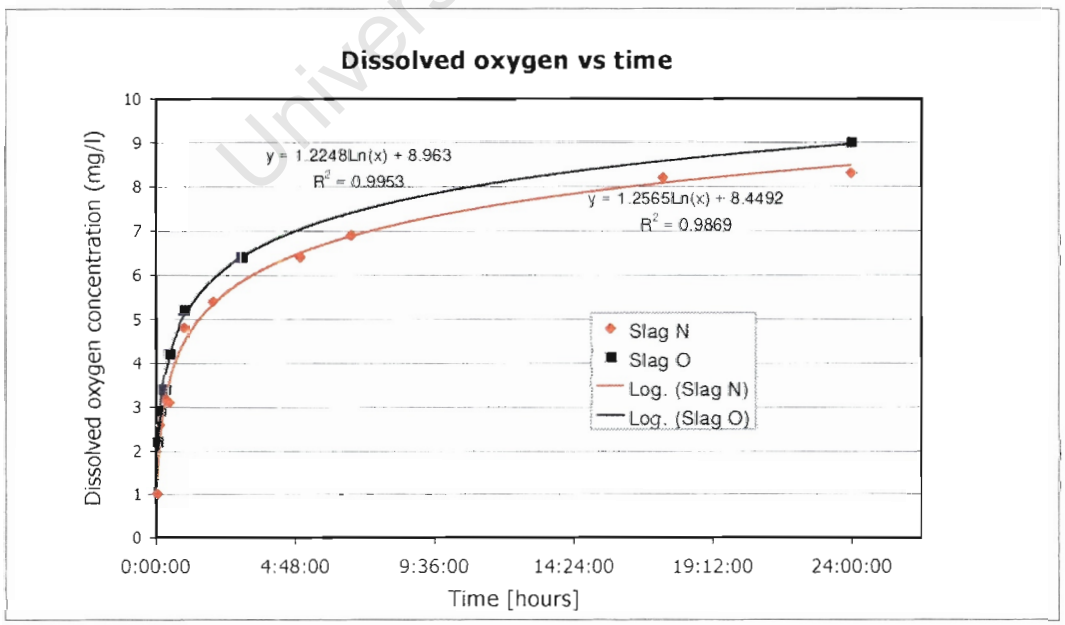

Figure 5.4-9 Dissolved oxygen concentration graph: 4 litre slag N experiment number 2

Figure 5.4-10 shows the graph for the determination of the oxidation rate constant for oxidation experiment number 4. This graph was plotted with the values of Table 2 in Appendix H-5. The linear fit had a regression coefficient of 0.99 and relative error of 0.0078 (equation for relative error calculation appears in Appendix H-5). The regression coefficients obtained for linearised plots of other base condition experiments are given in Table 5.4-1. Although experimental sampling and analytical error may have caused the scatter of results around the best-fit straight line, the results follow a typical trend also observed in other linearised oxidation plots. The initial three values indicate a greater gradient (hence a greater oxidation rate constant) than was actually determined on average for overall experiment. The next two values indicate a lower rate constant for that time period, followed by an increase as shown by the last two values.

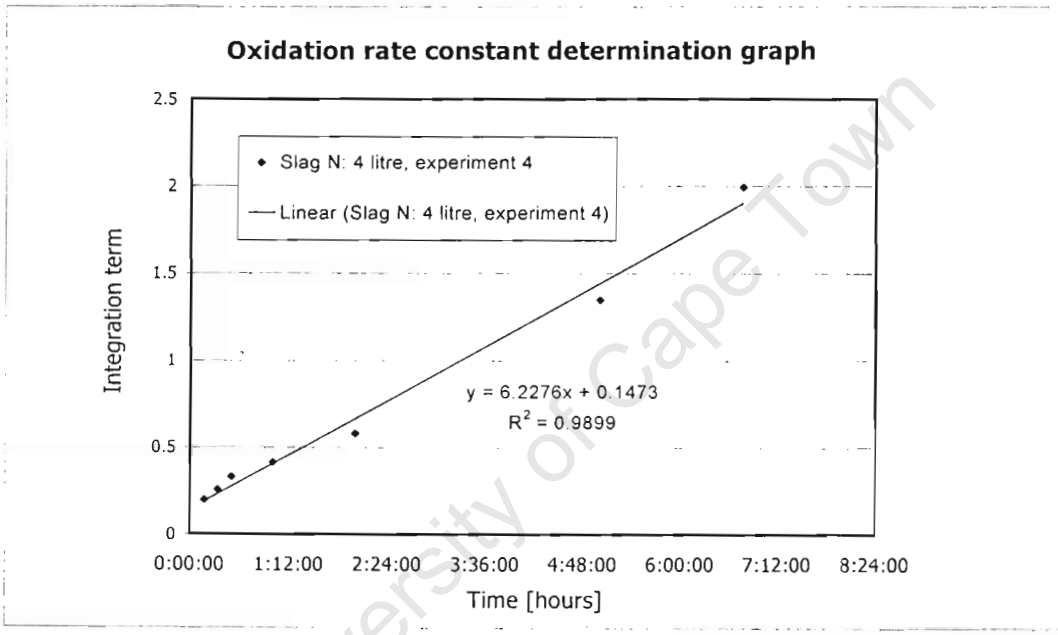

Figure 5.4-10 Linearised oxidation rate plot: experiment number 4

Table 5.4-1 shows the rate constants obtained for each experiment. These provide a measure of the repeatability of sulphide oxidation experimental results under base case conditions. The only significantly outlying value was experiment 7.

Slag type	Reactor	Experiment number	Initial sulphide concentration	Calculated sulphide oxidation rate constant [mg $^{-1.02}$. l $^{1.02}$. d^{-1}]	Regression coefficient
N	1.5 litre	1	121.8	6.9	0.999
		2	56.6	6.6	0.993
	4 litre	3	72.4	6.1	0.980
		4	210.0	6.2	0.990
O	1.5 litre	5	129.6	5.8	0.990
		6	96.2	5.5	0.970
		7	137.4	4.6	0.998
	4 litre	8	43.0	5.7	0.985

Table 5.4-5 Sulphide oxidation experiments: base condition experiments

Figure 5.4-11 shows the pH of the reactor solution during experiment number 4. The pH decreases as the oxidation experiment progresses.

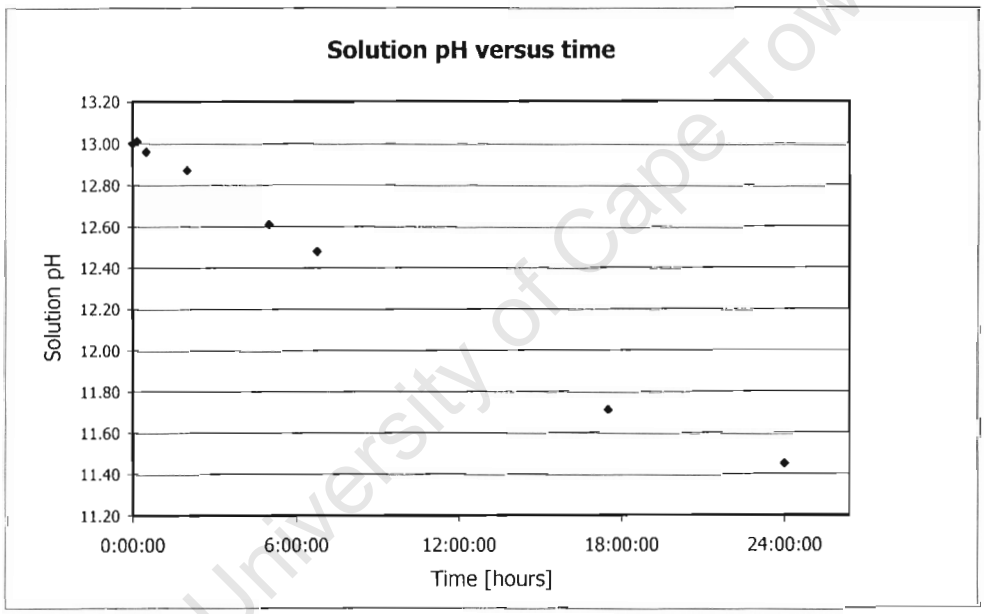

Figure 5.4-11 pH of reactor solution during experiment number 4

Effect of different starting sulphide concentration

Table 5.4-5 shows that the higher initial sulphide experiments typically did have slightly greater oxidation rate constants. However, this increase was not substantial. A linear fit to the reaction orders of Lefers *et al* (1978) was obtained for experiments covering a wide range of initial sulphide concentrations. These are given in Table 5.4-5.

Comparison of reactors of different volumes

Table 5.4-5 shows that, for the experiments using slag N, the rate constants for the 1.5 litre reactor exceed those obtained for the 4 litre reactor. For slag O, the 4 litre reactor value falls between the two 1.5 litre reactor values.

Comparison between slag N and slag O

Table 5.4-5 shows that all the oxidation rate constants that were determined for the slag N experimental experiments exceed those determined for slag O.

Investigation of conditions affecting the oxidation of aqueous slag sulphide

Temperature

Figure 5.4-12 shows the effect of temperature on the aqueous sulphide oxidation rate. It shows an appreciable increase in the sulphide oxidation rate with an increase in temperature. Table 5.4-6 shows that the oxidation rate constant evaluated for each of these experiments also increased appreciably.

Slag type	Slag starting condition	Temperature [°C]	Initial sulphide concentration	Calculated sulphide oxidation rate constant [$mg^{1.02}.l^{1.02}.d^{-1}$]	Regression coefficient
N	Pre-leached solution	20	121.8	6.9	0.99
		40	196.3	14.9	0.98
		60	317.5	25.3	0.98

Table 5.4-6 Sulphide oxidation experiments: varied temperature experiments

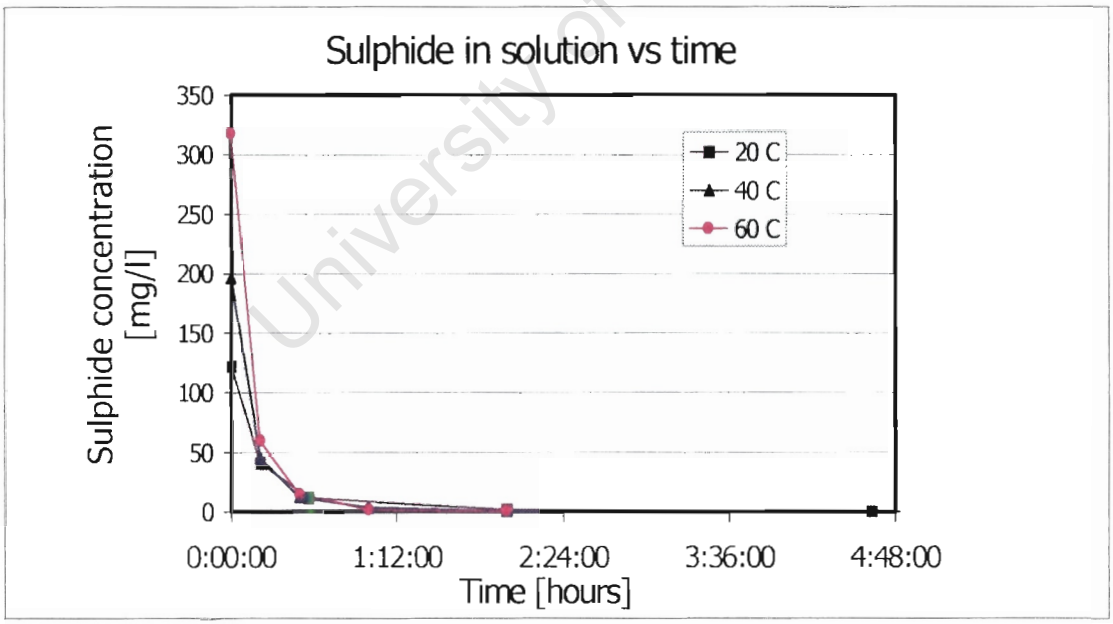

Figure 5.4-12 Sulphide in solution during temperature variation oxidation experiments: the fine fraction of slag N

A plot of the natural logarithm of the rate constant versus the inverse of temperature yielded a linearised plot as shown in Figure 5.4-13. The data used in this plot is given in Table 2 of Appendix H-5.

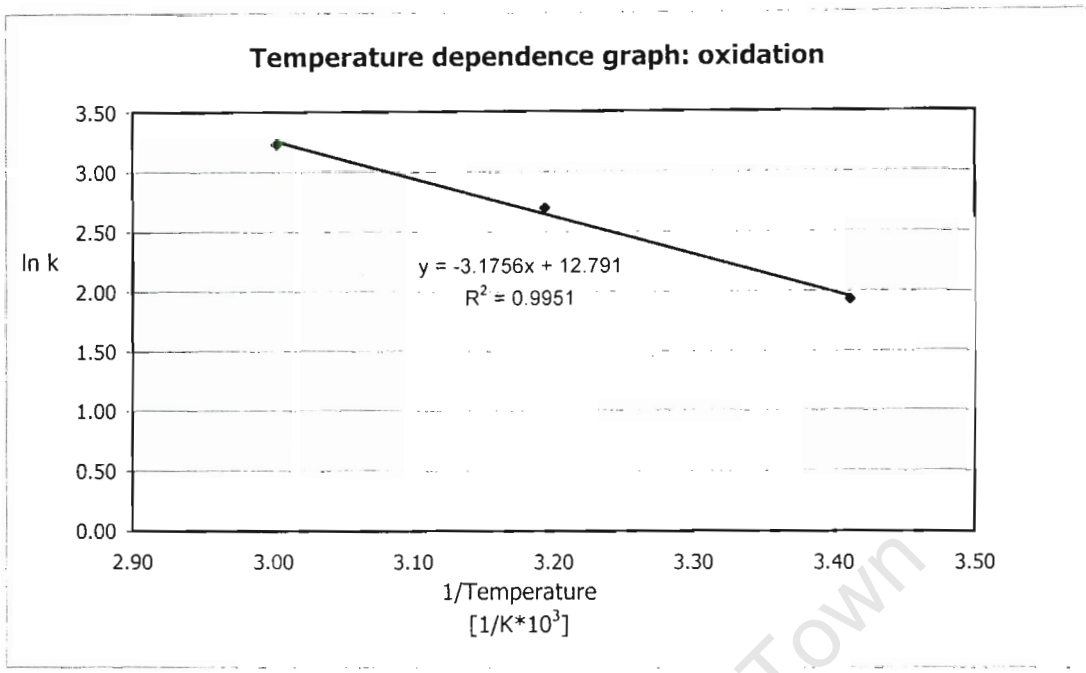

Figure 5.4-13 Plot of the natural logarithm of the rate constant versus the inverse of temperature: pulverised form slag N

Table 5.4-7 shows the constants in the Arrhenius equation that were evaluated using the plot in Figure 5.4-13.

Term	Determined from	Value	Units
$\frac{E_A}{R}$	Gradient of plot	3.2	[mg $^{-1.02}$. l $^{1.02}$. d^{-1}.K]
Frequency factor, k_o	Y-intercept of plot	5.4×10^5	[mg $^{-1.02}$. l $^{1.02}$. d^{-1}]

Table 5.4-7 Calculated constants in Arrhenius equation from ln k versus 1/T plot

Solid to liquid ratio

Table 5.4-8 shows the results of oxidation experiments to determine the effect of the solid to liquid ratio of the slag on the oxidation rate. Despite substantial differences in this ratio between experiments, Table 5.4-8 shows that the starting sulphide concentrations were not increased in proportion. This was a result of poor inhibition of aqueous sulphide oxidation during dissolution experiment, which produced the pre-leached feed solution. The calculated oxidation rate constant showed an increase with increasing solid to liquid ratio.

Slag type	Slag starting condition	Mass concentration of slag	Initial sulphide concentration	Calculated sulphide oxidation rate constant [mg $^{-1.02}$. l $^{1.02}$. d^{-1}]	Regression coefficient
N	Pre-leached solution	10 g/l	36.6	5.9	0.99
		50 g/l	56.6	6.6	0.99
		100 g/l	66.2	8.0	0.94

Table 5.4-8 Sulphide oxidation experiments: solid to liquid ratio experiments

Occurrence of oxidative leaching of insoluble slag sulphides

Table 5.4-9 shows the rate constants calculated for experiments where the insoluble component of the slag was removed from the pre-leached solution prior to the start of the experiment by filtration, in comparison with those of experiments where the pre-leached solution was unfiltered. The latter was the normal procedure for the oxidation experiments. These experiments were operated under base conditions. The starting sulphide concentration of the filtered pre-leached solution was significantly lower due to unavoidable oxidation of aqueous sulphide during filtration.

Slag type	Reactor	Condition of reactor solution prior to oxidation	Initial sulphide concentration [mg/l]	Calculated sulphide oxidation rate constant [mg $^{-1.02}$. l $^{1.02}$. d^{-1}]	Regression coefficient	Thiosulphate produced during experiment [mg/l]
N	4 litre	Filtered	84.6	0.6	0.99	802
		Unfiltered	210.0	6.2	0.99	7304
O	4 litre	Filtered	5.3	1.29	0.98	384
		Unfiltered	43.0	5.72	0.99	8176

Table 5.4-9 Sulphide oxidation experiments: effect of the presence of insoluble components

Figure 5.4-14 shows the comparison between thiosulphate production graphs for the filtered and unfiltered experiments. Some aqueous sulphide oxidation would have occurred during the dissolution experiment that produced the pre-leached solution. Thus, it must be noted that the initial thiosulphate concentration was not zero which makes comparison of the initial thiosulphate production rates difficult. It was evident that after 1 h the thiosulphate production rate for the filtered experiments was low while the production rate for the unfiltered experiment remains high throughout the experiment.

Table 5.4-9 gives the actual amount of thiosulphate produced during the respective oxidation experiments. The thiosulphate produced by the unfiltered experiments was several times higher than that produced by the filtered experiments, as was evident from Figure 5.4-14. The complete conversion of the unfiltered experiment starting sulphide concentrations to thiosulphate, i.e. 84.6 mg/l and 5.3 mg/l sulphide, should result in the production of 148 mg/l and 9.3 mg/l thiosulphate respectively.

Table 5.4-9 shows that the actual thiosulphate production for the filtered experiments exceeds this substantially, indicating that the filtration was not successful at removing all the insoluble sulphides.

Table 5.4-9 shows that the rate constants obtained for the experiments where the insoluble component was filtered out of the pre-leached solution were appreciably less than where the pre-leached solution was unfiltered. This was in excess of four times and ten times for slag types O and N respectively.

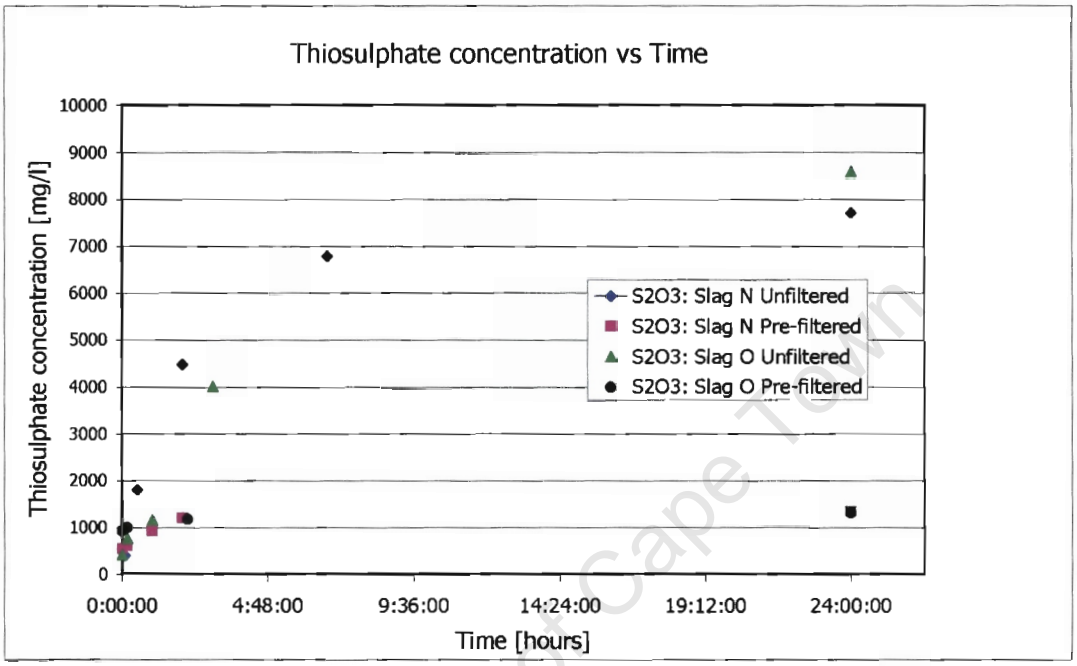

Figure 5.4-14 Thiosulphate concentration graphs for filtered and non-filtered pre-leached solution oxidation experiments

Comparison of rate constants obtained experimentally with literature values

Table 5.4-10 shows the literature oxidation rate constants converted from the values shown in Table 2-7 to units that can be compared to each other and the rate constants calculated in the oxidation experiments. The calculation for the conversion of the units from those given in the literature review is given in Appendix H-5. The converted units obtained are in most cases not exactly the same as those obtained for the oxidation rate constant in this study, due to the use of different reaction orders with respect to sulphide and oxygen in other investigations. The exception is the investigation of Lefers *et al* (1978) who used the same reaction orders. The difference in the 'z' values shown in Table 5.4-10 is small. Therefore this difference would not substantially affect the oxidation rate constant values obtained, and a comparison can be made. The literature oxidation rate constants are all several times smaller than those obtained in this study, except for the Fe^{2+} catalysed experiment of Zhang and Millero (1993), which is similar.

Author	Experimental Conditions			Rate Constant [(mg/l)$^{1-z}$. d^{-1}]	z
	pH	Temperature	Catalyst		
Lefers *et al* (1978)	12	48.5 °C	None	0.23	1.02
Chen and Morris (1972)	11.75	25 °C	None	0.03	0.9
	12.50	25 °C	None	0.04	0.9
O'Brien and Birkner (1977)	7.55	25 °C	None	0.04 to 0.09	1
Zhang and Millero (1993)	8.0	25 °C	None	0.14	1
	8.0	25 °C	Fe^{+2}	8.08	1
	10.0	25 °C	None	0.19	1

Table 5.4-10 Comparison of rate constants obtained from literature sources

6 Discussion of experimental results

6.1 Characterisation of the slag

6.1.1 Quantitative analysis

A relevant consideration in judging whether the results achieved by the leach – oxidation experiments are representative of the results that may have been achieved on other slags produced at the local refinery was determining whether the compositions of the slags selected were representative. The comparison of the slags selected for experimental test work to the historical data, given in Section 5.1.1, indicated that the slags selected for treatment were not significantly different to those produced on average. The time gap between the last recorded historical data and when the selected slags were collected made it impossible to judge whether these were representative of the slags produced by the local refiner at the time of collection.

6.1.2 Qualitative analysis

X-ray diffraction analysis

Compounds predicted to be present in the matte phase from knowledge of the secondary lead furnace reactions were not detected by XRD analysis. However, this analysis did provide information on the composition of the slag phase. The hydroxides of the slag phase oxide compounds predicted from furnace reactions by Queneau (1989), namely ferrous oxide (FeO) and sodium oxide (Na_2O), were detected. Their presence in the form of hydroxides, rather than oxides, from XRD analysis is likely to be as a result of exposure of the analysed slag sample to atmospheric water vapour. In addition to sodium oxide, evidence was found for the presence of sodium silicate matrix phases.

SEM analysis

The SEM images indicate the heterogeneity of the slag. The compounds predicted by the phase diagram for the matte phase, Na2S.FeS and FeS, successfully accounted for the elements detected for the matte phase.

In the slag phase, sodium could be assigned equally well to sodium silicate compounds as to sodium oxide. The actual composition was expected to be a combination of these compounds, as indicated by XRD analysis. Indirect evidence for the presence of sodium silicate compounds was the significant proportion of sodium that remained insoluble during leach – oxidation experiments, which may be a result of these compounds being bound up in an insoluble silicate matrix.

6.1.3 Indirect techniques

Mass balance over the furnace

The significant error between inputs and outputs is likely to be attributed mainly to errors in the estimation of the mass of feed materials, rather than sampling errors leading to an erroneously estimated composition of the slag. The discrepancies in masses of components fed to the furnaces were likely to be the most significant factor causing variability in the slag composition. The full mass balance presented in Appendix E is useful in indicating the origin of the slag components. If the

furnace feeds were changed, this balance would provide an indication of how this would affect the slag composition.

Carbonate analysis

From the results of the wet chemical tests it can be concluded that no carbonate was present in the slag samples analysed. Thus it appears that all the sodium carbonate present in the furnace feed is decomposed via the reaction of equation 2-5 to sodium oxide and carbon dioxide in the furnace. The relevance of whether carbonate is present or not is its function as a biological substrate in the second step of the BROSS process.

6.2 Leach – oxidation of slag under base conditions

6.2.1 End-of-run experimental results

A number of general observations can be made from the leach – oxidation results obtained under base conditions. Firstly, the majority of the slag remained in the insoluble phase at the end of the experiment, although a significant proportion was extracted to the aqueous phase.

Of the slag components extracted to the aqueous phase, sulphur was the most important in terms of the objectives of this study. The majority of the sulphur present in the feed slag was extracted to the aqueous phase, although a significant proportion remained in the insoluble phase. Significant increases were observed in overall slag extraction, sulphur extraction and conversion to thiosulphate when the results of the milled fine fraction were compared to the coarse fraction.

The mass balance shows that the sulphur extracted from the slag was virtually all converted to thiosulphate by the end of the 48 h experiment. A low conversion to sulphate was also found in some experiments. The product phases (insoluble, thiosulphate and sulphate) generally accounted for all the sulphur present in the feed slag. This indicates that, at the end of the experiment, there were no other significant sulphur aqueous products present in addition to thiosulphate and sulphate.

6.2.2 Sulphur species in solution during the experiment

The comparison of the sulphide and thiosulphate species concentration in solution during the experiment provides evidence that thiosulphate was formed by another mechanism in addition to the oxidation of the aqueous sulphide. Firstly, the maximum sulphide concentration is almost two orders of magnitude smaller than the maximum thiosulphate concentration. An extremely rapid sulphide leaching and oxidation rate from solution would be required if all the thiosulphate was produced by oxidation of aqueous sulphide. Secondly, and more conclusively, much of the increase in thiosulphate concentration occurs after the sulphide concentration has reached zero. A zero sulphide solution concentration suggests that the sulphide leaching rate into solution was very small, if it occurred at all. The oxidation rate when the sulphide concentration was below detectable levels would be very small due to its dependence on the solution sulphide concentration. For this to exceed the leaching rate implies that the leaching rate must have been negligible.

Comparison between the fine fraction and coarse fraction sulphur species graphs indicated that the starting particle size played a significant role in the rate at which sulphide leaching initially occurs. This was indicated by the initially higher sulphide and thiosulphate solution concentrations for the fine fraction. However, thiosulphate production towards the end of the run for the fine fraction is lower than that of the coarse fraction. Therefore, it would be expected that in an experiment of longer length, the respective thiosulphate conversions would approach each other more closely. This is inline with the hypothesis that the coarse fraction disintegrates during the leach – oxidation experiment and potentially may become exposed to leaching and oxidative leaching to a similar degree as the fine fraction.

For the fine fraction size, the soluble slag sulphide is exposed to leaching to a far greater degree than the coarse fraction at the beginning of the experiment, by virtue of the greater slag surface area. The result of this was that the initial leaching rate was significantly higher for the fine fraction, as evident from the difference between the maximum sulphide concentrations reached. A comparison between the leaching rate and particle size was given in Section 5.3.4.

During the coarse fraction experiments, the sulphide concentration did not decrease as rapidly after the initial peak as in the fine fraction experiments. Two factors are likely to cause this observation. Firstly, the leaching rate of soluble sulphide from the coarse fraction would become greater later in the experiment, compared to the fine fraction, as more sulphide becomes exposed to leaching via disintegration. Secondly, the oxidation rate is dependent on the sulphide concentration, thus a lower sulphide concentration in solution would result in a lower oxidation rate.

6.2.3 Sodium leaching

The results indicate that the extraction of sodium into the aqueous phase was incomplete. Table 2-4 shows that the sodium compounds that were expected to be present in the slag should be entirely soluble at a 50 g/l slag mass concentration. It was found in Section 4.1 that a portion of the sodium is likely to be bound up in, or form a component of, the insoluble silicate matrix phase. This is likely to account for the 15 – 30 mass-% that remains in the solid phase at the end of the experiment.

The end-of-run increased extraction of sodium in the case of the fine fraction indicates that a greater amount of the slag sodium was exposed to leaching for this case than the coarse fraction case, even with the occurrence of disintegration. The presence of an insoluble silicate matrix explains this. In the case of the coarse fraction, disintegration of the slag in solution is not likely to be effective in breaking down this silicate matrix due to its insolubility, while milling could achieve this increased exposure mechanically.

The sodium concentration graphs showed that the soluble sodium components that were exposed to leaching were leached at a rapid initial rate. The leaching rate of sodium provides an indication of the rate at which the sulphide and oxide soluble components of the slag are leached due to the ion-balance requirement. Due to the fact that the sulphide dissolution experiments could not be determined independently from depletion caused by oxidation, the trends in sodium leaching may be used to explain certain trends for soluble sulphide leaching.

The sodium concentration graphs indicate that the initial leaching rates of the fine fraction and coarse fraction were not appreciably different. The starting surface area exposed to leaching for the fine fraction was in the order of 224 times greater that the coarse fraction (see Appendix H-6). Equation 2-11 shows that the dissolution rate was directly proportional to the exposed surface area. Thus, the rate of sodium dissolution from the fine fraction starting size was expected to be appreciably higher than that from the coarse fraction, which was not the case. This indicated the property of the slag to disintegrate rapidly from the coarse fraction particle size to a form in which the components of the slag are exposed to leaching.

6.2.4 Iron leaching

Leach – oxidation results provided evidence for the presence of the $FeS.Na_2S$ compound. Firstly, early in the leach – oxidation experiment, the maximum solubility of FeS was exceeded. Secondly, the period of raised iron solubility corresponds to the period during which sulphide was present in significant quantities in the reactor solution after which it is decreased. This is an expected outcome if the iron in solution is associated with $FeS.Na_2S$, as ferrous sulphide was predicted (Section 2.4.1) to return to the solubility of FeS as shown in Table 2-4 once the sodium sulphide component was oxidised.

The presence of Fe^{2+} ions in solution was indicated by the green colour of the filtered solution. The observed transition of the filtered solution from green to clear indicates its removal. Firstly, this removal was a result of the overall removal of iron from solution after four hours. Secondly, the oxidation of the Fe^{2+} ions to Fe^{3+} ions may also contribute to this colour change. The change in colour of the unfiltered solution can be ascribed to the progressive conversion of insoluble ferrous sulphide (black) to ferric hydroxide (reddish-brown) (Perry, 1984).

6.2.5 pH change during leach – oxidation

The high solution pH caused by leach – oxidation of the slag was a result of the rapid leaching of sodium oxide (resulting in sodium hydroxide in solution) and aqueous sulphide components. The decrease in pH, particularly over the first 24 hours, can be ascribed to the removal of the aqueous sulphide from the solution.

6.2.6 Comparison between the slag types N and O

The higher sulphur composition of slag N resulted in consistently greater thiosulphate production in leach – oxidation experiments using this slag. However, the end-of-run results were compared in terms of the percentage conversion of feed slag sulphur to aqueous oxidation products, rather than overall extraction or thiosulphate production. This was done to compare the respective efficiency of sulphur extraction from the slag types. Although the percentage conversion was significantly higher for the slag O for the coarse fraction experiments, the fact that there were only two of these experiments makes it impossible to state that the one slag type yields significantly different results to the other. No significant difference was evident from the results of the fine fraction. This means that, either the difference observed for the coarse fraction experiments was a result of experimental error, or more of the sulphur present in slag O was exposed to leaching (dissolution or oxidative leaching). The latter may indicate that the disintegration of slag O is more extensive during the leach – oxidation experiment compared to slag N. This confirmed the finding of Section 5.4.1 that slag O disintegrates at a greater rate than slag N.

6.2.7 Comparison of reactors of differing volumes

The fact that only one base condition experiment was successfully completed in the 4 litre reactor for each slag type, makes it impossible to infer statistically if the results obtained for the 4 litre reactor are significantly different to the 1.5 litre reactor. The results do not show major inconsistencies. Small differences in reactor characteristics may have caused the differences in results evident in the

observations of Section 5.2.8. Possible reasons for the differences in results for sulphur extraction could include a lesser degree of solids suspension in the 4 litre reactor.

6.3 Investigation of conditions that affect the leach – oxidation process

6.3.1 Temperature

The results of Section 5.3.1 showed that increasing the temperature above the base condition temperature of 20 °C resulted in a substantial increase in sulphur extraction and conversion to thiosulphate. This variable had a significantly greater impact on the results than any other variable investigated. In Section 2.4.1, it was reported that the temperature dependence of leaching (via the diffusion coefficient), was less than the temperature dependence of chemical reactions (via the reaction constant) represented here by the aqueous and insoluble sulphide oxidation reactions. Thus, the variation of temperature should have a greater impact on sulphur extraction via the oxidative leaching route than the soluble sulphide leaching route.

Section 5.4.2 showed that the aqueous sulphide dissolution and oxidation route was responsible for typically 12 % of the extraction of slag sulphur under base conditions. The zero solution sulphide concentration that was obtained during all leach – oxidation experiments suggests that the subprocesses of leaching and oxidation of the soluble sulphides was typically virtually complete by the end of the experiment. Thus, these subprocesses would not be expected to have a substantial impact on the end-of-run conversion to thiosulphate. Thus, the impact of temperature on the end-of-run results (sulphur extraction and conversion to thiosulphate) should be primarily a result of the impact on the oxidative leaching of the insoluble sulphides. It is shown in Section 7.2.3 that the removal of the aqueous sulphide does affect the initial rate of leach – oxidation. But under base conditions this removal was sufficiently fast that increasing its rate even further by raising the temperature would not cause a substantial increase in the end-of-run results.

The low production of rate of thiosulphate over the second half of the fine fraction 60 °C experiment indicated that virtually all the slag sulphur had been converted to thiosulphate during the first 24 hours. The end-of-run conversion to thiosulphate (> 100%) confirmed that this was the case. The thiosulphate concentration of the 40 °C experiment was still increasing appreciably over the final 24 hours showing that, at that condition, the maximum thiosulphate conversion was not yet closely approached as is shown by the end-of-run thiosulphate conversion.

Oxidative leaching is thermodynamically less favoured when sulphide is present in solution. This provides an explanation for the smaller variation between thiosulphate readings at different temperatures at 2 h. Before this time, the leaching and oxidation of the soluble sulphides is likely to play a greater role in the conversion to thiosulphate. The dissolution step is likely to limit this process at high temperature, due to its smaller temperature dependence. After 2 h the oxidative leaching reaction would play a greater role, hence the greater effect of temperature on the results at 8 h. This provides additional evidence of more than one mechanism for thiosulphate production.

The greater effect of temperature on sulphur extractions for the fine fraction compared to the coarse fraction indicates that the disintegration subprocess limits the amount of slag sulphur that was exposed to oxidation via oxidative leaching. The lower sulphur extractions and hence thiosulphate conversions at the same temperature for the coarse fraction, provide an indication that not all of the sulphur was

exposed to the solution during these experiments. The smaller effect of temperature on the disintegration rate indicated by these results, is an outcome of the smaller effect of temperature on dissolution, the subprocess that causes disintegration.

The conversion to sulphate, the equilibrium thermodynamic product, is greater at higher temperatures. This is an expected outcome of the significant temperature dependence of chemical reaction rates. Despite the fact that these high temperature experiments had higher thiosulphate concentrations, this factor is unlikely to play a significant role in its conversion to sulphate. This is hypothesised due to the lack of conversion to sulphate at high thiosulphate concentrations in high solid to liquid ratio experiments.

Despite the fact that the soluble sulphide is removed from the slag prior to the end of the experiment in these 48 h experiments, the effect of temperature on the soluble sulphide concentration remains relevant for treatment of shorter duration. The increased effect of temperature on the oxidation rate compared to leaching rate is illustrated by the 10 min sulphide readings which were progressively lower for an increase in temperature. Higher temperature conditions also resulted in sulphide being removed from solution earlier.

6.3.2 Agitation rate

In a reasonably well-mixed reactor, the agitation rate would typically only affect the leaching rate and not the oxidation rate. However, in the experiments of this study, both the oxidation of soluble and insoluble sulphide was likely to be affected by the agitation rate. Firstly, this was due to the impeller motion being responsible for break up and dispersion of the air bubbles. Hence, a greater agitation rate would result in a greater gas – liquid interfacial area for oxygen transfer. Secondly, the transport of oxygen to the particle surface would be promoted by the shorter diffusion boundary layer at higher agitation rates. This would increase the oxidative leaching rate if this subprocess was limited by diffusion.

The sodium leaching graphs for the fine fraction showed that dissolution rate was increased as the agitation rate was increased. This was due to the effective boundary layer thickness around the solid particle being decreased at higher agitation rates, resulting in a shorter diffusion path. The fact that the 600 rpm and 1200 rpm results did not show appreciably different results, indicates that sodium leaching was not limited significantly at the base agitation rate of 600 rpm. The significantly lower leaching rate at 200 rpm compared to 600 rpm indicates that at 200 rpm, agitation does constrain the leaching rate of soluble slag components.

The same trend was evident from the end-of-run sulphur extraction results and thiosulphate conversions during the experiment. Both showed that the differences in results between 200 rpm and 600 rpm were significantly greater than the differences between 600 rpm and 1200 rpm, particularly for the fine fraction. Thus, the end-of-run results showed that agitation limited the conversion of slag sulphur to thiosulphate at 200 rpm but not at 600 rpm. The extraction rate of the soluble sulphides would be increased by increasing agitation as indicated by the sodium leaching results. However, the greatest contribution to the increased sulphur extraction would be the result of the increased oxidative leaching with increased agitation rate. This indicates that oxygen transport from the gas phase to the

particle surface via mass transfer from the gas to the liquid and diffusion limits oxidative leaching at 200 rpm but not at 600 rpm.

Comparing the coarse fraction and fine fraction results showed that agitation played a significantly greater role in the results of the coarse fraction experiments. Apart from the greater overall increase in sulphur extraction for the coarse fraction with increasing agitation, the increase of the agitation rate from 600 rpm to 1200 rpm also had a greater effect on the results obtained. The reason for this was that the process of dissolution, which was greatly affected by the agitation rate, was responsible for two subprocesses when the coarse fraction was used. Firstly, the disintegration of the coarse fraction and exposure of slag components to the solution and secondly, the conversion of these to aqueous phase compounds (in the case of the soluble components). For the fine fraction, the dissolution subprocess was only responsible for the latter.

The fact that the 10 min sulphide concentration peak for the 1200 rpm experiment was lower than that for lower agitation rates, despite the higher dissolution rate, shows the increase in the oxygen transfer rate to the aqueous phase. The oxidation reaction rate would be increased for the 1200 rpm experiment by the higher oxygen concentration of the solution. This result shows that early in the experiment the oxygen transfer rate to the aqueous phase was limited. A higher agitation rate than 600 rpm therefore promoted the oxidation reaction above that of the dissolution rate.

In summary, the discussion above indicates that no subprocesses were appreciably constrained by agitation at 600 rpm for the fine fraction. However at a lower agitation rate of 200 rpm, the mass transfer subprocesses were affected. For the coarse fraction, the role played by agitation was increased due to its role in the disintegration of the slag. This result indicates the effect of the rate at which disintegration occurs on the rate of the overall leach – oxidation process.

6.3.3 Solid to liquid ratio

The end-of-run results showed that the effect of the solid to liquid ratio was small relative to the degree by which it was varied. This indicates the small impact of this parameter on the oxidative leaching subprocess, which was shown in Section 5.4.2 to be responsible for the majority of slag sulphur extracted and converted to thiosulphate. The contribution to the end-of-run conversion to thiosulphate would be expected to be decreased by virtue of the extended presence of sulphide in solution at higher solid to liquid ratios. The results showed that the opposite occurred. Thus, this effect appears to have been offset by other advantages, including those for the leaching and oxidation of the soluble sulphides.

The driving force for the leaching of the soluble sulphides would be initially doubled for a mass concentration increase from 50 g/l to 100 g/l, assuming that the amount of sulphur present in the slag is doubled when the mass concentration is doubled. This would lead to an increased leaching rate. The presence of increased sulphide in solution would increase the aqueous sulphide oxidation rate. This increase would be higher than the proportional increase in the sulphide aqueous concentration due to the exponential rate law order being greater than unity for sulphide.

The increase in sulphur extraction and thiosulphate conversion from the 50 g/l to the 100 g/l experiment was not continued from 100 g/l to 133 g/l. This may be a result of the extended presence of sulphide in solution for the 133 g/l experiment, offsetting any advantages in soluble sulphide leaching and oxidation. This is supported by the thiosulphate concentration graph, which indicates that the production rate of thiosulphate was decreasing towards the end of the 100 g/l experiment, while that of 133 g/l experiment does not appear to be significantly reduced towards the end of the experiment. This could be a result of the removal of inhibition to oxidative leaching later in the experiment for the 133 g/l experiment. The fact that there was no sulphide present in the reaction solution between 32h25 and 48h00, during which time the thiosulphate concentration increased greatly, discounts the likelihood that this increase was due to the oxidation of soluble sulphide rather than oxidative leaching.

6.3.4 Particle starting size

The increase in thiosulphate conversion with decreasing particle size was not in proportion to the increase in surface area. Both the soluble sulphide and insoluble sulphide leaching rates should be proportional to the surface area exposed to the solution as shown by equation 2-17. The differences between the end-of-run results were not in proportion with the starting surface area difference. This indicates the propensity of the slag to disintegrate. Thus, it is only at the start of the experiment when the differences between the surface areas would be similar to their calculated values (Appendix H-6). Disintegration causes the surface area available for leaching to become increasingly similar as the experiment progresses for all particle sizes. This would explain the observation that the relative variation between thiosulphate concentrations does not increase significantly after 8 h.

Despite the decrease in the differences in surface area exposed to leaching over the course of the experiment due to disintegration, the results show that the slag starting size still plays a significant role in the end-of-run results obtained. Thus, the differences in the extent of disintegration that different sized slag blocks require, would have an impact on the rate at which slag sulphur is converted to thiosulphate.

6.3.5 Air flowrate

From the end-of-run results, it is evident that increasing the air flowrate does not have a significant effect on the extraction of sulphide from the slag. The comparatively small increase in dissolved oxygen concentration when the air flowrate was doubled, indicates that at 5.3 l/min the air flowrate does not appreciably limit the transfer of oxygen from the gas phase to the liquid phase in the 4 litre reactor.

6.3.6 Experimental run time

Doubling of the experimental run time caused a relatively small increase in the thiosulphate conversion. This suggests that, under base conditions, the total conversion of the slag sulphur to oxidised sulphur species was either approached very slowly or the maximum possible conversion is significantly less than 100 % conversion.

The thiosulphate production graphs indicate that the differences between the slag types in thiosulphate conversion, as shown by the extended experiment end-of-run results, were not likely to be as appreciable if the experiments were extended further. It is apparent that slag O achieved a greater conversion more quickly than slag N. This finding was also typical of many 48 h experiments.

6.4 Investigation of the subprocesses occurring during leach - oxidation

6.4.1 Disintegration rate

Disintegration was caused by dissolution of the soluble slag constituents. The fact that the slag disintegrates implies that the remaining insoluble components were not retained as a porous structure once the soluble components are removed, but are washed away. The experimental results of Section 5.4.1 showed that the slag blocks were rapidly reduced in mass and the block was observed to be correspondingly reduced in volume. This finding would not be consistent with a mechanism where the soluble components diffused out of the pores in the slag, leaving behind a solid that retains its structure as the slag is composed of only 15 % - 30 % soluble material.

The likely mechanism for disintegration in water is that the soluble components of the exposed outer layer of the slag block are dissolved, which weakens the surrounding structure of the insoluble components. This weakened outer layer would be washed away if sufficient shear stress was placed on it. If this occurred, a new layer would be exposed to dissolution and the process would repeat itself. Evidence for this mechanism was found in the experimental results where the agitation rate and slag block size were varied.

Effect of agitation

The results show that agitation had a considerable effect on the disintegration rate. This would be expected due to the increase in the rate of dissolution with increasing agitation. Increased agitation would decrease the boundary layer thickness around the slag block and therefore increase the rate of dissolution from the outside layer. Once the soluble components were removed from the outside layer, it would become structurally weakened. In the presence of agitation it is likely that this weakened layer would be washed away as a result of the shear stresses applied by the surrounding moving fluid. Thus, a new layer of slag would be exposed to dissolution. In the absence of agitation, dissolution from the outer layer would be slower and the outer layers would not be washed away, resulting in an increased resistance to transport of the solution and dissolved solutes through this layer.

This mechanism is consistent with the observed decrease in the disintegration rate for an agitated experiment, as the block became progressively smaller, see Figure 5-1. The percent disintegration was calculated relative to the mass of the original block of slag. Assuming that the block had a uniform density, the percent disintegration would also be relative to the volume of the original slag block. It would be expected that if the agitation rate remained constant, the outer layers should be washed away at the same rate no matter the size of the slag block, i.e. the thickness of the layer washed away should be constant with respect to time. The percent of the original volume accounted for by each subsequent layer of slag removed would be progressively smaller and smaller as the slag block decreased in size, corresponding to the decrease in the area of the outer layer. This explains the observed fall in the disintegration rate as the block became smaller.

It is also likely that certain phases provide more resistance to disintegration by virtue of having a lower soluble content would remain undisintegrated for longer. This would also cause a slowing in the disintegration rate after the more soluble phases are removed.

The relevance of agitation to the rate of disintegration of the slag, when large starting size slag blocks are used, would cause this subprocess to contribute with increasing significance to the rate at which the slag sulphur can be converted to a thiosulphate product.

Effect of slag mass

The slower rate of disintegration corresponding to an increase in the starting slag block mass is also consistent with the mechanism hypothesised. For a slag block of larger initial volume, the outside layer accounts for a smaller fraction of the original volume of the slag block, in comparison with a block of smaller volume. The rate at which the outer layers were washed away should be the same for each experiment regardless of the starting block size, due to the agitation rate being the same. Thus, the percent disintegration that occurs as each layer was removed would be lower for a block of larger initial volume, as was observed from the results.

By this mechanism, the starting block size plays an important role in determining the rate at which the slag disintegrates. As the starting block size is increased, the disintegration rate would be progressively decreased, and thus contribute with increasing significance to the rate at which the slag sulphur can be converted to a thiosulphate product.

6.4.2 Dissolution experiments

Analysis of dissolution rate data

Based on the measured sulphide solution concentrations, equation 2-13 was not successful in predicting the dissolution rate of sulphide from the fine fraction after 10 min. The major cause for this was that the sulphide oxidation reaction was not successfully inhibited, which resulted in the sulphide being depleted. Equation 2-13 would therefore over-estimate the actual solution sulphide concentration. Another likely cause was that this first order equation may only successfully predict the initial dissolution rate for the soluble slag components. Evidence of this was found in fitting the sodium dissolution results to equation 2-13. The equation was found to only adequately predict the dissolution rate for the first 30 min (regression coefficient of 0.97). The soluble sulphides were expected to be in the form of sodium sulphide, therefore the dissolution rates of sulphide and sodium should have been closely related. One potential reason why this hypothesis may not have been true, is the location of sodium compounds in phases that provide greater resistance to leaching than the phase in which the sodium sulphide is found. Sodium sulphide was found in Section 5.1 to be a constituent of the matte phase while sodium was also found to also be a constituent of the less soluble silicate phases.

Depletion of sulphide was not expected to significantly lower the concentration of sulphide readings within the first 10 min. This was indicated by the fit of equation 2-13 to the experimental results during the first 10 min. During this time the equation did successfully predict the sodium dissolution rate. Additionally, it was ensured that the dissolved oxygen concentration of the solution was zero prior to starting the dissolution experiments, therefore the oxidation rate would initially have been suppressed.

The initial leach rate constants, calculated for the first 10 min when the fit was adequate, were useful in comparing the initial dissolution rate under different conditions.

The accurate determination of the leach rate constant is dependent on the determination of the slag's maximum soluble sulphide. The method in calculating this could have been in error due to soluble thiosulphate or sulphate being present in the feed slag or oxidative leaching of the insoluble sulphides occurring during the dissolution experiment. No thiosulphate or soluble sulphate was detected in the slag under XRD analysis ($PbSO_4$ was detected). If these oxidised species were present (for example in the non-crystalline phases, which were not detected by XRD analysis) it is likely that they would be present in similar quantities in each experimental slag sample. Thus, the impact of using the leach rate constant for comparison between the initial dissolution rates of different experiments should not have been significantly affected.

Oxidative leaching of insoluble sulphides to thiosulphate and sulphate is unlikely to have occurred during dissolution experiments, due the presence of sulphide in significant quantities in solution. Oxidation experiments showed that, during the time that significant concentrations of sulphide were present, virtually all of the thiosulphate and sulphate production could be accounted for by aqueous sulphide oxidation (see Section 7.2.3).

Dissolution of sulphide under base case conditions

The initial rapid leaching rate evident from the base condition sulphide concentration graphs can be explained by the driving force term of the first order dissolution rate equation (equation 2-13). The driving force for dissolution is the difference between the maximum soluble sulphide present in the slag and the sulphide that has already leached. This was greatest early in the experiment when the latter value was low, hence the high initial dissolution rate.

After the initial sharp increase, the sulphide concentration was expected to increase slowly as the maximum soluble sulphide value was approached. Instead, the sulphide in solution was depleted at a greater rate than it was leached into solution causing a lowered sulphide concentration. This depletion was due to oxidation and shows that dissolved oxygen is present in the reaction solution despite the sparged nitrogen. The variation in the rates of decline of different experiments indicates that the removal of oxygen from the reactor solution was achieved to varying degrees of success.

The maximum soluble sulphide calculation assumes that all sulphide was leached out of the slag by the end of the 24 h dissolution experiment. This was not possible to determine from the sulphide concentration graph. However, the sodium concentration graphs show only a small increase in concentration over the final 12 h of the experiment, indicating that little further soluble sulphide goes into solution during this time.

The calculated maximum soluble sulphide concentrations account for only a small fraction of the total sulphur present in the feed slag and only approximately 12 % of the sulphur extracted from the slag. This firstly indicates the small relative contribution that the soluble sulphide fraction makes to converting the slag sulphur to thiosulphate. Secondly, it provides evidence for an alternative oxidation mechanism for the conversion of slag sulphur to thiosulphate.

Comparison of reactors of differing volumes

The results indicate that equivalent leaching rates are obtained for both 1.5 and 4 litre reactors under base conditions. More experiments would be required to prove if this observation is statistically significant.

Comparison between slag N and slag O

Comparison of the sulphide dissolution graphs showed that the initial dissolution rate was similar for slags N and O. Thus, the lower initial leach rate constant for slag N appears to be compensated for by its greater initial driving force for leaching. This greater driving force would be a result of the higher maximum soluble sulphide concentration that was calculated for this slag. The higher initial leach rate constant for slag O indicates a more efficient extraction of soluble sulphide for this slag. This was consistent with the disintegration rate experiments, which showed that under the same conditions, slag O disintegrated more rapidly.

Comparison of dissolution from the fine fraction and the coarse fraction

While the dissolution rate for the fine fraction was initially significantly greater, this difference was not in proportion to the difference between the surface areas exposed to leaching at the start of the experiment. This was a result of the rapid disintegration of the slag. Additionally, the calculated maximum soluble sulphide concentration of the coarse fraction was not appreciably less than the value for the fine fraction. This indicates that, in 24 h, the soluble sulphide contained in the coarse fraction was exposed to leaching to a degree not appreciably less than the fine fraction.

The regression coefficient for the coarse fraction (0.93) indicated that the linear fit for the initial dissolution (10 min) of the coarse fraction was significantly less accurate than for the fine fraction. This was explained by the assumption of the dissolution equation (equation 2-13) that all sulphide was exposed to leaching from the start of the experiment. This was expected to be the case with the fine fraction experiments, but not the coarse fraction experiments. Thus, even during the first 10 min of the coarse fraction experiment, equation 2-13 cannot be used to predict the dissolution rate.

Investigation of conditions affecting the dissolution subprocess

Temperature

The experimental results showed that temperature had a significant effect on both the value of the initial leach rate constant and the amount of soluble sulphide leached. The increased initial rate of soluble sulphide extraction, shown by the initial leach rate constant calculated, would have been caused by an increase in the diffusion coefficient. The leach rate constant encompassed this term in equation 2-13, and therefore is also a function of temperature.

The increase in the extraction of soluble sulphide shown by the 60 °C experiment appears to indicate that not all the soluble sulphide was extracted from the slag during dissolution experiments below this temperature. This may be a result of the increased rate of extraction at this temperature, but may also have been a result of the occurrence of oxidative leaching, Section 5.3.1 showed that oxidative leaching is greatly promoted by an increase in temperature. This would cause the calculated maximum soluble sulphide concentration to be artificially increased by thiosulphate that was not produced by aqueous sulphide oxidation.

Although the sulphide readings for the experiments run at temperatures higher than 20 °C obeyed a linear fit during the initial 10 min, it is likely that some oxidation did occur during this time. This would reduce the value of the calculated initial leach rate constant. This is a likely cause of the error in the fit of the calculated initial leach rate constants of the 20 °C, 40 °C and 60 °C experiments to an Arrhenius type equation. The only term encompassed by the leach rate constant that is a function of temperature is the diffusion coefficient, which is known to have an Arrhenius type temperature dependence (Section 2.4.1).

Agitation rate

The significant increase in the initial leach rate constant of the fine fraction with increasing agitation rate is due to the decrease in the boundary layer thickness, which is one of the terms that it encompasses. The significance of the boundary layer thickness to dissolution was discussed in Section 2.4.1.

The effect of the agitation rate was greater for the increase in agitation from 200 rpm to 600 rpm than an increase from 600 rpm to 1200 rpm. This was particularly evident from the relatively small increase in soluble sulphide extraction for the agitation rate increase from 600 rpm to 1200 rpm. This small increase in extraction occurred despite the significant increase in the initial leach rate constant by this agitation rate increase. This indicates that the agitation rate does not significantly limit extraction of the soluble sulphide at 600 rpm for an experiment of 24 h duration.

The fact that the initial rate of dissolution did not limit the extraction of soluble sulphide indicates that virtually all the soluble sulphide that could be extracted from the slag at 20 °C had been extracted by the end of the experiment. This shows that the maximum soluble sulphide values calculated do represent the soluble sulphide content of the slag.

Solid to liquid ratio

The driving force for dissolution would be increased by an increase in the solid to liquid ratio. This driving force is caused by the difference between the maximum possible soluble sulphide that can dissolve from the slag under the experimental conditions and the soluble sulphide that had already dissolved. Thus, the increased sulphide dissolution rate is a result of the increase in driving force rather than a significant change in the leach rate constant.

Although the dissolution rate was significantly greater for the 100 g/l experiment, the percent extraction of soluble sulphide from the slag was less. Twice as much soluble sulphide should have been extracted from 100 g/l experimental slag sample compared to the 50 g/l experimental sample. The fact that percent extraction was less for the 100 g/l experiment indicates that the run length was insufficient for the soluble sulphide extraction to closely approach the maximum percent that can be extracted. The similar degree of extraction achieved by the 10 g/l and 50 g/l experiments indicates that the run length was sufficient for all the extractable soluble sulphide to be removed at a solid to liquid ratio of 50 g/l. Thus, it appears that at the base condition solid to liquid ratio (50 g/l) and run length (24 h), the solid to liquid ratio would not limit the amount of soluble sulphide that can be extracted.

6.4.3 Oxidation of aqueous sulphides

Analysis of oxidation rate data

The linearised plots obtained in the calculation of the oxidation rate constants show that the exponential rate law equation (equation 2-19) together with the reaction orders of Lefers *et al* (1978) are valid for the experiments in this study. This is an expected result as the conditions under which Lefers *et al* (1978) determined their reaction orders were in the same initial sulphide concentration and pH range as the oxidation (and leach – oxidation) experiments of this study. The temperature difference between the base condition and the temperature at which Lefers *et al* (1978) determined their reaction orders should not affect the applicability of the reaction orders. This is because the only term in the rate equation (equation 2-19) that is a function of temperature is the oxidation rate constant.

Oxidation of aqueous slag sulphides under base conditions

The initial sulphide oxidation rate was rapid despite the low initial dissolved oxygen concentration. This was caused by the significantly greater value of the reaction order with respect to sulphide compared to that of oxygen. Hence, the sulphide oxidation rate is a significantly stronger function of the sulphide concentration. Similarly, once the sulphide concentration was depleted, oxidation proceeded at an appreciably lower rate.

The initially low values of the dissolved oxygen concentration are explained by the high consumption rate of dissolved oxygen due to the rapid initial sulphide oxidation rate. The rapid increase in the dissolved oxygen concentration after this time indicates that, after the initial 10 min, the sulphide oxidation rate was not significantly inhibited by the transfer of oxygen to the aqueous phase.

A natural logarithmic fit was obtained for the dissolved oxygen concentration of the 4 litre experiments. The assumption that the same natural logarithmic equation can be used to estimate the dissolved oxygen concentration in the 1.5 litre reactors would be a source of potential error in the rate constant determination. This error would be due to differences in the oxygen mass transfer characteristics of the 1.5 litre and 4 litre reactors as well as different initial sulphide concentrations resulting in varied initial oxygen consumption rates. O'Brien and Birkner (1977) used a similar assumption in modelling the dissolved oxygen concentration of their sulphide oxidation experiments, but they used a natural exponent fit.

Variation in the oxidation rate constant relative to the average rate constant determined over the whole experiment was observed during certain times in the experiment. Typically, only temperature affects reaction rate constants. However, the rate constant for the sulphide oxidation reaction has been shown to be a function of pH as well. The experiments of Chen and Morris (1972) showed an increase in the rate constant for a decrease in pH from 13 to 11. The oxidation rate constant would also be increased by the presence of Fe^{2+}, which was identified in Section 2.4.2 to be a catalyst for the aqueous sulphide oxidation reaction. Iron in the form of Fe^{2+} is present in significant quantities in the slag early in the experiment in the form of FeS and $Na_2S.FeS$. Although it is unknown whether this catalysis takes place homogeneously or heterogeneously, early in the experiment Fe^{2+} would be present in raised relative

amounts in both the aqueous phase due to $Na_2S.FeS$ and insoluble phase due to FeS. Thus, catalysis is likely to occur regardless of which mechanism (homogeneous or heterogeneous) is obeyed.

The increased presence of Fe^{2+} explains the apparent increase in the rate constant at early times in the experiment. The observed subsequent reduction in the oxidation rate constant corresponds to the reduction in the Fe^{2+} both from solution and in solid form by oxidative leaching to Fe^{3+}. The apparent increase in the rate constant after 2h00 (particularly from 5h00 to 6h46) can be attributed to the decrease in pH.

Comparison of reactors of differing volumes

The oxidation rate constant is not a function of the mass transfer characteristics of the reactor. Thus, the result that the oxidation rate constant was not significantly different for the reactors of different volumes is expected. However, the mass transfer characteristics would influence the observed rate of sulphide depletion through the dissolved oxygen concentration term of equation 2-22. These were hard to determine due to the different initial sulphide concentrations.

Comparison between slag N and slag O

A possible explanation for the increased oxidation rate constant of slag N compared to slag O is the greater iron component of slag N (see Section 5.1.1). Iron is expected to be initially all in the form of Fe^{2+}. Hence, the iron content would be directly proportional to the amount of potential catalyst present.

Investigation of conditions affecting the oxidation of aqueous sulphide

Temperature

The observed increase in the sulphide oxidation rate with increasing temperature is the result of the increase in the oxidation rate constant. The reaction rate constant is typically only a function of temperature, but for this reaction it is also a function of pH. If Fe^{2+} catalysis occurs, this would also affect its value.

The linear fit of the natural logarithm of the rate constant versus the inverse of temperature plot (Figure 5.4-13) indicates that the temperature dependence of the oxidation rate constant is given by the Arrhenius equation. The constants for the Arrhenius equation, shown in Section 5.4.3, theoretically allow the calculation of the rate constant at any temperature. However, calculated values would contain significant statistical error due to the plot containing only three data points. Extrapolation of the rate constant outside the experimental temperature range (20 °C to 60 °C) would cause substantial error.

Agitation rate

The oxidation rate constant is not a function of the agitation rate. Therefore, no oxidation experiments were run to determine its value under different agitation rates. However, the agitation rate would have an affect on the observed rate of sulphide oxidation, due to its effect on the dissolved oxygen concentration and sulphide concentration values. Increasing the agitation rate leads to an increased oxygen mass transfer and hence a greater dissolved oxygen concentration. Therefore, increasing the agitation of the reactor solution would cause the observed aqueous sulphide oxidation rate to increase due to its dependence on dissolved oxygen concentration. An increase in the agitation rate was also found to increase the rate of the dissolution of sulphide. A higher aqueous sulphide concentration would also increase the observed aqueous sulphide oxidation rate.

Solid to liquid ratio

The oxidation rate constant should not be a function of the solid to liquid ratio. A possible reason why the rate constant increased slightly with increasing solid to liquid ratio was the presence of higher relative quantities of Fe^{2+} catalyst. The differences between the starting sulphide concentrations for each experiment was relatively small, compared to the substantially increased initial quantity of Fe^{2+} present. Thus, the greater effective catalyst concentration may have been the cause of the increase in the calculated oxidation rate constant.

Absence of insoluble slag component

Two major findings were yielded by the comparison between the results obtained from the oxidation of pre-leached unfiltered solutions and filtered solutions. The first finding was that the removal of most of the insoluble sulphide component caused a substantial decrease in thiosulphate produced. This indicated that the insoluble component is responsible for much of the conversion of slag sulphur to thiosulphate. This confirms the hypothesis that the slag sulphur, which remains insoluble, is also converted to thiosulphate by oxidative leaching without appearing in the solution as aqueous sulphide.

The second finding was that the calculated sulphide oxidation rate constants were several times less for the filtered case compared to the unfiltered case. Since no other experimental conditions were changed, the reason for this appears to lie with the absence of the insoluble iron component, which in the form of Fe^{2+} is known to be a catalyst of the sulphide oxidation reaction. Even the substantial increase in the experimental rate constant in the presence of the Fe^{2+} does not match the increase found by Zhang and Millero (1993) which was 60 times, shown by Table 5-4.10. The thiosulphate production results showed that not all the insoluble FeS was removed by filtering, so there would still be some Fe^{2+} catalyst present in the filtered solution, but at a lower total concentration. Thus, the oxidation rate constants obtained for the filtered experiments are still likely to be greater than the value that would be obtained if no iron were present. This also provides an explanation as to why the increase in the oxidation rate constant where the pre-leached solution was unfiltered was less than the increase found by Zhang and Millero (1993).

Comparison of rate constants obtained experimentally with literature values

The oxidation rate constants obtained in the experiments of this study were found to be similar to an sulphide oxidation rate constant determined by Zhang and Millero (1993) for a Fe^{2+} catalysed experiment. The oxidation rate constants obtained were several times higher than that of non-catalysed literature oxidation rate constants. This provides another source of evidence that Fe^{2+} catalysis caused a substantial increase in the sulphide oxidation rate constant for the experiments in this study. Thus, the aqueous sulphide oxidation rate is correspondingly several times higher than would have been the case if no Fe^{2+} was present.

7 Evaluation of experimental results

7.1 Individual subprocesses

The results of the experimental and literature investigations allow the individual subprocesses that are relevant to the leach – oxidation step to be identified. These are as follows:

- Leaching of soluble components
- Oxidation of soluble sulphides
- Oxidative leaching of insoluble sulphides

The diagram shown in Figure 7-1 illustrates these subprocesses. The sequence in which the subprocesses occur is shown for each of the routes for converting the slag sulphur to thiosulphate and sulphate.

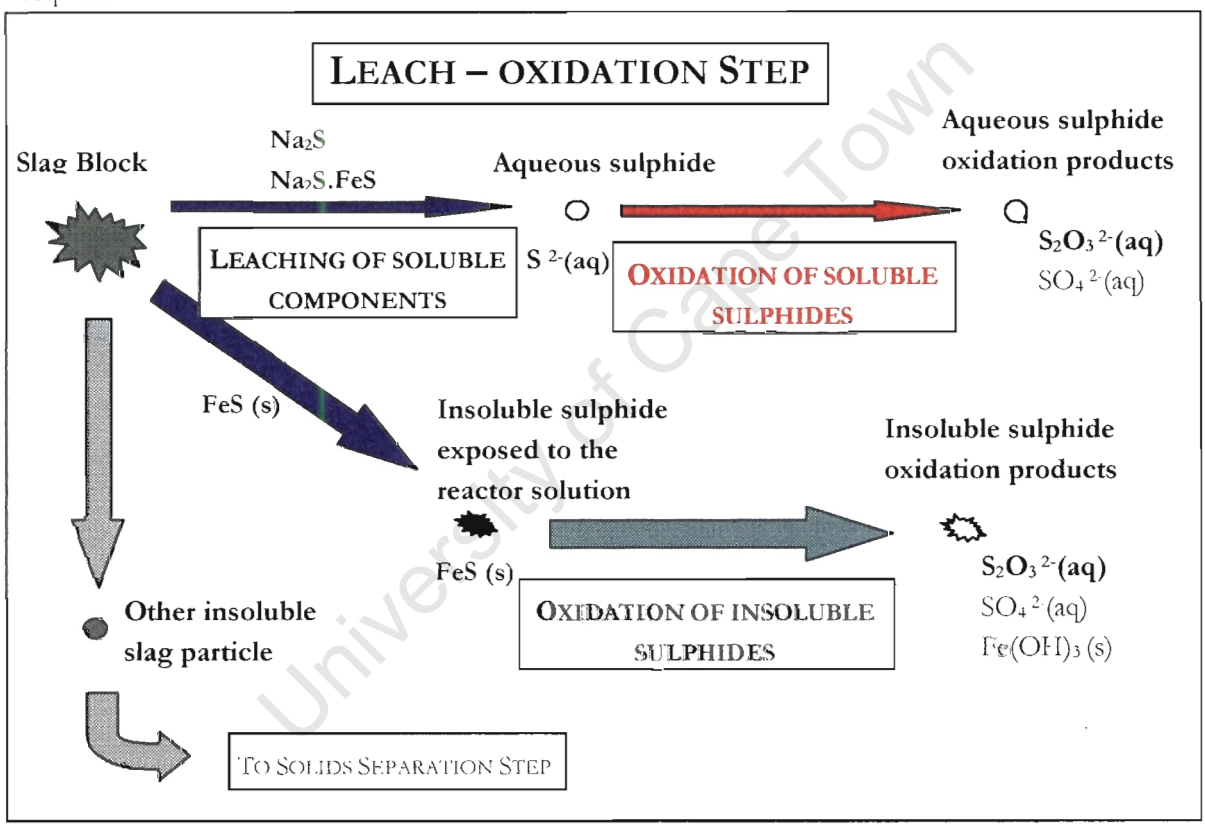

Figure 7-1 Subprocesses that occur during leach – oxidation

The individual subprocesses that were identified as relevant to the leach – oxidation step are discussed below in terms of:

- the contribution of their rates to determining the overall rate of the conversion of slag sulphur to thiosulphate under base conditions
- the understanding gained of the mechanism by which they occur, particularly in terms of sequence and interdependence
- the applicability of rate equations to modelling the aqueous sulphide dissolution and oxidation subprocesses

7.1.1 Leaching of soluble components

The 'leaching of the soluble components' subprocess encompasses dissolution and disintegration as discussed in Section 3.2. The process of dissolution of soluble slag components causes the disintegration of the slag. Disintegration results in the further exposure of soluble sulphides as well as the insoluble sulphides contained in the slag. Thus, the leaching of the soluble components is necessary for exposing the insoluble sulphides to the reactor solution and hence is also the first step for the oxidation of the insoluble sulphides.

Effect of the disintegration rate

The leach – oxidation and dissolution experimental results showed that the initial dissolution rate of the soluble sulphide was lowered when the coarse fraction was used in comparison with the fine fraction. However, the difference between the two observed rates was several times less than the difference that would be expected if leaching occurred in the absence of disintegration, i.e. only from the particle surface or by pore diffusion. This comparison shows the appreciable effect that disintegration has on the leach – oxidation process. The small relative differences between fine fraction and coarse fraction experiments for the overall conversion to thiosulphate, suggest that disintegration did allow sulphur components (soluble and insoluble) in the slag to be exposed to leaching to a similar degree during the 48 h experiment, regardless of the starting size.

Disintegration rate experiments allowed the effect of the disintegration rate of slag blocks of greater size to be evaluated under conditions similar to the base conditions. Increasing the slag starting size was found to have the effect of decreasing the disintegration rate. Hence, the rate of the exposure of the sulphur components (insoluble and soluble) to the leaching action of the solution would be reduced and in turn the rate conversion of slag sulphur to thiosulphate and sulphate would also be reduced.

An example of the difference that the change in slag starting size would cause is found by the fact that a slag block of approximately 85 mm diameter (398 g, slag O) took two hours to disintegrate to a size approximately equal to that of the coarse fraction under base conditions. Less favourable conditions for dissolution and hence disintegration are likely to be found in a scaled up reactor, as is discussed in section 7.2.1. This would cause this subprocess to occur at an even slower rate.

Dissolution of soluble components

Under base conditions, the initial dissolution rate of the soluble sulphide and sodium components was found to be rapid for the fine fraction. An example of this was the sodium concentration, which on average reached 92 % of the 24 h value after only 60 min. This shows that dissolution was rapid under base conditions if the soluble component was exposed to the solution (as in the case of the fine fraction).

A first order dissolution equation was found to fit the fine fraction dissolution experimental data for sulphide and sodium for only the initial 10 min and 30 min respectively. The lack of a fit to the sulphide data after this time was expected due to oxidation. However, the sodium dissolution rate after 30 min shows that the assumptions under which the dissolution equation was derived do not apply to

the dissolution of soluble components from the fine fraction. The equation predicts that all the soluble components are exposed to the solution at the start of the experiment and the dissolution rate swiftly approaches zero subsequent to the rapid initial dissolution. This was not the case for the observed dissolution rate in this study. This showed that even for the fine fraction, the soluble components were not all exposed to leaching from the beginning of the experiment. This is likely to be as a result of some of the soluble slag components, especially sodium, being bound up in less soluble phases which provide greater resistance to leaching.

The course fraction showed even greater deviations from the leaching trend predicted by the equation, as expected by the fact that only a small fraction of the soluble components are exposed to the solution at the beginning of the experiment. This deviation would have been more significant in the absence of any disintegration occurring.

Thus, if the dissolution process is to be modelled, a more rigorous model than the first order equation is required. To be successful it should take into consideration the effect of the differing resistances of different phases to leaching and the effect of particle size on the dissolution rate, which would be closely related to the disintegration behaviour of the slag.

7.1.2 Oxidation of soluble sulphides

The depletion of soluble sulphides by oxidation was observed to occur at a rapid rate in oxidation experiments under base conditions. The sulphide concentration was reduced on average to 13 % of the starting concentration after approximately 30 min. In leach – oxidation experiments, where dissolution occurs simultaneously, the sulphide concentration was reduced on average by 6.3 % of its 10 min peak after 60 min. Two factors would cause this rapid depletion of soluble sulphide during leach – oxidation to be retarded under a larger scale of operation. Firstly, the conditions for oxidation are likely to be less favourable, an aspect further discussed in section 7.2.3. Secondly, the removal of the soluble sulphide present in the slag would occur at a lower rate, due to the dependence of the dissolution rate on the particle size.

The rate law equation for the aqueous sulphide oxidation reaction, equation 2-19, together with the reaction orders of Lefers *et al* (1978), fitted the experimental data obtained from oxidation experiments. The dependence of the rate on the pH and presence of varied concentrations of Fe^{2+} catalyst during the experiment, explained deviations observed.

7.1.3 Oxidation of insoluble sulphides

The experimental investigation yielded evidence for the occurrence of this reaction, even though it is not directly evident from analysis (due to the aqueous reaction product being the same as that of the oxidation of soluble sulphide). The sources of this evidence are as follows:

- All matte phase spots analysed by EDS yielded iron to sodium molar ratios well in excess of 0.5 (for example this ratio was 1.1 for the matte phase spot analysed in Section 5.1.3). 0.5 is the molar ratio required for all iron and sodium to be accounted for by the $Na_2S.FeS$ compound. Thus, FeS

conversion to thiosulphate) for the experiments of Section 5.2 and Section 5.4.1 showed that more than just the sulphide associated with Na_2S or $Na_2S.FeS$ would have been extracted to the aqueous phase during leach – oxidation.

- Most of the thiosulphate production during the leach – oxidation experiments occurred after the solution sulphide concentration became zero.
- Oxidation experiments where the pre-leached solution was filtered yielded only a fraction of the thiosulphate produced by experiments which were unfiltered (Section 5.4.3)

The experimental investigation of this subprocess was aimed primarily at proving whether this reaction occurred, and did not yield much information about its mechanism. The driving force for oxidative leaching reactions is caused by the redox potential of the solution. Aqueous sulphide is a reducing agent, and therefore causes the redox potential of the solution to decrease. Thus, it was expected that the oxidative leaching reaction would be inhibited until sufficient depletion of the soluble sulphides by oxidation had taken place.

Experimental evidence for this was found from unfiltered oxidation experiments. For example for base oxidation experiment number 1, the depletion of the soluble sulphide by oxidation accounted for 92 % of the thiosulphate produced during the first 30 min. Over the whole 24 h of the experiment, the depletion of the soluble sulphide by oxidation accounted for only 4 % of the thiosulphate produced.

This result indicates that the aqueous sulphide has to be removed from solution to below a certain level before the oxidative leaching reaction is no longer significantly inhibited. This result indicates the sequence in which these subprocesses occur, showing that the oxidation reactions of soluble and insoluble sulphide do not proceed independently of each other.

It was shown in Section 5.4.2 that only a small fraction of the conversion to thiosulphate was due to oxidation of the soluble sulphides. However, the time taken to deplete the aqueous sulphides would have a significant impact on the conversion to thiosulphate due to inhibition of the oxidative leaching reaction.

This impact would not be considerable under base conditions due to the rapid depletion of the aqueous sulphide under these conditions. However, conditions applied in a scaled up reactor are unlikely to favour the dissolution and oxidation of the aqueous sulphide as much as base conditions, this would cause the oxidative leaching reaction to be retarded for a longer time. This is further discussed in Section 7.2.3.

The rate of dissolution of the soluble components, and hence the disintegration rate of the slag, therefore played a dual role in determining the extent of oxidative leaching during leach – oxidation. Firstly, this was due to the requirement that the insoluble sulphide must be exposed to the solution before oxidative leaching can occur. Secondly, the rate of extraction of the soluble sulphides will contribute to determining the time period during which oxidative leaching is inhibited.

7.2 Effect of processing conditions on leach – oxidation

In this section, the conditions that had a significant impact on each of the subprocesses and overall step are discussed. Where applicable, the conditions under which each of the subprocesses limit the rate of the overall leach – oxidation step were identified. Particular attention is given to those conditions that are likely to be altered significantly from the base conditions in a scaled up situation.

7.2.1 Leaching of the soluble components

Effect of disintegration rate

Agitation and slag starting size were observed to play significant roles in determining the time required for blocks of slag to reach a size equal to the coarse fraction. The mechanism which was proposed to explain the observed disintegration behaviour (see Section 5.4.1) showed the dual role that agitation plays in increasing the dissolution rate and removing weakened outer layers. Hence, agitation and slag starting size would play significant roles in the rate at which the soluble and insoluble sulphide species are exposed to leaching. The starting size in a full-scale operation is likely to be appreciably higher due to limitations imposed by the cost of communition. A full-scale operation is also unlikely to be able to achieve the same agitation rate as the base condition rate. Thus, under scaled up conditions, the disintegration rate would be expected to increasingly become rate-determining to the overall leach – oxidation rate (rate at which sulphur can be extracted from the slag and converted to thiosulphate), as these slag starting sizes and agitations become less favourable to dissolution and disintegration.

Dissolution of soluble components

Varying the agitation rate during dissolution experiments showed that the rate of dissolution at the base condition agitation rate was significantly less when a lower agitation rate was used. Variation of temperature and solid to liquid ratio also had a significant effect. However, the rate of dissolution was limited by the agitation rate when the lower agitation rate was used. Thus, the high agitation rate was primarily responsible for the rapid dissolution rate observed under base conditions. A lower agitation rate, which is likely under scaled up conditions, would lower the rate of this subprocess and therefore cause the disintegration rate to be reduced. Also, this would retard the oxidative leaching subprocess (see Section 7.2.3).

Although not as significant as agitation, the temperature and solid to liquid ratio did have an impact on the dissolution rate. Raising the temperature to increase the rate of this subprocess is unlikely to be cost effective. Although doubling the solid to liquid ratio did not double the sulphide extraction rate, the increase in soluble sulphide extraction at a higher solid to liquid ratio would allow an increased slag treatment capacity for the same volume of reactor.

7.2.2 Oxidation of aqueous sulphide

The depletion of aqueous sulphide was found to obey the rate law expression found in equation 2-19. This is stated in equation 7-1 with the successful reaction orders of Lefers *et al* (1978). The reaction

orders show the dependence of the aqueous sulphide oxidation rate on the sulphide and oxygen aqueous concentrations.

$$\frac{dC_S}{dt} = -k * C_S^{1.47} C_{O_2}^{0.55} \qquad \text{equation 7-1}$$

The reaction orders show that the oxidation rate is significantly more dependent on the aqueous sulphide concentration than dissolved oxygen concentration, which was evident in oxidation experiments. Therefore a factor that causes the sulphide concentration to be increased would be significantly more effective in raising the sulphide oxidation rate than another factor that causes a similar increase in the dissolved oxygen concentration. An increase in solid to liquid ratio was shown by leach – oxidation experiments to increase the extraction rate of soluble sulphide and hence achieve greater sulphide concentrations in solution, therefore this factor would raise the sulphide oxidation rate significantly. However, if the effluent were to be further treated by biological means, the solid to liquid ratio would be limited to approximately 50 g/l, a value determined by Barnes (1996).

The dissolved oxygen concentrations measured for the leach – oxidation and oxidation experiments showed that, with the possible exception of early in the run (first 10 min), oxygen transfer to the aqueous phase would not inhibit the reaction, i.e. excess oxygen is present in the solution. The dissolved oxygen concentration of the solution would still affect the rate of sulphide oxidation as shown by equation 7-1. The dissolved oxygen concentration remained significantly above zero and was observed to increase during the run. This shows that the rate of transfer to the solution exceeds the rate of depletion by the aqueous oxidation reaction. The agitation rate and airflow rates are known to be responsible for increasing the oxygen transfer. The air flowrate was not found to limit transfer at 1.33 (l air)(l solution)$^{-1}$(min)$^{-1}$, although this may become limiting at significantly lower air flowrates. A lower agitation rate would lower the oxygen transfer rate due to a lesser degree of bubble break-up. These two factors would influence the sulphide oxidation rate through the dissolved oxygen concentration term.

The oxidation reaction rate constant is typically only a function of temperature. However, for this reaction, it has also been found to be a function of pH. Fe^{2+} catalysis was responsible for significantly raising the oxidation rate. This was shown by comparing the oxidation rate constants of the filtered and unfiltered oxidation experiments. The greater effective initial catalyst concentration caused by an increased solid to liquid ratio provided an explanation for the corresponding increase in the rate constant. Thus, a greater solid to liquid ratio may favour the oxidation rate constant term of equation 7-1 in addition to the sulphide concentration.

7.2.3 Oxidation of insoluble sulphides

The goal of experiments investigating the oxidation of soluble sulphides by oxidative leaching were aimed at proving whether this reaction occurred rather than determining the effect of various conditions on this subprocess. However, due to the finding that only approximately 12 % (see Section 5.4.2) of the sulphur extracted from the slag was due to extraction of the soluble sulphides, the end-of-run results of leach – oxidation experiments where conditions were varied, provide an indication of the effect of those conditions on oxidative leaching.

Typically only 55 – 60% of the feed slag sulphur was converted to thiosulphate under base conditions for fine fraction slags N and O. An increase in the temperature was observed to cause the greatest effect, on the conversion of slag sulphur to thiosulphate, of all the conditions under which leach – oxidation was investigated. At an operating temperature of 60 °C, it was shown that virtually all the slag sulphur was converted to thiosulphate (and a small amount of sulphate).

The agitation rate, solid to liquid ratio and particle size were all observed to have an impact on the end-of-run conversion. However, no set of conditions apart from increased temperature caused the conversion to thiosulphate to exceed 65 %. While the agitation had a significant effect on the conversion when it was dropped below 600 rpm, an increase above 600 rpm to 1200 rpm only resulted in a small increase in the conversion (less than 2 % for fine fraction and coarse fraction). This indicates firstly, that under base conditions, the agitation rate (600 rpm) does not significantly limit the conversion to thiosulphate. Secondly, this indicates that oxidative leaching was not limited by the agitation rate at 600 rpm.

These results indicate that, under base conditions, temperature limits the conversion to thiosulphate. As the conversion to thiosulphate was found to be principally due to oxidative leaching, it is evident that temperature limits the oxidative leaching conversion under base conditions.

As discussed in Section 7.2.1, it is likely that scale-up would cause the agitation rate to be lowered and particle size to be increased compared to base conditions. If this occurred, the results of the dissolution and disintegration experiments showed that agitation would become increasingly important to determining the rate of the overall process and may become the limiting factor for the conversion to thiosulphate. The increased differences between the end-of-run sulphur extraction for the fine fraction and course fraction leach – oxidation experiments as temperatures were increased above 20 °C, showed the increased significance of the disintegration rate under conditions where temperature was not limiting.

7.3 Evaluation of process goals

7.3.1 Conversion to thiosulphate

The main goal for the first step of the BROSS process was the conversion of sulphur present in the slag to thiosulphate. The 'near quantitative' conversion of the sulphur component of the slag to thiosulphate was reported by Barnes (1996) for leach – oxidation laboratory experiments on the Enthoven slag. The overall reaction summarising the mass balance across the chemical pre-oxidation reactor showed that all sulphur was required to be converted to thiosulphate (equation 2-8). Typically only 55 % – 60 % of the feed slag sulphur was converted to thiosulphate under base conditions for fine fraction slags N and O. This shows that, either the composition differences between the Enthoven and local slags, or differences in operating conditions caused the conversion to thiosulphate for the local slag to be appreciably lower. It is not possible to make a comparison between the results as not all the operating conditions were reported by Barnes (1996) for treatment of the Enthoven slag.

The requirement for an near quantitative conversion of the slag sulphur to thiosulphate was obtained at an operating temperature of 60 °C. However, operation of the leach – oxidation step at temperatures above that of the Enthoven pilot plant (34.1 °C) would require the stream entering the biological stage to be pre-cooled. Thus this is unlikely to be cost effective.

7.3.2 Depletion of soluble sulphide

The removal of the soluble sulphide component of the slag is necessary for environmental reasons to prevent the contamination of liquids with which the slag comes into contact. The fine fraction base condition experiments all reached a zero sulphide concentration before 18h45, with the exception of one run, which only reached zero by 24h00. The coarse fraction base condition experiments all reached zero sulphide concentration before 24h00, again with the exception of one run which recorded a zero value at 36h00.

The reduction of the aqueous sulphide concentration to zero during the leach – oxidation experimental runs implies that under the experimental conditions all potentially soluble sulphide had been removed from the slag. It is unlikely that any significant leaching of soluble sulphide occurred after the solution concentration became zero. This is assumed, as the aqueous sulphide oxidation rate that would be required to maintain the sulphide concentration below a detectable level would very small due to its sulphide concentration dependence. Additionally, the rate of sodium leaching was found to become negligible toward the end of the 24 h dissolution experiments, this indicates that leaching of sulphide should also become negligible after this time due to the ion balance requirement.

8 Conclusions

The characterisation of the local refiners' slag with respect to the components relevant to leach – oxidation yielded the following conclusions:

1. The slag of the O 20 ton furnace and N 20 ton furnace selected for experimental investigation are not significantly different to those produced on average, based on historical data.

2. The molar ratio of iron to sodium was significantly in excess of 0.5 for all matte phase spots analysed by EDS. This provided evidence for the presence of insoluble sulphides (FeS), in addition to $Na_2S.FeS$, which were both converted to thiosulphate.

3. Evidence for the presence of $Na_2S.FeS$ was found by the increased iron solubility during times when sulphide was present in solution. This raised solubility of iron caused by $Na_2S.FeS$ was insufficient to account for the conversion to thiosulphate of this compound by aqueous phase oxidation.

4. Sodium is present in the slag phase as Na_2O and in silicate matrices. This provided an explanation for the 15 % - 30 % of the sodium remaining insoluble during leach – oxidation experiments.

5. No carbonate was detected in the slag. This indicated that all sodium carbonate was decomposed to sodium oxide in the furnace and that carbon substrate would have to be added if the aqueous effluent of leach – oxidation was to be further treated by biological means.

Investigation of the leach – oxidation process, from individual subprocess experiments and leach – oxidation experiments yielded the following conclusions on the mechanism by which leach – oxidation occurs.

1. The conversion of sulphur present in the slag to aqueous thiosulphate and sulphate oxidation products was found to occur via two different subprocess routes. These were firstly the dissolution and oxidation of the soluble sulphides and secondly the oxidative leaching of the sulphides that remain insoluble (FeS).

2. The leaching and oxidation of the soluble sulphides only accounts for a small fraction (approximately 12 %) of the extraction of sulphur from the slag under base conditions. The rest can be attributed to the oxidative leaching of insoluble sulphides.

3. The oxidative leaching of insoluble sulphides is dependent on the leaching and oxidation of the soluble sulphides. Firstly, the exposure of the insoluble sulphides to the solution is dependent upon the dissolution of the soluble components, which causes the slag to disintegrate. Secondly, evidence was found to confirm that the oxidative leaching is inhibited in the presence of aqueous sulphide. Thus, sufficient depletion of the aqueous sulphide via oxidation must take place before oxidative leaching of insoluble sulphide can take place.

4. A first order leaching model does not predict the rate at which the soluble components of the slag leach except for the initial 10 min. Reasons for this include the effect caused by the slag's heterogeneity and the process of disintegration.

5. The rate of oxidation of the aqueous sulphides is adequately predicted by the rate law of equation 2-19 with the reaction orders of Lefers *et al* (1978). These orders, with respect to sulphide and oxygen, were 1.47 and 0.55 respectively.

$$\frac{dC_S}{dt} = -k \cdot C_S^{\ m} C_{O_2}^{\ n} \qquad \text{equation 2-1}$$

Investigation of the effect of certain process conditions on the overall leach – oxidation of the slag and on the individual processes occurring in this step yielded the following conclusions:

1. Under base conditions, temperature limited the conversion of slag sulphur to thiosulphate. This was caused primarily by the dependence of the oxidative leaching subprocess on the temperature. The dependence of oxidative leaching on the presence of aqueous sulphide, means that the increase in the soluble sulphide dissolution and oxidation rates at higher temperatures would therefore decrease the time during which oxidative leaching was inhibited. The rapid dissolution and oxidation of the soluble sulphides under base conditions means that the impact of the further increase in these rates would not cause a substantial impact on the end-of-run results.

2. While the agitation rate was not limiting at the base condition of 600 rpm, both the end-of-run sulphur extraction and soluble component dissolution rate was limited by this variable when it was decreased to 200 rpm.

3. Agitation was shown to play a substantial role in determining the disintegration rate of slag blocks significantly larger than the coarse fraction size, through dissolution and the removal of weakened insoluble layers. Thus a decrease in agitation significantly below its base value may result in the disintegration rate becoming limiting to the conversion of slag sulphur to thiosulphate.

4. The disintegration rate was dependent on the slag block starting size. While the coarse fraction did not appreciably limit conversion, slag blocks of size 850 mm diameter and bigger took in excess of 2 h to disintegrate to a size equal to that of the coarse fraction under base conditions. Thus, as the slag block size is increased, the disintegration rate would become limiting to the conversion of slag sulphur to thiosulphate.

5. An increased solid to liquid ratio increased the rates of the dissolution and aqueous sulphide oxidation subprocesses and the overall conversion to thiosulphate. Although its impact on the results was not as significant as temperature or agitation, an increased solid to liquid ratio would have other benefits such as decreased water usage. If the aqueous product of leach – oxidation was to be further treated by the biological step of the BROSS process, the solid to liquid ratio would be limited by the ionic strength to a value of approximately 50 g/l, as reported by Barnes (1996).

6. The soluble sulphide oxidation rate constant was substantially raised by Fe^{2+} catalysis. Fe^{2+} is present in the feed slag in significant quantities.

In terms of the goals for the leach – oxidation process, the following conclusions can be made:

1. The 'near quantitative' conversion of the slag sulphur to thiosulphate, which was reported by Barnes (1996) for leach – oxidation treatment of the Enthoven slag, was not attained within a feasible processing time at the base conditions of the experimental investigation (conversion was typically 55% - 60% after 48 h). This conversion was not increased substantially by the doubling of the experimental run time. Only an increase in temperature caused this goal to be attained. Near quantitative conversion was accomplished at a temperature of 60 °C.

2. The environmentally hazardous soluble sulphide component of the slag can be removed from the slag by leach – oxidation. Under base conditions, a zero sulphide concentration was typically attained in leach – oxidation experiments before 24h00 for the coarse size fraction. For the fine fraction, which does not require disintegration, this removal was typically completed before 18h45.

9 Recommendations

The following recommendations can be made regarding the feasibility of using the leach – oxidation step to treat the local slag with respect to the goals of leach – oxidation given in Section 1.2.

1. If complete conversion of the slag sulphur to thiosulphate is a requirement for the leach – oxidation step, further investigation should only be carried out if operation at 60 °C is feasible.

2. If the removal of the environmentally hazardous soluble sulphide component is chosen to be the only criteria for determining the feasibility of the leach – oxidation step, then further investigation is should be carried out as this occurred within the experimental run length under the conditions of this investigation.

If further investigation of the leach – oxidation step is carried out, the following are recommended:

1. Leach – oxidation experiments should be operated on a larger scale, where the effect of the disintegration rate of large slag blocks (> 85 mm) on the rate of conversion to thiosulphate and removal of sulphide, can be properly assessed. The effect of lower agitation rates in collaboration with larger slag blocks on the conversion to thiosulphate and removal of sulphide should also be properly assessed.

2. If the removal of soluble sulphide is a priority, then the concentration of this component in solution should be modelled for the design a leach – oxidation reactor. This can be achieved by finding a suitable rate equation for the dissolution of the soluble sulphide. Combination of a suitable sulphide dissolution rate equation with the successful aqueous sulphide oxidation rate equation would allow the sulphide concentration of the reactor to be modelled under conditions where rate constants have been evaluated.

If further investigation of the leach – oxidation step, particularly with respect to incorporation into the BROSS process is required, then the following are recommended:

1. Investigate the separation of the slag components that remain insoluble during leach – oxidation. This would determine whether a lead rich fraction could be recovered from this leach – oxidation product.

2. Investigate the feasibility of biological oxidation of the leach – oxidation aqueous effluent.

3. Investigate the options for the treatment of the aqueous sodium sulphate effluent of the BROSS process.

References

Alferova, L.A. and Titova, G.A. (1969) "Study of the Reaction Rate and Mechanism for the Oxidation of Hydrogen Sulfide, Sodium Hydrosulphide and the Sulfides of Sodium, Iron and Copper in Aqueous Solution." *Zhurnal Prikladnoi Khimii trans.* **42,** 165–169.

Akkarapattanagoon, N., Itagaki, K. and Yazawa, A. (1989) "Phase distribution of the minor elements in the Fe-Sb-S and Fe-Sb-S-Na_2S systems at 1473 K" *Metallurgical Review of MMIJ.* **6,** 84–97.

Arai, K. and Toguri, J.M. (1994) "Leaching of lead sulphate in sodium carbonate solution". *Hydrometallurgy.* **12,** 49–59.

Avrahami, M. and Golding, R.M., (1968) "The Oxidation of the Sulphide Ion at Very Low Concentrations in Aqueous Solutions." *J. Chem. Soc.* **25,** 647–651.

Barnes, L.J. (1996) "BROSS process: bio-treatment of alkaline slags produced during lead recycling". *Institution of Mining and Metallurgy.* **105,** c113–c125.

Barnes, L.J. (1997a) (1997b) Personal communication. 12 December 1997.

Barnes, L.J. "Bio-Remediation of Sulphidic Slags" Slide presentation. University of Cape Town Chemical Engineering Department. 11 December 1997.

Bayrakceken, S., Yasar, Y. and Colak, S. (1990) "Leaching of FeS in Aqueous Chlorine Solution." *Hydrometallurgy* **25** (3), 357–365.

Bush, D.R., (1994) "Sodium Sulfides." *Encyclopedia of Chemical Technology* **22.** 4th edition, 411–419.

Chen, K.Y. and Morris, C.J. (1972) "Kinetics of Oxidation of Aqueous Sulifide by O_2." *Environmental Science and Technology.* **6** (6), 529–537.

Cline, J.D. and Richards, F.A. (1969) "Oxygenation of Hydrogen Sulphide in Seawater at Constant Salinity, Temperature, and pH." *Environmental Science and Technology.* **3** (9), 838–843.

Corrick, J.D. and Sutton, J.A. (1968) "Oxidation of lead blast furnace matte by ferrobacilus ferrooxidans or dilute acid solution." *US Bureau of Mines Report: Invest* **7126,** 1–19.

Coulson, J.M. and Richardson, J.F. (1991) *Chemical Engineering.* **2,** 4th edition. Pergamon Press, Oxford. 385–420.

Ferreira, D.C.H. (1975) "High - temperature Eh-pH diagrams for the systems S-H_2O and Fe-S-H_2O." *Leaching and Reduction in Hydrometallurgy ed. Burkin, A.R.*, 67–77.

Freeman, H. (1925) "The Genesis of Sulphide Ores." *Engineering and Mining Journal-Press.* **120** (25), 973–975.

Garrels, R.M. and Naeser, C.R. (1958) "Equilibrium Distribution of Dissolved Sulphur Species in Water at 25 °C and 1 atm Total Pressure." *Geochimica et Cosmochimica Acta* **15.** Pergamon Press Ltd, London, 113–130.

Guerrero, A., Romero, A., Morales, R.D. and Chavez, F. (1997) "Thermodynamic Analysis of the soda ash smelting of lead acid battery residue in a rotary furnace". *Canadian Metallurgical Quarterly* **36,** 121–130.

Heunisch, G.W. (1977) "Stoichiometry of the Reaction of Sulfites with Hydrogen Sulphide Ion." *Inorganic Chemistry,* **16,** 1411–1413.

Jackson, E. (1986) *Hydrometallurgical Extraction and Reclamation.* John Wiley & Sons, New York, 29–73.

Kammer, U., Schenker, G., Wieden, H.D. (1993) "Secondary Lead Smelting Using a Silica Slag." *EPD Congress 1993.* The Minerals, Metals and Materials Society, Pennsylvania, USA, 917–926.

Lefers, J.B., Koetsier, W.T. and Van Swaaij, W.P.M. (1978) "The Oxidation of Sulphide in Aqueous Solutions." *The Chemical Engineering Journal.* Netherlands, 111–120.

Levenspiel, O. (1972) *Chemical Reaction Engineering.* John Wiley & Sons, New York, 357–397.

Lewis, A.E., Hugo, A. and Beautement, C. (1999) "Waste Characterisation, Testing and Modification: A Case Study for Secondary Lead Slag." *International Mining and Environment Congress "Clean Technology: Third Millennium Challenge"* Lima, Peru, 471-482.

Majima, H. and Peters, E. (1966) "Oxidation Rates of Sulphide Minerals by Aqueous Oxidation at Elevated Temperatures." *Transactions of the Metallurgical Society of Aime.* **236,** 1409–1413.

Nagata, S. (1975) *Mixing: Principles and Applications* Halstead, New York, 249–296; 336–359.

O'Brien, D.J. and Birkner, F.B. (1977) "Kinetics of Oxygenation of Reduced Sulfer Species in Aqueous Solution." *Environmental Science and Technology.* **11** (12), 1114-1120.

Pehlken, A. (1997) *Secondary Lead Smelting and Treatment of Soda Slag at Fry's Metals.* Diplomarbeit, Rheinishch- Westfalische Technishce Hochschule Aachen, 1–63.

Perry, R.H. and Green, Don. (1984) *Perry's Chemical Engineers' Handbook,* 6th edition. McGraw-Hill Book Co., New York, 3-6 – 3-24.

Peters, E. (1976) "Direct Leaching of Sulfides: Chemistry and Applications." *Metallurgical Transactions B.* 7**B**, 505–517.

Prengaman, D.R. (1989) "Recovering Lead from Batteries." *The Journal of the Minerals, Metals, and Materials Society.* **47**, 31–33.

Queneau, P.B., Hansea, B.J. and Spilker, E.D. (1981) "Recycling Lead and Zinc in the United States: Hydrometallurgy and Physical Concentration Become Important Parts of the Secondary Smelter". *Harran Research*, Golden: Colorado, USA, Chapter 2.

Queneau, P.B., Cregar, D.E. and Mickey, D.K. (1989) "Optimising matte and slag composition in rotary furnace smelting of leady residues". *Primary and secondary lead processing*; Halifax, Nova Scotia, August 1989, proceedings, M.L. Laeck, New York, Pergamon Press, 145–178.

Richards, M.K. and Oberacker, D. (1992) "EPA SITE demonstration of the Horsehead Resource Development Company Flame Reactor Technology" *EPA Technical Report Contract no. 68-co-0047*, 675–678.

Shenkler, E.S., Graham, S. and Greenhut, V.A. (1991) "Secondary lead smelter slags: minimizing lead release levels". *Ceramic Transactions.* **23**, 5–84.

Steck, L.V., Slavin, M. and Ralston, O.C. (1929) "The System Sodium Sulfide-Ferrous Sulfide." *J. Chem. Soc.* **51**, 3241–3248.

Tender, A. and Wilhelmsson, A. (1975) "The kinetics of the Reaction Between Sulphide and Sulfite in aqueous solution." *Swedish Paper Journal.* **78** (13), 480–487.

Wakeman, R.J. (1994) "Extraction: Liquid – Solid." *Encyclopaedia of Chemical Technology* **10.** 4th edition, 181–195.

Willis, J. (1998) "A review of analytical techniques used in mineralogy" *Mineralogy for Mineral Processing engineers workshop* Cape Town, South Africa. 5 August 1998.

Wilmot, P.D, Cadee, K., Katinic, J.J. and Kavanagh, B.V. (1988) "Kinetics of Sulphide Oxidation by Dissolved Oxygen." *Journal WPCF.* **60** (7), 1264–1270.

Zhang, J.Z. and Millero, F.J. (1993) "The products from the Oxidation of H_2S in Seawater." *Geochimica et Cosmochimica Acta.* **57.** USA: Pergamon Press Ltd, 1705–1718.

Appendix A

1 Pre-treatment of the furnace feed: Paste desulphurisation

Typically, one spent battery gives rise to approximately 6kg of paste and has the composition shown in Table 1.

$PbSO_4$	60 mass-%
PbO_2	19 mass-%
Pb	21 mass-%

Table 1 Composition of lead acid battery paste (Arai and Toguri, 1983)

The process involves the removal of sulphur from the paste by leaching the lead sulphate with a sodium carbonate solution. Ammonium carbonate can also be utilised, but this reagent has not yet reached commercial scale implementation. This desulphurisation reaction is shown in equation 2-6.

$$PbSO_{4\,(S)} + Na_2CO3_{\,(aq)} \rightarrow PbCO_{3\,(s)} + Na_2SO_{4\,(aq)} \qquad \text{equation 1}$$

The thermodynamic and kinetic considerations for this reaction are discussed by Arai and Toguri (1983). Reaction thermodynamics predict that the reaction of equation 2-6 should go to completion at 298 K. The authors indicate that PbS can be converted to $PbSO_4$, and thus be amenable to reaction of equation 2-6.

Pyrometallurgical Treatment of the Desulphurised Paste Fraction

The reduction in the non-lead bearing furnace feed requirement, when the feed paste is desulphurised, results in the production of a smaller quantity of slag. At the Oker secondary lead smelter, which utilizes paste desulphurisation, 170 kg slag is produced per ton of lead bullion (Kammer, 1993). The local smelter produces 330 kg slag per ton lead bullion (Pehlken, 1997). In addition to the reduction in the slag quantity, the silicate based slag that is produced, resists leaching better than sulphidic slag due to its greater stability in the presence of water.

A disadvantage of paste desulphurisation treatment is the production of an aqueous sodium sulphate stream, which is unsuitable for discharge into the environment. Removal of the sodium sulphate via crystallisation is required. This is a high cost operation, but does result in a potentially saleable solid sodium sulphate product. A higher furnace operating temperature is also required (Kammer, 1993). The main advantage of the process, namely the large reduction in SO_2 emissions, is not likely to be as important in South Africa (compared to other countries where it is used commercially) due to the less stringent gaseous emission requirements.

Hydrometallurgical treatment of the desulphurised paste fraction

A number of processes have been proposed to recover lead hydrometallurgically from the desulphurised paste fraction instead of furnace smelting. These processes incorporate a leaching step to solubilise the lead components followed by an electrowinning step. The literature available report that these processes have not yet reached commercial implementation. However, several variations have been investigated up to a pilot plant level. Hydrometallurgical treatment has the advantage of low temperature operation and the elimination of sulphur dioxide gaseous emissions. A disadvantage of these processes is the

requirement for desulphurisation of the paste prior to hydrometallurgical recovery of the lead and the need for a very aggressive electrolyte to dissolve the lead components arising from the desulphurisation step. Prengaman (1995) has reviewed a number of these hydrometallurgical processes.

2 Glassification

This involves thermal processing of the slag in a pot furnace at 1200 °C together with silica (glass former) and sodium carbonate (glass modifier). The results of this investigation, summarized in Table 2.

Slag Sample	Untreated slag TCLP lead release [ppm]	Glassified slag TCLP lead release [ppm]
A	60	0.85
B	14	0.3
C	60	2

Table 2 Comparison of TCLP results for untreated and glassified secondary lead slags (Shenkler *et al*, 1991)

3 Volatilisation of heavy metals

Fuming of a secondary lead slag has been demonstrated by Richards and Oberacker (1992) of the United States Environmental Protection Agency (EPA) utilising a flame reactor, shown in Figure 1.

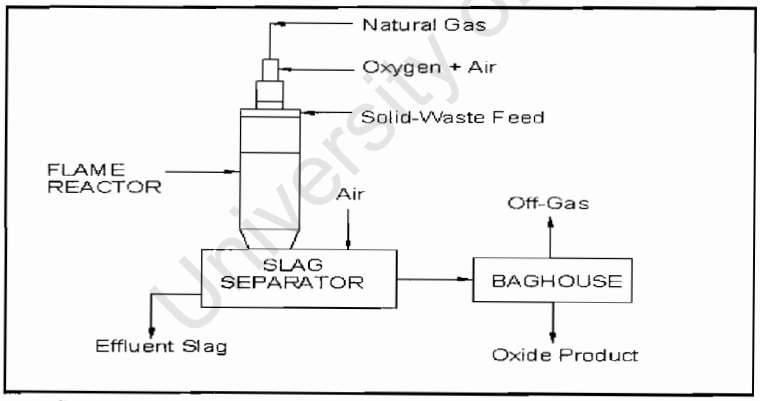

Figure 1 EPA flame reactor for the treatment of a secondary lead slag

This treatment yielded two main products:

- A heavy metal oxide product that can potentially be recycled (96.9% and 99.7% recovery of lead and zinc respectively to this product)
- A vitrified slag which is non-leachable (complies with EPA standards for the TCLP test)

4 Oxidation of a secondary lead matte

Corrick and Sutton (1968) investigated the oxidation of sulphide components and found this to occur via the reaction of equation 2-7.

$$CuS + FeS + PbS + 4O_2 + H_2SO_4 \rightarrow CuSO_4\,(aq) + FeSO_4(aq) + PbSO_4\,(s) + H_2S \qquad \text{equation 2}$$

They reported that the oxidation reaction of equation 2-7 could be accomplished by the methods shown in Table 3.

Method	Results
Roasting	Large heating requirement, large SO_2 emission. Lead recovery was not quantified in this study.
Ferrobacillus Ferrooxidans	69.8% Lead Recovery
Dilute Sulphuric Acid Leach	82.3 % Lead Recovery

Table 3 Methods for oxidising a secondary lead blast furnace matte

5 Hazard characterisation of the toxic metal components of the slag

Currently the local refiner employs a waste disposal company to remove the slag from the premises and dispose of it in a hazardous class H waste tip. This is required as the toxic heavy metals present in the slag leach in excess of the South African acceptable risk limits (ARL) in a standard Toxic Characteristic Leaching Procedure (TCLP) test. The results of TCLP tests on the slag are given by Lewis *et al* (1999). The results indicate that lead and zinc exceed the South African limits. These results, together with the fact that lead and zinc are class II hazardous substances, preclude the possibility of de-listing the slag to a less hazardous class G site, which has lower disposal costs.

The acetic acid based TCLP test simulates the current practice of co-disposal of the slag with domestic waste and the potential for the formation of a lead species of increased solubility, namely lead acetate. Thus, it was thought that mono-disposal of the slag would substantially decrease the leachability of lead. This leaching environment was simulated by means of the synthetic precipitation leach procedure (SPLP) test, in which the leachant is a simulated acid rain mixture. This test is recommended by the American National Mining Association as being more appropriate for mineral processing wastes (Koren *et al*, 1977). The SPLP results of Lewis *et al* (1999) showed that while a decrease in lead leaching occured, leaching still significantly exceeded the South African ARL limit, and zinc leaching was in fact increased. Thus, it appears that mono-disposal will still result in the slag requiring disposal to a class H site.

Appendix B

Abridged composition of the Enthoven slag as reported by Barnes (1996). An elemental analysis of the Enthoven slag was done by ICP emission spectroscopy. An abridged elemental composition of only the main elements is presented in Table 1. The above elemental analysis is the averaged values for the ICP analysis of 14 slags and it was thus assumed that this was representative of the slags to be treated. The Table 2 gives a computation of the expected main compounds present in the slag.

Element	Average mass %
Sulphur	16.82
Sodium	22.39
Iron	19.96
Lead	2.55
Zinc	0.64
Calcium	1.2
Silicon	2.41
Chlorine	1.5
Sum	**67.47%**

Table 1 ICP Elemental analysis of the Enthoven slag

Slag Compound	Average Mass %
Na2S	11.12
Na2CO3	33.74
FeS	31.39
Pb	2.55
ZnS	0.95
CaSiO3	2.71
Na3PO4	1.83
SiO2	3.3
NaCl	2.47
Sum	**90.60**

Table 2 Calculated component analysis of the Enthoven slag

Appendix C

Analytical techniques used in slag characterisation

Quantitative

The total amount of a certain element in a slag sample can be determined quantitatively by digesting the sample and analysing the resultant solution by Atomic Absorption Spectroscopy (AAS) or Inductively Coupled Plasma (ICP) analysis. AAS and ICP analysis is especially suitable for the metal elements. Although sulphur could be analysed by ICP analysis at the local secondary lead refiner, the ICP – OES (Optical Emission Spectroscopy) used at the University of Cape Town did not have the necessary detector. Therefore sulphur analysis was done using a LECO sulphur analyser, which combusts the sulphur present in a solid slag sample and analyses the resultant sulphur dioxide gaseous emission.

ICP analysis has the advantage of being able to analyse a number of elements simultaneously, and has a lower limit of detection (0.1 – 60 ppb) compared to AAS (0.002 – 2 ppm) (Willis, 1998). However, the requirement to dilute ICP analysed samples to 1 - 2 % dissolved solids concentration negates this advantage in the case of the digested slag sample.

Qualitative

X-ray diffraction (XRD) is an analytical technique that allows the identification of crystalline phases in the slag via their characteristic diffraction peaks. The limitations of this analysis are that only crystalline phases are identified. By matching diffraction angles and peak displacements obtained from the slag analysis to those for particular pure component compounds, a number of compounds that are potentially present in a particular phase are found. Photographic images of the slag were taken using a backscatter detector by a Scanning Electron Microscope (SEM) at magnifications of between 1000× and 5000×.

Tests for carbonate

Barium carbonate precipitation

Aqueous extracts were prepared from slag samples and filtered. The high solubility of sodium carbonate should cause this compound to dissolve. The presence of carbonate in this extract was to be determined by addition of barium chloride and observation of the formation of a white barium carbonate precipitate. As the fresh extract solution is too dark, this test was also done on a clearer partially oxidised solution, however no precipitation was observed. The quantitative standard test for carbonate described in Vogel (1989) is not applicable in this case as it assumes that only carbonate ions contribute to the alkalinity of the aqueous extract. This is not the case here.

Evolution of carbon dioxide

A hydrochloric acid solution was added to the aqueous slag extract in a closed vessel. The resultant gas that was evolved from the solution was analysed on a Perkin Elmer Auto-system Gas Chromatograph. Only peaks for air (oxygen nitrogen combined peak) and for hydrogen sulphide appeared on the resultant chromatogram. If carbonate was present in the extract, carbon dioxide should be evolved on addition of an acid. However, this gas was not detected by the column.

Appendix D

SEM Analysis of Slags O & N

Photographic images of the slag were taken using a backscatter detector by a Scanning Electron Microscope (SEM) at magnification of between 1000X and 5000X. The backscatter image is especially useful at determining differences in slag composition, as elements of greatest atomic weight appear brighter in the photo. Different spots of typical appearance (for each phase) was focussed in on and analysed in order to determine their elemental composition using electron dispersive spectroscopy (EDS).

Matte phases

Slag O

An additional example of the matte fraction of slag O is given in photo no. 1 below:

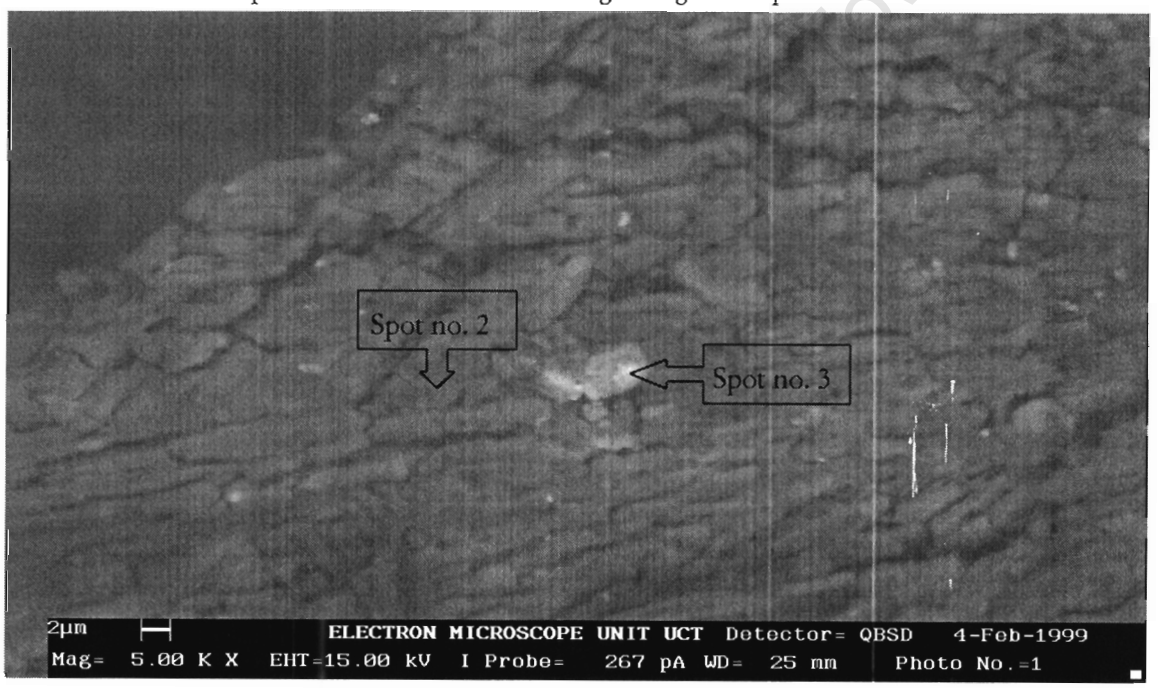

An elemental analysis of the spot labeled 2 on photo no.1 is presented below:

Element		Mass %	Mol %
Sulphur	S	36.48	40.18
Sodium	Na	10.41	15.99
Iron	Fe	37.03	23.41
Zinc	Zn	5.6	3.02
Chlorine	Cl	2.7	2.69
Oxygen	O	5.6	12.36

Table 1 Elemental Analysis for Spot no.2 on Photo no. 1

This composition indicates that this spot has a FeS wt% of 64% (relative to Na2S) and again this composition falls within the region of FeS.Na2S and FeS as predicted by Steck *et al* (1929).

These elements were thus assigned to the following compounds:

Compound	Mol %
FeS	40
$FeS.Na_2S$	16
ZnS	9
NaCl	5
O	30

Table 2 Elemental Assignation to Compounds for Spot no.2 on Photo no. 1

Evidence of the compound ZnS was found via XRD analysis for both slags under investigation here, other zinc compounds were also detected (e.g. Zn(OH)2 and sodium zinc silicate), however this assignment accounted for all the sulphur present in the analysed spot and the other compounds are more likely to be found in the slag phase. Again a large amount of excess oxygen is present; the explanation for this has been given above.

EDS analysis of the spot labeled 1 on the photo yielded a similar analysis to that given above, as suggested by the similar appearance of these regions on the SEM backscatter photo. The bright spot labeled 3 on the photo was found to be a metallic iron inclusion (85 wt % Fe) as well as a small amount of tin (2.8 wt %) in the surrounding matte region.

Slag N

A example of the matte phases present in this slag are given by the spots labeled 1 and 2 on photo no. 5.

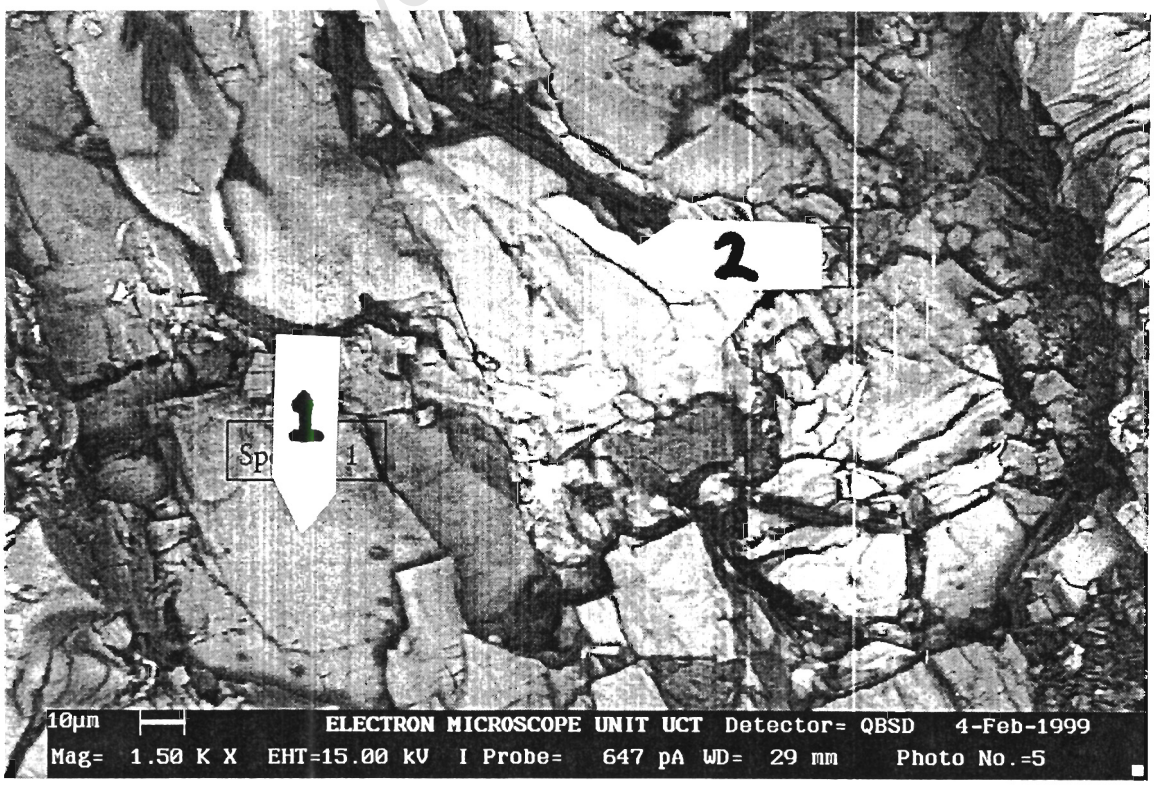

These spots had the following EDS elemental analysis:

Element		Mass %	Mol %
Sulphur	S	36.31	38.79
Sodium	Na	14.81	22.06
Iron	Fe	35.59	21.82
Chlorine	Cl	9.45	9.13
Oxygen	O	3.83	8.20

Table 5 Elemental Analysis for Spot no.1 on Photo no. 5

Element		Mass %	Mol %
Sulphur	S	36.44	43.65
Sodium	Na	9.2	15.37
Iron	Fe	49.54	34.06
Chlorine	Cl	3.53	3.82
Oxygen	O	1.29	3.10

Table 5 Elemental Analysis for Spot no. 2 on Photo no. 5

Spot no. 2 was selected as it is a lighter region in contrast to the relatively darker region surrounding spot no. 1. This difference is clearly explained by the different relative elemental compositions, spot no. 2 has more of the higher molecular weight iron. Spots 1 and 2 have FeS wt % of 54.6% and 72.9% respectively (relative to Na2S) and again these compositions fall within the region of $FeS.Na_2S$ and FeS as predicted by Steck et al (1929). Thus it was expected that the elements would be found in the following compounds for each spot respectively:

Compound	Mol %
FeS	42
$FeS.Na_2S$	17
NaCl	21
O	21

Table 6 Elemental Assignation to Compounds for Spot no.1 on Photo no. 5

Compound	Mol %
FeS	69
$FeS.Na_2S$	14
NaCl	10
O	8

Table 7 Elemental Assignation to Compounds for Spot no.2 on Photo no. 5

The iron and sodium account for all the sulphur and chlorine present in the analysis and again an excess of oxygen is present.

Slag Phases

Predictions of slag phase composition from thermodynamics and observed composition of typical secondary lead slags (Queneau *et al*, 1989) assign the major slag phase elements to Na_2O, FeO and SiO_2.

Slag R (new 20 t Furnace)

Spot no. 1 on photo no. 7 is another example of a slag phase region.

The elemental analysis was as follows:

Element		Mass %	Mol %
Sulphur	S	1.35	1.11%
Sodium	Na	23.71	27.24%
Iron	Fe	33.86	16.02%
Silica	Si	16.46	15.48%
Oxygen	O	24.08	39.76%

Table 11 Elemental Analysis for Spot no. 1 on Photo no. 7

Again two assignments of sodium can be again employed:

Compound	Mol %
FeO	28
Na_2O	23

SiO_2	28
O	21
Na2S.FeS	1

Table 12 Elemental Assignation One to Compounds for Spot no.1 on Photo no. 7

Compound	Mol %
FeO	31
Na_2SiO2	13
SiO_2	31
O	24
Na2S.FeS	1

Table 13 Elemental Assignation Two to Compounds for Spot no.1 on Photo no. 7

As for slag L above, both assignments account for the elemental quantities present in the EDS analysis. The percentage of sodium in the slag which remains insoluble has been found to be 46 %, so again the true composition is likely to fall between the two given component estimations given above.

Appendix E

Elemental Mass Balance

Furnace N 20 ton

FURNACE INPUTS

Lead inputs

Metallics (1)		
Component	[mass %]	[kg]
Ag	0.003	0.048
As	0.011	0.176
Cu	0.060	0.96
Ni	0.001	0.016
Pb	97.062	1552.992
S	0.003	0.048
Sb	2.640	42.24
Sn	0.040	0.64
Total	99.8	1600

Dross		
Component	[mass %]	[kg]
Cu	0.50	17
O	6.30	214.2
Pb	79.00	2686
Sb	0.20	6.8
Sn	0.10	3.4
Plastic	13.90	472.6
Total	100.00	3400

Sludge		
Component	[mass %]	[kg]
O	17.27	345.4
Pb	73.85	1477
S	8.50	170
Sb	0.37	7.4
Sn	0.01	0.2
Total	100.00	2000

Battery Plates		
Component	[mass %]	[kg]
As	0.40	28.8
Plastics	4.00	288
Cu	0.40	28.8
H2O	4.00	288
Pb	78.00	5616
PbO	8.40	604.8
- Pb		561.4
PbSO4	3.60	259.2
- Pb		177.1
- S		28.9
Sb	1.20	86.4
Total	100.00	7200

Cell Plates		
Component	[mass %]	[kg]
As	0.40	0
Plastics	4.00	0
Cu	0.40	0
H2O	4.00	0
Pb	70.20	0
PbO	8.40	0
PbSO4	3.60	0
Sb	9.00	0
Total	100.00	0

Slag In (Slag Bottoms)		
Component	[mass %]	[kg]
Lead	38.6	1603.7
Sulphur	13.3	553.3
Iron	19.5	812.1
Sodium	8.5	353.4
Zinc	2.6	108.3
Aluminium	0.5	22.7
Silicon	2.0	84.2
Oxygen	13.8	575.7
Total		4160

Flux inputs

Cast Iron Borings		
Component	[mass %]	[kg]
C	4.24	38.16
Fe	95.72	861.5
S	0.04	0.4
Total	100	900

Soda Ash		
Component	[mass %]	[kg]
Na2CO3	99.50	2288.5
- Na		993.1
- O		1036.3
- C		259.1
Total		2300

Coal		
Component	[mass %]	[kg]
H2O	2.40	38.4
Ash	10.40	166.4
Volatiles	10.60	169.6
C	76.60	1225.6
S	0.94	15.04
Total	100.94	1600

Salt		
Component	[mass %]	[kg]
NaCl	100.00	0
Total		0

Gascor Gas		
Component	[mass %]	[kg]
C2H2	2.13	31.95
CH4	32.82	492.3
CO	42.46	636.9
- C		273.0
- O		363.9
CO2	13.34	200.1
- O		145.5
- C		54.6
H2	7.12	106.8
N2	2.12	31.8
Total	99.99	1500

Oxygen		
Component	[mass %]	[kg]
O2	100.00	1404
Total		1404

Fume		
Component	[mass %]	[kg]
Cl	6.70	134
Fe	2.32	46.4
Na	5.98	119.6
O	5.84	116.8
Pb	69.30	1386
S	7.95	159
Sb	0.34	6.8
Sn	0.80	16
Zn	0.77	15.4
Total	100.00	2000

Elemental Inputs

Element	[kg]
Pb	13,674
Fe	1,674
Na	1,347
S	926
C	1,850
Ag	0
As	29
Cu	47
Ni	0
Sb	143
Sn	4
Zn	108
Si	84
Al	23
Plastic	761
O	3,871
H	
N	
Total	24540.53

Elemental Outputs

Element	[kg]
Pb	17,615
Fe	1,230
Na	1,041
S	832
C	1,551
Ag	
As	3
Cu	42
Ni	2
Sb	245
Sn	2
Zn	53
Si	116
Al	105.1
Cl	
O	5,191
H	
N	
Total	28028.81

FURNACE PRODUCTS

Bullion Metal

Component	[mass %]	[kg]
Sn	0.014	2.28
Sb	1.458	244.94
Se	0.003	0.47
As	0.019	3.23
Ca	0.003	0.42
Ag	0.004	0.64
Cu	0.054	8.99
Ni	0.012	1.93
Bi	0.011	1.90
S	0.050	8.32
Pb	98.374	16,527
Total		16,800

Slag

Component	[mass %]	[kg]
Sulphur	11.4	711.4
Iron	19.18	1196.8
Lead	1.72	107.3
Sodium	15.33	956.6
Magnesium	0.27	16.7
Copper	0.53	33.3
Antimony	0.25	15.5
Silica	1.85	115.6
Ca	0.61	38.1
Sn	1.55	97.0
Al	1.70	106.1
C	2.14	133.5
Zn	0.68	42.4
As	0.10	6.1
Cr	0.20	12.5
Rest: O2 by dif	42.49	2651.1
Total		6240

Exhaust Gas

Compone	[kg]
CO	2170.98
CO2	1785.89
- C	1417.481
- O	2539.389
SO2	20.0945
H2	143.009
H2O	1486.088
Pb	0.005
	8615

Fume

Compone	[mass %]	[kg]
Cl	6.70	94.8
Fe	2.32	32.8
Na	5.98	84.6
O	5.84	82.6
Pb	69.30	980.3
S	7.95	112.5
Sb	0.34	4.8
Sn	0.80	11.3
Zn	0.77	10.9
Total		1414.6

Appendix E

Elemental Mass Balance

Furnace	Old 20 ton

FURNACE INPUTS

Lead inputs

Metallics (1)		
Component	[mass %]	[kg]
Ag	0.003	0
As	0.011	0
Cu	0.060	0
Ni	0.001	0
Pb	97.062	0
S	0.003	0
Sb	2.640	0
Sn	0.040	0
Total	99.8	0

Dross		
Component	[mass %]	[kg]
Cu	0.50	17
O	6.30	214.2
Pb	79.00	2686
Sb	0.20	6.8
Sn	0.10	3.4
Plastic	13.90	472.6
Total	100.00	3400

Sludge		
Component	[mass %]	[kg]
O	17.27	863.5
Pb	73.85	3692.5
S	8.50	425
Sb	0.37	18.5
Sn	0.01	0.5
Total	100.00	5000

Battery Plates		
Component	[mass %]	[kg]
As	0.40	25.2
Plastics	4.00	252
Cu	0.40	25.2
H2O	4.00	252
Pb	78.00	4914
PbO	8.40	529.2
- Pb		491.2
PbSO4	3.60	226.8
- Pb		154.9
- S		25.3
Sb	1.20	75.6
Total	100.00	6300

Cell Plates		
Component	[mass %]	[kg]
As	0.40	0
Plastics	4.00	0
Cu	0.40	0
H2O	4.00	0
Pb	70.20	0
PbO	8.40	0
PbSO4	3.60	0
Sb	9.00	0
Total	100.00	0

Flux inputs

Cast Iron Borings		
Component	[mass %]	[kg]
C	4.24	38.16
Fe	95.72	861.5
S	0.04	0.4
Total	100	900

Soda Ash		
Component	[mass %]	[kg]
Na2CO3	99.50	2338.25
- Na		1014.7
- O		1058.8
- C '		264.7
Total		2350

Coal		
Component	[mass %]	[kg]
H2O	2.40	38.4
Ash	10.40	166.4
Volatiles	10.60	169.6
C	76.60	1225.6
S	0.94	15.04
Total	100.94	1600

Salt		
Component	[mass %]	[kg]
NaCl	100.00	0
Total		0

Fume

Component	[mass %]	[kg]
Cl	6.70	134
Fe	2.32	46.4
Na	5.98	119.6
O	5.84	116.8
Pb	69.30	1386
S	7.95	159
Sb	0.34	6.8
Sn	0.80	16
Zn	0.77	15.4
Total	100.00	2000

Slag In (Slag Bottoms)

Component	[mass %]	[kg]
Lead	38.6	1202.8
Sulphur	13.3	415.0
Iron	19.5	609.1
Sodium	8.5	265.0
Zinc	2.6	81.2
Aluminium	0.5	17.0
Silicon	2.0	63.2
Oxygen	13.8	431.8
Total		3120

Gascor Gas		
Compone	[mass %]	[kg]
C2H2	2.13	31.95
CH4	32.82	492.3
CO	42.46	636.9
- C		273.0
- O		363.9
CO2	13.34	200.1
- O		145.5
- C		54.6
H2	7.12	106.8
N2	2.12	31.8
Total	99.99	1500

Oxygen		
Compone	[mass %]	[kg]
O2	100.00	1404
Total		1404

Elemental Inputs

Element	[kg]
Pb	13,141
Fe	1,471
Na	1,280
S	1,039
C	1,856
Ag	-
As	25
Cu	42
Ni	-
Sb	101
Sn	4
Zn	81
Si	63
Al	17
Plastic	725
O	4,268
H	
N	
Total	24112.89

Furnace

FURNACE PRODUCTS

Elemental Outputs

Eleme	[kg]
Pb	15,425
Fe	1,468
Na	840
S	1,275
C	1,551
Ag	
As	4
Cu	47
Ni	0
Sb	176
Sn	1
Zn	76
Si	131
Al	106.1
Cl	
O	4,629
H	
N	
Total	25728.994

Bullion Metal

Component	[mass %]	[kg]
Sn	0.005	0.76
Sb	1.222	175.97
Se	0.003	0.36
As	0.027	3.83
Ca	0.003	0.39
Ag	0.003	0.46
Cu	0.041	5.96
Ni	0.001	0.19
Bi	0.018	2.52
S	0.016	2.26
Pb	98.662	14,207
Total		14,400

Slag

Component	[mass %]	[kg]
Sulphur	18.6	1160.6
Iron	23	1435.2
Lead	3.8	237.1
Sodium	12.1	755.0
Magnesium	0.11	7.0
Copper	0.65	40.6
Antimony	0.35	21.6
Silica	2.11	131.4
Ca	0.61	38.1
Al	1.70	106.1
C	2.14	133.5
Zn	1.05	65.3
As	0.10	6.1
Cr	0.20	12.5
Rest: O2 by dif	33.49	2089.9
Total		6240

Exhaust Gas

Componen	[kg]
CO	2170.98
CO2	1785.89
- C	1417.481
- O	2539.389
SO2	20.0945
H2	143.009
H2O	1486.088
Pb	0.005
	8615

Fume

Componen	[mass %]	[kg]
Cl	6.70	94.8
Fe	2.32	32.8
Na	5.98	84.6
O	5.84	82.6
Pb	69.30	980.3
S	7.95	112.5
Sb	0.34	4.8
Sn	0.80	11.3
Zn	0.77	10.9
Total		1414.6

Appendix F

Formulae for calculation of extraction and recovery from analysis of leach – oxidation products

Overall percent of feed slag remaining insoluble

$$Total\ insolubes = \frac{mass\ insolble}{mass\ \ feed\ slag}$$

Feed slag sulphur remaining in insoluble phase

$$sulphur\ recovery\ to\ insoluble\ \ phase = \frac{mass\ insolble}{mass\ \ feed\ slag} \times \frac{sulphur\ \ fraction\ in\ insoluble\ \ phase}{sulphur\ \ fraction\ in\ \ feed\ slag}$$

Recovery of feed slag sulphur to aqueous phase oxidised sulphur species (mass basis)

$$sulphur\ recovery\ to\ soluble\ component = \frac{volume\ of\ \ solution}{mass\ \ feed\ slag} \times \frac{concentration\ of\ \ sulphur\ component}{sulphur\ \ fraction\ in\ \ feed\ slag}$$

Sulphur accounted for by product phases as percent of feed slag sulphur

$$sulphur\ recovery\ to\ \ product\ \ phases =$$
$$sulphur\ \ recovery\ to\ insoluble\ \ phase + sulphur\ \ recovery\ to\ aqueous\ \ phase$$

Appendix G

Slag Type N

Agitation 600 rpm

Container mass	[g]	691.8
Combined mass	[g]	1005.3
Slag Mass	[g]	**313.5**

Start time 1/2/00 11:10

Actual Time	Ellapsed Time	Mass	Slag Mass	% Disintegrated
[dd:hh:mm]	[minutes]	g		
59:10:00	0:00:00	1005.3	313.5	0%
1/2/00 11:20	0:10:00	876.8	185.0	41%
1/2/00 11:40	0:30:00	736.6	44.8	86%
1/2/00 12:10	1:00:00	706.2	14.4	95%
1/2/00 12:40	1:30:00	698.1	6.3	98%
1/2/00 13:10	2:00:00	696.5	4.7	99%
1/2/00 15:10	4:00:00	691.8	0.0	100%
1/2/00 17:10	6:00:00			
1/2/00 19:10	8:00:00			
1/3/00 11:10	24:00:00			

Table 1 Disintegration experiment 1

Slag Type O

Agitation 600 rpm

Container mass	[g]	694.7
Combined mass	[g]	1093.1
Slag Mass	[g]	**398.4**

Start time 1/2/00 11:10

Actual Time	Ellapsed Time	Mass	Slag Mass	% disintegrated
[dd:hh:mm]	[minutes]	g		
59:10:00	0:00:00	1093.1	398.4	0%
1/2/00 11:20	0:10:00	913.8	219.1	45%
1/2/00 11:40	0:30:00	739.7	45.0	89%
1/2/00 12:10	1:00:00	706.7	12.0	97%
1/2/00 12:40	1:30:00	700.7	6.0	99%
1/2/00 13:10	2:00:00	694.7	0.0	100%
1/2/00 15:10	4:00:00			
1/2/00 17:10	6:00:00			
1/2/00 19:10	8:00:00			
1/3/00 11:10	24:00:00			

Table 2 Disintegration experiment 2

Slag Type N

Agitation 0 rpm

Container mass	[g]	693.5
Combined mass	[g]	974.2
Slag Mass	[g]	**280.7**

Start time 1/2/00 9:10

Actual Time	Ellapsed Time	Mass	Slag Mass	% disintegrated
[dd:hh:mm]	[minutes]	g		
1/2/00 9:10	0:00:00	974.2	280.7	0%
1/2/00 9:20	0:10:00	968.6	275.1	2%
1/2/00 9:40	0:30:00	948.9	255.4	9%
1/2/00 10:10	1:00:00	932.1	238.6	15%
1/2/00 10:40	1:30:00	918.1	224.6	20%
1/2/00 11:10	2:00:00	901.2	207.7	26%
1/2/00 13:10	4:00:00	863.6	170.1	39%
1/2/00 15:10	6:00:00	828.8	135.3	52%
1/2/00 17:10	8:00:00	797.6	104.1	63%
1/3/00 9:10	24:00:00	717.6	24.1	91%

Table 3 Disintegration experiment 3

Slag Type N

Agitation 600 rpm

Container mass	[g]	695.7
Combined mass	[g]	1827.7
Slag Mass	[g]	**1132.0**

Start time 1/2/00 9:10

Actual Time	Ellapsed Time	Mass	Slag Mass	% disintegrated
[dd:hh:mm]	[minutes]	g		
1/2/00 9:10	0:00:00	1827.7	1132.0	0%
1/2/00 9:20	0:10:00	1488.1	792.4	30%
1/2/00 9:40	0:30:00	1171.1	475.4	58%
1/2/00 10:10	1:00:00	1001.3	305.6	73%
1/2/00 10:40	1:30:00	927.8	232.1	80%
1/2/00 11:10	2:00:00	849.7	154.0	86%
1/2/00 13:10	4:00:00	782.9	87.2	92%
1/2/00 15:10	6:00:00	741.0	45.3	96%
1/2/00 17:10	8:00:00	718.3	22.6	98%
1/3/00 9:10	24:00:00	695.7	0.0	100%

Table 4 Disintegration experiment 4

RUN NUMBER	1
CONDITION	Base
VALUE	
Slag type	N
Slag fraction	fine fraction

Start Time 1/2/00 11:10

Liquid Samples

Sample no.	Actual Time	lapsed Ti	pH	Eh	emperatur	DO 2	iltrate Colo	S - 2		S-2	S2O3		S2O3	SO4	
	[dd:hh:mm]	[minutes]			[C]	[mg / L]			[mg / L]	[mol/m^3]		[mg / L]	[mol/m^3]		[mg / L]
Dilution Factor	1/2/00 11:10	0:00:00						2	0	0.0	200	0	0	200	0
1	1/2/00 11:20	0:10:00	12.8	-326	21.3			144.9	289.8	9.0	-			-	
2	1/2/00 11:40	0:30:00	12.84	-329				43.2	86.4	2.7	-			-	
3	1/2/00 12:10	1:00:00	12.83	-328				8.9	17.8	0.6	-			-	
4	1/2/00 13:10	2:00:00	12.82	-325			1.9%	2.7	5.4	0.2	6.875	1375	12.3	0.18	36
	1/2/00 15:10	4:00:00						1.6	3.2	0.1					
5	1/2/00 19:10	8:00:00	12.49	-305				0.8	1.66	0.1	19.379	3875.8	34.6	0.21	42
	1/3/00 5:10	18:00:00	12.21					0.0	0	0.0					
6	1/3/00 11:10	24:00:00	12	-278				0.0	0	0.0	38.449	7689.8	68.6	0.18	36
7	1/4/00 1:10	38:00:00	11.77	-264				0.0	0	0.0	46.761	9352.2	83.4	0.1	20
10	1/4/00 11:10	48:00:00	11.68	-281	19.3			0.0	0	0.0	50.413	10082.6	89.9	0.27	54
11	1/4/00 11:10	48:00:00						0.0	0	0.0	52.995	10599	94.5	0.35	70

		Slag S 1	Slag S2	Slag S3	Insol S1	Insol S2	Insol S3	13	14	15	16
Mass digested	[g]	0.111	0.125	0.111	0.099						
Volume made up	[mL]	100.0	100.0	100.0	100.0	100.0	100.0	100.0	100.0	100.0	100.0
Concentration	[mg / L]	1105.0	1252.0	1107.0	993.0	0.0	0.0	0.0	0.0	0.0	0.0

	Slag
Slag	[g] 75.3
Water	[L] 1.5
Slag Concentration	[g / L] 50.2

	Mass	Percentage
	[g]	[%]
Insolubles		
Total Insolubles	56.95	75.6%
Mass % Extracted		24%
S Recovered to Soluble Form		58%
S Recovered to Thiosulphate		58%
S Recovered to Combined S2O3 and SO4		58%
Na Recovered to soluble form		0%
S Recovered to Sulphate		0%

Digestions

	Sulphur	Sodium		Iron		Lead		Zinc		
	[mass %]	[mg / L]	[%]	[mg / L]	[%]	[mg / L]	[%]	[mg / L]	[%]	
Slag	20%		13%		20%		11%		2%	65%
S1	20.6%	126.5	11%	230.00	21%	146.00	13%	17.60	2%	68%
S2	20.4%	170	14%	266.00	21%	145.00	12%	20.30	2%	68%
S3	19.9%	152	14%	189.00	17%	82.10	7%	14.70	1%	
Insols	9%		5%		21%		13%		2%	
S1	8.7%	46.5	5%	210.00	21%	125.00	13%	18.40	2%	
S2	9.1%									
S3										

RUN NUMBER	2
CONDITION	Base
VALUE	
Slag type	N
Slag fraction	fine fraction

Start Time 1/2/00 11:15

Liquid Samples

Sample no.	Actual Time	lapsed Ti	pH	Eh	S - 2		S2O3		SO4		Total Sulphur	
	[dd:hh:mm]	[minutes]				[mg / L]		[mg / L]		[mg / L]	[mg / L]	[mg]
Dilution Factor	1/2/00 11:15	0:00			2	0	200	0	200	0		
1	1/2/00 11:25	0:10	12.86	-329	142.9	285.7	-		-			
2	1/2/00 11:45	0:30	12.84	-329	36.7	73.5	-		-			
3	1/2/00 12:15	1:00	12.84	-329	9.6	19.2	-		-			
4	1/2/00 13:15	2:00:00	12.84	-328	4.8	9.5	6.86	1372.0	0.32	64	816	1223
5	1/2/00 19:15	8:00:00	12.49	-305	1.1	2.2	22.08	4416.0	0.06	12	2532	3798
6	1/3/00 11:15	24:00:00	12.11	-286	0.0	0.0	39.27	7854.0	0.12	24	4500	6750
7	1/4/00 1:15	38:00:00	11.39	-242	0.0	0.0	-		-		0	0
10	1/4/00 11:15	48:00:00	11.88	-273	0.0	0.0	55.84	11168.0	0.09	17.8	6394	9590
11	1/4/00 11:15	48:00:00			0.0	0.0	51.66	10332.0	0.09	17.8	5915	8873

		Slag S 1	Slag S2	Slag S3	Insol S1	Insol S2	Insol S3	13	14	15	16
Mass digested	[g]	0.111	0.125	0.111	0.095						
Volume made up	[mL]	100.0	100.0	100.0	100.0	100.0	100.0	100.0	100.0	100.0	100.0
Concentration	[mg / L]	1105.0	1252.0	1107.0	950.0	0.0	0.0	0.0	0.0	0.0	0.0

Slag	[g]	75.3
Water	[L]	1.5
Slag Concentration	[g / L]	50.2

	Mass	Percentage
Insolubles	[g]	[%]
Total Insolubles	55.88	74.2%
Mass % Extracted		26%
S Recovered to Soluble Form		60%
S Recovered to Thiosulphate		60%
S Recovered to Combined S2O3 and SO4		60%
Na Recovered to soluble form		
S Recovered to Sulphate		0%

Digestions

	Sulphur	Sodium		Iron		Lead		Zinc		
	[mass %]	[mg / L]	[%]	[mg / L]	[%]	[mg / L]	[%]	[mg / L]	[%]	
Slag	20%		13%		20%		11%		2%	65%
S1	20.6%	126.5	11%	230.00	21%	146.00	13%	17.60	2%	68%
S2	20.4%	170	14%	266.00	21%	145.00	12%	20.30	2%	68%
S3	19.9%	152	14%	189.00	17%	82.10	7%	14.70	1%	
Insols	9%		7%		22%		9%		2%	
S1	8.9%	68.5	7%	208.00	22%	88.60	9%	18.50	2%	
S2										
S3										

RUN NUMBER	3
PARAMETER	Base
VALUE	
Slag:	N
Slag Condition:	fine fraction

Start Time 1/2/00 16:30

Liquid Samples

Sample no.	Actual Time	Ellapsed Time	S - 2		S2O3		SO4		Total Sulphur	
	[dd:hh:mm]	[minutes]		[mg / L]		[mg / L]		[mg / L]	[mg / L]	[mg]
Dilution Factor	1/2/00 16:30	0:00	2	0	200	0	200	0		
1	1/2/00 16:40	0:10	130.6	261.1	-		-			
2	1/2/00 17:00	0:30	41.2	82.4	-		-			
3	1/2/00 17:30	1:00	6.1	12.2	-		-			
4	1/2/00 18:30	2:00:00	5.0	10.0	7.31	1462	0.38	76	872	1307
5	1/2/00 20:30	4:00:00	3.0	6.0	15.68	3136	0.502	100.4	1833	2750
6	1/3/00 0:30	8:00:00	0.3	0.6	25.01	5002	0.18	36	2874	4310
7	1/3/00 11:15	18:45:00	0.0	0.0	40.34	8068	0.07	14	4619	6929
9	1/4/00 11:00	42:30:00	0.0	0.0	47.62	9524	0.17	34	5459	8188
10	1/4/00 16:30	48:00:00	0.0	0.0	50.24	10048	0.1	20	5754	8631
	1/4/00 16:30	48:00:00	0.0	0.0	49.18	9836	0.21	42	5640	8460

Sodium			Iron	
[mg / L]		[mol/m^3	[mg / L]	
210.5263	0	0	4	0
15.79	3324.2	144.5		
16.40	3452.6	150.1	5.75	23.0
18.08	3806.3	165.5		
18.69	3934.7	171.1	2.60	10.4
			0.42	1.7
20.21	4254.7	185.0		
			0.22	0.9
25.88	5448.4	236.9		
26.23	5522.1	240.1	0.14	0.6

Slag	[g]	75.3
Water	[L]	1.5
Slag Concentration	[g / L]	50.2

	Mass	Percentage
Insolubles	[g]	[%]
Total Insolubles	59.1	78%
Mass % Extracted		22%
S Recovered to Soluble Form		56%
S Recovered to Thiosulphate		56%
S Recovered to Combined S2O3 and SO4		56%
Na Recovered to soluble form		85%
S Recovered to Sulphate		0%

		Slag S 1	Slag S2	Slag S3	Insol S1	Insol S2	Insol S3
Mass digested	[g]	0.111	0.125	0.111	0.104		
Volume made up	[mL]	100.0	100.0	100.0	100.0	100.0	100.0
Concentration	[mg / L]	1105.0	1252.0	1107.0	1037.0	0.0	0.0

Digestions

	Sulphur	Sodium		Iron		Lead		Zinc	
	[mass %]	[mg / L]	[%]	[mg / L]	[%]	[mg / L]	[%]	[mg / L]	[%]
Slag	20%		13%		20%		11%		2%
S1	20.6%	126.5	11%	230.00	21%	146.00	13%	17.60	2%
S2	20.4%	170	14%	266.00	21%	145.00	12%	20.30	2%
S3	19.9%	152	14%	189.00	17%	82.10	7%	14.70	1%
Insols	10%		5%		16%		15%		3%
S1	10.1%	55.5	5%	170.00	16%	155.00	15%	28.40	3%
S2									
S3									

RUN NUMBER	4
CONDITION	Base
VALUE	
Slag type	N
Slag fraction	fine fraction

Slag	[g]	75.3
Water	[L]	1.5
Slag Concentration	[g / L]	50.2

	Mass	Percentage
Insolubles	[g]	[%]
Total Insolubles	59.61	79.2%
Mass % Extracted		20.8%
S Recovered to Soluble Form		59.5%
S Recovered to Thiosulphate		59.5%
S Recovered to Combined S2O3 and SO4		59.5%
Na Recovered to soluble form		77.6%
S Recovered to Sulphate		0.0%

Start Time 1/2/00 16:35

Liquid Samples

Sample no.	Actual Time	lapsed Ti	S - 2		S2O3		SO4		Total Sulphur
	[dd:hh:mm]	[minutes]		[mg / L]		[mg / L]		[mg / L]	[mg / L]
Dilution Factor	1/2/00 16:35	0:00	2	0	200	0	200	0	
1	16:45:00	0:10	157.1	314.285714	-			0	314
2	17:05:00	0:30	40.4	80.8	-			0	81
3	17:35:00	1:00	6.7	13.3	-			0	13
4	18:35:00	2:00:00	5.3	10.5	6.86	1372	0.32	64	817
5	20:35:00	4:00:00	4.3	8.5	-			0	9
6	1/3/00 0:35	8:00:00	0.9	1.88	22.08	4416	0.06	12	2532
7	1/3/00 11:20	18:45:00	0.0	0.05	37.27	7454	0.12	24	4271
9	1/4/00 11:00	42:25:00	0.0	0	-			0	0
10	16:35:00	48:00:00	0.0	0	54.85	10970	0.089	17.8	6280
	16:35:00	48:00:00	0.0	0	51.09	10218		0	5844
								0	0

		Slag S 1	Slag S2	Slag S3	Insol S1	Insol S2	Insol S3
Mass digested	[g]	0.111	0.125	0.111	0.112		
Volume made up	[mL]	100.0	100.0	100.0	100.0	100.0	100.0
Concentration	[mg / L]	1105.0	1252.0	1107.0	1117.0	0.0	0.0

Digestions

	Sulphur	Sodium		Iron		Lead		Zinc	
	[mass %]	[mg / L]	[%]	[mg / L]	[%]	[mg / L]	[%]	[mg / L]	[%]
Slag	20%		13%		20%		11%		2%
S1	20.6%	126.5	11%	230.00	21%	146.00	13%	17.60	2%
S2	20.4%	170	14%	266.00	21%	145.00	12%	20.30	2%
S3	19.9%	152	14%	189.00	17%	82.10	7%	14.70	1%
Insols	10%		7%		17%		13%		2%
S1	9.9%	75.8	7%	187.00	17%	141.00	13%	21.90	2%
S2									
S3									

RUN NUMBER	5
CONDITION	Base
VALUE	96 h
Slag type	N
Slag fraction	fine fraction

Start Time 1/2/00 11:30

Liquid Samples

Sample no.	Actual Time	Ellapsed Time	pH	Eh	S - 2		S2O3		SO4	Total Sulphur		
	[dd:hh:mm]	[minutes]				[mg / L]		[mg / L]		[mg / L]	[mg / L]	[mg]
Dilution Factor	1/2/00 11:30	0:00			2	0	200	0	200	0		
1	1/2/00 11:40	0:10	12.70	-323	102.5	205	-		-			
2	1/2/00 12:00	0:30	12.76	-327	32.5	65	-		-			
3	1/2/00 12:30	1:00	12.66	-322	11.7	23.4	-		-			
4	1/2/00 13:30	2:00:00	12.62	-321	2.56	5.12	7.29	1458	0.169	33.8	850	1275
5	1/2/00 19:30	8:00:00	12.29	-301	0	0	23.74	4748	0.13	26	2724	4087
6	1/3/00 11:30	24:00:00	11.55	-255	0	0	41.31	8262	0.167	33.4	4737	7105
10	1/4/00 11:30	48:00:00	11.53	-254	0	0	48.62	9724	0.114	22.8	5569	8354
11	1/5/00 11:30	72:00:00	10.41	-190	0	0	54.08	10816	0.268	53.6	6204	9306
12	1/6/00 11:30	96:00:00	9.94	-163	0	0	58.76	11752	0.304	60.8	6742	10113
						0		0		0	0	0
						0		0		0	0	0

		Slag S 1	Slag S2	Slag S3	Insol S1	Insol S2	Insol S3	13	14	15	16
Mass digested	[g]	0.111	0.125	0.111	0.098						
Volume made	[mL]	100.0	100.0	100.0	100.0	100.0	100.0	100.0	100.0	100.0	100.0
Concentration	[mg / L]	1105.0	1252.0	1107.0	979.0	0.0	0.0	0.0	0.0	0.0	0.0

Slag	[g]	75.3
Water	[L]	1.5
Slag Concentration	[g / L]	50.2

96 hours

	Mass	Percentage
Insolubles	[g]	[%]
Total Insolubles	53.82	71.5%
Mass % Extracted		29%
S Recovered to Soluble Form		66%
S Recovered to Thiosulphate		66%
S Recovered to Combined S2O3 and SO4		66%
Na Recovered to soluble form		
S Recovered to Sulphate		0.2%

48 hours

	Mass	Percentage
Insolubles	[g]	[%]
Total Insolubles		
Mass % Extracted		
S Recovered to Soluble Form		55%
S Recovered to Thiosulphate		54.6%
S Recovered to Combined S2O3 and SO4		55%
Na Recovered to soluble form		

Digestions

	Sulphur	Sodium		Iron		Lead		Zinc		
	[mass %]	[mg / L]	[%]	[mg / L]	[%]	[mg / L]	[%]	[mg / L]	[%]	
Slag	20%		13%		20%		11%		2%	65%
S1	20.6%	126.5	11%	230.00	21%	146.00	13%	17.60	2%	68%
S2	20.4%	170	14%	266.00	21%	145.00	12%	20.30	2%	68%
S3	19.9%	152	14%	189.00	17%	82.10	7%	14.70	1%	
Insols	9%		8%		20%		13%		2%	
S1	8.7%	80.5	8%	197.00	20%	124.00	13%	18.60	2%	
S2										
S3										

RUN NUMBER	6
CONDITION	Base
VALUE	
Slag type	N
Slag fraction	fine fraction

Slag	[g]	200.5
Water	[L]	4
Slag Concentration	[g / L]	50.1

	Mass	Percentage
Insolubles	[g]	[%]
Total Insolubles	161.59	81%
Mass % Extracted		19%
S Recovered to Soluble Form		60%
S Recovered to Thiosulphate		60%
S Recovered to Combined S2O3 and SO4		60%
Na Recovered to soluble form		0%
S Recovered to Sulphate		0%

Start Time	1/2/00 15:52

Liquid Samples

Sample no.	Actual Time	Ellapsed Time	DO 2	S - 2		S2O3	
	[dd:hh:mm]	[minutes]	[mg / L]		[mg / L]		[mg / L]
Dilution Factor	1/2/00 15:52	0:00	0	2		200	
1	16:02:00	0:10	2.8	107.2	214.4		0
2	1/2/00 16:12	0:20	4	44.4	88.8		
3	16:22:00	0:30	4.5	24.3	48.6		0
4	16:52:00	1:00	5.2	9.8	19.6		0
5	1/2/00 18:20	2:28:00	6.2	4.3	8.6	12.64	2528
6	19:52:00	4:00:00	6.6	1.1	2.2		0
7	23:52:00	8:00:00	8.2	0.0	0		0
8	1/3/00 11:30	19:38:00	8.7	0.0	0		0
9	15:52:00	24:00:00	9	0.0	0	39.19	7838
10	1/4/00 15:52	48:00:00		0.0	0	53.06	10612
11	1/4/00 15:52	48:00:00			0	52.92	10584

		Slag S 1	Slag S2	Slag S3	Insol S1	Insol S2	Insol S3
Mass digested	[g]	0.111	0.125	0.111	0.119		
Volume made up	[mL]	100.0	100.0	100.0	100.0	100.0	100.0
Concentration	[mg / L]	1105.0	1252.0	1107.0	1190.0	0.0	0.0

Digestions

	Sulphur	Sodium		Iron		Lead		Zinc	
	[mass %]	[mg / L]	[%]	[mg / L]	[%]	[mg / L]	[%]	[mg / L]	[%]
Slag	20%		13%		20%		11%		2%
S1	20.6%	126.5	11%	230.00	21%	146.00	13%	17.60	2%
S2	20.4%	170	14%	266.00	21%	145.00	12%	20.30	2%
S3	19.9%	152	14%	189.00	17%	82.10	7%	14.70	1%
Insols	10%		10%		23%		8%		2%
S1	10.4%	115.5	10%	278.00	23%	93.20	8%	22.60	2%
S2	9.3%								
S3									

RUN NUMBER	7
CONDITION	Base
VALUE	
Slag type	O
Slag fraction	fine fraction

Start Time 1/2/00 16:30

Liquid Samples

Sample no.	Actual Time	Ellapsed Time	S - 2		S2O3		SO4		Sodium	
	[dd:hh:mm]	[minutes]		[mg / L]		[mg / L]		[mg / L]	[mg / L]	
Dilution Factor	1/2/00 16:30	0:00	2	0	200	0	200	0	210.5263158	0
1	1/2/00 16:40	0:10	110.0	220.0				0	12.62	2656.8
2	1/2/00 17:00	0:30	31.1	62.1				0	14.08	2964.2
3	1/2/00 17:30	1:00	8.9	17.9				0	14.79	3113.7
4	1/2/00 18:30	2:00:00	3.7	7.3	9.36	1872	0.77	154	16.02	3372.6
5	1/2/00 20:30	4:00:00	2.8	5.7	14.29	2858	0.516	103.2		0.0
6	1/3/00 1:30	9:00:00	1.8	3.6	24	4800	0.4	80	17.92	3772.6
7	1/3/00 11:15	18:45:00	0.0	0.0	37.03	7406	0.55	110		0.0
9	1/4/00 11:00	42:30:00	0.0	0.0	40.98	8196	0.47	94	25.77	5425.3
10	1/4/00 16:30	48:00:00	0.0	0.0	44.38	8876	0.52	104	26.32	5541.1
	1/4/00 16:30	48:00:00	0.0	0.0	42.87	8574	0.58	116		0.0
								0		0.0

Slag	[g]		75.3
Water	[L]		1.5
Slag Concentration	[g / L]		50.2

	Mass	Percentage
Insolubles	[g]	[%]
Total Insolubles	58.43	78%
Mass % Extracted		22%
S Recovered to Soluble Form		54%
S Recovered to Thiosulphate		53%
S Recovered to Combined S2O3 and SO4		54%
Na Recovered to soluble form		82%
S Recovered to Sulphate		0%

		Slag S 1	Slag S2	Slag S3	Insol S1	Insol S2	Insol S3
Mass digested	[g]	0.103	0.129	0.116	0.107		
Volume made up	[mL]	100.0	100.0	100.0	100.0	100.0	100.0
Concentration	[mg / L]	1033.0	1288.0	1163.0	1072.0	0.0	0.0

Digestions

	Sulphur	Sodium		Iron		Lead		Zinc	
	[mass %]	[mg / L]	[%]	[mg / L]	[%]	[mg / L]	[%]	[mg / L]	[%]
Slag	19%		13%		19%		3%		2%
S1	17.6%	134.5	13%	167.00	16%	29.80	3%	17.10	2%
S2	18.4%	185	14%	256.00	20%	40.40	3%	23.90	2%
S3	19.9%	151	13%	234.00	20%	32.20	3%	22.40	2%
Insols	13%		9%		15%		11%		2%
S1	13.0%	92.5	9%	164.00	15%	113.00	11%	18.80	2%
S2	12.4%								
S3									

RUN NUMBER	8
CONDITION	Base
VALUE	96 h
Slag type	O
Slag fraction	fine fraction

Start Time 1/2/00 11:30

Liquid Samples

Sample no.	Actual Time	Ellapsed Tim	pH	Eh	S - 2		S2O3		SO4
	[dd:hh:mm]	[minutes]				[mg / L]		[mg / L]	
Dilution Factor	1/2/00 11:30	0:00	8		2	0	200	0	200
1	1/2/00 11:40	0:10	12.72	-324.00	97.1	194.3			
2	1/2/00 12:00	0:30	12.75	-326.00	35.6	71.2			
3	1/2/00 12:30	1:00	12.68	-323.00	13.5	27.0			
4	1/2/00 13:30	2:00:00	12.62	-320.00	0.3	0.7	7.97	1594	0.47
5	1/2/00 19:30	8:00:00	12.44	-307.00	0.0	0.0	19.17	3834	0.37
6	1/3/00 11:30	24:00:00	11.51	-252.00	0.0	0.0	40.07	8014	0.41
10	1/4/00 11:30	48:00:00	11.35	-242.00	0.0	0.0	45.12	9024	0.46
11	1/5/00 11:30	72:00:00	10.03	-167.00	0.0	0.0	49.83	9966	0.56
12	1/6/00 11:30	96:00:00	9.70	-149.00	0.0	0.0	50.58	10116	0.87
					0.0	0			

		Slag S 1	Slag S2	Slag S3	Insol S1	Insol S2	Insol S3
Mass digested	[g]	0.103	0.129	0.116	0.115		
Volume made up	[mL]	100.0	100.0	100.0	100.0	100.0	100.0
Concentration	[mg / L]	1033.0	1288.0	1163.0	1148.0	0.0	0.0

Slag	[g]	75.1
Water	[L]	1.5
Slag Concentration	[g / L]	50.1

96 hours

	Mass	Percentage
Insolubles	[g]	[%]
Total Insolubles	53.39	71%
Mass % Extracted		29%
S Recovered to Soluble Form		63%
S Recovered to Thiosulphate		62%
S Recovered to Combined S2O3 and SO4		63%
Na Recovered to soluble form		0%
S Recovered to Sulphate		1%

48 hours

	Mass	Percentage
Insolubles	[g]	[%]
Total Insolubles		
Mass % Extracted		
S Recovered to Soluble Form		55.7%
S Recovered to Thiosulphate		55.3%
S Recovered to Combined S2O3 and SO4		55.7%
S Recovered to sulphate		

Digestions

	Sulphur	Sodium		Iron		Lead		Zinc	
	[mass %]	[mg / L]	[%]	[mg / L]	[%]	[mg / L]	[%]	[mg / L]	[%]
Slag	19%		13%		19%		3%		2%
S1	17.6%	134.5	13%	167.00	16%	19.80	2%	17.10	2%
S2	18.4%	185	14%	256.00	20%	40.40	3%	23.90	2%
S3	19.9%	151	13%	234.00	20%	32.20	3%	22.40	2%
Insols	8%		9%		19%		4%		2%
S1	7.0%	102.5	9%	223.00	19%	51.50	4%	21.20	2%
S2	8.1%								
S3									

RUN NUMBER	9
CONDITION	Base, 4 l
VALUE	
Slag type	O
Slag fraction	fine fraction

Start Time 1/2/00 21:03

Liquid Samples

Sample no.	Actual Time	Ilapsed Tim	DO 2	S - 2		S2O3		SO4	
	[dd:hh:mm]	[minutes]	[mg / L]		[mg / L]		[mg / L]		[mg / L]
Dilution Factor		0		2		200		200	
1	1/2/00 21:13	0:10	3	12.8	25.6	9.49	1898	0.85	170
	1/2/00 21:23	0:20	3.5	5.32	10.64				
2	1/2/00 21:33	0:30	4	5.62	11.24		0		0
3	1/2/00 23:03	2:00:00	6.3	0.02	0.04	11.74	2348	0.75	150
4	1/3/00 11:03	14:00:00	8.7	0	0	31.91	6382	0.4	80
	1/4/00 1:50	28:47:00	9.4	0	0		0		0
10	1/4/00 21:03	48:00:00	9.7	0	0	43.08	8616	0.54	108
11	1/4/00 21:03	48:00:00	9.7	0	0	43.85	8770	0.69	138
					0		0		0

		Slag S 1	Slag S2	Slag S3	Insol S1	Insol S2	Insol S3
Mass digested	[g]	0.103	0.129	0.116	0.112		
Volume made up	[mL]	100.0	100.0	100.0	100.0	100.0	100.0
Concentration	[mg / L]	1033.0	1288.0	1163.0	1122.0	0.0	0.0

	Mass	Percentage
Insolubles	[g]	[%]
Total Insolubles	157.9	79%
Mass % Extracted		21%
S Recovered to Soluble Form		59%
S Recovered to Thiosulphate		58%
S Recovered to Combined S2O3 and SO4		59%
Na Recovered to soluble form		
S Recovered to Sulphate		0%

	Slag	[g]	200.5
	Water	[L]	4
	Slag Concentration	[g / L]	50.1

Digestions

	Sulphur	Sodium		Iron		Lead		Zinc	
	[mass %]	[mg / L]	[%]	[mg / L]	[%]	[mg / L]	[%]	[mg / L]	[%]
Slag	17%		13%		19%		3%		2%
S1	17.6%	134.5	13%	167.00	16%	19.80	2%	17.10	2%
S2	16.5%	185	14%	256.00	20%	40.40	3%	23.90	2%
S3	16.9%	151	13%	234.00	20%	32.20	3%	22.40	2%
Insols	8%		10%		19%		3%		2%
S1	7.4%	113.5	10%	218.00	19%	30.90	3%	23.60	2%
S2	8.8%								
S3									

RUN NUMBER	10
CONDITION	Base
VALUE	
Slag type	N
Slag fraction	course fraction

Start Time 1/2/00 11:25

Liquid Samples

Sample no.	Actual Time	lapsed Ti	pH	Eh	S - 2		S2O3	
	[dd:hh:mm]	[minutes]				[mg / L]		[mg / L]
Dilution Factor	1/2/00 11:25	0:00:00	8		2	0	200	0
1	1/2/00 11:35	0:10:00	12.98	-338	63.2	126.4		
2	1/2/00 11:55	0:30:00	13.09	-344	44.4	88.8		
3	1/2/00 12:25	1:00:00	13.08	-343	12.75	25.5		
4	1/2/00 13:25	2:00:00	13.09	-344	6.45	12.9	5.12	1024
5	1/2/00 15:05	3:40:00	13.09	-344	1.8	3.6		0
6	1/3/00 1:05	13:40:00	12.57	-315	0.054	0.108		0
7	1/3/00 11:25	24:00:00	12.42	-307	0	0	24.15	4830
8	1/3/00 23:25	36:00:00	11.56	-258	0	0	28.93	5786
10	1/4/00 11:25	48:00:00	10.96	-226	0	0	33.68	6736
	1/4/00 11:25	48:00:00			0	0	32.27	6454
						0		0

Sodium			Iron	
[mg / L]		[mol/m^3]	[mg / L]	
210.5263	0	0	4	0
13.24	2787.4	121.1899	5.41	21.6
			2.26	9.0
14.96	3149.5	136.9336	1.04	4.2
			0.91	3.6
19.68	4142.5	180.1098	0.53	2.1
20.07	4224.3	183.6659		
20.90	4398.9	191.2586	0.38	1.5
	0.0			
	0.0			

Slag	[g]	75.3
Water	[L]	1.5
Slag Concentration	[g / L]	50.2

	Mass	Percentage
Insolubles	[g]	[%]
Total Insolubles	59.19	79%
Mass % Extracted		21%
S Recovered to Soluble Form		39%
S Recovered to Thiosulphate		39%
S Recovered to Combined S2O3 and SO4		39%
Na Recovered to soluble form		67%
S Recovered to Sulphate		0%

		Slag S 1	Slag S2	Slag S3	Insol S1	Insol S2	Insol S3
Mass digested	[g]	0.111	0.125	0.145	0.102		
Volume made up	[mL]	100.0	100.0	100.0	100.0	100.0	100.0
Concentration	[mg / L]	1105.0	1252.0	1449.0	1023.0	0.0	0.0

Digestions

	Sulphur	Sodium		Iron		Lead		Zinc
	[mass %]	[mg / L]	[%]	[mg / L]	[%]	[mg / L]	[%]	[mg / L]
Slag	19%		13%		22%		11%	
S1	20.6%	126.5	11%	230.00	21%	146.00	13%	17.60
S2	20.4%	170	14%	266.00	21%	145.00	12%	20.30
S3	17.0%	208	14%	327.00	23%	110.00	8%	25.10
Insols	11%		7%		23%		6%	
S1	10.6%	74	7.18%	231.00	22.58%	65.60	6.41%	20.90
S2	12.1%							
S3								

RUN NUMBER	11
CONDITION	Base
VALUE	
Slag type	N
Slag fraction	course fraction

Start Time 1/2/00 9:55

Slag	[g]	75.3
Water	[L]	1.5
Slag Concentration	[g / L]	50.2

	Mass	Percentage
Insolubles	[g]	[%]
Total Insolubles	61.56	82%
Mass % Extracted		18%
S Recovered to Soluble Form		43%
S Recovered to Thiosulphate		43%
S Recovered to Combined S2O3 and SO4		43%
Na Recovered to soluble form		
S Recovered to Sulphate		0%

Liquid Samples

Sample no.	Actual Time	Ellapsed Tim	pH	Eh	S - 2		S2O3	
	[dd:hh:mm]	[minutes]				[mg / L]		[mg / L]
Dilution Factor	1/2/00 9:55	0:00:00	8		2	0	200	0
1	1/2/00 10:10	0:15:00	12.85	-338	74.5	149		0
2	1/2/00 10:28	0:33:00	13	-346	67.5	135		0
3	1/2/00 11:00	1:05:00	13.06	-349	19.2	38.4		0
4	1/2/00 11:55	2:00:00	13.01	-348	15.2	30.4	3.5	700
5	1/2/00 17:45	7:50:00	12.86	-339	4.77	9.54	10.57	2114
6	1/3/00 9:10	23:15:00	12.22	-303	0	0	20.92	4184
7	1/3/00 21:40	35:45:00	11.6	-268	0	0	31.8	6360
10	1/4/00 9:55	48:00:00	11.68	-216	0	0	35.94	7188
11	1/4/00 9:55	48:00:00	11.68	-216	0	0	36.81	7362
						0		0

		Slag S 1	Slag S2	Slag S3	Insol S1	Insol S2	Insol S3
Mass digested	[g]	0.111	0.125	0.111	0.098	0.109	
Volume made up	[mL]	100.0	100.0	100.0	100.0	100.0	100.0
Concentration	[mg / L]	1105.0	1252.0	1107.0	980.0	1090.0	0.0

Digestions

	Sulphur	Sodium		Iron		Lead		Zinc	
	[mass %]	[mg / L]	[%]	[mg / L]	[%]	[mg / L]	[%]	[mg / L]	[%]
Slag	19%		13%		20%		11%		2%
S1	17.0%	126.5	11%	230.00	21%	146.00	13%	17.60	2%
S2	20.4%	170	14%	266.00	21%	145.00	12%	20.30	2%
S3	19.9%	152	14%	189.00	17%	82.10	7%	14.70	1%
Insols	11%		10%		20%		9%		2%
S1	10.40%	97	10%	193.00	20%	89.50	9%	17.20	2%
S2	11.9%								
S3									

RUN NUMBER	12
CONDITION	Base
VALUE	
Slag type	N
Slag fraction	course fraction

Start Time 1/2/00 11:15

Slag	[g]	75.3
Water	[L]	1.5
Slag Concentration	[g / L]	50.2

	Mass	Percentage
Insolubles	[g]	[%]
Total Insolubles	62.73	83%
Mass % Extracted		17%
S Recovered to Soluble Form		43%
S Recovered to Thiosulphate		43%
S Recovered to Combined S2O3 and SO4		43%
Na Recovered to soluble form		0%
S Recovered to Sulphate		0%

Liquid Samples

Sample no.	Actual Time	lapsed Ti	pH	Eh	S - 2			S2O3			SO4			SO4*10
	[dd:hh:mm]	[minutes]				[mg / L]	[mol/m^3]		[mg / L]	[mol/m^3]		[mg / L]	[mol/m^3]	
Dilution Factor	1/2/00 11:15	0:00:00	8		2	0	0.00	200	0	0	200	0	0	0
1	1/2/00 11:25	0:10:00	12.58	-313	52.5	105	3.27							
2	1/2/00 11:45	0:30:00	12.96	-333	48.75	97.5	3.04							
3	1/2/00 12:15	1:00:00	12.97	-334	13.84	27.68	0.86							
4	1/2/00 13:15	2:00:00	12.95	-334	6.5	13	0.41	4.44	888	7.9	0.08	16	0.166667	1.666667
5	1/2/00 15:15	4:00:00	12.85	-329	6.15	12.3	0.38							
6	1/2/00 19:15	8:00:00	12.73	-320	4.12	8.24	0.26	13.58	2716	24.2	0.14	28	0.291667	2.916667
7	1/3/00 1:15	14:00:00	12.37	-299	1.84	3.68	0.11							
8	1/3/00 11:20	24:05:00	12.01	-280	0.23	0.46	0.01	26.91	5382	48.0	0			
9	1/3/00 23:10	35:55:00	11.73	-265	0	0	0.00	32.88	6576	58.6	0.18	36	0.375	3.75
10	1/4/00 11:15	48:00:00	11.36	-244	0	0	0.00	37.124	7424.8	66.2	0			
	1/4/00 11:15	48:00:00			0	0	0.00	39.472	7894.4	70.4	0.12	24	0.25	2.5

		Slag S 1	Slag S2	Slag S3	Insol S1	Insol S2	Insol S3
Mass digested	[g]	0.111	0.1252	0.111	0.119	0.098	
Volume made up	[mL]	100.0	100.0	100.0	100.0	100.0	100.0
Concentration	[mg / L]	1105.0	1252.0	1107.0	1185.0	980.0	0.0

Digestions

	Sulphur	Sodium		Iron		Lead		Zinc	
	[mass %]	[mg / L]	[%]	[mg / L]	[%]	[mg / L]	[%]	[mg / L]	[%]
Slag	20%		13%		20%		11%		2%
S1	20.6%	126.5	11%	230.00	21%	146.00	13%	17.60	2%
S2	20.4%	170	14%	266.00	21%	145.00	12%	20.30	2%
S3	19.9%	152	14%	189.00	17%	82.10	7%	14.70	1%
Insols	10%		4%		19%		8%		2%
S1	9.6%	52.5	4%	230.00	19%	92.30	8%	19.80	2%
S2	9.9%								
S3									

RUN NUMBER	13
CONDITION	Base
VALUE	
Slag type	N
Slag fraction	course fraction

Start Time 1/2/00 11:20

Liquid Samples

Sample no.	Actual Time	lapsed Ti	pH	Eh	S - 2		S2O3	
	[dd:hh:mm]	[minutes]				[mg / L]		[mg / L]
Dilution Factor	1/2/00 11:20	0:00:00	8		2	0	200	0
1	1/2/00 11:30	0:10:00	12.75	-325	49.6	99.2		0
2	1/2/00 11:50	0:30:00	13	-339	24.4	48.8		0
3	1/2/00 12:20	1:00:00	13.02	-340	8.16	16.32		0
4	1/2/00 13:20	2:00:00	13.05	-343	2.32	4.64		0
5	1/2/00 15:05	3:45:00	13.09	-344	2.28	4.56		0
6	1/3/00 1:00	13:40:00	12.91	-334	1.6	3.2	17.46	3492
7	1/3/00 11:20	24:00:00	12.93	-335	0			
8	1/3/00 23:20	36:00:00	12.77	-325	0	0	33.4	6680
10	1/4/00 11:20	48:00:00	12.61	-318	0	0	36.49	7298
	1/4/00 11:20	48:00:00	12.61	-318	0	0	34.081	6816.2
						0		0

		Slag S 1	Slag S2	Slag S3	Insol S1	Insol S2	Insol S3
Mass digested	[g]	0.111	0.125	0.111	0.109	0.110	
Volume made up	[mL]	100.0	100.0	100.0	100.0	100.0	100.0
Concentration	[mg / L]	1105.0	1252.0	1107.0	1088.0	1100.0	0.0

Slag	[g]	75.3
Water	[L]	1.5
Slag Concentration	[g / L]	50.2

	Mass	Percentage
Insolubles	[g]	[%]
Total Insolubles	63.93	85%
Mass % Extracted		15%
S Recovered to Soluble Form		40%
S Recovered to Thiosulphate		40%
S Recovered to Combined S2O3 and SO4		40%
Na Recovered to soluble form		
S Recovered to Sulphate		0%

Digestions

	Sulphur	Sodium		Iron		Lead		Zinc
	[mass %]	[mg / L]	[%]	[mg / L]	[%]	[mg / L]	[%]	[mg / L]
Slag	20%		13%		20%		11%	
S1	20.6%	126.5	11%	230.00	21%	146.00	13%	17.60
S2	20.4%	170	14%	266.00	21%	145.00	12%	20.30
S3	19.9%	152	14%	189.00	17%	82.10	7%	14.70
Insols	11%		3%		16%		17%	
S1	12.1%	28	2.53%	177.00	16.27%	184.00	16.91%	15.30
S2	10.7%							
S3								

RUN NUMBER	14
CONDITION	Base
VALUE	
Slag type	O
Slag fraction	course fraction

Slag	[g]	75.3
Water	[L]	1.5
Slag Concentration	[g / L]	50.2

	Mass	Percentage
Insolubles	[g]	[%]
Total Insolubles	60.75	81%
Mass % Extracted		19%
S Recovered to Soluble Form		52%
S Recovered to Thiosulphate		52%
S Recovered to Combined S2O3 and SO4		52%
Na Recovered to soluble form		71%
S Recovered to Sulphate		0%

Start Time 1/2/00 13:25

Liquid Samples

Sample no.	Actual Time	Ellapsed Time	pH	Eh	S2O3		SO4		Sodium
	[dd:hh:mm]	[minutes]				[mg / L]		[mg / L]	[mg / L]
Dilution Factor	1/2/00 13:25	0:00:00	8		200	0	200	0	210.5263158
1	1/2/00 13:35	0:10:00	12.59	-312		0		0	10.97
2	1/2/00 13:55	0:30:00	12.73	-322		0		0	12.24
3	1/2/00 14:25	1:00:00	12.77	-325		0		0	12.86
4	1/2/00 15:00	1:35:00	12.81	-326	5.07	1014	0.29	58	13.93
5	1/2/00 17:35	4:10:00	12.86	-329		0		0	
6	1/2/00 21:45	8:20:00	12.9	-327	15.1	3020	0.27	54	15.58
7	1/3/00 10:50	21:25:00	12.61	-314	28.29	5658	0.31	62	
8	1/3/00 22:30	33:05:00	12.13	-286		0		0	22.41
10	1/4/00 13:25	48:00:00	11.86	-271	38.95	7790	0.39	78	22.89
	1/4/00 13:25	48:00:00			40.27	8054	0.34	68	
						0		0	

		Slag S 1	Slag S2	Slag S3	Insol S1	Insol S2	Insol S3
Mass digested	[g]	0.103	0.129	0.116	0.138		
Volume made up	[mL]	100.0	100.0	100.0	100.0	100.0	100.0
Concentration	[mg / L]	1033.0	1288.0	1163.0	1381.0	0.0	0.0

Digestions

	Sulphur	Sodium		Iron		Lead		Zinc	
	[mass %]	[mg / L]	[%]	[mg / L]	[%]	[mg / L]	[%]	[mg / L]	[%]
Slag	17%		13%		19%		3%		2%
S1	17.6%	134.5	13%	167.00	16%	19.80	2%	17.10	2%
S2	16.5%	185	14%	256.00	20%	40.40	3%	23.90	2%
S3	17.9%	151	13%	234.00	20%	32.20	3%	22.40	2%
Insols	8%		7%		20%		2%		2%
S1	8.0%	95.5	7%	279.00	20%	27.60	2%	30.60	2%
S2	8.9%								
S3									

RUN NUMBER	15
CONDITION	Base
VALUE	
Slag type	O
Slag fraction	course fraction

Start Time 1/2/00 11:25

Liquid Samples

Sample no.	Actual Time	Ellapsed Tim	S2O3		SO4	
	[dd:hh:mm]	[minutes]		[mg / L]		[mg / L]
Dilution Factor		0	200		200	
1	1/2/00 11:30	0:05		0		0
2	1/2/00 11:50	0:25		0		0
3	1/2/00 12:20	0:55		0		0
4	1/2/00 13:20	1:55:00	11.52	2304		0
5	1/2/00 15:05	3:40:00		0		0
6	1/3/00 1:00	13:35:00	18.64	3728		0
7	1/3/00 11:20	23:55:00		0		0
8	1/3/00 23:20	35:55:00	33.13	6626		0
10	1/4/00 11:20	47:55:00	34.97	6994		0
			34.11	6822		0
				0		0

		Slag S 1	Slag S2	Slag S3	Insol S1	Insol S2	Insol S3
Mass digested	[g]	0.103	0.129	0.116	0.115		
Volume made up	[mL]	100.0	100.0	100.0	100.0	100.0	100.0
Concentration	[mg / L]	1033.0	1288.0	1163.0	1153.0	0.0	0.0

Slag	[g]	75.3
Water	[L]	1.5
Slag Concentration	[g / L]	50.2

	Mass	Percentage
Insolubles	[g]	[%]
Total Insolubles	63.82	85%
Mass % Extracted		15%
S Recovered to Soluble Form		46%
S Recovered to Thiosulphate		46%
S Recovered to Combined S2O3 and SO4		46%
Na Recovered to soluble form		0%
S Recovered to Sulphate		0%

Digestions

	Sulphur	Sodium		Iron		Lead		Zinc	
	[mass %]	[mg / L]	[%]	[mg / L]	[%]	[mg / L]	[%]	[mg / L]	[%]
Slag	17%		13%		19%		3%		2%
S1	17.6%	134.5	13%	167.00	16%	19.80	2%	17.10	2%
S2	16.5%	185	14%	256.00	20%	40.40	3%	23.90	2%
S3	16.9%	151	13%	234.00	20%	32.20	3%	22.40	2%
Insols	9%		6%		20%		2%		2%
S1	8.7%	75	6.46%	225.00	19.51%	26.90	2.33%	23.00	1.99%
S2	9.1%								
S3									

CONDITION	agitation
VALUE	200 rpm
Slag type	N
Slag fraction	fine fraction

Start Time 1/2/00 11:10

Liquid Samples

Sample no.	Actual Time	llapsed Tim	pH	Eh	mperatu	DO 2	ltrate Colo	S - 2		S2O3		SO4	
	[dd:hh:mm]	[minutes]			[C]	[mg / L]			[mg / L]		[mg / L]		[mg / L]
Dilution Factor	1/2/00 11:10	0:00	8					2	0	200	0	200	0
1	1/2/00 11:20	0:10	12.7	-321	21.3			108.4	216.8		0		0
2	1/2/00 11:40	0:30	12.77	-325				66.7	133.4		0		0
3	1/2/00 12:10	1:00	12.79	-326				15.5	31		0		0
4	1/2/00 13:10	2:00:00	12.84	-327				7.1	14.2	5.23	1046		0
5	1/2/00 19:45	8:35:00	12.88	-327				3.4	6.8				0
6	1/3/00 11:10	24:00:00	12.75	-322				0.98	1.96	28.30	5660.74074		0
7	1/4/00 1:10	38:00:00	12.48	-305				0	0				0
10	1/4/00 11:10	48:00:00	12.2	-290	19.3			0	0	44.12	8824		0
11	1/4/00 11:10	48:00:00						0	0	41.79	8358		0
													0

		Slag S 1	Slag S2	Slag S3	Insol S1	Insol S2	Insol S3	13	14	15	16
Mass digested	[g]	0.111	0.125	0.111	0.119						
Volume made up	[mL]	100.0	100.0	100.0	100.0	100.0	100.0	100.0	100.0	100.0	100.0
Concentration	[mg / L]	1105.0	1252.0	1107.0	1185.0	0.0	0.0	0.0	0.0	0.0	0.0

		Mass	Percentage
Insolubles	[g]		[%]
Total Insolubles	60.57		80%
Mass % Extracted			20%
S Recovered to Soluble Form			48%
S Recovered to Thiosulphate			48%
S Recovered to Combined S2O3 and SO4			48%
Na Recovered to soluble form			62%
S Recovered to Sulphate			0%

	[g]	
Slag		75.3
Water	[L]	1.5
Slag Concentration	[g / L]	50.2

Digestions

	Sulphur	Sodium		Iron		Lead		Zinc	
	[mass %]	[mg / L]	[%]	[mg / L]	[%]	[mg / L]	[%]	[mg / L]	[%]
Slag	20%		13%		20%		11%		2%
S1	20.6%	126.5	11%	230.00	21%	146.00	13%	17.60	2%
S2	20.4%	170	14%	266.00	21%	145.00	12%	20.30	2%
S3	19.9%	152	14%	189.00	17%	82.10	7%	14.70	1%
Insols	10.9%		10%		20%		2%		2%
S1	10.7%	115.5	10%	233.00	20%	23.20	2%	28.40	2%
S2	11.1%								
S3									

CONDITION	agitation
VALUE	600 rpm
Slag type	N
Slag fraction	fine fraction

Slag	[g]	75.3
Water	[L]	1.5
Slag Concentration	[g / L]	50.2

	Mass	Percentage
Insolubles	[g]	[%]
Total Insolubles	59.1	78.5%
Mass % Extracted		22%
S Recovered to Soluble Form		56%
S Recovered to Thiosulphate		56%
S Recovered to Combined S2O3 and SO4		56%
Na Recovered to soluble form		85%
S Recovered to Sulphate		0%

Start Time 1/2/00 16:30

Liquid Samples

Sample no.	Actual Time	llapsed Tim	pH	Eh	emperatur	DO 2	ltrate Colo	S - 2		S2O3		SO4	
	[dd:hh:mm]	[minutes]			[C]	[mg / L]			[mg / L]		[mg / L]		[mg / L]
Dilution Factor	1/2/00 16:30	0:00	8					2	0	200	0	200	0
1	1/2/00 16:40	0:10						130.6	261.1	-	#VALUE!	-	#VALUE!
2	1/2/00 17:00	0:30						41.2	82.4	-	#VALUE!	-	#VALUE!
3	1/2/00 17:30	1:00						6.1	12.2	-	#VALUE!	-	#VALUE!
4	1/2/00 18:30	2:00:00						5.0	10.0	7.31	1462	0.38	76
5	1/2/00 20:30	4:00:00						3.0	6.0	15.68	3136	0.502	100.4
6	1/3/00 1:30	9:00:00						1.3	2.5	28.01	5602	0.18	36
7	1/3/00 11:15	18:45:00						0.0	0.0	40.34	8068	0.07	14
9	1/4/00 11:00	42:30:00						0.0	0.0	47.62	9524	0.17	34
10	1/4/00 16:30	48:00:00						0.0	0.0	50.24	10048	0.1	20
								0.0	0.0	49.18	9836	0.21	42

		Slag S 1	Slag S2	Slag S3	Insol S1	Insol S2	Insol S3	13	14	15	16
Mass digested	[g]	0.111	0.125	0.111	0.104						
Volume made up	[mL]	100.0	100.0	100.0	100.0	100.0	100.0	100.0	100.0	100.0	100.0
Concentration	[mg / L]	1105.0	1252.0	1107.0	1037.0	0.0	0.0	0.0	0.0	0.0	0.0

Digestions

	Sulphur	Sodium		Iron		Lead		Zinc	
	[mass %]	[mg / L]	[%]	[mg / L]	[%]	[mg / L]	[%]	[mg / L]	[%]
Slag	20%		13%		20%		11%		2%
S1	20.6%	126.5	11%	230.00	21%	146.00	13%	17.60	2%
S2	20.4%	170	14%	266.00	21%	145.00	12%	20.30	2%
S3	19.9%	152	14%	189.00	17%	82.10	7%	14.70	1%
Insols	10%		7%		16%		15%		3%
S1	10.0%	75.5	7%	170.00	16%	155.00	15%	28.40	3%
S2	10.2%								
S3									

CONDITION	agitation
VALUE	1200 rpm
Slag type	N
Slag fraction	fine fraction

Start Time 1/2/00 16:35

Liquid Samples

Sample no.	Actual Time	Ellapsed Time	pH	Eh	mperatu	DO 2	ltrate Colo	S - 2		S2O3		SO4	
	[dd:hh:mm]	[minutes]			[C]	[mg / L]			[mg / L]		[mg / L]		[mg / L]
Dilution Factor	1/2/00 16:35	0:00	8					2	0	200	0	200	0
1	16:45:00	0:10						74.4	148.8				0
2	17:05:00	0:30						26.4	52.8				0
3	17:35:00	1:00						11.8	23.6				0
4	18:35:00	2:00:00						8.5	17	8.56	1712		0
5	20:35:00	4:00:00						2	4				0
6	1/3/00 1:35	9:00:00						2.3	4.6	32.46	6492	0	0
7	1/3/00 11:20	18:45:00						0	0	40.21	8042	0.16	32
9	1/4/00 11:00	42:25:00						0	0				0
10	16:35:00	48:00:00						0	0	50.11	10022	0.205	41
	16:35:00	48:00:00						0	0	52.37	10474	0.189	37.8
									0		0		0

		Slag S 1	Slag S2	Slag S3	Insol S1	Insol S2	Insol S3	13	14	15	16
Mass digested	[g]	0.111	0.125	0.111	0.105						
Volume made up	[mL]	100.0	100.0	100.0	100.0	100.0	100.0	100.0	100.0	100.0	100.0
Concentration	[mg / L]	1105.0	1252.0	1107.0	1046.0	0.0	0.0	0.0	0.0	0.0	0.0

	Mass	Percentage
Insolubles	[g]	[%]
Total Insolubles	56.85	75%
Mass % Extracted		25%
S Recovered to Soluble Form		58%
S Recovered to Thiosulphate		58%
S Recovered to Combined S2O3 and SO4		58%
Na Recovered to soluble form		92%
S Recovered to Sulphate		0%

Slag	[g]	75.3
Water	[L]	1.5
Slag Concentration	[g / L]	50.2

Digestions

	Sulphur	Sodium		Iron		Lead		Zinc	
	[mass %]	[mg / L]	[%]	[mg / L]	[%]	[mg / L]	[%]	[mg / L]	[%]
Slag	20%		13%		20%		11%		2%
S1	20.6%	126.5	11%	230.00	21%	146.00	13%	17.60	2%
S2	20.4%	170	14%	266.00	21%	145.00	12%	20.30	2%
S3	19.9%	152	14%	189.00	17%	82.10	7%	14.70	1%
Insols	10.0%		7%		19%		12%		2%
S1	9.7%	75.5	7%	202.00	19%	124.00	12%	19.80	2%
S2	10.2%								
S3									

CONDITION	s-l
VALUE	50 g/l
Slag type	N
Slag fraction	fine fraction

Start Time 1/2/00 16:35

Liquid Samples

Sample no.	Actual Time	Ellapsed Tim	pH	Eh	mperatu	DO 2	ltrate Colo	S - 2		S2O3		SO4	T
	[dd:hh:mm]	[minutes]			[C]	[mg / L]			[mg / L]		[mg / L]		[mg / L]
Dilution Factor	1/2/00 16:35	0:00	8					2	0	200	0	200	0
1	16:45:00	0:10						93.5	187.0				0
2	17:05:00	0:30						15.0	30.0				0
3	17:35:00	1:00						8.8	17.6				0
4	18:35:00	2:00:00						5.5	11.0	6.86	1372	0.32	64
5	20:35:00	4:00:00						0.0	0.0				0
6	1/3/00 1:35	9:00:00						0.0	0.0	22.08	4416	0.06	12
7	1/3/00 11:20	18:45:00						0.0	0.1	37.27	7454	0.12	24
9	1/4/00 11:00	42:25:00						0.0	0.0				0
10	16:35:00	48:00:00						0.0	0.0	51.09	10218	0.089	17.8
	16:35:00	48:00:00						0.0	0.0	54.85	10970		0
								0.0	0.0				0

		Slag S 1	Slag S2	Slag S3	Insol S1	Insol S2	Insol S3	13	14	15	16
Mass digested	[g]	0.111	0.125	0.111	0.112						
Volume made up	[mL]	100.0	100.0	100.0	100.0	100.0	100.0	100.0	100.0	100.0	100.0
Concentration	[mg / L]	1105.0	1252.0	1107.0	1117.0	0.0	0.0	0.0	0.0	0.0	0.0

	Mass	Percentage
Insolubles	[g]	[%]
Total Insolubles	59.61	79.2%
Mass % Extracted		20.8%
S Recovered to Soluble Form		59.5%
S Recovered to Thiosulphate		59.5%
S Recovered to Combined S2O3 and SO4		59.5%
Na Recovered to soluble form		0.0%
S Recovered to Sulphate		0.0%

Slag	[g]	75.3
Water	[L]	1.5
Slag Concentration	[g / L]	50.2

Digestions

	Sulphur	Sodium		Iron		Lead		Zinc	
	[mass %]	[mg / L]	[%]	[mg / L]	[%]	[mg / L]	[%]	[mg / L]	[%]
Slag	20%		13%		20%		11%		2%
S1	20.6%	126.5	11%	230.00	21%	146.00	13%	17.60	2%
S2	20.4%	170	14%	266.00	21%	145.00	12%	20.30	2%
S3	19.9%	152	14%	189.00	17%	82.10	7%	14.70	1%
Insols	10%		9%		17%		13%		2%
S1	9.9%	95.5	9%	187.00	17%	141.00	13%	21.90	2%
S2									
S3									

CONDITION	s-l
VALUE	100
Slag type	N
Slag fraction	fine fraction

Start Time 1/2/00 11:35

Liquid Samples

Sample no.	Actual Time	llapsed Tim	pH	Eh	mperatu	DO 2	ltrate Colo	S - 2		S2O3		SO4	
	[dd:hh:mm]	[minutes]			[C]	[mg / L]			[mg / L]		[mg / L]		[mg / L]
Dilution Factor	1/2/00 11:35	0:00	8					2	0	200	0	200	0
1	1/2/00 11:45	0:10						161.5	323		0		0
2	1/2/00 12:05	0:30						23.1	46.2		0		0
3	1/2/00 12:35	1:00						9.75	19.5		0		0
4	1/2/00 13:35	2:00:00						8.175	16.35	8.74	1748	0.322	64.4
5	1/2/00 19:35	8:00:00						0.285	0.57	36.54	7308	0.436	87.2
6	1/3/00 11:35	24:00:00						0	0				
7	1/3/00 20:00	32:25:00						0	0	91.68	18336	0.565	113
10	1/4/00 11:35	48:00:00						0	0	113.47	22694	0.502	100.4
	1/4/00 11:35	48:00:00						0	0	110.06	22012		0
											0		0

		Slag S 1	Slag S2	Slag S3	Insol S1	Insol S2	Insol S3	0	14	15	16
Mass digested	[g]	0.111	0.125	0.111	0.119						
Volume made up	[mL]	100.0	100.0	100.0	100.0	100.0	100.0	100.0	100.0	100.0	100.0
Concentration	[mg / L]	1105.0	1252.0	1107.0	1190.0	0.0	0.0	0.0	0.0	0.0	0.0

		Mass	Percentage
Insolubles		[g]	[%]
Total Insolubles		116.71	78%
Mass % Extracted			22%
S Recovered to Soluble Form			64%
S Recovered to Thiosulphate			64%
S Recovered to Combined S2O3 and SO4			64%
Na Recovered to soluble form			0%
S Recovered to Sulphate			0%

Slag	[g]	150									
Water	[L]	1.5									
Slag Concentration	[g / L]	100.0									

Digestions

	Sulphur	Sodium		Iron		Lead		Zinc	
	[mass %]	[mg / L]	[%]	[mg / L]	[%]	[mg / L]	[%]	[mg / L]	[%]
Slag	20%		13%		20%		11%		2%
S1	20.6%	126.5	11%	230.00	21%	146.00	13%	17.60	2%
S2	20.4%	170	14%	266.00	21%	145.00	12%	20.30	2%
S3	19.9%	152	14%	189.00	17%	82.10	7%	14.70	1%
Insols	8%		5%		18%		16%		2%
S1	7.6%	63.5	5%	215.00	18%	189.00	16%	18.20	2%
S2									
S3									

CONDITION	s-l
VALUE	133 g/l
Slag type	N
Slag fraction	fine fraction

Start Time 1/2/00 11:35

Liquid Samples

Sample no.	Actual Time	llapsed Tim	pH	Eh	mperatu	DO 2	ltrate Colo	S - 2		S2O3		SO4	
	[dd:hh:mm]	[minutes]			[C]	[mg / L]			[mg / L]		[mg / L]		[mg / L]
Dilution Factor	1/2/00 11:35	0:00	8					2	0	200	0	200	0
1	1/2/00 11:45	0:10						129.2	258.4		0		0
2	1/2/00 12:05	0:30						18.0	36		0		0
3	1/2/00 12:35	1:00						10.5	20.9		0		0
4	1/2/00 13:35	2:00:00						9.0	18	10.29	2058	0.47	94
5	1/2/00 19:35	8:00:00						1.2	2.4	45.54	9108	0.42	84
6	1/3/00 11:35	24:00:00						0.2	0.36				
6	1/3/00 20:00	32:25:00						0.0	0	113.45	22690	0.478	95.6
10	1/4/00 11:35	48:00:00						0.0	0	153.61	30722	0.54	108
	1/4/00 11:35	48:00:00						0.0	0		0		0
											0		0

		Slag S 1	Slag S2	Slag S3	Insol S1	Insol S2	Insol S3		14	15	16
Mass digested	[g]	0.111	0.125	0.111	0.102						
Volume made up	[mL]	100.0	100.0	100.0	100.0	100.0	100.0	100.0	100.0	100.0	100.0
Concentration	[mg / L]	1105.0	1252.0	1107.0	1020.0	0.0	0.0	0.0	0.0	0.0	0.0

Slag	[g]	200
Water	[L]	1.5
Slag Concentration	[g / L]	133.3

	Mass	Percentage
Insolubles	[g]	[%]
Total Insolubles	152.14	76%
Mass % Extracted		24%
S Recovered to Soluble Form		65%
S Recovered to Thiosulphate		65%
S Recovered to Combined S2O3 and SO4		65%
Na Recovered to soluble form		0%
S Recovered to Sulphate		0%

Digestions

	Sulphur	Sodium		Iron		Lead		Zinc	
	[mass %]	[mg / L]	[%]	[mg / L]	[%]	[mg / L]	[%]	[mg / L]	[%]
Slag	20%		13%		20%		11%		2%
S1	20.6%	126.5	11%	230.00	21%	146.00	13%	17.60	2%
S2	20.4%	170	14%	266.00	21%	145.00	12%	20.30	2%
S3	19.9%	152	14%	189.00	17%	82.10	7%	14.70	1%
Insols	8%		5%		21%		9%		2%
S1	7.7%	48.5	5%	211.00	21%	92.10	9%	18.70	2%
S2									
S3									

CONDITION	temperature
VALUE	20 C
Slag type	N
Slag fraction	fine fraction

Start Time 1/2/00 16:30

Liquid Samples

Sample no.	Actual Time	llapsed Tim	pH	Eh	emperatu	DO 2	ltrate Colo	S - 2		S2O3		SO4	
	[dd:hh:mm]	[minutes]			[C]	[mg / L]			[mg / L]		[mg / L]		[mg / L]
Dilution Factor	1/2/00 16:30	0:00	8					2	0	200	0	200	0
1	1/2/00 16:40	0:10						130.6	261.1	-	#VALUE!	-	#####
2	1/2/00 17:00	0:30						41.2	82.4	-	#VALUE!	-	#####
3	1/2/00 17:30	1:00						6.1	12.2	-	#VALUE!	-	#####
4	1/2/00 18:30	2:00:00						5.0	10.0	7.31	1462	0.38	76
5	1/2/00 20:30	4:00:00						3.0	6.0	15.68	3136	0.502	100.4
6	1/3/00 1:30	9:00:00						1.3	2.5	28.01	5602	0.18	36
7	1/3/00 11:15	18:45:00						0.0	0.0	41.34	8268	0.07	14
9	1/4/00 11:00	42:30:00						0.0	0.0	47.62	9524	0.17	34
10	1/4/00 16:30	48:00:00						0.0	0.0	50.24	10048	0.1	20
	1/4/00 16:30	48:00:00						0.0	0.0	49.18	9836	0.21	42

		Slag S 1	Slag S2	Slag S3	Insol S1	Insol S2	Insol S3	13	14	15	16
Mass digested	[g]	0.111	0.125	0.111	0.104						
Volume made up	[mL]	100.0	100.0	100.0	100.0	100.0	100.0	100.0	100.0	100.0	100.0
Concentration	[mg / L]	1105.0	1252.0	1107.0	1037.0	0.0	0.0	0.0	0.0	0.0	0.0

Slag	[g]	75.3
Water	[L]	1.5
Slag Concentration	[g / L]	50.2

	Mass	Percentage
Insolubles	[g]	[%]
Total Insolubles	59.1	78.5%
Mass % Extracted		22%
S Recovered to Soluble Form		56%
S Recovered to Thiosulphate		56%
S Recovered to Combined S2O3 and SO4		56%
Na Recovered to soluble form		85%
S Recovered to Sulphate		0%

Digestions

	Sulphur	Sodium		Iron		Lead		Zinc	
	[mass %]	[mg / L]	[%]	[mg / L]	[%]	[mg / L]	[%]	[mg / L]	[%]
Slag	20%		13%		20%		11%		2%
S1	20.6%	126.5	11%	230.00	21%	146.00	13%	17.60	2%
S2	20.4%	170	14%	266.00	21%	145.00	12%	20.30	2%
S3	19.9%	152	14%	189.00	17%	82.10	7%	14.70	1%
Insols	10%		7%		16%		15%		3%
S1	10.1%	75.5	7%	170.00	16%	155.00	15%	28.40	3%
S2									
S3									

CONDITION	temperature
VALUE	40 C
Slag type	O
Slag fraction	fine fraction

Start Time 1/2/00 15:55

Liquid Samples

Sample no.	Actual Time	Ellapsed Time	pH	Eh	mperatu	DO 2	ltrate Colo	S - 2		S2O3		SO4	
	[dd:hh:mm]	[minutes]			[C]	[mg / L]			[mg / L]		[mg / L]		[mg / L]
Dilution Factor	1/2/00 15:55	0:00	8					2	0	200	0	200	0
1	1/2/00 16:05	0:10	12.94					120	240		0		0
2	1/2/00 16:25	0:30	12.94					13.4	26.8		0		0
3	1/2/00 16:55	1:00	12.97					12	24		0		0
4	1/2/00 17:55	2:00:00	12.87					10.2	20.4	9.38	1876		0
5	1/2/00 23:55	8:00:00	12.24					0	0	32.65	6530	0.509	101.8
6	1/3/00 15:55	24:00:00	10.78					0	0	52.201	10440	0.56	112
10	1/4/00 15:55	48:00:00	10.04					0	0	66.109	13221.8	1.169	233.8
	1/4/00 15:55	48:00:00	10.04					0	0	64.829	12965.8	0.972	194.4
									0		0		0

		Slag S 1	Slag S2	Slag S3	Insol S1	Insol S2	Insol S3	13	14	15	16
Mass digested	[g]	0.103	0.129	0.116	0.132						
Volume made up	[mL]	100.0	100.0	100.0	100.0	100.0	100.0	100.0	100.0	100.0	100.0
Concentration	[mg / L]	1033.0	1288.0	1163.0	1322.0	0.0	0.0	0.0	0.0	0.0	0.0

Slag	[g]	75.3
Water	[L]	1.5
Slag Concentration	[g / L]	50.2

	Mass	Percentage
Insolubles	[g]	[%]
Total Insolubles	53.06	70.5%
Mass % Extracted		29.5%
S Recovered to Soluble Form		85.6%
S Recovered to Thiosulphate		84.8%
S Recovered to Combined S2O3 and SO4		85.6%
Na Recovered to soluble form		0.0%
S Recovered to Sulphate		0.8%

Digestions

	Sulphur	Sodium		Iron		Lead		Zinc		
	[mass %]	[mg / L]	[%]	[mg / L]	[%]	[mg / L]	[%]	[mg / L]	[%]	
Slag	19%		13%		19%		3%		2%	56%
S1	17.6%	134.5	13%	167.00	16%	19.80	2%	17.10	2%	50%
S2	19.5%	185	14%	256.00	20%	40.40	3%	23.90	2%	59%
S3	19.9%	151	13%	234.00	20%	32.20	3%	22.40	2%	
Insols	4.9%		5%		22%		2%		3%	
S1	4.6%	67.5	5%	287.00	22%	24.50	2%	34.20	3%	
S2	5.1%	74.9	6%	299.00	23%					
S3										

CONDITION	temperature
VALUE	60 C
Slag type	O
Slag fraction	fine fraction

Start Time 1/2/00 15:50

Liquid Samples

Sample no.	Actual Time	Ellapsed Tim	pH	Eh	mperatu	DO 2	ltrate Colo	S - 2		S2O3		SO4		
	[dd:hh:mm]	[minutes]			[C]	[mg / L]			[mg / L]		[mg / L]		[mg / L]	[mg / L]
Dilution Factor	1/2/00 15:50	0:00	8					2	0	200	0	200	0	
1	1/2/00 16:00	0:10			27			97.4	194.8		0		0	195
2	1/2/00 16:20	0:30						13.2	26.4		0		0	26
3	1/2/00 16:50	1:00						9.8	19.6		0		0	20
4	1/2/00 17:50	2:00:00						7.4	14.8	13.46	2692	0.336	67.2	1577
5	1/2/00 23:50	8:00:00						0	0	39.13	7826	0.39	78	4502
6	1/3/00 15:50	24:00:00						0	0	78.547	15709.4	1.435	287	9081
10	1/4/00 15:50	48:00:00			34			0	0	82.088	16417.6	5.871	1174.2	9782
	1/4/00 15:50	48:00:00						0	0	80.691	16138.2	11.325	2265	9987

		Slag S 1	Slag S2	Slag S3	Insol S1	Insol S2	Insol S3	13	14	15	16
Mass digested	[g]	0.139	0.129	0.116	0.108						
Volume made up	[mL]	100.0	100.0	100.0	100.0	100.0	100.0	100.0	100.0	100.0	100.0
Concentration	[mg / L]	1390.0	1288.0	1163.0	1075.0	0.0	0.0	0.0	0.0	0.0	0.0

Slag	[g]		75.3
Water	[L]		1.5
Slag Concentration	[g / L]		50.2

	Mass	Percentage
Insolubles	[g]	[%]
Total Insolubles	51.93	69.0%
Mass % Extracted		31.0%
S Recovered to Soluble Form		111.9%
S Recovered to Thiosulphate		105.4%
S Recovered to Combined S2O3 and SO4		111.9%
Na Recovered to soluble form		0.0%
S Recovered to Sulphate		6.5%

Digestions

	Sulphur	Sodium		Iron		Lead		Zinc	
	[mass %]	[mg / L]	[%]	[mg / L]	[%]	[mg / L]	[%]	[mg / L]	[%]
Slag	19%		24%		18%		3%		2%
S1	17.6%	370.0	27%	270.00	19%	42.90	3%	26.90	2%
S2	19.5%	337	24%	256.00	18%	40.40	3%	23.90	2%
S3	19.9%	303	22%	234.00	17%	32.20	2%	22.40	2%
Insols	2.2%		15%		22%		10%		2%
S1	2.6%	203.0	15%	307.00	22%	136.00	10%	25.50	2%
S2	1.7%								
S3									

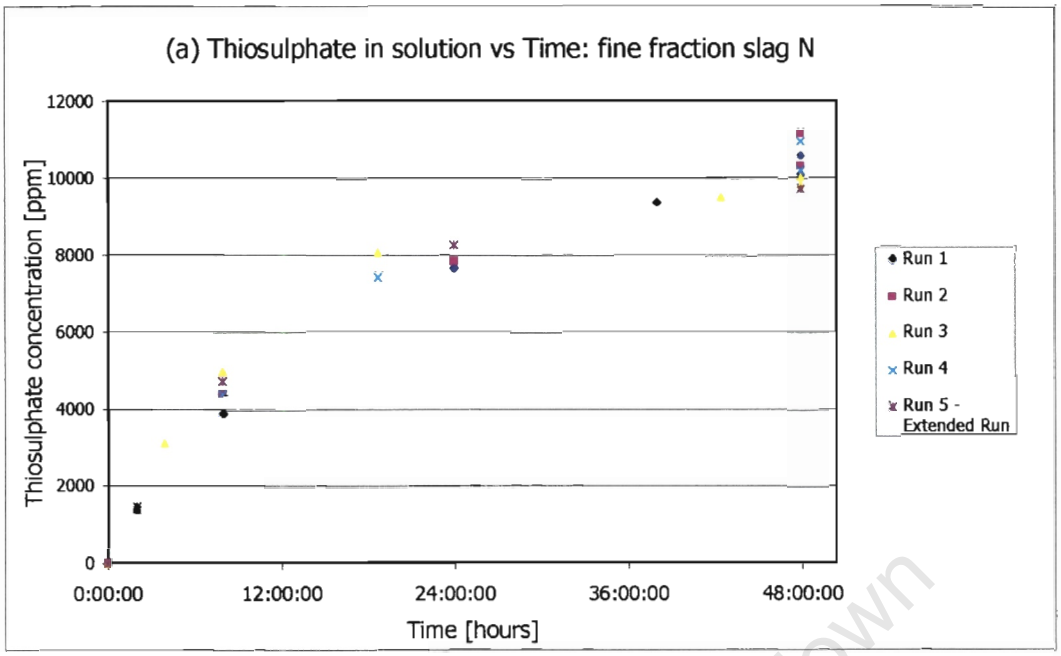

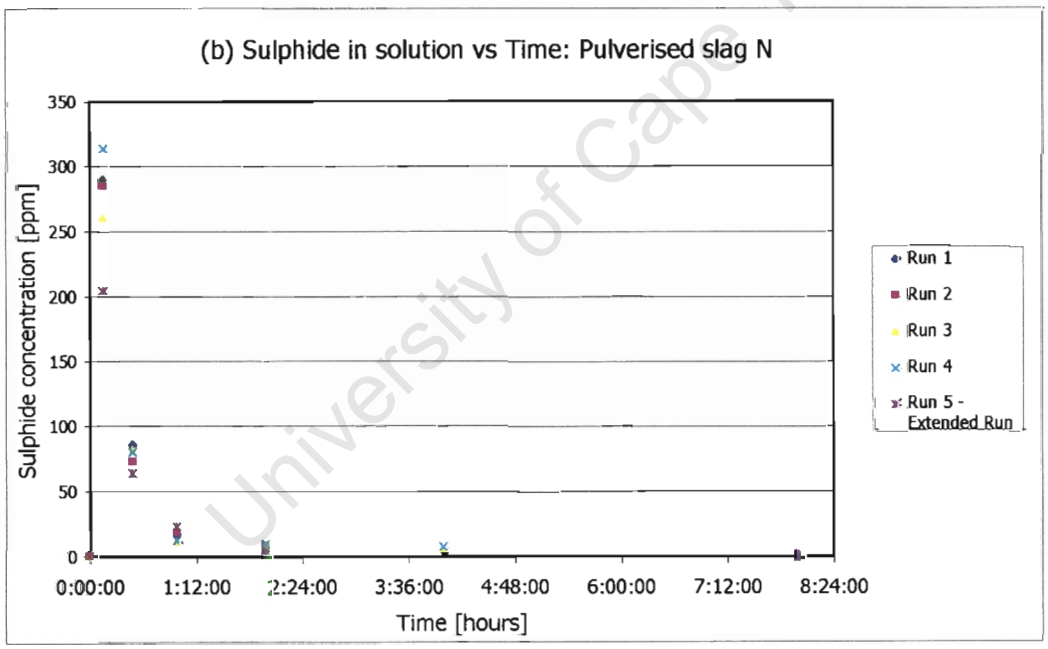

Figure 1 (a) and (b) Base condition experiments: comparison of thiosulphate and sulphide concentration graphs for the fine fraction

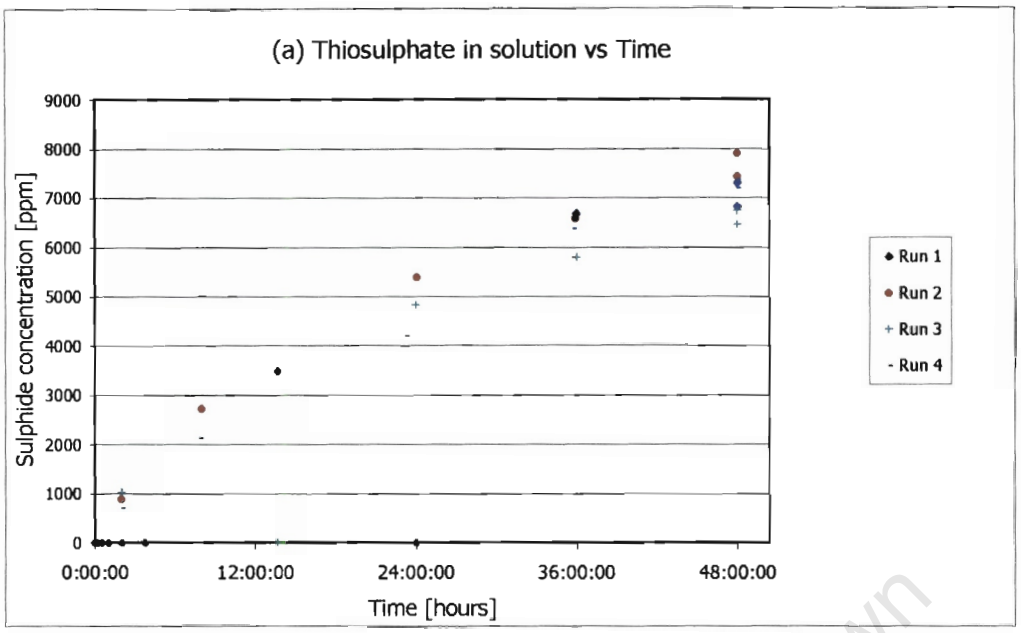

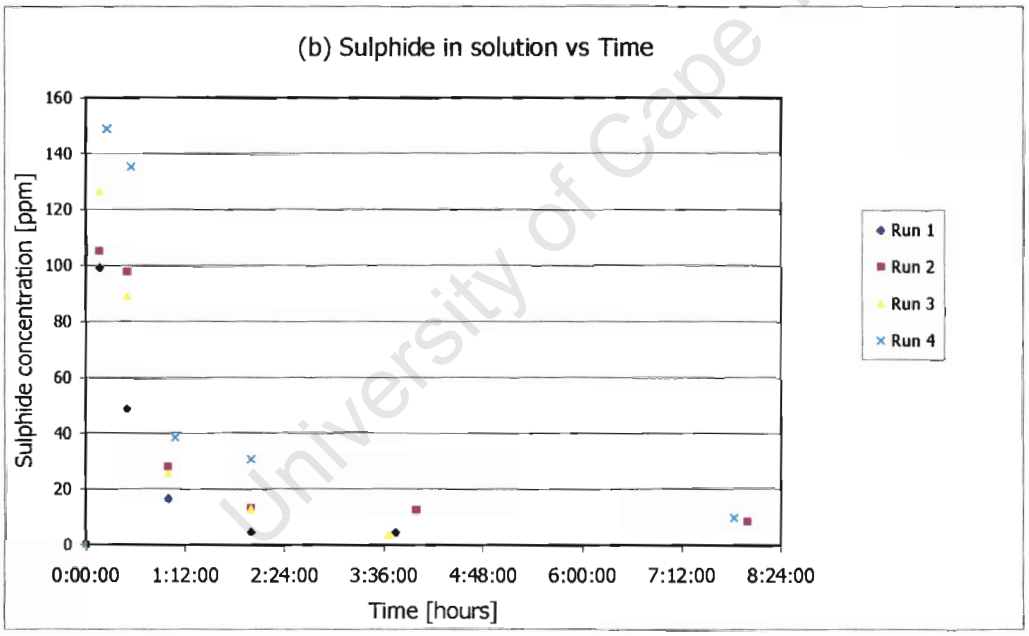

Figure 2(a) and (b) Thiosulphate and sulphide concentration curves for a course fraction, slag N base condition experiment

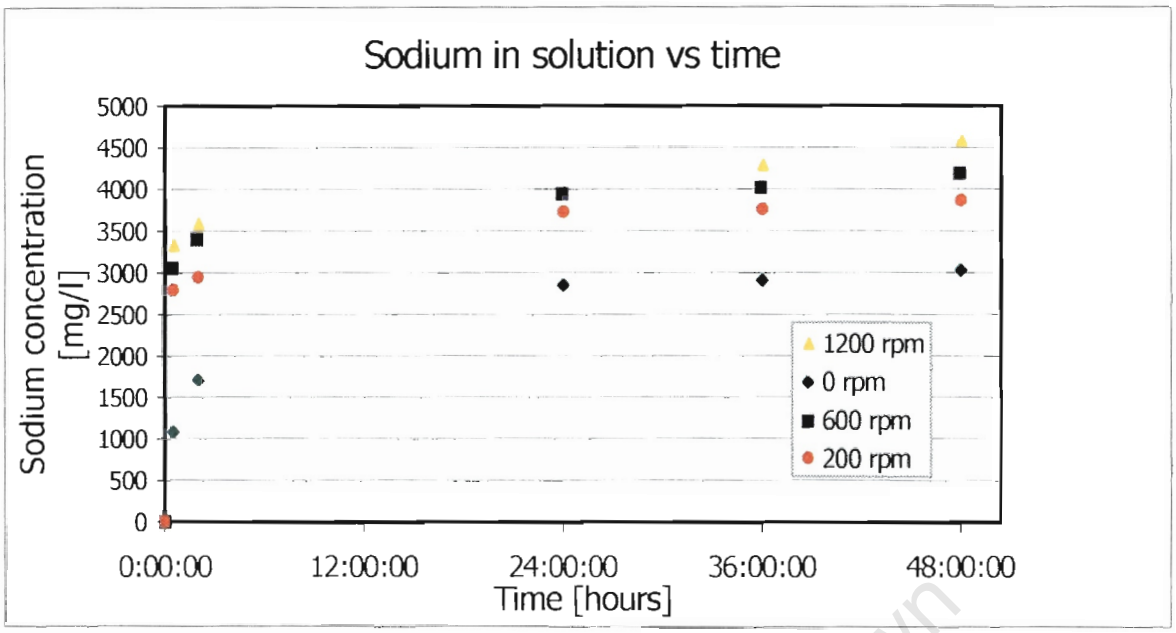

Figure 1 Variation of sodium concentration in solution for different agitation rates for coarse fraction slag N

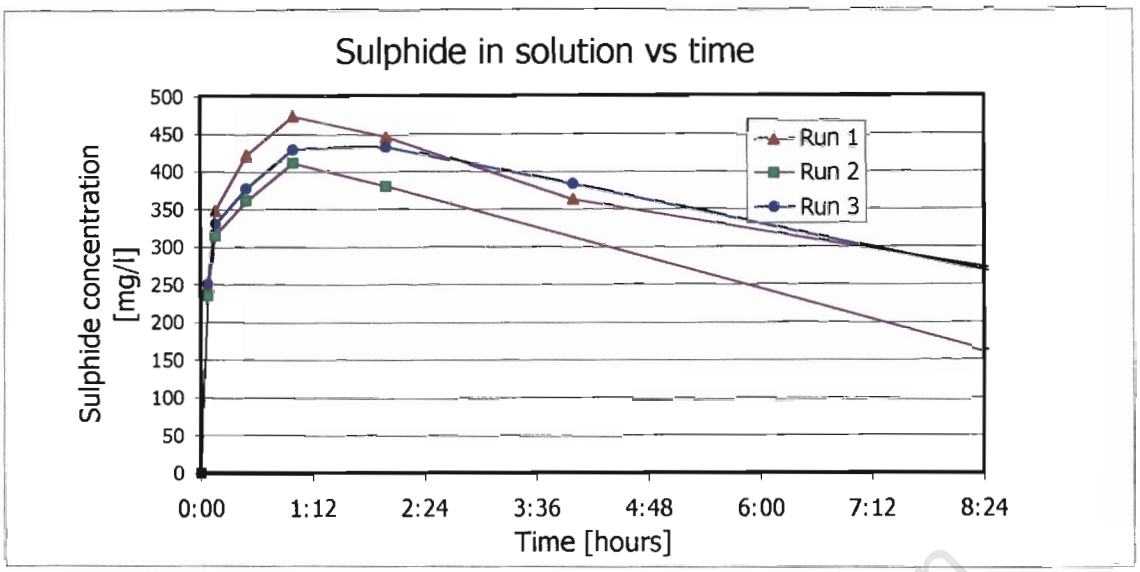

Figure 1 Sulphide in solution during leaching experiments: fine fraction slag O

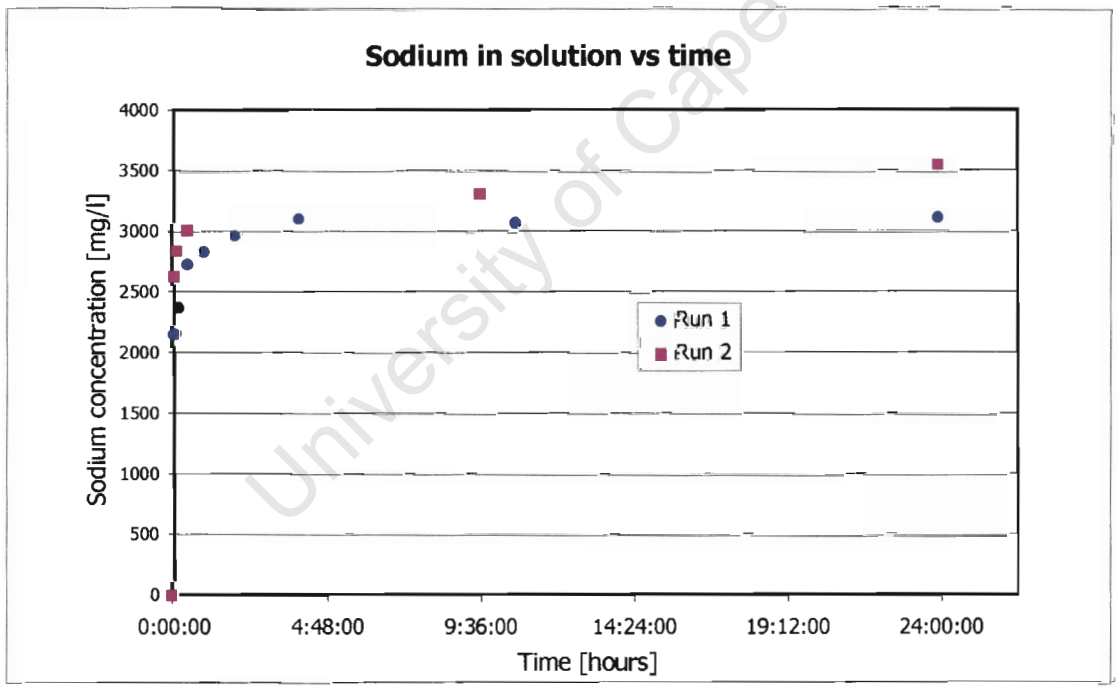

Figure 2 Sodium in solution during leaching experiments: fine fraction slag O

Csmax	793.97

Time [hours]	sulphide [mg/l]	ln[Csmax/Csmax - Cs]	Absolute error $\sum x_{Data} - x_{Regression}$
0:00	0.0	0.000	0.024
0:05	228.4	0.339	0.048
0:10	328.6	0.534	0.024
0:30	378.0	0.646	0.980
1:00	437.2	0.800	2.429

Table 1 Analytical data for calculation of leach rate constant of dissolution experiment 2

Calculation of relative error

$$relative\ error = \frac{\left|\sum x_{Data} - x_{Regression}\right|}{n}$$

x_{Data}	Value calculated from analytical data
$x_{Regression}$	Value calculated from linear regression formula
n	Number of data points

Relative error calculated for 0 min, 5 min, 10 min data points

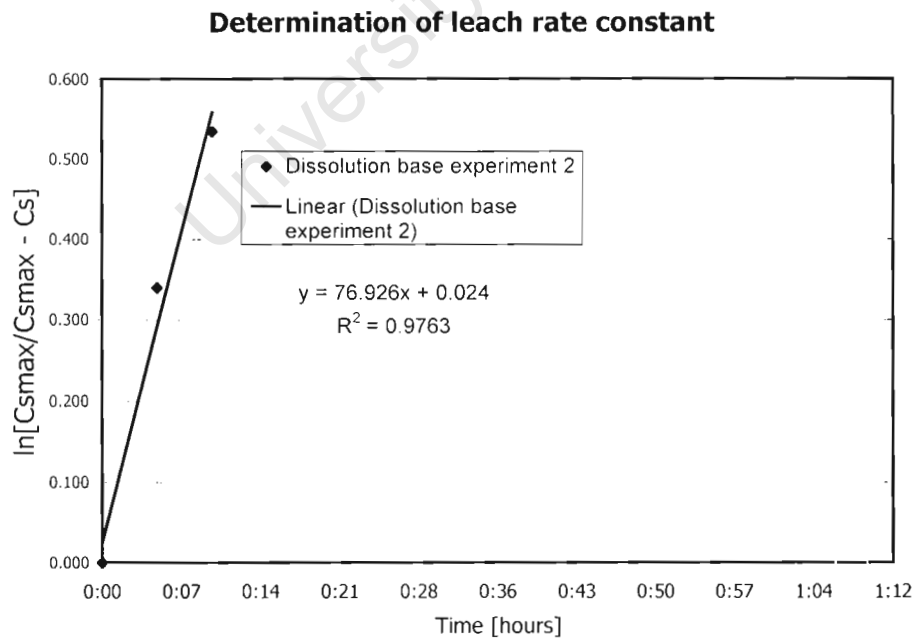

Figure 1 Determination of leach rate constant for base condition dissolution experiment 2

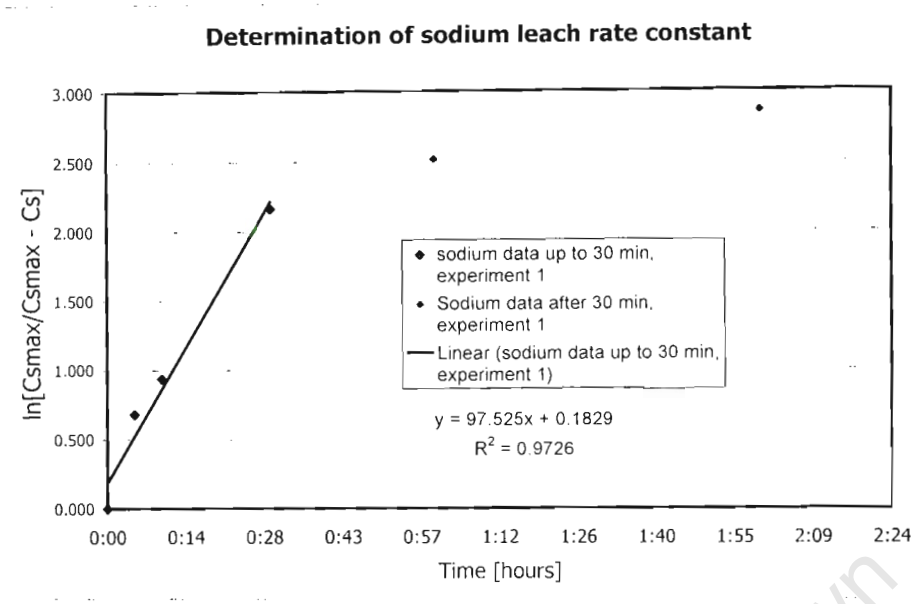

Figure 2 Determination of leach rate constant for sodium base condition dissolution experiment 1

Leaching temperature dependence calculation

Temperature [C]	Temperature [K]	1/Temperature [1/K]	1/Temperature [1/K*10^3]	k	ln(k)
20	293.1	0.00341	3.41	77.5	4.35
40	313.1	0.00319	3.19	95.6	4.56
60	333.1	0.00300	3.00	142.1	4.96

Table 2 Calculation of Arrhenius coefficients for leach rate constant temperature dependence

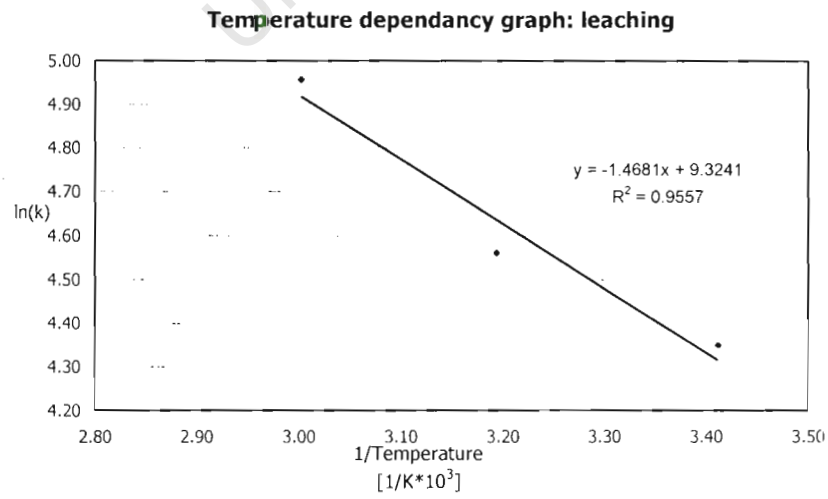

Figure 3 Calculation of Arrhenius coefficients for leach rate constant temperature dependence

Oxidation rate constant determination				
Sulphide order	m	1.47		
Oxygen order	n	0.55		

Time	Oxygen concentration	Sulphide concentration	$\frac{-1}{C_{O_2}^{\,n}} \times \frac{C_S^{\,-m+1}}{-m+1}$	absolute error
[hours]	[mg/l]	[mg/l]		$\lvert\sum x_{Data} - x_{Regression}\rvert$
0:10:00	4.2	69.2	0.1319	0.0208
0:20:00	5.4	37.4	0.1534	0.0036
0:30:00	7.9	19.8	0.1677	0.0065
1:00:00	8.2	15.8	0.1827	0.0088
2:00:00	8.5	11.6	0.2072	0.0077
4:00:00	9.2	6.8	0.2549	0.0044
15:00:00	9.1	1.46	0.5286	0.0026

Table 1 Analytical data for calculation of oxidation rate constant of oxidation experiment 2

Calculation of relative error

$$relative\ error = \frac{\lvert\sum x_{Data} - x_{Regression}\rvert}{n}$$

x_{Data} Value calculated from analytical data
$x_{Regression}$ Value calculated from linear regression formula
n Number of data points

Oxidation temperature dependency calculation

Temperature	Temperature	1/Temperature	1/Temperature	k	ln(k)
[C]	[K]	[1/K]	[1/K*10^3]		
20	293.1	0.00341	3.41	6.9	1.93
40	313.1	0.00319	3.19	14.9	2.70
60	333.1	0.00300	3.00	25.3	3.23

Table 2 Calculation of Arrhenius coefficients for oxidation rate constant temperature dependence

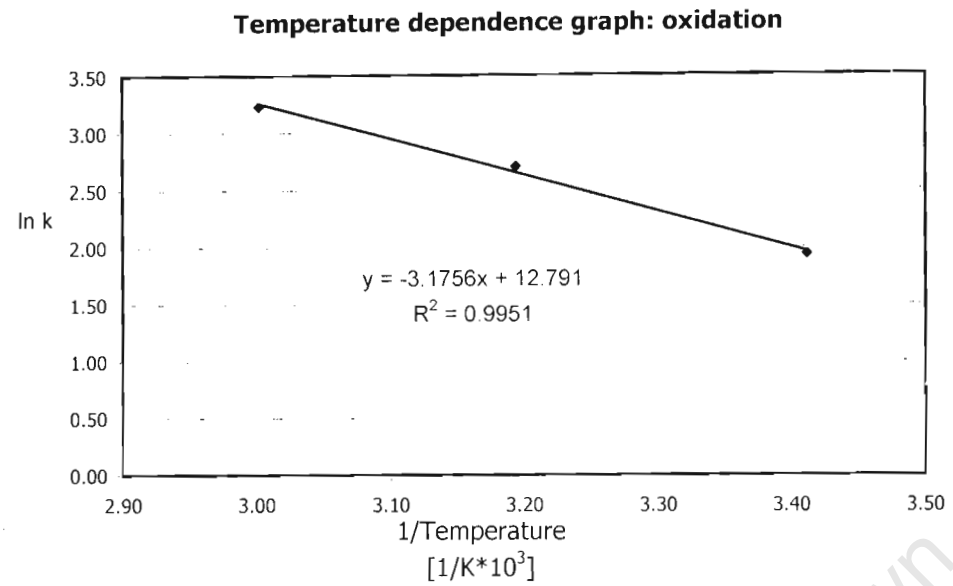

Figure 1 Calculation of Arrhenius coefficients for leach rate constant temperature dependence

Author	Literature value [various units]	Converted units [M^{-n} min^{-1}]	n	[mg -1.02. l 1.02. d-1]
Chen & Morris	15.45	0.2575	0.9	0.03
	19.42	0.323666667	0.9	0.04
Lefers	0.103	6.18	1.02	0.23
O'Brein & Birkner	0.97	0.97	1	0.04
	1.97	1.97	1	0.09
Zhang & Millero	3.00	3.00	1	0.14
	4.22	4.22	1	0.19
	179.47	179.47	1	8.08

Unit conversion	
mol/l	mg/l
2.00E-04	6.414

Table 3 Calculation for the conversion of the units from those given in the literature review

Figure 1 picture of slag

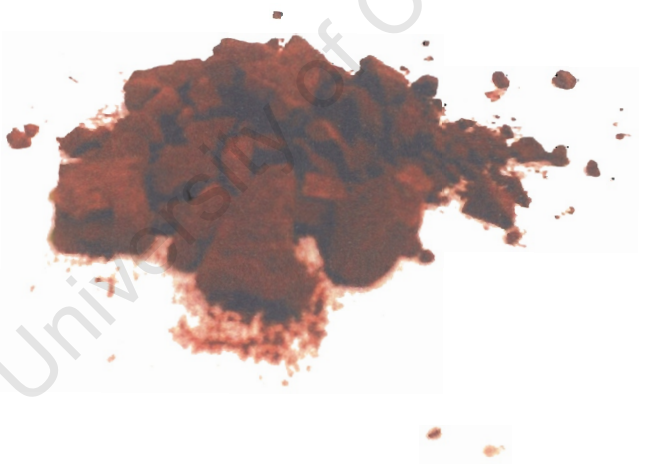

Figure 2 Picture of insoluble product